AGULHAS RETROFLECTION RINGS IN THE SOUTH ATLANTIC OCEAN

Christopher Michael DUNCOMBE RAE

B.Sc. (Rhodes), B.Sc. Hons. (Cape Town)

Sea Fisheries Research Institute, Private Bag X2, Rogge Bay 8012, South Africa

Supervisor: Prof. F.A. Shillington

Thesis presented for the degree of

DOCTOR OF PHILOSOPHY

in the Department of Oceanography,

UNIVERSITY OF CAPE TOWN.

June 1994

ABSTRACT

AGULHAS RETROFLECTION RINGS IN THE SOUTH ATLANTIC OCEAN
Christopher Michael DUNCOMBE RAE
S.F.R.I., Private Bag X2, Rogge Bay 8012, South Africa.
Ph.D. Thesis, Dept. of Oceanography, University of Cape Town.

The western boundary current rings shed from the Agulhas retroflection may be responsible for a considerable transfer of heat, salt and energy from the South Indian into the South Atlantic Ocean. Few hydrographic measurements have been collected from Agulhas rings in the South Atlantic Ocean and their characteristics and influence on the waters of the Cape Basin through which they pass are thus little known. The temperature, salinity, and nutrient data presented in the thesis were collected from three Agulhas rings on a number of recent hydrographic cruises in the South Atlantic Ocean. Temperature profiles, conductivity-temperature-depth measurements, nutrient data, GEOSAT altimeter data, and NOAA-11 satellite imagery were used to investigate one of the rings in May 1989. It had previously been postulated that the rings could have an important effect on the Benguela upwelling system and this thesis demonstrates the interaction of the ring with a filament from the upwelling system. An adverse influence of this interaction on the anchovy larval population is postulated, and cited as a possible cause of the very poor anchovy yearclass of 1989. The other two rings were encountered during winter (August 1990 and June 1992), closer to the retroflection, and only hydrographic observations were possible. One of the rings showed a very deep isothermal surface layer and evidence of a deep pycnostad at its centre. The deep stad is shown to be likely due to vortex stretching and possible sources for the water in the stad are suggested. Comparative hydrographic characteristics, water mass structure, velocity fields, and the potential for contribution to interbasin transfer of the three rings are presented and discussed in the thesis.

SUMMARY

The most energetic western boundary current rings in the World Ocean are shed from the Agulhas retroflection, south of Africa. It has been suggested that these rings are responsible for a considerable transfer of heat, salt and energy from the South Indian into the South Atlantic Ocean, as a mechanism for closing the global thermohaline circulation. In addition, it has been postulated that the rings have an important local effect on the Benguela upwelling system in their passage across the Cape Basin. Their importance in the global circulation has only recently (since 1983) been realised and few hydrographic measurements have been collected from Agulhas rings in the South Atlantic. Their characteristics and their influence on the waters of the Cape Basin through which they pass are thus little known. Data from three rings encountered hydrographically within the Cape Basin are presented in the thesis. The characteristics (temperature, salinity, nutrients) and geostrophic structure of these rings are presented and discussed.

The first ring was detected using expendable bathythermograph probes on a cruise between Cape Town and Vema Seamount in the south-east Atlantic Ocean during April 1989. CTD and nutrient data, collected on a second cruise in May 1989, GEOSAT altimeter data for February to April 1989 and cloud-free NOAA-11 satellite imagery from June 1989 were used to characterise the ring. The ring was elliptical (330 km east to west and 165 km north to south, relative to the 16°C isotherm at 200 m depth), evident to at least 1200 m, and centred on 30.5°S; 9.2°E in May, about 700 km west of the Orange River. Its drift velocity was 6.4±1 $cm.s^{-1}$ towards the north-west. Maximum anticyclonic geostrophic surface currents near its edge were 55 $cm.s^{-1}$ relative to 1150 db. The available potential energy was estimated to be 38.8×10^{15} J and the kinetic energy 2.3×10^{15} J using a two layer model of the ring.

Interaction of this ring with a filament from the upwelling front of the Benguela Ecosystem was demonstrated and this interaction was investigated. An adverse influence of this interaction on the anchovy larval population is postulated, and cited as a possible cause of the very poor anchovy yearclass of 1989. A cool filament extending 450 km offshore from the Benguela upwelling front was identified in the

hydrography and the NOAA-11 imagery. Entrainment velocities (maximum of 75 $cm.s^{-1}$) of mature upwelled water from the Benguela frontal region were inferred from feature tracking.

The other two rings discussed in the thesis were encountered during winter closer to the retroflection. Satellite infra-red imagery and altimetry were not available for these rings. Observations were made on cruises during August 1990 and June 1992. One ring, examined during August 1990 and centred at 35°16'S; 11°43'E, was shed during mid-winter. This ring, 430 km in diameter east to west and 385 km north to south, showed a very deep isothermal surface layer (330 m) of 16.3°C and evidence of a thick stad of 10-11°C water which had the characteristics of South Indian Subantarctic Mode Water at its centre. Other possible explanations are suggested for this 11°C thermostad: vorticity stretching; entrainment of Agulhas Bank bottom and slope water; and entrainment of Subantarctic water. The available potential and the kinetic energies of the ring were estimated to be 26.0×10^{15} J and 2.6×10^{15} J respectively. Maximum geostrophic velocities were 74 $cm.s^{-1}$ with respect to 1150 db. The second ring was encountered during June 1992 at 35°47'S; 14°57'E, was shed just prior to the onset of winter and also showed a deep isothermal layer (280 m) but no evidence of the 11°C stad. Both rings showed characteristics little changed from the source Agulhas Current water, an unusual feature as rings are often modified by mixing with South Atlantic and Subantarctic water during separation from the Agulhas Current. The potential of these rings for interbasin transfer is discussed in the thesis. It is suggested that Agulhas rings and the associated flows between the ring and the African continent may contribute 50 to 80% of the volume flux required to close the global thermohaline circulation.

ACKNOWLEDGEMENTS

This thesis is dedicated to three people whose influence and guidance was felt long before the work was begun: Prof. Brian Allanson, whose good advice put me on the path to research in Oceanography; the late Dr Amy Jacot-Guillarmod; and the late Dr Brian Boden. I am also extremely grateful to Prof. Frank Shillington whose interest, assistance and advice during his supervision of the progress of this thesis were invaluable.

I thank: Dr Vere Shannon, Director of the Sea Fisheries Research Institute, for his support in allowing the use of data collected and papers written under the auspices of the S.F.R.I. for the thesis; Mr Geoff Bailey and Dr Alan Boyd for allowing the use of data from their cruises; Prof. Johann Lutjeharms and his group at U.C.T. for access to publications and SCARC and other data; Roy van Ballegooyen and John Taunton-Clark whose comments and suggestions were a great help in the initial stages; Prof. Arnold Gordon and Ms Deirdre Byrne for their comments on the final draft of the thesis while at sea on R.R.S. *Discovery* during May 1993; Ms Christine Illert for drawing some of the figures; Prof. Geoff Brundrit for his patient suffering through innumerable changes in direction and topic before I settled on this one; Sarah Searson for assisting in final completion of the text.

The work embodied in this thesis is based on a series of measurements made on, amongst others, an Agulhas ring for which GEOSAT altimetry, NOAA imagery and hydrographic data were available. It is this which has occasioned the multi-author nature of the papers emanating from the work. This thesis deals with the hydrography of this Agulhas ring, while the NOAA imagery also appears in Kobus Agenbag's Ph.D. thesis, and the GEOSAT altimetry in John Taunton-Clark's M.Sc. thesis. Prof. Frank Shillington supervised all three theses and was present on most of the cruises. His contributions, advice and comments necessitated his inclusion in the list of authors as did Dr Marten Gründlingh's comments and provision of the altimeter data. Drs Alan Boyd and Rob Crawford, while at first somewhat sceptical about my ideas on the influence of Agulhas rings on the anchovy fishery, were finally convinced and contributed their knowledge of the anchovy life cycle and the West Coast upwelling ecosystem. A number of anonymous reviewers of the papers greatly improved their content. The assistance of co-authors, scientific and technical staff and ship's crews is recognized in an Acknowledgements section at the end of each Chapter where appropriate.

TABLE OF CONTENTS

LIST OF FIGURES

LIST OF TABLES

CHAPTER 1: INTRODUCTION

The mid-ocean gyral circulations of the South Atlantic and Indian Oceans are connected (Gordon *et al.* 1992) and one of the mechanisms for maintaining this interbasin flow is the shedding of Agulhas rings from the Agulhas retroflection south of Africa into the South Atlantic Ocean. These Agulhas rings thus form an important link in the global ocean circulation. Formation of cold, deep water in the North Atlantic Ocean requires the return of water and heat through the South Atlantic in the surface layers from the equatorial Pacific and Indian Oceans (Bryan 1962, Gordon and Piola 1983, Gordon 1986, Broecker 1991). Here again it is believed that Agulhas rings perform an important function in this process (Gordon 1985).

In spite of their now evident importance (Gordon 1985, Gordon and Haxby 1990, Gordon *et al.* 1992), it is only recently that the function, structure and characteristics of these rings has begun to be elucidated (Duncombe Rae 1991). Satellite thermal imagery can resolve the shedding and movement of these rings in the immediate vicinity of the retroflection where they are spawned, but they rapidly lose their surface thermal signature and within a few weeks are undetectable by this means except under exceptional circumstances. In addition, cloud cover often obscures the thermal image of the ocean surface. Satellite altimetry, a recent addition to the oceanographer's toolbox, does not suffer from these limitations and has enabled great advances to be made in our understanding of the global circulation and Agulhas rings (e.g. Cheney *et al.* 1983, Sandwell and Zhang 1989, Douglas and Cheney 1990, Gordon and Haxby 1990, Wakker *et al.* 1990b, Feron *et al.* 1992). However, as valuable as remote sensing can be, there are some features of the ocean interior which still require ship-based observations. Agulhas rings are difficult to detect at sea: until the inception of the WOCE programme, hydrographic stations were seldom occupied at sufficiently fine spatial resolution in the deep ocean around South Africa for these features to be resolved. With the advent of satellite remote sensing it is now possible to some extent to indicate where ship-based searches for rings will be most profitable. Up until 1989, however, there were only two sets of hydrographic measurements of Agulhas rings which had been made some distance away from the immediate

vicinity of the retroflection (Gordon and Haxby 1990, McCartney and Woodgate-Jones 1991). Both these rings were detected by chance in the course of large-scale surveys and neither measurement consisted of more than one line of hydrographic and bathythermograph measurements through each ring. Even close to the retroflection there are few historical cruises which have examined Agulhas rings in detail. Only the Agulhas Retroflection Cruise in 1983 (Gordon 1985, Camp *et al.* 1986), and the Subtropical Convergence and Agulhas Retroflection Cruise in 1987 (Lutjeharms 1987, Valentine *et al.* 1988), could claim to have produced truly comprehensive measurements of rings adjacent to the Agulhas retroflection.

I participated in a cruise of F.R.S. *Africana* in April 1989, during which an Agulhas ring was detected on a line of expendable bathythermograph (XBT) stations near Vema Seamount in the Cape Basin (the Vema ring). Although ship's time is always at a premium and *ad hoc* cruises of the type which we wished to do to examine deep ocean eddies are normally not possible, the opportunity to undertake an intensive study of this ring presented itself. Since R.S. *Benguela* was then fortuitously uncommitted, she was made available at short notice by Sea Fisheries Research Institute for ten days during May 1989 and I was chief scientist of the cruise which returned to the ring. The anticipated new position of the ring in May 1989 was estimated from the April 1989 data using translation speeds of rings encountered closer to the retroflection (Olson and Evans 1986) and an appropriate search strategy devised. The ring was duly located on 17 May 1989 with an exploratory XBT section and subsequently two lines of 16 hydrographic stations were occupied across it, measuring temperature, salinity and nutrient concentrations to a depth of 1100 m (Duncombe Rae *et al.* 1992b).

Not only was this ring unusual in its accessibility to ship-based study, but it was also later found to be clearly evident in remote sensing data from two different satellites. The ring had entrained a filament of cold Benguela frontal water, and was thus clearly differentiated from its surroundings in the NOAA infra-red satellite imagery for June 1989. GEOSAT, from which no useful altimetric data were available for the South Atlantic after April 1989, revealed the ring from the time it first became distinguishable from the retroflection in February 1989 and confirmed the path it had taken to its first

hydrographic detection in April 1989. We were thus equipped with a unique suite of hydrographic and remotely sensed measurements of this ring.

I participated in further cruises which yielded other evidence of rings in XBT sections across the South Atlantic. Then, in August 1990, F.R.S. *Africana* was made available for a physical oceanographic survey and it was proposed that a deliberate search for an Agulhas ring in the South Atlantic be made. This cruise proposal was approved and I was again appointed chief scientist. I devised a cruise track which extended along the basin edge from south-west of Cape Town to Port Nolloth and out into the South Atlantic Ocean which was likely to locate a ring of 350-400 km diameter if it were present. Using this track a ring was detected with XBT probes on 18 August 1990 and 16 hydrographic stations were occupied across it, measuring temperature, salinity, oxygen and nutrient concentrations to a maximum depth of 3000 m. This was the first Agulhas ring detected hydrographically which had been shed from the retroflection during mid-winter, and it exhibited some unique features: a deep isothermal surface mixed-layer; a deep pycnostad within the main thermocline, with characteristics corresponding to Subantarctic Mode Water; baroclinic reversal at the ring centre; and clear evidence of unaltered Agulhas water within the core of the ring. In this case, however, no follow-up cruise was available; the entire region remained obstinately under cloud cover; and the GEOSAT radar altimeter had been dead for nearly a year. We sorrowfully waved this Agulhas ring "goodbye". During the BEST-1 cruise in June 1992 another Agulhas ring was detected on a line south-west of Cape Town during the deployment of three inverted echo-sounders, and again two lines of detailed hydrographic measurements were made across the ring. This last ring is dealt with only cursorily in this thesis.

The main objective of this thesis is to describe and characterize the hydrography of individual Agulhas rings in the South Atlantic Ocean. Further questions that will be addressed pertain to both the regional and global influences of Agulhas rings:

i) What is the physical and biological impact of an Agulhas ring passing close to the adjacent Benguela Upwelling system?

ii) What is the potential for Agulhas rings to contribute to the global ocean circulation?

The thesis arises from research conducted at the Sea Fisheries Research Institute and part of the work has already been reported in a series of recent publications while further aspects are in preparation for publication.

The structure of the thesis is as follows: Chapter 2 reviews the appropriate literature and is an updated and slightly modified version of a recent overview of Agulhas rings by Duncombe Rae (1991). Methods of data collection and their subsequent digital processing for each cruise are presented in Chapter 3 from data reports in preparation (Duncombe Rae *et al.* 1989a, Duncombe Rae and Shillington 1989). Some of the basic theoretical considerations required for the data processing are also reviewed in this Chapter. A discussion of XBT data collected in the south-east Atlantic Ocean and the way these describe the background circulation of the Cape Basin follows in Chapter 4. The main body of the thesis is contained in Chapter 5 which discusses the hydrography of Agulhas rings (from Duncombe Rae *et al.* 1992b, Duncombe Rae and Shillington in prep.). Aspects of the interaction of Agulhas rings with the Benguela upwelling system and the implications for fisheries are explored in Chapter 6 (from Duncombe Rae *et al.* 1992a, 1992b). The heat, salt and volume transport potentials of Agulhas rings with implications for global circulation are discussed in Chapter 7 (an extension of Duncombe Rae *et al.* 1989b, Duncombe Rae *et al.* 1992b). Each chapter has a discussion associated with it and Chapter 8 summarises the findings of the work.

CHAPTER 2: LITERATURE REVIEW

The Agulhas Current flows south along the south-eastern coast of Africa from Mozambique, guided by the edge of the continental shelf. Near 36°S at the Agulhas Bank it separates from the continental shelf as a free jet, develops oscillations of increasing amplitude (Harris and Bang 1974) and turns eastward in a great anticyclonic loop, named the Agulhas "retroflexion" by Bang (1970a). The current then returns to the South Indian Ocean as the Agulhas Return Current. Periodically the loop of the retroflection can pinch off, forming a ring which is ejected into the South Atlantic Ocean (Lutjeharms and Gordon 1987). The Agulhas Current and the rings formed at the retroflection form an important link in the global thermohaline circulation (Gordon 1986). In addition, they affect their immediate surroundings in the South-East Atlantic Ocean (Duncombe Rae *et al.* 1992b).

In this review, current knowledge of these Agulhas rings and their contribution to both the thermohaline circulation and the local oceanography is summarized.

2.1 THE THERMOHALINE CONVEYOR BELT

The deep water which occupies the World Ocean basins between about 2000 and 4000 m depth is formed in the North Atlantic Ocean, in the Norwegian Sea (Warren 1981, Killworth 1983a) by the loss of heat to the atmosphere and during the winter formation of pack ice. These processes increase the salinity and lower the temperature, forming dense (cold and saline) water which sinks and forms North Atlantic Deep Water. Deep water is only formed in the North Atlantic Ocean. In the North Pacific, the salinity of the near-surface water is too low for the cold water formed to penetrate the thermocline and enter the deep water layer (Warren 1983). Dense water formed around Antarctica, on the other hand, is even more dense and forms the majority of the bottom water of the World Ocean.

The water formed in the North Atlantic moves southward within the Deep Western Boundary Currents (Warren 1981) and rises above the Antarctic Bottom Water in mid-Atlantic. The deep water crosses the equator

(Speer and McCartney 1991) and spreads through the Atlantic and into the Indian and Pacific Oceans. Global circulation models (Semtner and Chervin 1991, 1992) and theoretical studies (Kawase 1987) suggest that the deep water percolates to the surface at the equator, principally in the Pacific, as opposed to the uniform upwelling proposed by Stommel and Arons (1960). The upwelled water returns to the North Atlantic near the surface in the Intermediate and thermocline (Central) waters to replace the outflow of mass and salt in the deep water.

There are two possible routes for this return flow of Intermediate and Central Waters (Fig. 2.1). Antarctic Intermediate Water from the Pacific Ocean can enter the Atlantic through the Drake Passage and join the South Atlantic gyre to feed the Gulf Stream. This is called the "cool freshwater path" (Georgi 1979, Piola and Georgi 1982). The other possible route for the return of water and salt is the "warm-water path" (Gordon 1986, Piola and Gordon 1986) from the tropical Pacific across the Indonesian seas and the tropical Indian Ocean. Via the Agulhas Current the warm water reaches the southern point of Africa.

In the warm-water path the water may enter the South Atlantic as rings shed from the Agulhas Retroflection (Lutjeharms 1981a, Gordon 1985, Gordon 1986) or as intermittent direct leakage of Agulhas Current water (Harris and Van Foreest 1978, Gordon 1985, Shannon *et al.* 1990). This flow into the Atlantic from the Indian Ocean has been observed in global ocean circulation models (e.g. Semtner and Chervin 1988, 1992, Webb *et al.* 1991, FRAM Group 1991, Fujio 1992a, 1992b). Gordon *et al.* (1987a) found that direct intermittent flow was on one occasion associated with the passage of an Agulhas ring. A small quantity of water from the Agulhas Bank also enters the Benguela Current and upwelling system (Nelson and Hutchings 1983, Shannon 1985) in the shelf-edge jet associated with the upwelling front.

Heat and freshwater fluxes through the Atlantic are sensitive to the proportions of the two inflows. If the salty Agulhas path predominated, the Atlantic would be expected to become saltier, whereas if the Antarctic Intermediate Water path predominated, the Atlantic would become fresher. Estimates of the heat and salt budgets for the Atlantic demonstrate a net northward flux of heat through the South Atlantic (Gordon and Piola 1983). Inverse method analysis of non-

synoptic sections bordering the South Atlantic implies that most of the return flow is through the Drake Passage (Rintoul 1991) and Piola and Gordon (1989) showed a strong northward flow of freshwater in the intermediate layers of the south-western South Atlantic. However, recent research, showing that Agulhas rings are shed and move into the South Atlantic (Lutjeharms 1981a, Gordon 1986) together with direct leakage into the Benguela system (Gordon 1985, Shannon *et al.* 1990), indicates that the warm water path may make a significant contribution to the flow. The ocean circulation model of Semtner and Chervin (1991, 1992) would seem to favour this route, without excluding the other, while the FRAM model (Webb *et al.* 1991) shows no heat transport through the Drake Passage (FRAM Group 1991). Matano and Philander (1993) suggest that the transport of the Antarctic Circumpolar Current and associated meridional displacements of the Subtropical Front could control which route is favoured, by changing the amount of heat gained by the South Atlantic Ocean from the atmosphere. This would moderate the amount of heat required to be provided by the warm-water path and the Agulhas Current.

Recent data have revealed that the thermocline circulations of the South Atlantic and South Indian Oceans are linked. Examining chemical tracer data and water mass characteristics, Gordon *et al.* (1992) have suggested that the cool intermediate water input from the Drake Passage is first cycled through the Indian Ocean before entering the South Atlantic gyre circulation through the Agulhas Current.

2.2 SOUTH ATLANTIC CIRCULATION

It is appropriate to survey here the upper level circulation of the South Atlantic Ocean before examining in detail the source, formation and structure of Agulhas rings. The South Atlantic hydrography is reviewed completely in a series of papers by Stramma and Peterson (Stramma 1989, Stramma and Peterson 1989, Stramma *et al.* 1990, Stramma and Peterson 1990, Peterson and Stramma 1991, Stramma 1991).

2.2.1 CLIMATOLOGY

A climatology of the South Atlantic has been provided by Höflich (1984). The South Atlantic Ocean climate is dominated by a semi-permanent high pressure system in the subtropics. The South Atlantic

subtropical high pressure system is centred near 32°S, 5°W in summer and in winter this high moves to 27°S, 10°W. Pressure differences between the centre of the high pressure and the adjacent African and South American coastlines is greatest during summer, due to thermal lows which develop over the continents in this season. Consequently along-shore winds and the associated upwelling along the eastern South Atlantic boundary are strongest in summer. As the centre of the oceanic high pressure system is over the eastern basin of the South Atlantic Ocean the trade winds near southern Africa are stronger than those near the South American continent. At mid- and high-latitudes the zonal isobars and associated pressure gradients produce westerly winds.

Air-sea heat energy fluxes are strongly seasonal. During summer the greatest oceanic heat gain occurs in the region of upwelled water off the western coast of southern Africa. Large heat gains also occur in the cool regions of the Falkland Current and the Antarctic Circumpolar Current. The Agulhas Current system provides the only region of heat loss from the ocean to the atmosphere during summer (>50 $W.m^{-2}$). During winter the greatest areas of heat loss from the ocean are in regions of strong evaporation (~250 $W.m^{-2}$ in the Agulhas Current region).

2.2.2 CIRCULATION

The topography and the large-scale upper-level circulation of the South Atlantic Ocean are shown in Figure 2.2 (from Peterson and Stramma 1991). For the purpose of this discussion, the equatorial and Angola Basin current systems are described first, and then the circulation round the basin is considered, ending with the Benguela Current system.

2.2.2.1 The Equatorial Current System

The equatorial current system varies greatly over both time and space, driven essentially by atmospheric forcing (Eriksen and Katz 1987, Garzoli 1987) and dominated by wave-like motions (Siedler 1983, Garzoli and Richardson 1989). Differences between ship's drift observations and geostrophic calculations are accounted for by Ekman drift which has larger amplitudes than the geostrophic component of the flow (Arnault 1987). At the equator the Coriolis parameter is zero, the geostrophic component of the flow vanishes and the Ekman drift is the only component of the flow. Ship's drift is westward at all longitudes and

seasons as is the Ekman drift. Surface geostrophic flow is eastward in all months except June to September. In these months the "Angola Dome" (discussed below) is absent in the thermocline of the Gulf of Guinea and the northern Angola Basin.

The Angola Dome is a feature of the shallow thermocline of the Angola Basin (Fuglister 1960, Mazeika 1967). It appears in southern summer by uplifting, under the influence of lowered atmospheric pressure, of a permanent sub-thermocline thermal dome formed from the South Equatorial Undercurrent (Voituriez 1981, Voituriez and Herbland 1982, Wacongne and Piton 1990). Also within the Angola Basin and distinct from the Angola dome is a cyclonic gyre bounded in the north by the South Equatorial Countercurrent (Moroshkin *et al.* 1970, Shannon *et al.* 1987, Gordon and Bosley 1991).

Wacongne and Piton (1990) suggest that the Equatorial Undercurrent is continuous with the Gabon-Congo Undercurrent, a poleward eastern boundary current of the Angola Basin, and supplies water to the Angola Current in the south.

The system of equatorial currents comprises a complex array of westward currents and eastward countercurrents typified by the schematic representation for the southern winter (Fig. 2.3). Straddling the equator is the South Equatorial Current (Wacongne 1989). There is a velocity minimum at the equator, above the Equatorial Undercurrent, a narrow jet about 3° latitude wide, 100 m deep with eastward velocities over 100 $cm.s^{-1}$. Below, on either side of, and distinct from this jet are the North and South Equatorial Undercurrents near 4.5°S and 4.5°N. The southern current averages 100 km wide and transports 15×10^6 $m^3.s^{-1}$ at 150 to 200 m depth (Cochrane *et al.* 1979, Molinari *et al.* 1981).

Between two branches of the South Equatorial Current is the eastward flowing South Equatorial Counter Current, whose maximum velocities are encountered below the surface. This current also feeds into the Angola Basin (Moroshkin *et al.* 1970, Shannon *et al.* 1986). Stramma *et al.* (1990) found that the southern branch of the South Equatorial Current carries 16×10^6 $m^3.s^{-1}$ in the upper 500 m across 30°W.

2.2.2.2 The Western Boundary Currents

The South Equatorial Current (Stramma 1991) flows to the South American coast where it is split by Cabo de São Roque into the North Brazil Current and the Brazil Current, of which the North Brazil Current is the stronger (Stramma *et al.* 1990, Peterson and Stramma 1991). Of the 16×10^6 $m^3.s^{-1}$ carried by the South Equatorial Current, 12×10^6 $m^3.s^{-1}$ flows into the North Brazil Current and only 4×10^6 $m^3.s^{-1}$ feeds into the Brazil Current. This loss of cross-equatorial flow from the South Atlantic gyre is responsible for the weakness of the Brazil Current in comparison to other western boundary currents.

The northern Brazil Current is shallow and confined to the shelf. The Brazil Current transport between 19° and 25°S is estimated to be 11×10^6 $m^3.s^{-1}$ or less (Peterson and Stramma 1991). There is no systematic strengthening of the current (Stramma *et al.* 1990) until it reaches 24°S from where it intensifies at the rate of 5% per 100 km (Gordon and Greengrove 1986). South of 30°S this intensification is linked to a recirculation cell (Stramma 1989). Recent inverted echo-sounder and hydrographic measurements have determined the mean flow of the Brazil Current at 37°50'S, relative to 800 m, to be 11×10^6 $m^3.s^{-1}$, reaching a maximum of 23×10^6 $m^3.s^{-1}$ (Garzoli and Clements 1986, Garzoli and Bianchi 1987, Garzoli and Garraffo 1989).

The Brazil Current separates from the continental shelf between 33° and 38°S. This separation appears to be seasonal (Peterson and Stramma 1991). Once separated from the shelf the Current continues southward to a southern limit where it experiences a retroflection which fluctuates over a two-month cycle between 38° and 46°S (Legeckis and Gordon 1982) analogous to the westward penetrations of the Agulhas retroflection (Lutjeharms and Van Ballegooyen 1988a; discussed in detail below). Also analogously to the Agulhas system, the Brazil Current retroflection sheds warm core rings (Legeckis and Gordon 1982, Gordon 1989).

2.2.2.3 South Atlantic Current

The South Atlantic Current forms the southern arm of the South Atlantic subtropical gyre. This current is distinct from the Antarctic Circumpolar Current and separated from it by the Subtropical Front (Stramma and Peterson 1990). The Subtropical Front was described by

Deacon (1933), who called it the Subtropical Convergence, as an abrupt surface thermal discontinuity of between 4° and 0.5°C, lying 2° or 3° north of about 40°S. Surface waters just north of the front were described as ranging from 11.5°C in winter to 14.5°C in summer, with salinity values of at least 34.9 psu.

The Subtropical Front starts at the confluence of the Brazil and Falkland Currents, the frontal regions of these two currents finally separating near 42°W, with the Brazil Current Front turning northwards to delimit the recirculation cell of the Brazil Current. Surface velocities of the South Atlantic Current are greatest in the Argentine Basin, estimated from 20 $cm.s^{-1}$ (Roden 1986) to 27 $cm.s^{-1}$ (Stramma and Peterson 1990) decreasing to values half as large in the Cape Basin (Whitworth and Nowlin 1987, Stramma and Peterson 1990); near the longitude of the Tristan da Cunha Islands, at 13°W, geostrophic current speeds relative to 1500 m of 8 and 16 $cm.s^{-1}$ have recently been measured (Chapman *et al.* in prep.). This trend is followed by the volume transport: 30 to 37×10^6 $m^3.s^{-1}$ in the Argentine basin and 15×10^6 $m^3.s^{-1}$ in the Cape Basin (Stramma and Peterson 1990). Transport relative to 1200 db along a section from 36°S to 42°S (13°W) west of the Tristan Islands was 14×10^6 $m^3.s^{-1}$ in February 1990, while along the same section in April 1989 transport relative to 1500 db was 15×10^6 $m^3.s^{-1}$ (Chapman *et al.* in prep.). As the South Atlantic Current flows east, it encounters the Agulhas retroflection and some of this flow turns north as the source of the Benguela Current (Stramma and Peterson 1990). However, Gordon *et al.* (1992) found that the source of the Benguela Current was primarily Indian Ocean/Agulhas Current water and not the South Atlantic Current.

2.2.2.4 The Eastern Boundary Currents

As has been noted by Stramma and Peterson (1989), some confusion has arisen about the terminology in referring to the Benguela Current and the adjacent upwelling ecosystem. Throughout the thesis I shall follow the usage of Stramma and Peterson (1989) and use the term "Benguela Current" for the off-shore gyre component of the flow off the west coast of Africa. The term "shelf-edge jet" will be used to refer to the intense flows along the shelf-edge over the 300 to 400 m isobath which are most evident between Cape Point and Cape Columbine. The term

"Benguela upwelling system" will be used to refer to the inshore wind-induced upwelling regime and the shelf-related flows as a whole.

The Benguela Current begins as a northward flow off the Cape of Good Hope before bending north-west to separate from the African coast at about 30°S and widening rapidly (Stramma and Peterson 1989). In addition to the input of the South Atlantic Current (Stramma and Peterson 1990), the Benguela Current receives an input from the Agulhas Current more or less sporadically. Gordon *et al.* (1992) found the content of the Benguela Current to be primarily of Indian Ocean or Agulhas origin and not from the South Atlantic Current. Sverdrup *et al.* (1942) estimated a northward geostrophic transport at 30°S of 16×10^6 $m^3.s^{-1}$ with respect to 1200 db. Stramma and Peterson (1989) noted a northward transport of 18.7×10^6 $m^3.s^{-1}$ in the upper 600 m of the data of Wüst (1957) and obtained a northward transport at 32°S of 21×10^6 $m^3.s^{-1}$. They found that near 30°S the Benguela Current begins to separate from the shelf and turn towards the northwest, carrying 18×10^6 $m^3.s^{-1}$ of water across 28°S. At this point the current turns westward and flows over a relatively deep section of the Walvis Ridge. About 3×10^6 $m^3.s^{-1}$ of surface flow leaves the Cape Basin to the north and enters the Angola Basin.

Nelson and Hutchings (1983), Shannon (1985) and Nelson (1989) provide a comprehensive overview of the wind-induced upwelling system and associated currents along the coastal shelf inshore of the Benguela Current.

2.3 THE AGULHAS CURRENT

The Agulhas Current (Fig. 2.4) closes the circulation of the South Indian Subtropical gyre. Harris (1972) and Fu (1986) identified the source of the current in the Mozambique Channel. Saetre and Jorge da Silva (1984), however, suggested that the Mozambique circulation was dominated by small eddies without a flow-through. This has not yet been resolved (Gründlingh *et al.* 1991). Some input to the Agulhas Current was found to arise from the East Madagascar Current (Lutjeharms 1976, Lutjeharms *et al.* 1981, Lutjeharms 1988a). However, the majority of the Agulhas Current flow is provided through recirculation within an

anticyclonic sub-gyre in the South West Indian Ocean (Wyrtki 1971, Harris 1972, Lutjeharms 1976, Gordon *et al.* 1987a).

The current moves southward, remaining just offshore of the continental shelf edge (Lutjeharms *et al.* 1989, Goschen and Schumann 1990). Near Algoa Bay (25°E) it moves away from the coast as the shelf widens, developing oscillations and beginning to separate from the continental shelf between 20° and 22°E (Harris and Bang 1974, Lutjeharms 1981a, Schumann and Van Heerden 1988). South of Cape Agulhas the shelf-edge turns abruptly north-westwards, but the current continues to the south or south-west leaving the continental shelf topography behind it. Estimates of the flow of the current when it separates from the shelf vary from 95×10^6 $m^3.s^{-1}$ (Gordon *et al.* 1987a) to 136×10^6 $m^3.s^{-1}$ (Jacobs and Georgi 1977) relative to the bottom. The current turns towards the east in a large loop, the Agulhas retroflection (Bang 1970a, 1970b, Bang and Pearse 1970) becoming the Agulhas Return Current. Lutjeharms (1989), Valentine (1990), Peterson and Stramma (1991) and Gründlingh *et al.* (1991) provide recent reviews of most aspects of the Agulhas Current and retroflection.

2.4 RETROFLECTION

Some other western boundary currents also exhibit a retroflection (Brazil, East Australian Currents). However, they differ from the Agulhas Current retroflection in that their currents turn eastward before the continent ends.

Lutjeharms and Van Ballegooyen (1988a) found the Agulhas retroflection to occur preferentially at 20°E with a secondary retroflection at 16°E. Lutjeharms (1988b) observed the most westerly extent of Agulhas water at 8°E. Occasionally (two or three times a year) retroflection occurs upstream of these positions, at about 25°E (Lutjeharms and Van Ballegooyen 1988b), possibly triggered by a "Natal pulse". These large meanders are formed from eddies shed intermittently and rarely from the Natal Bight at about 29°S (Gründlingh 1979, Lutjeharms 1981b, Lutjeharms and Roberts 1988). Whether these anomalous early retroflections have an effect on the shedding of Agulhas rings (see below) is unknown. The diameter of the retroflection is reasonably constant (342 ± 66 km; Lutjeharms and Van Ballegooyen 1988a) and comparable to

the diameter of rings encountered in the South Atlantic (discussed below). Extension of the retroflection into the South Atlantic creates broad zones of warm Agulhas water adjacent to the Subtropical Front and stretching over distances of more than 500 km, with important climatic and dynamic implications (Lutjeharms and Van Ballegooyen 1988a).

The retroflection of the Agulhas Current is incomplete and some of the current flows into the South Atlantic (Shannon 1966, Bang 1973, Gordon 1985, Shannon *et al.* 1990). Estimates of this transfer range from 3 to 14×10^6 $m^3.s^{-1}$. In addition, Agulhas rings shed from the retroflection (discussed below) introduce 10 to 15×10^6 $m^3.s^{-1}$ of Indian Ocean water into the South Atlantic (Gordon and Haxby 1990).

Modelling studies have provided some insight into the conditions prompting retroflection in the Agulhas system. Free-inertial jet models (Darbyshire 1972, Lutjeharms and Van Ballegooyen 1984) showed that small changes in bottom topography greatly affected the path of the Agulhas Current after its separation from the shelf. The magnitude of the jet transport was an important factor in determining the position of retroflection in the model, with low volume transports producing greater westerly penetrations of the retroflection into the Atlantic.

Wind-driven models of the Agulhas Current by De Ruijter (1982) could not produce a retroflection, and he therefore suggested that inertia and friction were responsible for closing the Indian subtropical gyre. De Ruijter and Boudra (1985) showed that a strong retroflection could be produced with a high Rossby number in a one-layer model of the current, whereas low Rossby numbers produced little or no retroflection. Boudra and De Ruijter (1986) extended this model to two and three layers and showed that the change in vorticity balance when the current separated from the shelf was responsible for retroflection.

The model of Ou and De Ruijter (1986) included the ß-effect, inertia and the curvature of the topography and revealed a separation from the coast and retroflection strongly dependent on the volume flux of the current. For instance, a decrease of 10% in the model volume flux induced the current to continue around the continent with no separation from the coast. Boudra and Chassignet (1988) determined that vertical

stretching of vorticity was as important as the planetary component in generating the retroflection, and that representing the shape of the Agulhas Bank more realistically produced greater leakage and ring formation in the model.

2.5 RETROFLECTION RINGS IN THE SOUTH ATLANTIC

Periodically, the loop of the Agulhas retroflection pinches off, shedding a ring which moves into the South Atlantic (Lutjeharms 1981a, Gordon 1985, 1986, Lutjeharms and Gordon 1987).

2.5.1 OCCURRENCE

Rings have long been known to be associated with western boundary currents. Both cold-core (Fuglister 1972) and warm-core (Joyce 1985) rings are formed from the Gulf Stream; the Kuroshio forms rings in a manner similar to that of the Gulf Stream (Solomon 1978); two rings per year are produced from the East Australian Current (Nilsson and Cresswell 1981) and one every two months from the Brazil Current (Legeckis and Gordon 1982). Cyclonic cold-core eddies are frequently encountered within the recirculation cell of the Agulhas Current and associated with the Mozambique Ridge Current (Gründlingh 1978, 1983, 1988, Gründlingh and Pearce 1984).

In the regimes discussed above, the rings are pinched off from meanders in the currents and remain in the ocean in which they were formed, often being re-absorbed into the main current again (Gulf Stream: The Ring Group 1981; Kuroshio: Solomon 1978; East Australian: Nilsson and Cresswell 1981). Cresswell (1982) found that rings may also coalesce. These events have also been observed in the Agulhas system. Recent examination of GEOSAT altimeter data suggests that coalescence may be a feature of Agulhas rings constrained within the Cape Basin by the Walvis Ridge (D.A. Byrne, Lamont-Doherty Earth Observatory, pers. comm.). Hydrographic data taken within the region between the Agulhas Current and the Agulhas Return Current showed evidence of reabsorption of rings into the Agulhas circulation (Gordon *et al.* 1987a).

However, these features may not be common in Agulhas rings since the rings are not constrained by topography or dynamics to the proximity of the mother current and can move great distances from their source of

formation into the South Atlantic. Reabsorption and coalescence may occur more frequently in the region between the Agulhas Current and the Agulhas Return Current in the South-West Indian Ocean and south of the Subtropical Front, where an eddy formed from the Agulhas Return Current has recently been examined (Dower and Lucas subm., Lucas *et al.* in prep. a, b).

Cruises which have encountered warm-core rings in the South Atlantic and near the retroflection are summarized in Table 2i. The positions of the rings are shown on Figure 2.5. Circles on the figure indicate the radii of rings from Table 2ii.

From satellite thermal infra-red data, Lutjeharms (1981a) demonstrated the instability of the Agulhas retroflection and that it could form rings (Lutjeharms 1981b). Rings were found hydrographically near the retroflection before their true nature was realized. Duncan (1968) detected a large ring, almost certainly from the Agulhas retroflection, but was in some doubt as to the mechanism responsible for it. He raised the possibility that the explanation of the rings lay in the dynamics of the Agulhas Current stating (p. 532) that "The eddy may have been caused by the Agulhas Current impinging on the West Wind Drift or by inherent instability in the Agulhas Current once it departed from the continental slope....". The station spacing on the cruise discussed by Duncan was too great to fully characterize the ring.

A major three-ship survey of the Agulhas Current in March 1969 (Bang 1970a, 1970b, Harris and Van Foreest 1978) showed the inherent generative nature of the retroflection and that the terminal region was populated by a range of eddies. Bang (1970a) suggested that these eddies might move into the South Atlantic. He stated (p. 73) "... the resultant intrusions are probably best represented as *tongues** of warmer water thrusting into the South Atlantic. It is likely nevertheless that some geostrophic component exists so that, should the tongues separate to form individual patches of Agulhas water, some rotation may be expected.". Noting that these patches of warm water had not been detected north of 32°S, Bang failed to recognise their

* Bang's italics

importance. He goes on (p. 74) "It must thus be assumed that such patches rapidly lose their dynamic integrity and are dissipated by spreading and mixing."

Harris and Van Foreest (1978), who presented the vertical sections from the cruises, showed that Bang's "patch" was a deep-reaching eddy. This eddy had the characteristics of an Agulhas ring and appeared in nearly the same position as the various "Cape Town eddies" described below, which occur with regularity in this position (Lutjeharms and Valentine 1988b). Other rings were later encountered close to or just spawning from the retroflection.

The first in-depth hydrographical study of rings undertaken at the Agulhas retroflection was the Agulhas Retroflection Cruise (ARC) in November 1983 (Camp *et al.* 1986, Gordon *et al.* 1987b). Three vessels (R.V. *Knorr*, M.V. *S.A. Agulhas* and R.V. *Meiring Naudè*) surveyed the Agulhas Current system from the Transkei coast to west of Cape Town. Two recently spawned rings were detected, the Cape Town and Retroflection eddies (Olson and Evans 1986).

Another warm-core anticyclonic ring was encountered south-west of Cape Town on a survey undertaken on R.V. *Thomas Washington* during 1985 (Bennett 1988). A third large-scale study, the Subtropical Convergence and Agulhas Retroflection Cruise (SCARC) during February 1987, found at least five rings in the retroflection area whose isothermal depressions suggested that they were from the Agulhas and not spun up from the mid-ocean gyres or the Subtropical Front (Lutjeharms 1987, Valentine *et al.* 1988). Upper-layer sections from this cruise were presented by Shannon *et al.* (1989a).

In the South Atlantic, the detection by hydrographic measurements of rings from the retroflection has been rare. In 1983 a cruise of *Oceanus* crossed an Agulhas ring in mid-Atlantic (McCartney and Woodgate-Jones 1991), confirming the estimated range and track of these rings. In 1987 a cruise of *Discovery* also crossed a ring (Gordon and Haxby 1990) in the same area as a later cruise of F.R.S. *Africana*. On the *Africana* cruise in 1989, a ring was encountered near Vema Seamount and this discovery led to a second cruise, on R.S. *Benguela*, to examine the same ring a month later (Duncombe Rae *et al.* 1989b, Duncombe Rae *et*

al. 1992b). These cruises represent the only intensive full-scale hydrographic examination of a ring within the South Atlantic, away from the immediate vicinity of the retroflection. Other hydrographic measurements have consisted of only one line of conductivity-temperature-depth probe (CTD) or expendable bathythermograph (XBT) data through each ring. The data collected from the Vema ring consisted of two cruises of hydrographic measurements, NOAA satellite sea-surface temperatures and GEOSAT altimetry. A recent South Atlantic Ventilation Experiment cruise (SAVE-4) crossed two Agulhas rings in January 1990 (Gordon *et al.* 1992). The westernmost, R90.1 (Table 2i; Fig. 2.5), could possibly have been the Vema ring (R89.1) examined by R.S. *Benguela* delayed by the Walvis Ridge, because the estimated time of shedding of both rings was the end of 1988.

A cruise of F.R.S. *Africana* in August 1990, examined hydrographically, for the first time, a ring shed from the Agulhas during winter (the Winter ring; Duncombe Rae and Shillington in prep.). This study unfortunately only led to one comprehensive set of hydrographic measurements and a later attempt to seed the ring with a satellite-tracked drifter failed.

During the deployment cruise of the Benguela Sources and Transports (BEST-1) programme, in June 1992, an Agulhas ring was encountered, centred mid-way along a line of inverted echo sounders deployed south-west of Cape Town. This ring, in approximately the same position as the Cape Town eddy and Winter ring, was surveyed with CTD and XBT measurements.

Very recently (January 1993) a German WOCE cruise on F.S. *Meteor*, along line 30°S (WOCE line A10) crossed a ring with Agulhas water characteristics at 3°W (pers. obs.).

2.5.2 FORMATION

The process of ring-separation from the retroflection was documented by Lutjeharms and Van Ballegooyen (1988a) from METEOSAT imagery (Fig. 2.6). Within each event, westward penetrations of the retroflection showed an increasing rate of progress with time, followed by what appears in the satellite imagery to be a sudden discontinuous eastward jump, accompanied by the flow of Subantarctic or South Atlantic water

into the gap. This sequence of events was related directly to the shedding of an Agulhas ring. Ring shedding was observed at sea during the Agulhas Retroflection Cruise (Lutjeharms and Gordon 1987). The process is similar to that undergone during the shedding of Brazil Current eddies. Legeckis and Gordon (1982) identified three mechanisms for formation of Brazil Current eddies: formation from meanders in the current (like the Gulf Stream); pinching off of a loop of the Brazil Current extension; and wave instabilities in the western boundary of the current. The Agulhas Current shows all these eddy generation mechanisms (Lutjeharms 1981a). Agulhas ring shedding from the retroflection corresponds to the second type.

Subantarctic surface water has been shown by Shannon *et al.* (1989a) to penetrate the Subtropical Front and enter the South Atlantic. On that occasion the influx persisted for some months. Gordon *et al.* (1992) cites this process as one of the source inputs of the Benguela Current.

Estimates of the formation rate of Agulhas rings vary. From studies of METEOSAT images, over a three-year period of observation, Lutjeharms and Van Ballegooyen (1988a) detected approximately nine ring-shedding events per year, on average every 39 days. Feron *et al.* (1992) found eighteen pulses, corresponding to six ring-shedding events per year, from principal component and harmonic analysis of 150 weeks of GEOSAT altimeter data. Byrne (1993) also estimated 6 rings shed per year from GEOSAT observations in the South Atlantic. Gordon and Haxby (1990) estimated, from ring translation speeds in the South Atlantic determined by GEOSAT altimetry, that five rings per year enter the South Atlantic from the retroflection.

Boudra and De Ruijter's (1986) and Boudra and Chassignet's (1988) multi-layer modelling studies of the wind-driven South Atlantic/Indian Ocean circulation and Agulhas retroflection region showed the formation of rings at the retroflection. Chassignet and Boudra (1988) concluded that, in the model domain, a weak mixed barotropic/baroclinic instability was associated with ring-formation. Experiments in which rings formed showed a greater transfer of mean kinetic to eddy kinetic energy than cases where rings were not formed. The instability required for ring-formation depended on the shape of the Agulhas Bank shelf-break. Increasing inertia in the model reduced the number of

rings formed. Boudra *et al.* (1989) consolidated and refined these models further but obtained results not significantly different from those outlined above.

2.5.3 LIFE HISTORY

Once an Agulhas ring has been shed from the retroflection, it moves into the South Atlantic. Depending on the position of the shedding event, some of these rings may move southwards to be returned to the Indian Ocean by the Antarctic Circumpolar Current. Satellite altimetric maps of the sea surface height (SEASAT: Cheney *et al.* 1983; GEOSAT: Sandwell and Zhang 1989, Chelton *et al.* 1990, Gordon and Haxby 1990, Shum *et al.* 1990, Wakker *et al.* 1990b) show the region of variability associated with the Agulhas retroflection (>30 $cm.s^{-1}$ r.m.s. geostrophic velocity: Gordon and Haxby 1990) to extend north-west into the South Atlantic (>10 $cm.s^{-1}$ r.m.s. geostrophic velocity: Gordon and Haxby 1990), indicating the track of rings and eddies separated from the Agulhas retroflection (Fig. 2.7). The region of strong variability also extends into the West Indian Ocean, indicating the path of the Agulhas Return Current and instabilities in the Subtropical Front.

Individual rings tracked by GEOSAT altimetry (Fig. 2.8) confirm the drift of the rings to the north-west (Gordon and Haxby 1990, Duncombe Rae *et al.* 1992b, Wakker *et al.* 1990a). Tracks of seven selected eddies from GEOSAT data (Fig. 2.7) show drift rates of 5 to 8 $cm.s^{-1}$ (Gordon and Haxby 1990). A total of 11 eddies could be seen in the GEOSAT data from the South Atlantic for the period November 1986 to November 1987 (Gordon and Haxby 1990), while 13 large eddies were observed in the altimeter data for July 1987 to July 1988 (Wakker *et al.* 1990a).

Once the rings have crossed the Cape Basin under the influence of the Benguela Current, they are stalled for a time by the Walvis Ridge (see Fig. 2.2), before moving westwards again. The family of features in the GEOSAT images can be traced into the western South Atlantic between 20° and 30°S reaching to at least 30°W in two to three years. Byrne (1993) found that almost all of approximately 30 Agulhas rings identified in GEOSAT altimeter data propagated westwards across the Atlantic between 25°S and 35°S. Gordon and Haxby (1990) suggest that the rings are absorbed by the Brazil Current, thereby joining the

circulation of the South Atlantic gyre and eventually contributing to the flow across the equator to balance the production of North Atlantic Deep Water.

The lifetimes of Agulhas rings appears to conform to those of other western boundary currents. McCartney and Woodgate-Jones (1991) estimated an age of 2.2 years for the Agulhas ring at 23°S, 5°W. Byrne's (1993) study suggests a lifetime of 3.5 to 4 years before the rings reach the Brazil Current. Nilsson and Cresswell (1981) obtained an average lifetime of 650 days for rings from the East Australian Current. Lai and Richardson (1977) also obtained lifespans of the order of 650 days for Gulf Stream rings, and The Ring Group (1981) estimated values of up to four years for the same rings.

2.5.4 ANATOMY

Data obtained for some of the rings in Table 2i are shown in Table 2ii. Depression of the 10° isotherm for most of these rings is around 300-400 m (e.g. the Vema ring, Fig. 2.9). The two anomalous rings, R90.4 (the Winter ring; Fig. 2.10) and R87.1 (SCARC ring Susan), have isotherm depressions of 510 and 145 m respectively. On the other hand, rings with a more westerly motion, being further south and closer to subantarctic water (R83.2 [ARC Cape Town] and R87.4 [SCARC Erina]) also show large isotherm depressions. R87.1 (SCARC Susan) is very close to the continental shelf, possibly accounting for the small isotherm depression. However, R87.5 (SCARC Helen), very far south, does not show excessive isothermal depression. This is possibly due to the line of data not bisecting the ring.

In comparison with other current systems such as the Brazil Current and Kuroshio Agulhas eddies are larger in size: Kuroshio eddies are typically 150 km in diameter (Kitano 1975); and Brazil eddies also about 150 km in diameter (Legeckis and Gordon 1982). Gulf Stream rings are closer in size to Agulhas rings, extending 200-300 km in diameter (Richardson 1983). Greater vertical mixing within the rings has been observed in systems' other than the Agulhas. Gulf Stream and Kuroshio rings have been observed with mixed layers up to 500 m thick; Agulhas rings only to 320 m.

2.5.4.1 Water Transport

An account of the kinematics of trapping a body of water within a ring is given by McCartney and Woodgate-Jones (1991) and is summarized briefly here. Flierl (1981) calculates two types of paths followed by fluid particles as an eddy moves through a region: closed loops representing particles trapped in and moving with the eddy; and meanders corresponding to a wave-like disturbance induced by the passage of the eddy. A non-dimensional parameter ϵ, the ratio of the maximum azimuthal speed at a depth to the eddy drift speed, determines whether a trapped region exists at the given depth.

For depths when the maximum azimuthal speed is less than the eddy drift speed there is no trapped region in the eddy and only the induced disturbance occurs. Although a net transport of the fluid particles is experienced, the particles are eventually left behind by the eddy. For depths where the maximum azimuthal speed is greater than the drift speed, the trapped region is a teardrop shape centred equatorward of the (anti-cyclonic warm-core) eddy centre which moves along with the eddy at the eddy drift speed. For eddies of the size and translational speeds of those detected by Olson and Evans (1986) and Gordon and Haxby (1990), McCartney and Woodgate-Jones (1991) calculate trapped depths between 1100 m (for slow drift speeds) and 670 m (for faster drift speeds). Therefore, although the expression of Agulhas rings (e.g. depressed isotherms) extends throughout the water column (>4000 m; Gordon and Haxby 1990), only the upper water masses (i.e. Intermediate, Central and Surface waters) may be expected to be translated with the ring as it moves.

An alternative interpretation of how fluid is trapped within an eddy is provided by, for example, Kamenkovitch *et al.* (1986, p. 221). A cyclonic ring with the distributions of potential vorticity and potential density indicated is shown in Figure 2.11. The situation would be similar for an anticyclonic eddy. For mixing to take place between the core and the surroundings of the eddy, a fluid parcel must move along isopycnals. Conservation of potential vorticity implies that this fluid parcel must maintain a constant potential vorticity. From the figure, it is clear that the fluid would be blocked in its path along isopycnals by the lobes of high vorticity at the ring edges.

2.5.4.2 Water Masses

Table 2iii, compiled from Bennett (1988), shows some of the extreme parameter values and the water types associated with the major water masses of interest in the South Atlantic and South Indian Oceans. Valentine (Valentine 1990, Valentine *et al.* 1993), in a fine-scale volumetric census of the Agulhas retroflection region, recognised the following water masses and their characteristics (shown in Table 2iv): Surface Water, Central Water, Antarctic Intermediate Water, two types of deep water: North Atlantic and Circumpolar, and Antarctic Bottom Water. The origin and characteristics of the upper water masses are discussed briefly here.

Antarctic Intermediate Water is formed near the surface in the Antarctic regions between the Antarctic Polar Front and the Subantarctic Front where precipitation is high. The cold, relatively fresh Subantarctic Surface Water sinks and spreads northward (Sverdrup *et al.* 1942). The newly-formed Intermediate water circulates through the Indian Ocean as a salinity-minimum layer between the Central Water thermocline and the Deep Water salinity maximum. It enters the retroflection area through the Agulhas Current after the occasional addition of Red Sea Water of high salinity (Duncan 1970, Gründlingh 1985). The occurrence of Antarctic Intermediate Water around South Africa has been reviewed by Shannon and Hunter (1988).

The Central Water of the Agulhas retroflection is the South Indian Central Water, which occupies the entire South Indian thermocline and includes the Subtropical and the Subantarctic mode waters (Schmitt 1981, Bennett 1988). Mode waters are formed at the sea surface during winter overturning, and are capped during spring by surface warming of the upper layer, allowing them to enter the thermocline (McCartney 1977). Mode waters appear as anomalously thick isopycnal layers with weak stratification, and are associated with oxygen maxima and relative vorticity minima.

During winter, convective overturning north of the Antarctic Circumpolar Current in the Subantarctic zone creates Subantarctic Mode Water in the south-western Atlantic and southern Indian Oceans. This water moves northwards generating a thick, nearly isopycnal layer forming part of the Central Water thermocline (McCartney 1977,

McCartney 1982, Georgi 1979). The results of Piola and Georgi (1982) imply that only a small quantity of Subantarctic Mode Water is generated in the South Atlantic. The Subantarctic Mode Water present in the Agulhas system originates in the south-western Indian Ocean.

The surface water of the retroflection is formed in the South Indian Subtropical gyre. Within the Agulhas Current and the retroflection the freshwater and heat flux from the sea surface to the atmosphere exceeds that of any other region in the southern hemisphere (Höflich 1984, Olson *et al.* 1992). This air-sea exchange is responsible for an increased salinity and convective overturning which creates a mode water different from South Indian Subtropical Mode Water, closer in characteristics to the South Atlantic Surface water (Olson *et al.* 1992).

By using chlorofluoromethane and hydrographic data, Fine *et al.* (1988) showed that the Agulhas retroflection is responsible for mixing of South Atlantic and Indian Intermediate and Central waters. It is therefore likely that Agulhas rings shed from the retroflection are also not pure Indian water, but some admixture of Indian and Atlantic water. This is also evident in the upper layers. Chapman *et al.* (1987), using upper layer nutrient and oxygen data, obtained ratios of 56% and 58% (±10%) Agulhas water in the northern (Cape Town) eddy of the Agulhas Retroflection Cruise (ARC) at 200 and 100 m respectively.

2.5.4.3 Energetics

Rings formed at the retroflection rapidly lose their heat to the atmosphere in the South Atlantic. This rapid heat loss drives deep convective overturning and causes the generation of deep isothermal surface layers, particularly during winter (Fig. 2.10; Duncombe Rae and Shillington in prep.). The loss of heat to the atmosphere diminishes the amount of heat transferred by the rings to the South Atlantic (Olson *et al.* 1992).

The ability of a ring to stir the fluid around it as it passes depends on the energy imparted in its formation, which is steadily eroded by dissipative processes. After its formation the instantaneous ability of the ring to affect its surroundings is determined by the conversion of available potential energy (APE) in the initial mass field to

kinetic energy in the flow around the ring (Olson *et al.* 1985). The APE and kinetic energy for some of these Agulhas rings have been calculated. The APE ranges from 26.2 to 51.4×10^{15} J. The Winter ring is anomalous, having a much smaller APE than the others, possibly due to its smaller diameter. Kinetic energies range from 2.3 to 8.7×10^{15} J. Comparison of Agulhas rings to other western boundary current rings shows that they are the most energetic encountered in the World Ocean (Olson and Evans 1986).

2.5.5 INTERBASIN TRANSFER

In currents like the Gulf Stream, warm- and cold-core rings exchange water across the current into cold and warm environments respectively (Olson 1991). In the case of the Agulhas Rings in the South Atlantic, warm water pinches off from the Agulhas retroflection and moves towards the centre of the South Atlantic gyre, where warm water also resides.

Gordon and Haxby (1990) calculated a volume flux per ring of 2 to 3×10^6 $m^3.s^{-1}$ of water above the Antarctic Intermediate Water layer. They postulate that this does represent an input of heat and salt into the cool eastern arm of the South Atlantic gyre and will become incorporated into the gyre.

Bennett (1988) uses the 1985 data to obtain values of the heat flux westward across the retroflection region. ".... a steady upper level ($z < 2000$ m) heat flux of between -0.029 and -0.22 PW* (westward) is associated with westward upper-layer transport of 12 ± 8 Sv# inshore of the Agulhas water-mass boundary and an eastward return transport on the south side of the Return Current. Westward heat flux increases by -0.019 PW for every Sv diverted from this upper-level exchange into overturning exchange between upper-level water and NADW$." (Bennett 1988, p. 133). She also found that exchange with the atmosphere could only account for 50% of the westward heat flux implying that "the steady upper-level heat flux must be balanced by more remote heat sinks" (Bennett 1988, p. 129).

---

* 1 PW = 1 Petawatt = 10^{15} W
\# 1 Sv = 1 Sverdrup = 10^6 $m^3.s^{-1}$
$ North Atlantic Deep Water

In the upper layers of the South Atlantic Ocean, there is a net northward transport across the equator. Sverdrup *et al.* (1942) estimated the cross-equatorial surface flow as 6×10^{6} $m^{3}.s^{-1}$ together with 2×10^{6} $m^{3}.s^{-1}$ of Intermediate Water and 1×10^{6} $m^{3}.s^{-1}$ of Bottom Water, compensating a southward transport of 9×10^{6} $m^{3}.s^{-1}$ of Deep Water. This is comparable to Roemmich (1983) who obtained a net northward upper-layer transport of 10×10^{6} $m^{3}.s^{-1}$.

For the Vema ring, R89.1, Duncombe Rae *et al.* (1989b) calculated an excess heat content of the ring relative to the surrounding South Atlantic of 7.8×10^{20} J over the upper 750 m. This gave a heat energy flux of 0.2×10^{15} W. The volume flux of the Vema ring was 13×10^{6} $m^{3}.s^{-1}$ and the salt flux 2×10^{13} kg (Duncombe Rae *et al.* 1989b).

Agulhas input to the South Atlantic at the retroflection can also occur via intermittent direct flow (Gordon 1985). Gordon *et al.* (1992) have argued that the thermoclines of the South Indian and South Atlantic are linked, with the South Atlantic Current (cf. Stramma and Peterson 1990) flowing into the Indian Ocean.

2.5.6 LOCAL EFFECTS OF AGULHAS RINGS

In addition to their possible importance to global climate the Agulhas rings have a far more obvious local effect. In crossing the South Atlantic, they will leave behind a trail of mixed and stirred water and the frictional energy transfer will heighten the background energy field of the ocean basin while ageing and spinning down the ring. If a ring moves more northwards than westwards from the retroflection, possibly steered by the topography of the West Coast shelf, it will likely come into contact with or affect the Benguela upwelling system which supports the fishing industries of Namibia and South Africa. This interaction (Fig. 2.12) has been demonstrated by Duncombe Rae and Shillington and others (Duncombe Rae *et al.* 1989b, Lutjeharms *et al.* 1991, Duncombe Rae *et al.* 1992b).

Filaments from the Benguela Upwelling Front may be formed in a similar manner to those off the California coast (Brink 1992, Shillington *et al.* 1992) in which the filament is a meander of the frontal current. Surface current vectors shown by Agenbag (1992) indicate that the filament observed by Duncombe Rae *et al.* (1992b) was supplied by water

from the front. In this way the ring may "capture" the frontal jet and remove eggs, larvae, or juvenile fish which are being carried by it. This removal may have a serious detrimental effect on certain fisheries (e.g. anchovy: Duncombe Rae *et al.* 1992a). The volume of water entrained by a passing Agulhas ring during an interaction of this nature may be large. Duncombe Rae *et al.* (1992b) suggest that a volume equivalent to a strip of water 100 m deep, 50 km wide and 1000 km long could be extracted from the upwelling system in the space of 1½ months (a rate of 1.3×10^{6} $m^{3}.s^{-1}$). The rings may also provide a transport mechanism for the distribution of biotic material around the ocean basin.

Eddies in conjunction with the Benguela Upwelling frontal system have been observed previously (Kaz'min and Sutyrin 1990, Kaz'min *et al.* 1990, Shillington *et al.* 1990). It is unlikely that these features were retroflection rings (as suggested by Shillington *et al.* 1990) since they are too small and not very deep (e.g. 90 km radius, 11° isotherm at 250 m: Kaz'min and Sutyrin 1990).

High rates of surface cooling in new rings destroy the surface expressions (Lutjeharms and Gordon 1987, Walker and Mey 1988). Olson and Evans (1986) show that heat is quickly lost to the atmosphere, leaving the salt. These additional sources of heat to the lower atmosphere may influence passing weather systems affecting the climate of South Africa (Walker 1990).

Source: DUNCOMBE RAE, C.M. 1991 - Agulhas retroflection rings in the South Atlantic Ocean: an overview. *S. Afr. J. mar. Sci.* 11: 327-344.

CHAPTER 3: DATA COLLECTION, THEORY AND METHODS

This thesis presents an analysis of data collected by the author on several research cruises in the South Atlantic Ocean. This chapter describes briefly the methods of data collection and processing used on each cruise, the details of which are fully presented in unpublished reports (Duncombe Rae *et al.* 1989a, Duncombe Rae and Shillington 1989). The theoretical background and methods used for calculating the geostrophic velocities and transports, the available potential energy and kinetic energy, and the heat and salt anomalies are presented here. The theory of mesoscale ocean eddies is treated fully by Kamenkovitch *et al.* (1986), Robinson (1983) and Gill (1982). For the development of the layer model and the calculation of the kinetic and available potential energies contained in Agulhas rings I have followed e.g. Olson *et al.* (1985) and Reid *et al.* (1981).

3.1 HYDROGRAPHIC DATA

The principal vessel used was the F.R.S. *Africana* (V071 - Walvis Ridge Cruise; V080 - Antarctic/Chile Cruise; V085 - Winter Ring Cruise; V105 - BEST-1 Deployment Cruise). R.S. *Benguela* was used on one cruise (V246 - Vema Ring Cruise). Some data from the Agulhas Bank Boundary Processes Cruise (F.R.S. *Africana* V099) are used for comparison of the rings' water masses with Agulhas Current water. Cruise tracks are shown in Figure 4.1.

3.1.1 DATA COLLECTION

In general the recommendations of SCOR Working Group 51 (UNESCO 1988) were followed in the data acquisition and processing.

3.1.1.1 *Africana* Voyage 071

Temperature and salinity profiles of the water column throughout the cruise were determined using a Neil Brown Instruments Systems Mk III Conductivity Temperature Depth probe (CTD). Temperature profiles were obtained with Sippican T5 and T7 expendable bathythermograph (XBT) probes. Water samples through the water column for chemical and chlorophyll-a analysis were collected using 8-litre Niskin-type bottles on a 24-bottle Hydro-Bios Rosette Sampler. Only the XBT and CTD temperature profiles from this cruise were used for the thesis.

3.1.1.2 *Benquela* Voyage 246

A Mark III Neil Brown CTD was deployed at a descent rate of 1 $m.s^{-1}$, with a data value stored once per metre, down to the safe deployment length of the cable, effectively about 1200 m depth. Temperature profiles were obtained with Sippican T7 XBT probes. Water samples for chemical analysis were taken at nominal depths of 0, 50, 100, 200, 250, 300, 500, 750, 1000 and 1200 m on the up-cast using 2-litre Niskin-type bottles on a 10-bottle rosette sampler. Results of the oxygen determinations were not consistent and most results were discarded.

3.1.1.3 *Africana* Voyage 080

The data used from this cruise were from XBT data only, from two sections across the Cape Basin. Profiles were taken with Sippican T7 XBT probes at 2 hour intervals, nominally 40 km spacing.

3.1.1.4 *Africana* Voyage 085

For temperature and salinity profiles an IG&G Mk V CTD was deployed at 1 $m.s^{-1}$. The entire data stream from the Mk V CTD was stored for analysis. Samples for chemical analysis were taken through the water column using 5-litre Niskin-type bottles on a 12-bottle rosette sampler on the up-cast. Intermediate temperature profiles were obtained using Sippican T7 XBT probes.

3.1.1.5 *Africana* Voyage 105

This cruise was undertaken when the thesis was in an advanced stage of preparation and results are presented only for completeness in the tables comparing properties of the rings encountered. A Neil Brown Mk III CTD probe was used in obtaining temperature and salinity profiles of the water column. The entire data stream was stored for analysis. Most CTD casts on this cruise were taken to within 50 m of the bottom with the exception of four profiles between the edge and centre of the ring encountered. These latter profiles were taken to 1500 m. Sippican T7 probes were used to obtain intermediate temperature profiles. Water samples for salinity, oxygen, nutrient and alkalinity determinations were obtained on the up-cast with 5-litre Niskin-type bottles on a 12-bottle rosette sampler.

3.1.2 DATA PROCESSING

3.1.2.1 CTD Data

3.1.2.1.1 Recording

Data were recorded from the digital output of the CTD deck unit onto $5\frac{1}{4}$" magnetic media (360 kilobyte diskette) as records of four 6-byte real numbers using an IBM compatible XT. For the Mk III CTDs (with the exception of V105) the software scanned the incoming data selecting the data from integral units of pressure, in most cases every metre. On deeper casts (3000 m and 5000 m) the data were recorded at 2 or 3 metre intervals. For the Mk V probe and the Mk III probe on V105 the entire data stream was recorded, approximately 32 frames per second, on the hard-disk and archived to the diskette for transfer to the laboratory. Some preliminary processing was done at sea but the entire data set was used for the final data correction and filtering done ashore after the cruise.

3.1.2.1.2 Data Reduction

Obvious data spikes and spurious readings near the surface and bottom were edited interactively. The data were then filtered using a seven-point median filter passed once forward through the data. Discarded readings were not replaced, and were compensated for where necessary in later processing by linear interpolation. The data were not further reduced. For the Mk V probe and V105 data a five point median filter was passed twice forward through the data. Discarded readings were replaced by interpolation to maintain the time base. Due to different response times for the conductivity and temperature sensors, the data from these sensors potentially represent different parts of the water column. The data were lagged to synchronise the sensors and pressure reversals were removed during this step. A final median filter in which discarded data were not replaced reduced the data to approximately 1 metre intervals.

3.1.2.1.3 Sensors and Calibration

The temperature, conductivity and pressure sensors were calibrated before the cruise in the laboratory against a Hewlett-Packard Quartz thermometer, IOS Standard Seawater and a Budenberg Dead Weight Tester respectively. Corrected data for the North Atlantic Deep and Antarctic Bottom Water from the deeper stations were checked and found consistent with the results of the AJAX expedition (Anon. 1985) and with the South

Atlantic IGY data (Fuglister 1960) within the limits of error in the data.

3.1.2.1.4 Calculations

The various densities required were calculated from the algorithms presented by Millero *et al.* (1980) and Millero and Poisson (1981). With the exception of *Benguela* V243, salinity values were calculated using the Practical Salinity Scale 1978 (UNESCO 1983, 1988) at the appropriate time during the data editing and filtering process (UNESCO 1988). On *Benguela* V243, due to limitations in the software available, salinity values were calculated during the data recording process using a pre-Practical Salinity Scale 1978 (PSS-78) algorithm, that of Brown and Allentoft (1966; referenced in Brown and Morrison 1978) and Bradshaw and Schleicher (1965). This algorithm uses the International Practical Temperature Scale, 1948 (IPTS-48). The probe provided temperatures in accordance with IPTS-68, which were converted back to 1948 IPTS values by the data capture software to use the Brown and Allentoft salinity algorithm. After the cruise the results of Lewis and Perkin (1981) were used to adjust the salinity data to PSS-78.

3.1.2.2 XBT Data

Thermal traces through the water column were obtained using Sippican T5 and T7 XBT probes. Data were recorded from the XBT deck unit onto $5\frac{1}{4}$" magnetic media (360 kilobyte diskette) as 2-byte integers in records of 11 integers per record, at a rate of 1 record per second, using an IBM compatible XT. This gave a data density of approximately 2 readings per metre. The same deck unit was used on all cruises. Calculations, filtering and data reduction were done in the laboratory after each cruise. Data from the underway thermosalinograph and surface values from CTD casts were used to check the temperature calibration of the XBT probes. A seven-point median filter was passed once forward through the data. No further data reduction was done.

3.1.2.3 Bottle Data

Determination of oxygen concentration was done by Winkler titration while at sea, immediately after hydrographic sampling on all cruises. Chemical analyses for the micronutrient ions silicate, nitrate+nitrite and phosphate were done using a Technicon AutoAnalyzer system following the methods of Mostert (1983, 1988). On *Africana* V071 analyses were

done at sea, within three to four hours of sampling. A comparison with AJAX data (Anon. 1985) showed good agreement (to better than 2% in the deep water). On other cruises samples were collected and stored frozen at -18°C for analysis ashore.

3.2 REMOTE SENSING DATA

Details of the processing of the remote sensing data presented are not strictly relevant to this thesis. They are fully described by Agenbag (1992) and Taunton-Clark (1993). A brief outline of the processing is presented here for completeness.

3.2.1 NOAA IMAGERY

Images from NOAA data were transformed to Mercator projection using an ARIES II image processing system and software developed for this purpose by the Sea Fisheries Research Institute (Agenbag 1992). The surface circulation pattern was then constructed by manual tracking of small-scale thermal features in two images approximately 24 hours apart (Agenbag and Shannon 1988).

3.2.2 GEOSAT ALTIMETRY

GEOSAT altimeter data were processed using the Satellite Altimetry Data System (SADS) software developed by the Division for Earth, Marine and Atmospheric Technology (EMATEK) of the CSIR at Stellenbosch (Lewis 1990a,b,c and Lewis and St. Ange, 1990). The one-second along-track averages of sea height from the geophysical data records (GDR) received from the National Oceanic and Atmospheric Administration (NOAA, USA) were corrected for tidal and atmospheric effects using values supplied with the GDRs. Spurious data were edited following rejection criteria similar to those employed by Wakker *et al.* (1990a).

The collinear option in SADS was used in which the sea height variability along a ground track is studied and the mean sea surface elevation profile for a track or pass (repeated every 17 days) is computed. This mean profile approximates to the marine geoid. The approximate geoid was subtracted from the individual passes, leaving residual height profiles which contain details of the mesoscale ocean circulation.

To fill in data gaps and obtain a less temporally smeared horizontal picture, data from several passes over seven-day periods were interpolated and contoured, giving seven-day 'snapshot' pictures. While giving a better temporal representation than contouring over the full 17-day cycle the results of these snapshots were still not totally satisfactory and could give only a qualitative indication of the features present.

3.3 GEOSTROPHIC VELOCITIES

For the calculation of relative geostrophic velocities between stations where the vertical density structure was known (i.e. CTD stations) discrete versions of the geostrophic balance equations (Gill 1982, pp. 215-216) were used directly:

$$-f\,(\vec{v}_{p1} - \vec{v}_{p2}) = \frac{\partial}{\partial r}(\Phi_{p1} - \Phi_{p2}) \qquad [1]$$

where f is the coriolis parameter, v the relative velocity and Φ the geopotential, at pressure levels p_1 and p_2, and $\partial/\partial r$ indicates the change (in geopotential) over the distance r.

To enable the use of the large amount of vertical temperature data obtained from XBTs, and to estimate the energy content of the rings, a two-layer model (e.g. Gill 1982) of the rings was assumed. A discussion of this model as applied in the thesis follows.

3.3.1 THEORETICAL BACKGROUND

The equation of motion of an inviscid fluid is

$$\frac{\partial \mathbf{u}}{\partial t} + (\mathbf{u}\cdot\nabla)\mathbf{u} + 2\boldsymbol{\Omega}\times\mathbf{u} = -\frac{1}{\varrho}\nabla p - \boldsymbol{g} \qquad [2]$$

where u is the velocity vector, ∇ is the gradient operator, Ω is the angular velocity vector, p is the pressure, ϱ the density and g the acceleration due to gravity (Gill 1982).

In a cylindrical coordinate system, Eqn. [2] can be expanded to:

$$\frac{\partial u}{\partial t} + u\frac{\partial u}{\partial r} - \frac{v^2}{r} + \frac{v}{r}\frac{\partial u}{\partial \theta} + w\frac{\partial u}{\partial z} = -\frac{1}{\varrho}\frac{\partial p}{\partial r} + fv \qquad [3]$$

$$\frac{\partial v}{\partial t} + \frac{vu}{r} + u\frac{\partial v}{\partial r} + \frac{v}{r}\frac{\partial v}{\partial \theta} + w\frac{\partial v}{\partial z} = -\frac{1}{\varrho r}\frac{\partial p}{\partial \theta} - fu \qquad [4]$$

$$\frac{\partial w}{\partial t} + u\frac{\partial w}{\partial r} + \frac{v}{r}\frac{\partial w}{\partial \theta} + w\frac{\partial w}{\partial z} = -\frac{1}{\varrho}\frac{\partial p}{\partial z} - g \qquad [5]$$

where u, v and w are the radial (r), azimuthal (θ), and vertical (z) components of the velocity respectively, p is the pressure, ϱ is the density and f the coriolis parameter (Chassignet *et al.* 1990). If the ring is perfectly symmetric, u = const = 0 and Eqn. [3] reduces to

$$\frac{v^2}{r} + fv = \frac{1}{\varrho}\frac{\partial p}{\partial r} = fv_g \qquad [6]$$

where v_g is the total geostrophic velocity. If the ring is asymmetric and/or evolving with time then the other terms in Eqns. [3] and [4] might start to play a significant role.

The two-layer model is used and applied to the ring. The two-layer model (e.g. Gill 1982) is based on two layers of fluids of different densities $\varrho_1 < \varrho_2$. Differences in level (h) in the surface of the lower layer are adjusted by a reduced pressure $\delta p = (\varrho_2-\varrho_1)gh$. Adjustment processes are then the same as if a reduced gravity $g' = g(\varrho_2-\varrho_1)/\varrho_2$ were acting. For the system under consideration, i.e. Agulhas rings, the thermocline is used as an interface between the upper and lower layers and the pressure field created by the deformation of the thermocline is $p = \varrho g'h$, where h is the depth of an isotherm indicative of the thermocline.

Then the gradient velocity balance, Eqn. [6], becomes

$$\frac{v^2}{r} + fv = g'\frac{\partial h}{\partial r} \qquad [8]$$

Boundary conditions that $v = 0$ when $r = 0$ and $h = h_\infty$ when $r \to \infty$ are applied.

3.3.2 GEOSTROPHIC CALCULATIONS

The velocity field of rings is composed of both barotropic and baroclinic components. Assuming that the rings are in geostrophic balance the baroclinic component of the velocity field can be calculated from the two-layer model giving an indication of the volume transport associated with the ring. In applying the model, g' is obtained by empirically fitting the depth of the isotherm to the dynamic height field in the ring. Following Olson *et al.* (1985) and Olson and Evans (1986), the regression of the depth of even-numbered isotherms (8°, 10°, 12°, 14°C) with the geopotential anomaly (GPA) relative to 1150 db, the deepest CTD data available for all stations, was plotted for the *Benguela* V246 data. The depth of the 10°C isotherm (h_{10}) gave the best fit ($r^2 = 0.982$) so that the GPA (D_{1150}) could be estimated from the relation

$$D_{1150} = 0.01513\ h_{10} + 7.7585.$$

Using Olson *et al.*'s two-layer model with g' = 0.01513 (standard error in g' of ± 0.0005) to obtain GPAs from the XBT traces the surface geostrophic velocities could be calculated from both the CTD and XBT data. In spite of the good correlation between the depth of the isotherm and the GPA, the velocity distribution shows greater horizontal shear than one would expect from the distribution obtained from the CTD traces alone. This reflects the greater detail evident in the temperature, and hence density, structure revealed by the XBT data.

For the entire Cape Basin, all cruise data were combined to determine the relationship between the GPA relative to 1100 db and the 10°C isotherm. This relationship is shown in Figure 3.1. The regression is

$$D_{1100} = 0.00972\ h_{10} + 10.271$$

($r^2 = 0.925$; n = 105).

3.4 POTENTIAL AND KINETIC ENERGY CALCULATIONS

Reid *et al.* (1981) give a broad definition of the available potential energy as the difference between the total potential energy for the sample and that state of the same fluid which could exist in the same basin after an isentropic readjustment to a stable hydrostatic

reference state (denoted by subscript r) in which isosteric and isobaric surfaces are level. This treatment of the energetics of rings is restricted to the baroclinic field.

The available potential energy (APE) is not the purely gravitational potential energy. It includes the elastic part of the internal energy which must also be considered. This elastic energy accounts for up to 20% of the APE (Reid *et al.* 1981). In the ocean the contribution of the elastic internal energy is negative, i.e. its contribution reduces the APE. The correct approximation for the baroclinic APE in oceanography (Reid *et al.* 1981) derives from the work required to produce small vertical displacements ζ from equilibrium of the isentropic surfaces in vertically stratified fluids. This is the Boussinesq approximation

$$\mathrm{APE}_b = \int_V \tfrac{1}{2} \varrho_r N_r^2 \zeta^2 \, dV \qquad [9]$$

where ϱ_r is the density and V the volume of water for which the APE is required.

$$N_r^2 = -\frac{g}{\varrho_0} \frac{d\varrho_0}{dz} \qquad [10]$$

is the Brunt-Väisäla stability parameter for the stable reference state. Eqn. [9] is valid for a hydrostatic fluid in which the barotropic component is ignored. In the two-layer model of a ring this becomes

$$APE = \tfrac{1}{2} \varrho g' \int_A (h-h_-)^2 \, dA \qquad [11]$$

integrated over the area A of the ring.

Baroclinic kinetic energy is obtained by integrating the geostrophic velocities (Eqn. [8]) over the area of the ring

$$\mathrm{KE} = \tfrac{1}{2} \varrho \int_A h v^2 \, dA \qquad [12]$$

Eqns. [11] and [12] are as used by Olson *et al.* (1985) and Olson and Evans (1986).

3.5 HEAT AND SALT ANOMALIES

Consider a body of water of volume V with $T=T(p)$, $S=S(p)$, $\varrho=\varrho(p)$ and heat content Q in an environment of volume V_r with $T_r=T_r(p)$, $S_r=S_r(p)$, $\varrho_r=\varrho_r(p)$ and heat content Q_r. The heat content per unit volume of the body is $q=Q/V$ and of the surroundings is $q_r=Q_r/V_e$.

The difference in heat content per unit volume $\delta q=q-q_r$ between the body of water and the surroundings is

$$\begin{aligned}\delta q &= C_p \varrho T - C_p \varrho_r T_r \\ &= C_p(\varrho T - \varrho_r T_r)\end{aligned} \qquad [13]$$

where C_p is the heat capacity.

Mixing of properties takes place along neutral buoyancy surfaces (McDougall 1987, 1989). On the scale of Agulhas rings neutral surfaces are not much different from potential density levels (R.C. van Ballegooyen, University of Cape Town, pers. comm.) and isopycnals can be used to approximate mixing lines. Eqn. [13] can then be written:

$$\delta q = C_p \varrho (T-T_r) \qquad [14]$$

since $\varrho_r=\varrho$.

To obtain the total excess heat content, δQ, which will eventually mix into the surroundings, δq is integrated over the water body taking the temperature differences at the same potential density levels in the environment and the surroundings.

$$\delta Q = \int_V \delta q \, dV = \int_V C_p \varrho (T-T_r) \, dV \qquad [15]$$

$$\delta Q = \iint_{A\,z} C_p \varrho (T-T_r) \, dz \, dA \qquad [16]$$

From the hydrostatic equation, $\int dp = \int \varrho g dz$, $dz = \frac{dp}{\varrho g}$ is obtained. Then

$$\delta Q = \frac{1}{g}\iint_{A\,z} C_p\,(T-T_r)\,dp\,dA \qquad [19]$$

Since the mass of salt in a parcel of water is $S\varrho V$ (cf. heat content = $C_pT\varrho V$), a similar expression for calculating the salt anomaly of the water body is obtained directly:

$$\delta\Sigma = \frac{1}{g}\iint_{A\,z} (S-S_r)\,dp\,dA \qquad [20]$$

In practice the properties of the water body are compared to the environment by considering a typical reference station which has the characteristics of the environment. In cases where the density level is not represented e.g. surface water at the centre of an eddy where $\varrho_r < \varrho_s$, the salt and heat content at the denser station are taken as equal to zero.

3.6 SCALING PARAMETERS FOR RINGS

In order to provide a baseline for the inter-comparison of different rings, it is useful to introduce a number of different scales (Olson 1991). These are the Rossby number, the Burger number and the Richardson number. The gradient velocity balance equation (Eqn. [8]) can then be scaled as

$$R_o^2 + R_o = B' \qquad [21]$$

where $R_o = \frac{U}{fL}$ is a Rossby number for the gradient flow and $B' = g'\frac{\delta h}{f^2L^2}$ is a Burger number for the interface displacement ($\delta h = h-h_\infty$) across the ring. The horizontal length scale, L, is chosen as the radius of maximum velocity, while this maximum velocity is taken as the velocity scale, U. Rossby numbers provide a measure of the importance of rotation, while traditional Burger numbers provide a measure of stratification (Pedlosky 1979). These dimensionless numbers can also be used to provide other interesting information about rings.

When the deviation of the interface height (indicated by the displacement Burger number, B') is of the order of the interface depth

(indicated by a traditional Burger number, $B = g' \frac{h}{f^2 L^2}$) i.e. $B' \approx B$, then the Richardson number, $R_I = g' \frac{h}{U^2}$, approximately represents the ratio of the potential energy to the kinetic energy of the ring (Olson (1991), although it will be seen later that for Agulhas rings this is not generally the case. It is also useful to note that $B = R_I R_o^2$.

In the two-layer model, the Rossby radius can be derived as $R_d = \frac{(g'h)^{\frac{1}{2}}}{f}$ which indicates the distance over which the gravitational tendency to flatten the free surface is balanced by the tendency of the coriolis acceleration to deform the surface (Pedlosky 1979).

The data collected on the cruises listed in this Chapter are examined and discussed in detail in the following Chapters.

Acknowledgements: Although I was responsible for the CTD (except Africana V071) and XBT data collection on all cruises, data collection would have been an impossible task without the assistance of the scientific and technical staff and crews of the vessels used. I would like to acknowledge the assistance of: F.R.S. *Africana* - Captains Derek Krige and Kevin Denning, Bosuns Hector Golding and Eddie May and crew; R.S. *Benguela* - Captain Louis Swart and crew; F.R.S. *Africana* V071 - John Taunton-Clark (SFRI), Rob Cooper (SFRI); R.S. *Benguela* V246 - Frank Shillington (UCT), Shaun Courtney (UCT), Steve Cruikshank (SFRI), Jamie Fearon (SFRI), Colin Willies (SFRI), Des Wright (UCT); F.R.S. *Africana* V080 - Alan Borcher (SFRI); F.R.S. *Africana* V085 - Frank Shillington (UCT), John Taunton-Clark (SFRI), Rob Cooper (SFRI), Corné Erasmus (SFRI), Gus Goatley (SFRI), Christine Illert (SFRI), Chris Rohleder (SFRI), Heather Sessions (SFRI), Hannes Smit (SFRI), Edwin Scheffers (SFRI); F.R.S. *Africana* V105 - Geoff Bailey (SFRI), Frank Shillington (UCT), Rob Cooper (SFRI), Gert "Obie" Oberholster (SFRI), Jon Mantel (UCT), Sarah Searson (UCT), Brian Super (SFRI). All CTD and XBT data collection relied heavily on data capture software written by Peter Claassen (SFRI). The expertise of members of the Electronic Workshop at SFRI in keeping recalcitrant electronic equipment functioning was invaluable. NOAA imagery was processed by Kobus Agenbag (SFRI). GEOSAT data were made available by Marten Gründlingh (CSIR).

Sources: DUNCOMBE RAE, C.M., CHAPMAN, P. and L.V. SHANNON 1989 - *Data Report of R.S. Africana Voyage 071 - South East Atlantic Ocean, April 1989 (Vema, Walvis Ridge, Tristan da Cunha, Gough).* Internal report, Sea Fisheries Research Institute, manuscript in preparation.

DUNCOMBE RAE, C.M. and F.A. SHILLINGTON 1989 - *Data Report of R.S. Benguela Voyage 246 - South Atlantic Eddy Cruise, May 1989.* Internal report, Sea Fisheries Research Institute, manuscript in preparation.

CHAPTER 4: CAPE BASIN CIRCULATION

A knowledge of the average background circulation of the South Atlantic Ocean, particularly within the Cape Basin, is important to the understanding of how Agulhas rings move through this system. Within the Cape Basin, the Benguela Current begins as a northward flow off the Cape of Good Hope before bending north-west to separate from the African coast at about 30°S while widening rapidly (Stramma and Peterson 1989). In addition to the input from the South Atlantic Current (Stramma and Peterson 1990), the Benguela Current receives an input from the Agulhas Current more or less sporadically. The Benguela Current is confined to the upper layers, the flow at 1500 m being all to the south (Reid 1989).

The atmospheric pressure systems which develop over the South Atlantic and the southern African continent during summer cause prevailing winds from the south and south-east, producing an offshore Ekman drift and subsequent upwelling of cold, nutrient rich water on the shelf, which supports a rich ecosystem and fishery (Nelson and Hutchings 1983, Shannon 1985). The main upwelling occurs on the southern part of the coastal ocean during the summer and moves northwards during winter (Jones 1971). The most vigorous upwelling occurs during spring, when the winds are the strongest (Schell 1968). Traces of Agulhas Current water (from the Agulhas Bank and not necessarily from the main stream of the current) are almost always found in the off-shore region of the Cape upwelling regime in summer (Shannon 1966, Bang 1973). A northward jet extending from Cape Point (Bang and Andrews 1974, Nelson and Hutchings 1983, Nelson 1991) to Cape Columbine flows at 50 $cm.s^{-1}$, 20 to 30 km wide, over the 200 to 300 m isobaths at the shelf-edge (Nelson and Hutchings 1983, Nelson 1991).

In comparison to the upwelling system, the Benguela Current has been little studied. Sverdrup *et al.* (1942) estimated the northward geostrophic transport at 30°S as being 16×10^6 $m^3.s^{-1}$ with respect to 1200 db. Stramma and Peterson (1989) noted a northward transport of 18.7×10^6 $m^3.s^{-1}$ in the upper 600 m of the data of Wüst (1957) and obtained a northward transport at 32°S of 21×10^6 $m^3.s^{-1}$. They found that near 30°S the Benguela Current begins to separate from the shelf and

the northwest carrying 18×10^6 $m^3.s^{-1}$ of water across 28°S. At this point it turns westward and flows over a relatively deep section of the Walvis Ridge. About 3×10^6 $m^3.s^{-1}$ of surface flow leaves the Cape Basin to the north and enters the Angola Basin.

It is my intention in this chapter to describe the background circulation for the Cape Basin using temperature data obtained from expendable bathythermograph (XBT) probes and CTD stations done on research cruises in which I have participated.

4.1 TEMPERATURE DATA

Between April 1989 and July 1992 five cruises were undertaken by vessels of the Sea Fisheries Research Institute (S.F.R.I.) over the Cape Basin west of southern Africa, on F.R.S. *Africana* and R.S. *Benguela* (See Chapter 3). On each of these cruises temperature profiles of the water column were obtained at approximately 35 to 50 km intervals while the vessel was underway (Figure 4.1 shows the cruise tracks, indicated by station positions for the five cruises). From two of these cruises (*Africana* V071 and *Africana* V080) four lines crossing the entire Cape Basin were obtained. In the case of *Africana* V071, the base of the triangle made by the ships track from and back to Cape Town was also completed by XBT and CTD stations taken along the Walvis Ridge. Two cruises (*Africana* V085 and *Benguela* V246) were specifically targeted to study Agulhas rings shed from the retroflection. The final cruise (*Africana* V105, designated BEST-1) was undertaken to deploy the moorings for the Benguela Sources and Transports (BEST) programme and yielded data on the circulation within the basin. Consequently the data collected on these latter three cruises do not extend completely across the basin. The XBT traces collected between Cape Town and the study regions are, however, useful in contributing to the data set in the south-eastern part of the basin. Vertical temperature sections from these cruises are shown in Figure 4.2, arranged geographically from north to south.

4.2 DISCUSSION

The temperature profile obtained on the XBT line from Cape Town to Vema Seamount and the Walvis Ridge in April 1989 is shown in Figure 4.2b.

The depression of the isotherms indicating the position of the Vema ring which was first encountered on this cruise, is marked in the figure. On the large-scale the bowl-shape of the isotherms within the mid-ocean gyre was evident. Smaller scale features due to topographic effects (Vema Seamount and the Walvis Ridge) were also discernable. From the scale and extent of the isotherm excursions in these sections it is reasonable to assign at least some of the features to other rings or eddies in the basin (both anticyclonic and cyclonic). GEOSAT altimeter data has shown up to 11 anticyclonic rings at any one time within the South Atlantic (Gordon and Haxby 1990). GEOSAT altimeter (Taunton-Clark 1993) and unpublished hydrographic data from the BEST-1 cruise suggest that cyclonic eddies are frequently associated with the anticyclonic Agulhas rings in the southern part of the basin.

In the sections across the southern part of the basin, some features of the frontal systems of the Antarctic Circumpolar Current were evident. Chapman *et al.* (in prep.) show that the Subtropical Front occurred at about 40°S on the sections along 13°W (see Fig. 4.1). Thus in Figures 4.2d and 4.2e the lines of stations cut obliquely across the Subtropical Front. In the southernmost section (Fig. 4.2e) the line of stations crossed both the Subantarctic and the Subtropical Fronts. The influence of the Agulhas retroflection region as the eastern boundary is approached was seen in the high surface temperatures and depression of the isotherms (Figs 4.2d,e). It was not possible to distinguish whether these features were due to the retroflection itself or to rings shed from it.

The 10°C isotherm can be used to represent the geopotential anomaly relative to some pressure level in a two layer system (Chapter 3). This assumption is good within the rings sampled and even though it does not necessarily hold as well outside them, the correlation is acceptable and has been used before.

The depths of the 10°C isotherm were averaged over 1° squares with data taken in or near known rings included (Fig. 4.3). Since the depth of the 10°C isotherm is simply related to the GPA, this figure represents qualitatively the direction of the flow of water over the Cape Basin. Depths of the 10°C isotherm were also averaged with the data from known Agulhas rings omitted (Fig. 4.4). These figures show the flow of the

South Atlantic Current from the west, extending across the basin with little inflow into the centre of the basin. Data for the western part of the basin are sparse and with more data the structure of the contours may be different. However, the flow as presented here from the available data, with the South Atlantic Current continuing eastward into the Indian Ocean, supports the conclusions of Gordon *et al.* (1992). Also suggested from the sections is the shelf-edge flow around the tip of the continent from the Indian Ocean into the Benguela Current (cf. Stramma and Peterson 1989).

Surface dynamic topographies of the South Atlantic (Gordon and Bosley 1991, Gordon *et al.* 1992, Chelton *et al.* 1990) show essentially the same features. In the figures (Fig. 4.5) presented by Gordon and Bosley (1991) flow crossing 0° longitude south of 38°S does not return to the Atlantic but passes to the south of the retroflection region into the Indian Ocean. Flow entering the basin south of 35°S returns to the basin by passing around Agulhas rings shed from the retroflection. From Figures 4.3 and 4.4 it appears that flow entering the basin south of about 35°S does not return. The Agulhas rings entering the basin from the east appear to represent a barrier to flow returning to the South Atlantic, possibly because these pictures represent averaged data over five non-synoptic cruises. However, each individual ring may still represent a conduit for flow to return to the west. Levitus (1982) data (Fig. 4.6) shows that most of the (geostrophic) flow entering the eastern Cape Basin north of 41°S returns to the South Atlantic, particularly when combined with the Ekman velocities (Gordon and Bosley 1991).

The flow patterns thus indicated by the 10°C depths represents the general flow within the basin but still does not assist in elucidating the detail of the flow within the "mixing zone" of the area where the Agulhas retroflection, South Atlantic Current and Benguela Currents meet. Chemical tracer data of Gordon *et al.* (1992) shows, however, that the shedding of Agulhas rings may indeed present a partial barrier to South Atlantic Current water entering the Benguela Current as suggested by Figures 4.3 and 4.4.

CHAPTER 5: CHARACTERISTICS OF AGULHAS RINGS IN THE SOUTH ATLANTIC OCEAN

The hydrographic characteristics of Agulhas rings within the South Atlantic are little known. Up to 1989, only two hydrographic measurements of Agulhas rings had been made away from the immediate vicinity of the retroflection (Gordon and Haxby 1990, McCartney and Woodgate-Jones 1991). In 1990 another two rings were detected hydrographically far from the retroflection (Gordon *et al.* 1992). All of the above-mentioned rings were detected during the course of large-scale surveys and each measurement consisted of only one line of hydrographic and bathythermograph data. Close to the retroflection, rings have been more readily detected: the Agulhas Retroflection Cruise (Gordon 1985, Camp *et al.* 1986), in 1983, examined two recently shed rings in detail; during 1985 a large scale survey of the Agulhas Current retroflection detected a ring south-west of Cape Town (Bennett 1988); and the Subtropical Convergence and Agulhas Retroflection Cruise (Lutjeharms 1987, Valentine *et al.* 1988), in 1987, detected five rings to the south, west and northwest of the retroflection.

During April 1989 on a physical oceanographic survey to the Walvis Ridge, a ring was encountered near Vema Seamount and this encouraged Sea Fisheries Research Institute to mount a second cruise to examine the same ring a month later (Duncombe Rae *et al.* 1989b, Duncombe Rae *et al.* 1992b). These two cruises represent the only intensive full-scale hydrographic examination of a ring within the South Atlantic, far from the immediate vicinity of the retroflection. This particular ring was also evident in NOAA satellite derived sea-surface temperatures and GEOSAT altimetry. In August 1990 another ring, shed during winter from the retroflection, was detected on a further physical oceanographic survey in the Cape Basin. In June 1992, during deployment of inverted echo-sounders for the Benguela Sources and Transports programme (BEST-1 cruise) yet another ring was encountered. For the three rings encountered hydrographically by Sea Fisheries Research Institute vessels, at least two hydrographic sections were obtained in each case.

In this Chapter, the hydrographic characteristics of these three Agulhas rings are presented and discussed in detail. A comparison of

these and other Agulhas rings is undertaken in an attempt to identify typical Agulhas ring characteristics.

5.1 THE VEMA RING

5.1.1 DATA

5.1.1.1 Hydrographic Measurements

During Voyage 071 of F.R.S. *Africana* (Shannon *et al.* 1989b), vertical temperature sections were obtained from expendable bathythermographs (XBT) launched at approximately 40 km intervals between Cape Town (34°S, 18°E) and Vema Seamount (31°40'S, 8°20'E) in April 1989 (Fig. 5.1: A...A) and, on this leg, an Agulhas ring was discovered. A follow-up cruise on R.S. *Benguela* was undertaken in May 1989 to make a more detailed hydrographic survey of the feature found in April 1989 (Fig. 5.1: A..V..B). From the known position of the ring during April from the *Africana* cruise, and ring translation rates given by Olson and Evans (1986), a projected ring position for the *Benguela* cruise in May was calculated. An appropriate search grid was laid out and the ring was rediscovered on the first east - west exploratory XBT transect. Two detailed conductivity-temperature-depth (CTD) sections to 1200 m depth were then made at 30 nautical mile (55.5 km) intervals from south-east to north-west and north-east to south-west through the ring. Unfortunately insufficient time was available to allow further sections to be conducted.

5.1.1.2 NOAA Imagery

NOAA-11 AVHRR infrared imagery was examined for the period January to July 1989. Cloud-free images showing the ring were available for 24 and 30 April as well as 15 and 16 June 1989. The latter pair of images, approximately 24 hours apart, were used to manually track small-scale thermal features, and so produce surface velocity vectors. Details of the processing, outlined in Chapter 3, are described by Agenbag and Shannon (1988) and Agenbag (1992).

5.1.1.3 GEOSAT Altimetry

GEOSAT altimeter data were available for the period prior to the cruises, from 29 December 1988 to 27 April 1989, ie. cycles 47, 48, 49, 52, 53 and 54 of the satellite. Complete data were not available for

cycles 50 and 51. Details of the GEOSAT altimetry processing are outlined in Chapter 3 and by Taunton-Clark (1993).

5.1.2 RESULTS

5.1.2.1 Hydrography

5.1.2.1.1 Horizontal sections

The temperature field at 200 m (Fig. 5.2) from the *Benguela* cruise data in May 1989 indicates that at this time the ring was highly elliptical, with the 16°C isotherm giving a major axis diameter of 330 km and a minor axis diameter of 165 km (a ratio of about 2:1). The geostrophic surface velocity with respect to a level of no motion of 1150 db (Fig. 5.3), calculated from the CTD station data shows that the highest speeds were found between stations 6 and 7 (currents to the south-west at 55 $cm.s^{-1}$) and stations 3 and 4 (to the north-east at 46 $cm.s^{-1}$). The anticyclonic nature of the circulation was also confirmed by ship's drift obtained from SATNAV fixes while the vessel was on station (winds were less than 5 $m.s^{-1}$ throughout the cruise).

5.1.2.1.2 Vertical profiles

5.1.2.1.2.1 F.R.S. *Africana* data - April 1989

It is clear from the vertical XBT section obtained in April 1989 between Cape Town (CT) and Vema Seamount (V) (Fig. 5.4) that the ring had little surface expression. The upper 100 m layer was well-mixed with a temperature of 21°C at the ring's centre. A horizontal diameter of the ring at this stage can be determined from the section to be 240 km, while the 6°C isotherm was depressed by 320 m at the centre of the ring. Referenced to a level surface at 500 m the temperature difference between water at the centre of the ring and at the edge was 5°C.

5.1.2.1.2.2 R.S. *Benguela* data - May 1989

Three vertical temperature sections were made through the ring in May 1989. It is evident from the east - west XBT section (Fig. 5.5a) that the western edge of the ring had not been reached as the isotherms were still rising towards the surface. The horizontal east - west dimension was estimated by taking twice the distance from the eastern edge (where the isotherms level off) to the centre yielding a scale of 530 km. An estimate of the north - south extent (180 km) was obtained in the same way from combined CTD and XBT sections (Figs 5.5b and 5.5c). These

sections revealed a surface mixed layer of 19°C down to a depth of 100 m across the centre of the ring.

The vertical salinity sections from the two CTD transects (Fig. 5.6) showed an isohaline mixed layer of 35.66 psu to a depth of 100 m. These sections indicate that the ring core water was 0.6 psu more saline than the surrounding water at 400 m depth.

The vertical nutrient distribution (Fig. 5.7) measured on the CTD transect from south to north through the ring (line B..B' on Fig. 5.2) shows that the concentrations of silicate, phosphate and nitrate in the surface water surrounding the ring were typical of oligotrophic Atlantic Ocean water. Water within the ring had even lower nutrient concentrations, typical of the Agulhas Current (Chapman *et al.* 1987), particularly in the upper 300 m. However, use of these nutrient values to assist in differentiating Agulhas (Indian Ocean) water from Atlantic water can be problematic (Chapman *et al.* 1987) due to mixing at the Agulhas Retroflection of Agulhas water with both Atlantic water and water south of the Subtropical Front during the ring separation. The silicate distribution was similar to that reported by Gordon *et al.* (1987b) for the ring which they examined.

The potential density sections (Fig. 5.8) computed via the equation of state (e.g. Gill 1982) from the potential temperature and salinity for the two CTD transects of the ring show most of the features discussed in the temperature and salinity sections. From the potential density data the geopotential anomalies (GPA) were calculated relative to 1150 db, enabling the calculation of geostrophic velocities between CTD stations through the water column relative to that pressure (Fig. 5.9). For these stations, the volume flux in Sverdrup (Sv = 10^6 $m^3.s^{-1}$) was also calculated and is indicated below the reference level in Figure 5.9.

Following Olson and Evans (1986), the depth of the 10°C isotherm (h_{10}) was plotted against the distance from the ring centre (d) and a normal curve was fitted to the data ($h_{10} = h_\infty + a_1 \exp(a_2.d^2)$; where h_∞ is the depth of h_{10} far from the ring) to model the ring. Integrating over the model, values of 38.8×10^{15} J for the available potential energy (APE) and 2.3×10^{15} J for the kinetic energy (KE) of the ring (Chapter 3) were

calculated. These values are of the same order as those obtained for similar rings by Olson and Evans (1986) and also an order of magnitude greater than similar Gulf Stream rings. The kinetic energy of the ring under consideration here was slightly lower, suggesting that some of this energy had already been lost by friction to the South Atlantic, due to the longer time elapsed since shedding from the retroflection.

The NOAA satellite imagery (discussed below) showed a cool filament, originating in the Benguela upwelling front, surrounding the northern edge of the ring (Fig. 5.11). In order to determine water mass characteristics of the ring water, temperature-salinity (TS) diagrams were constructed for all the stations (Duncombe Rae and Shillington 1989). From these TS diagrams it became clear that there was indeed something very unusual about the north-western part of the first CTD transect (line B..B', Stations 8 and 9). The salinity between depths of 50-150 m was much lower (35.2 psu) than that of the other "edge" stations. In other "edge" stations, this low salinity value was found at about 200 m, and associated with a temperature of about 13.20°C.

Water with such characteristics (T = 13.20°C; S = 35.2 psu) is commonly found in the Benguela Upwelling Frontal region much closer inshore, and has recently been observed in a decaying filament off Lüderitz (Shillington *et al.* 1990). The contrast between this low-salinity near-surface layer and the water in the centre of the ring is shown in the TS diagram in Figure 5.10. This water is evident in Figure 5.6a as the low salinity (35.20 psu) 100 m thick layer from 50 to 150 m depth at the north-western edge of the ring.

The only plausible explanation for this low salinity water being present in this region near the surface, is that it was mature upwelled frontal water from the Benguela Upwelling region (Shillington *et al.* 1990) drawn into the proximity of the ring by the filament, as suggested by the satellite observations. The ring-filament interaction is discussed more completely in Chapter 6.

5.1.2.2 Remote Sensing

5.1.2.2.1 NOAA imagery

The NOAA satellite image from 15 June 1989 showed the origin of the anomalous edge water described above to be a filament captured from the

Benguela upwelling system (Fig. 5.11a). The ring was first observed in contact with the filament in satellite infra-red images from 24 and 30 April (not shown). From feature tracking between the two images from 15 and 16 June 1989, velocity vectors were constructed on the perimeter of the ring showing anti-cyclonic motion with speeds up to a maximum of 70 $cm.s^{-1}$ to the north-east of the ring (Fig. 5.11b). Elsewhere speeds were of the order of 50 $cm.s^{-1}$. At the base of the filament current speeds were of the order of 25 $cm.s^{-1}$. The filament was 50 km wide and 550 km long, extending from the edge of the Benguela Upwelling Front. The water within the filament originated in the current associated with the upwelling front (Agenbag 1992).

5.1.2.2.2 GEOSAT altimetry

From the cycle-averaged pictures (Chapter 3) obtained from the GEOSAT altimeter data, a region of elevated sea surface could be identified in the region of the Agulhas Retroflection, to the south-west of Cape Town. This region remained relatively static over several cycles, within a few hundred kilometres of the area marked "14 February" in the composite (Fig. 5.12). On the snapshot representing 1 March, a feature of markedly greater elevation than the surroundings appeared to bud off from this elevated region and moved north-westwards approximately along ascending ground track A158. The positions of this feature on 14 March and 14 April in the weekly snapshots are indicated.

No GEOSAT altimeter data were available after the end of April. This is unfortunate as the three sets of data (altimeter, hydrographic and infra-red) do not overlap in time to any great extent. However, some corroboration is obtained: the position of the ring centre on 6 April, 20 May and 15 June is indicated by crosses on Figure 5.12. The hydrographic data from 6 April showed the ring crossed by the *Africana* to be in the same region as the sea surface elevation revealed in the altimeter data at about the same time, and tracked back to the region of the Agulhas Retroflection two months earlier.

The 17-day average altimeter data depict spatially smoothed sea surface elevations and are thus quite difficult to interpret if the features are of the same order of magnitude as the grid spacing of the satellite ground-track. It is easier to identify features and to follow their progress along individual tracks sampled by the GEOSAT altimeter.

Along ascending pass A158 the ring appeared to move north-westwards and could be seen (Fig. 5.13) in successive cycles 52, 53, and 54 (24 March to 27 April). For this pass (A158), GEOSAT data were bad or missing for cycles 50 and 51 (before 24 March) and for cycles after 27 April. The region of sea-surface elevation corresponding to the Agulhas Retroflection was evident between 36°S and 38°S. The anticyclonic ring was seen to move progressively towards the equator, as indicated by the dashed line in Figure 5.13, at a speed of 6.8 $cm.s^{-1}$. The sea surface elevation relative to the general background sea level (assumed to be 0 cm on Figure 5.13) was about 30 cm and the north - south diameter was between 200-300 km. Sea surface slopes were calculated from Figure 5.13 to be 3.2×10^{-6}. From the geostrophic balance (e.g. Gill 1982, p. 193), and including any barotropic component, speeds of 40 $cm.s^{-1}$ were calculated. Speeds calculated from GEOSAT data compared very well with the hydrographically calculated velocities due to the baroclinic component and referenced to 1100 db (Taunton-Clark 1993).

5.1.3 DISCUSSION

The general direction of translation of the ring, the NOAA imagery before the hydrographic cruises from January to May 1989 (Duncombe Rae *et al.* 1989b) and the distribution of similar rings followed using satellite altimetry (Gordon and Haxby 1990) suggested that the ring originated at the Agulhas Retroflection. This hypothesis was confirmed from GEOSAT altimetry during and prior to the period of the cruises.

At the Agulhas retroflection, water with a temperature above 16°C is isohaline at 35.6 psu (Camp *et al.* 1986, Valentine *et al.* 1988) and "tends to be less saline than the thermocline of the South Atlantic" (Fig. 5.14; Gordon and Haxby 1990: p. 3123). The Vema ring centre exhibited two isohaline layers: one of 35.66 psu with temperature greater than 19°C near the surface and another of 35.61 psu with a temperature of 17.5°C at 150 m (Fig. 5.6a). Water in the surrounding South Atlantic had a salinity greater than 35.7 psu at temperatures greater than 17°C. The greater salinity of the near-surface isohaline layer compared to the lower isohaline layer at the Vema ring centre was most likely due to evaporation increasing the salinity in the wind mixed layer.

Olson *et al.* (1992) observed that South Indian Subtropical Mode Water (STMW) of 17.4-17.8°C occurs as a thermostad in the Agulhas Current and retroflection. In the Cape Town eddy, the upper thermostad had temperatures of 16.1-16.5°C (Olson *et al.* 1992). In the lower halostad (35.61 psu) of the Vema ring the temperature was 17.2°C (Duncombe Rae *et al.* 1992b). Modification of the upper salinity layer in the Vema ring subsequent to shedding changed the characteristics while the lower layer had characteristics similar to those observed by Olson *et al.* (1992).

These features are indicative of the Agulhas origin of the ring. Further confirmation of the Agulhas origin of the ring was given by the sections of silicate, phosphate and nitrate which showed the concentrations of these nutrients to be depressed relative to the surrounding water (Fig. 5.7).

From the two measured XBT sections (one from the F.R.S. *Africana* and the other from the R.S. *Benguela*) it was inferred that the ring translated 230 km in 42 days, which yields a velocity of 6.4 $cm.s^{-1}$ in a north-westerly direction. An error of 50 km in the first ring location (e.g. due to the first transect not exactly bisecting the ring) would imply an uncertainty in the speed estimate of about 1 $cm.s^{-1}$. From the GEOSAT altimetry data presented in Figure 5.12, the ring is seen to move 200 km in 34 days, a speed of 5.9 $km.day^{-1}$ (6.8 $cm.s^{-1}$) immediately prior to the *Africana* cruise which is in good agreement with the speed deduced from the hydrographic data.

Cushman-Roisin *et al.* (1990) show theoretically that rings of the dimension seen here should have a westward translation of some 2 $cm.s^{-1}$ due to the planetary beta effect. (They use a one-moving-layer model for their main result, and in attempts to generalise to a two-layer system, suggest that there will be an additional equatorward component.) Olson and Evans (1986) obtained theoretical westward values of 1.6 and 2.1 $cm.s^{-1}$ for the rings they studied, while observed westward values were 7.5 and 3.8 $cm.s^{-1}$. The theoretical westward translation calculated for the Vema ring was consistent with these results (2.1 $cm.s^{-1}$, calculated following Nof 1981 and Flierl 1984a). The observed westward component of the translation was 2.1 $cm.s^{-1}$ calculated between the ring positions in May and June. Although this

is similar to the theoretical value, extrapolating back to the retroflection region requires a higher value of the westward velocity. Note that Olson and Evans (1986) also observed drift speeds higher than the theoretically determined values implying that the background flow must be an important additional effect to drive the ring in a north-westerly direction at a speed three times the theoretical rate. The only other known case of an Agulhas ring drifting along a similar path is the one described in detail by Gordon and Haxby (1990). They described a ring which GEOSAT data showed was moving at 8.4 $cm.s^{-1}$. The continuation of the ring path described by Gordon and Haxby (1990) has been evaluated from subsequent GEOSAT data by Wakker *et al.* (1990a). They found the ring had a mean speed of 4 $cm.s^{-1}$ and stalled somewhat as it passed over the Walvis Ridge. Most rings observed recently in the South Atlantic (e.g. Olson and Evans 1986, Gordon and Haxby 1990, Wakker *et al.* 1990a) have had a more westerly orientated direction. Olson and Evans (1986) found the speed of translation for the two rings closer to the retroflection which they discussed to be 4.8 and 8.5 $cm.s^{-1}$.

Duncombe Rae *et al.* (1989b) calculated that the heat loss of the upper mixed layer to the atmosphere between the XBT temperature sections from the two cruises was of the order of 1.8×10^{19} J. (The time between the sections was 42 days.) This is consistent with an estimated heat loss of 80 $W.m^{-2}$ which is considered to be the climatic mean for this region (Höflich 1984). Duncombe Rae *et al.* (1989b) also estimated that the volume flux of the ring per annum was about 1.2×10^{6} $m^3.s^{-1}$.

5.1.4 SUMMARY

Temperature sections from two cruises were used by Duncombe Rae *et al.* (1989b) to calculate heat fluxes to the atmosphere and the mean drift rate of an Agulhas ring discovered in the South Atlantic in April 1989. The second more detailed CTD survey in May 1989 revealed the basic physical structure of the ring in a position adjacent to the Benguela Frontal region. Characteristics of the salinity in the upper 300 m, energy considerations and the general translation of the ring revealed by GEOSAT altimetry, confirmed its Agulhas origin. The vertical nutrient structure (phosphate, silicate, nitrate) was also suggestive of Agulhas water.

The ring was elliptical, with dimensions 530 km from east to west, and 180 km from north to south. This is considerably larger than the ring described by Gordon and Haxby (1990), which was 290 km in diameter. Using a slightly different criterion, the Gordon and Haxby (1990) data are consistent with an east-west dimension of 380 km. Maximum geostrophic surface speeds of 55 $cm.s^{-1}$ with respect to 1150 db were found at the north-western edge of the ring. NOAA-11 infra-red imagery and feature tracking demonstrated that the Benguela Frontal water had been entrained into the outer perimeter of the ring. A dominant characteristic of Benguela upwelled water near the surface is its low salinity. Low salinity (35.2 psu) water was found between 50 and 150 m depth in the north-western edge of the ring. Using Olson and Evans's (1986) two-layer model the available potential and kinetic energies of the ring were estimated to be 38.8 and 2.3×10^{15} J respectively.

5.2 THE WINTER RING

Near the retroflection a number of Agulhas rings have been examined hydrographically (Duncan 1968, Gordon 1985, Olson and Evans 1986, Lutjeharms 1987, Valentine *et al.* 1988, Harris and Van Foreest 1978, Bennett 1988) but farther from their source few confirmed Agulhas rings have been detected at sea (Duncombe Rae 1991). The above hydrographic measurements relate to rings spawned at the Agulhas retroflection during spring or autumn, or, in the case of the Oceanus ring (McCartney and Woodgate-Jones 1991), at some undetermined time.

Although Gordon (1986) suggested that a ring detected during November 1983 south-west of Cape Town (the Cape Town eddy) consisted of winter-cooled Indian Ocean water, translation rates from satellite-tracked drifters (Olson and Evans 1986) indicated that the ring was spawned in late September or October 1983. While early spring may still produce some spectacular gales, the ring would not have been subjected to the full fury of the austral winter around the "Cape of Storms".

The following is a discussion on a ring detected hydrographically south-west of Cape Town during August 1990 which separated from the retroflection during austral mid-winter (the Winter ring).

5.2.1 DATA

5.2.1.1 Cruise Track

A cruise of F.R.S. *Africana* was undertaken during August 1990 extending along the shelf edge from Engelbrecht Seamount towards Port Nolloth, in which XBT probes were used to search for a ring. The proposed grid was restricted to the region between the 2000 m isobath and a line drawn between Vema (31°41'S; 08°20'E) and Engelbrecht (36°11'S; 14°09'E) Seamounts. Grid lines were approximately 3/4 eddy diameter apart (Fig. 5.15).

Rings moving across the Cape Basin close to the shelf-edge should be constrained by the topography to waters deeper than 2000 m. From prior experience, it was felt that the presence of an Agulhas ring could be detected if the XBT stations came within 1/4 ring diameter of the centre of the ring. This allowed lines of the grid to be kept 3/4 ring diameter from the 2000 m isobath. The grid lines were perpendicular to the isobaths and one ring diameter long. Thus any Agulhas ring with a diameter greater than 300 km which was completely within 2.5 ring diameters of the 2000 m isobath was sure to be detected.

Using the proposed search pattern (Fig. 5.15), a warm-core ring was indeed detected in the offshore section between the first and second lines of the grid. It was estimated to have been shed during June 1990 and was named the Winter ring. Once the ring centre had been found, at 35°16'S; 11°43'E, further CTD and XBT measurements were used to characterize it (Fig. 5.16).

5.2.1.2 Hydrography

The expression of the ring found extended down to at least 3000 m: its maximum dimensions were 430 km E-W and 385 km N-S (cf. Vema ring = 530 x 180 km) while the diameter of the maximum geostrophic velocity (Fig. 5.17) was 180 km. Isotherm depression for the Winter ring varied from 250 m (15°C isotherm) to 500 m (9°C isotherm) (cf. Vema ring = 320 m) and the temperature anomaly of the centre with respect to the edge was 4°C at 500 m (cf. Vema ring = 5°C). The available potential energy for the Winter ring, calculated in the same way as for the Vema ring (Duncombe Rae *et al.* 1992b) was 26.0×10^{15} J and the kinetic energy was 2.6×10^{15} J. Maximum geostrophic velocities were 74 $cm.s^{-1}$ with respect to 1150 db (Fig. 5.17). It was not possible to

determine the translation speed of the ring as it was only encountered once and a blind attempt to seed it with a drifter on a subsequent cruise failed owing to lack of ship's time. Cloud cover and lack of surface signature prevented the use of satellite tracking. However, from the position of the ring relative to the retroflection and translation speeds of other rings in that vicinity (Olson and Evans 1986), it was estimated that the ring separated from the retroflection in late June or early July 1990 (austral mid-winter).

The Winter ring had a deep isothermal surface mixed-layer, extending from the surface to a depth of 320 m at a temperature of 16.3°C (Fig. 5.18). The density profile for the Winter ring (Fig. 5.19) showed doming of the isopycnals at the ring centre in the upper 400 m, indicating a reversal of baroclinicity. This is a common feature of rings and eddies in the World Ocean (Onken 1990) and has been observed in other Agulhas rings (Lutjeharms and Gordon 1987). A plausible explanation for this is provided by a recent numerical model of the formation of rings (Onken 1990) which ascribes the reversal of baroclinicity and the generation of subsurface jets to vortex stretching between the seasonal and the main thermoclines during ring formation. Differences in diabatic mixing attributable to changes in surface heat fluxes can also contribute to the reversal of baroclinicity (Williams 1988).

5.2.2 DISCUSSION

The water types evident in the Winter ring core are considered in relation to profiles taken on other cruises within the South Atlantic Ocean and the Agulhas Current. One of these water types, the Subantarctic Mode Water, is discussed separately. The deep surface mixed layer is also discussed briefly.

5.2.2.1 Winter Ring Core Water Types

A notable feature of the Winter ring was the integrity of the water masses at the centre (Fig. 5.20). The water masses of the retroflection region are (e.g. Bennett 1988, Valentine 1990, Valentine *et al.* 1993; see Tables 2iii, p. 168, and 2iv, p. 169): (1) Surface Water, (2) Central Water, including South Indian Subantarctic Mode Water, (3) Antarctic Intermediate Water and the deep water masses. The deep and bottom waters are not directly influenced by or involved in the water

mass modification and mixing undergone by the dynamic upper layers of the retroflection and rings and are therefore omitted in the following discussion.

The temperature and salinity characteristics of the water mass at the centre of the Winter ring are compared with the water masses of the Cape Basin and Agulhas Current system (Fig. 5.22) represented by stations occupied on recent cruises (Fig. 5.21). A profile at the centre of the ring is compared first with a station occupied in the immediate surroundings (Pos. 2 on Fig. 5.21) then subsequently with profiles obtained nearer the centre of the South Atlantic gyre (Pos. 3) and closer to the Subtropical Front (Pos. 4). The Winter ring profile is also compared with stations occupied in the Agulhas Current (Pos. 7 & 8) and on the edge of the western Agulhas Bank (Pos. 5 & 6). The TS diagram (Fig. 5.22a) for Station 7 (Pos. 1) at the centre of the Winter ring (Fig. 5.16) is shown for identification of the traces in the following figures (Fig. 5.22b-h).

The water masses in the core of the Winter ring were significantly different from those at a position on the edge of the ring (Fig. 5.22b) on the same cruise. The Deep Water showed the same characteristics at both stations. Above that level, the Antarctic Intermediate, Central and Surface waters outside the ring were fresher and cooler along isopycnal lines. At the Antarctic Intermediate Water (AAIW) level this indicates water more recently produced. The Winter ring thus still retained some characteristics of AAIW from the Indian Ocean, since Shannon and Hunter (1988) show that within the Agulhas Current system, AAIW from the Indian Ocean is more saline than that in the South Atlantic.

This situation is also evident in the comparison with Pos. 3 close to the Walvis Ridge (Fig. 5.22c). AAIW near the Walvis Ridge was closer to the intruding characteristics of the Winter ring, due to modification of AAIW as it circulates northward through the South Atlantic. Central Water and Surface Water were much less saline near the Walvis Ridge than within the Winter ring. AAIW farther south on a different cruise (Fig. 5.22d), however, was slightly more saline than that at the Winter ring core and showed evidence of mixing and interleaving. This particular station was occupied in the vicinity of

the BEST ring (discussed below), close to the Subtropical Front zone, and thus may not be typical of AAIW at high latitudes.

Comparison of the Winter ring core water with Agulhas Current water shows that although the ring AAIW had some Agulhas characteristics, true Agulhas Current AAIW is much saltier (Fig. 5.22g and h). AAIW in the Agulhas Current is sometimes modified to even more saline characteristics by the inclusion of Red Sea Water (Gründlingh 1985). However, only the upper 700 to 1000 m of the water column is transported by Agulhas rings (McCartney and Woodgate-Jones 1991) and the AAIW within the Winter ring may already have been left behind or altered by mixing.

The Winter ring Central water had characteristics nearly identical to the Agulhas Central water encountered to the east of the Agulhas Bank, the only deviations occurring near the surface and at the pycnostad layer around 900 m (Fig. 5.22g). The Winter ring TS profiles are very close to those of the western Agulhas Bank both at the shelf edge (Fig. 5.22e) and further offshore near the retroflection (Fig. 5.22f) where similar mixing of South Atlantic and Agulhas waters to that experienced during ring shedding may be expected. The surface layers of all Agulhas stations (Fig. 5.22e to h) are, of course, much warmer than the ring surface water, due to both the cooling experienced by the ring and the fact that the Agulhas stations were occupied during summer. The surface layers of the Winter ring are discussed in detail below in section 5.2.2.3.

5.2.2.2 Subantarctic Mode Water

Within the Central Water of the Winter ring, the layer of almost isothermal (9.8°C) and isohaline (34.85 psu) (therefore isopycnal) water between 800 and 950 m lies within the range of salinity (34.8-35.2 psu), and close to the range of temperature (10-12°C), characteristics for South Indian Subantarctic Mode Water (SAMW) observed in the Agulhas Current south of Africa (Bennett 1988). SAMW is recognised as a deep isothermal layer within the thermocline, with temperature and salinity characteristics dependent on distance from a source near the Subantarctic Front where the water type is formed during winter overturning, as defined by McCartney (1977). It is therefore initially tempting to identify this layer within the Winter ring as SAMW.

However, alternative explanations for the presence of this water within Agulhas rings exist and it is not possible within the context of this thesis to make an exhaustive study of these alternatives, and confirm that it is SAMW. The deep isopycnal layer, when observed within Agulhas rings, will therefore be referred to as a "lower stad" or "lower stad water" for the purposes of the discussion below.

A lower stad layer may be present within the thermocline of Agulhas rings due to the influence of a number of factors: the water may be supplied directly from the Agulhas Current; it may be entrained from south of the Subtropical Front during ring formation; it may be formed and/or modified on the Agulhas Bank; and in all these cases the dynamics of ring formation may play a role in increasing the thickness of the stad layer. The possible sources of the water within the lower stad are discussed briefly below.

5.2.2.2.1 The Agulhas Current as Source

The presence within Agulhas rings shed from the Agulhas Current of a very clear lower stad with SAMW characteristics, particularly within the Winter ring, cannot be fully explained by merely noting the presence of SAMW in the Agulhas or Return Currents. Although SAMW has been observed in the Agulhas and Agulhas Return Currents (e.g. Bennett 1988, Gordon *et al.* 1987a), there is no evidence in traces taken within the Agulhas Current of such a pronounced SAMW layer as that seen in the Winter ring. If the lower stad <u>is</u> supplied purely from Agulhas Current water, the explanation for its thickness relative to that observed within the Agulhas Current must lie elsewhere, such as in "stretching" or concentration of the source thermocline water within rings during the process of ring shedding (see Onken 1990). In this case, its close resemblance to the characteristics of SAMW may be fortuitous since with slightly different dimensions the ring may entrain a different part of the water column.

An observation possibly pertinent to this argument is that the SAMW present within the Agulhas Current at the time of shedding of the Winter ring was likely generated at the Subtropical Front in the South Indian Ocean (McCartney 1977, 1982) during the previous winter to the observation of the Winter ring. It has been speculated that the 1989 austral winter was unusually severe (Brundrit and Shannon 1989) and

this may account for the prominence of the SAMW layer. However, no observations are available to test this conjecture.

5.2.2.2.2 A Subantarctic Water Source

A second potential source of the lower stad water of the Winter ring in the region of the Agulhas retroflection is in the water drawn into the gap created by the separation of the ring from the retroflection during shedding. In satellite imagery of ring formation at the Agulhas retroflection, Subantarctic water is often observed to be drawn into the gap between the newly shed ring and the reformed retroflection (Lutjeharms and Van Ballegooyen 1988a). Incorporated into the ring during the formation process, the intruding water may be the source of the lower stad layer observed in Agulhas rings. Observation of the shedding of an Agulhas ring at sea (Lutjeharms and Gordon 1987) confirms that not only the surface layers observed in the satellite imagery but also the entire water column entering the gap could have come from the Subantarctic region. However, in the sections presented in that publication (and from profiles in Camp *et al.* 1986), although a SAMW signature (thermostad between 10-12°C) is evident in the section outside the ring, this layer is only slightly enhanced within the newly shed ring. Here again the dynamics of ring formation may contribute to the formation of the lower stad.

5.2.2.2.3 A Source on the Agulhas Bank

A third, somewhat unexpected, potential source of the lower stad water lies on the Agulhas Bank. The Agulhas Bank is a shallow, triangular extension of the continental shelf south of Africa, enclosing approximately 100 000 km^2 within the 200 m isobath. On this bank a bottom mixed layer up to 50 m thick is frequently observed (Swart and Largier 1987, Chapman and Largier 1989, pers. obs. 1992 Agulhas Bank Boundary Processes (ABBP) Cruise). This bottom mixed layer has temperature and salinity characteristics (approx. 8 - 11°C; 34.7 - 34.9 psu) close to those of the lower stad observed in the Winter ring (pers. obs. ABBP Cruise 1992, Chapman and Largier 1989). Wind-induced coastal upwelling in the vicinity of Cape St. Francis on the eastern Agulhas Bank (M. Roberts, Sea Fisheries Research Institute, pers. comm.) combined with topographically-induced shelf-edge upwelling (Chapman and Largier 1989) may continuously draw water from 600 to 800 m depth in the Agulhas Current onto the eastern Agulhas Bank. Here

it may reside for a time, becoming mixed and modified, before leaving the bank on the western edge. It is possible that it is this water which is entrained within the retroflection during the formation of an Agulhas ring. This hypothesis is currently being explored (Duncombe Rae and Roberts in prep.).

5.2.2.2.4 Discussion

It is possible that some combination of all the above sources had an influence on the composition of the lower stad within the Winter ring.

A dynamical explanation for the lower stad within rings is the most attractive, and it is within rings that the layer is most frequently seen. Two of the five rings encountered in February 1987 on the SCARC cruise showed some evidence of a lower stad within the thermocline (Fig. 5.23a & b). However, observations of a lower stad within the Agulhas and the Agulhas Return Currents such as that observed at a station on the SCARC cruise (Fig. 5.23c; Valentine *et al.* 1988) and a stad between 600 and 750 m, identified then as highly modified Subtropical Mode Water, observed in the November 1983 survey of the region (Gordon *et al.* 1987a), may indicate an actual source of a thick isopycnal layer of water such as SAMW or Agulhas Bank bottom water. A full investigation of this topic is considered to be beyond the scope of this thesis and is not attempted here. It is noted from a preliminary calculation using typical scales for Agulhas rings, however, that in moving water from outside an Agulhas ring to the centre, a large amplification may be expected in the height of a stad due to the change in potential vorticity.

5.2.2.3 Surface Mixed Layer

The deep isothermal surface mixed layer observed in the Winter ring (320 m; Fig. 5.18) was the deepest thus far reported for Agulhas rings. Rings with deep surface mixed layers have been found in other current systems, up to 400 m deep (Kamenkovitch *et al.* 1986). Agulhas rings, however, have generally been observed with shallower surface mixed layers. The Vema ring (Duncombe Rae *et al.* 1992b) had a mixed-layer depth at the centre of just over 100 m. Rings sampled in November 1983 showed mixed layer depths of 220 m and 260 m (Camp *et al.* 1986). In two rings sampled in February 1987, mixed layer depths of 120 m and

140 m were encountered (Valentine *et al.* 1988). In the other three rings from that cruise only shallow surface mixed layers were found.

The surface mixed layer of the Winter ring had temperature and salinity characteristics corresponding to cooled local Subtropical Mode Water (STMW) (Bennett 1988) which originated within the recirculating Agulhas Current. From synoptic weather charts for the winter of 1990 (S.A. Weather Bureau 1990), the highest wind speeds experienced over the retroflection were of the order of 40-50 $m.s^{-1}$. Production of the 320 m deep isothermal layer observed from an initially stratified Agulhas Current water column by the action of a mean wind-speed of 45 $m.s^{-1}$, requires an ocean-to-atmosphere heat flux of 225 $W.m^{-2}$ over the two-month period from the estimated time of shedding of the ring to the time it was sampled (calculated following Pollard *et al.* 1973, Thompson 1973). This value is high but within the range experienced over the Agulhas retroflection during winter (Höflich 1984, Mey *et al.* 1990). It is concluded therefore that the 320 m deep surface mixed-layer at the centre of the Winter ring was produced by rapid heat exchange with the atmosphere, driving deep convective overturning, and aided by wind-induced mixing.

5.2.3 SUMMARY

An anticyclonic ring shed from the Agulhas retroflection in late June or early July 1990 (austral mid-winter) was encountered in the South Atlantic Ocean south-west of Cape Town. The maximum diameter of the ring was 430 km E-W and 385 km N-S while the diameter of the maximum geostrophic velocity was 180 km. Isotherm depression at the centre of the ring was approximately 500 m compared to the surrounding water and the temperature anomaly of the centre was 4°C higher at 500 m with respect to the edge. The APE and KE for the Winter ring were calculated to be 26.0×10^{15} J and 2.6×10^{15} J respectively. Maximum geostrophic velocities were 74 $cm.s^{-1}$ with respect to 1150 db. Translation speeds for the ring could not be determined.

Water masses observed at the centre of the Winter ring were compared with the water masses of the Cape Basin and Agulhas Current system and showed substantial differences from the South Atlantic water and a marked similarity to Agulhas Current water. Some modification of the Winter ring relative to Agulhas water was observed in the AAIW layer

and was ascribed to stripping off of the deeper layers in its movement away from the retroflection. The surface layer of the Winter ring was seen to correspond to cooled STMW, while a deep pycnostad between 800 and 950 m was observed. Three possible sources for this deep stad layer were suggested: the Agulhas Current itself; newly formed SAMW entrained from south of the Subtropical Front; and modified Agulhas Bank bottom water. It was evident that vortex stretching contributed to the enhanced height of this layer relative to similar pycnostads observed in the surrounding environment.

The Winter ring showed a deep isothermal (16.3°C) surface mixed-layer, extending from the surface to a depth of 320 m. This is the deepest mixed layer for Agulhas rings thus far reported and its formation was attributed to a combination of ocean to atmosphere heat exchange and wind mixing.

5.3 THE BEST RING

A cruise undertaken as part of the Benguela Sources and Transports (BEST) programme during June 1992 encountered another ring (35°47'S; 14°57'E) in approximately the same position as the Winter ring (35°16'S; 11°43'E). It was estimated that this ring was shed just prior to the onset of winter, during austral autumn, and its characteristics differed markedly from those of the Winter ring. Again CTD and XBT measurements were used to define and characterize the ring. The BEST-1 cruise was undertaken to deploy a line of inverted echo-sounders and current meters along 30°S and along a line extending south-west from Cape Town. Fortuitously the ring was at the mid-point of this southern line and its position was such that echo-sounder deployment positions were situated on either side and at the centre of the ring. The cruise was undertaken while this thesis was in an advanced state of preparation and a full analysis of the hydrographic data has not yet been completed. Some initial results are presented here, however, to enable a comparison of this ring with the other data presented.

The expression of the anticyclonic warm-core ring was evident throughout the water column, to 4500 m depth. The horizontal extent of the ring was 300 km (E-W) x 260 km (N-S). Vertical temperature sections

for the ring are shown in Figure 5.24. Depression of the 10°C isotherm was 350 m. The temperature anomaly of the centre with respect to the edge was 4°C at 500 m. The BEST ring showed an isothermal surface layer of 16.45°C extending to 280 m depth. There was no evidence of a lower stad, possibly due to the smaller size of the ring relative to the Winter ring.

The geostrophic velocity structure for the line of BEST CTD stations south-west of Cape Town relative to the deepest common level (Fig. 5.25), in this case the bottom, was calculated. A net volume flux of 12.4×10^6 $m^3.s^{-1}$ was observed crossing the line of stations towards the north-west. This excess was concentrated in the flow between the ring and the southern African coast. A shorter line of stations across the Cape Town eddy in November 1983 demonstrated a net northward flow of 13×10^6 $m^3.s^{-1}$ between the eddy and the coast (Gordon 1985).

5.4 COMPARISON OF AGULHAS RING CHARACTERISTICS

Comparative data for some Agulhas rings (Table 2i) are shown in Tables 2ii and 5i. Depression of the 10°C isotherm (Table 2ii) for most of these rings was 300-400 m. The two anomalous rings, R90.4 (the Winter ring) and R87.1 (SCARC ring Susan), had isotherm depressions of 510 and 145 m respectively. On the other hand, other rings with a more westerly motion, being further south and closer to subantarctic water (R83.2 [ARC Cape Town] and R87.4 [SCARC Erina]) also showed large isotherm depressions. R87.1 (SCARC Susan) was very close to the continental shelf, possibly accounting for the small isotherm depression. However, R87.5 (SCARC Helen), very far south, did not show excessively large isothermal depression. This was possibly due to either the line of data not bisecting the ring or the ring being not completely detached and actually part of R87.4 (SCARC Erina), to the north.

The radii of Agulhas rings varied from 90 to 150 km. Radii in Table 2ii represent the radius of maximum azimuthal velocity where this was known. Other radii in the Table are for the distance at which the eddy shear signature disappears and thus represent a maximum radius. The Vema ring which is discussed in detail in this Chapter was one of

the largest of those considered. Of the rings studied in sufficient detail within the South Atlantic (Cape Town, Vema, Winter, BEST) three showed marked elipticity (Vema, Winter, BEST). Whether this is typical of Agulhas rings is uncertain. However, diagrams of the Discovery ring from GEOSAT altimetry also suggest that it was elliptical during much of its passage through the Cape Basin (Gordon and Haxby 1990).

As has been seen, some Agulhas rings retain their Agulhas water mass characteristics (refer to Table 2iii, and Table 2iv, for extremes and water types associated with the major water masses of interest in the South Atlantic and South Indian Oceans) with little evidence of intermixing with the South Atlantic thermocline at the core (Winter ring). Further from the retroflection, although there are some modifications to the original Agulhas characteristics, the origin of the water is still identifiable (Vema ring; Oceanus ring: McCartney and Woodgate-Jones 1991; Discovery ring: Gordon and Haxby 1990). McCartney and Woodgate-Jones (1991) give the explanation for this in the dynamics of the transfer of water within mesoscale eddies. The longer time since shedding allows greater opportunity for mixing of the core waters. Indeed McCartney and Woodgate-Jones (1991) suggest that most of the original water may be stripped away within one or two eddy diameters, leaving a greatly reduced cone of the source water. However, some rings close to the retroflection experience substantial mixing of the core water with the South Atlantic thermocline (e.g. Cape Town eddy: Olson and Evans 1986, Chapman *et al.* 1987, Fine *et al.* 1988).

Rossby numbers (R_o = V/fL) for Agulhas rings (Table 5i) show that, in spite of the elliptical nature of some of the rings, non-linear advective terms can be ignored and the assumptions allowing the use of the two-layer model are valid. The most linear of the rings is the Vema ring, the most non-linear the Winter ring. Burger numbers, estimating the importance of the isotherm displacement relative to the length scale of the rings, calculated for the rings show that interface displacement and interface depth relative to the length scale for both the Cape Town eddy and the Winter ring are greater than other rings shown in the Table. Both these rings showed evidence of a lower stad in the water column at the centre.

The ratio of available potential (APE) to kinetic (KE) energies is seen to increase with distance from the retroflection: the Cape Town and Agulhas eddies (Olson and Evans 1986), relatively recently shed, have the lowest ratios, the Vema ring, shed six months prior to detection, the highest. The Winter ring is somewhat anomalous. In approximately the same position as the Cape Town eddy (Fig. 2.5), slightly further west, it could have been expected to have nearly the same characteristics. However, its energy ratio is a factor of two greater than that of the Cape Town eddy. The Vema ring, in spite of its greater distance from the retroflection, shows one of the highest values of APE in the Table. These observations suggest that the Vema ring was atypical.

Agulhas rings within the South Atlantic thus show a range of characteristics. As a class, however, they are amongst the most energetic in the World Ocean (Olson and Evans 1986) and their influence on the Cape Basin through which they pass could be profound. The following Chapters examine and discuss this influence. Interaction of the Vema ring with a filament from the Benguela upwelling frontal system is considered in the light of possible effects on the fisheries of the shelf region; and heat, salt, and energy fluxes calculated for the three rings discussed in this Chapter are put into the context of their influence on the global thermohaline circulation.

Acknowledgements: Marten Gründlingh (CSIR) and John Taunton-Clark (SFRI) were responsible for extracting and producing the GEOSAT data; Kobus Agenbag (SFRI) generated the NOAA satellite images and did the feature tracking.

Sources: DUNCOMBE RAE, C.M., SHANNON, L.V. and F.A. SHILLINGTON 1989 - An Agulhas ring in the South Atlantic ocean. *S. Afr. J. Sci.* 85, 747-748.

DUNCOMBE RAE, C.M. and F.A. SHILLINGTON (in prep.) - A winter ring from the Agulhas.

DUNCOMBE RAE, C.M., SHILLINGTON, F.A., AGENBAG, J.J., TAUNTON-CLARK, J. and M.L. GRÜNDLINGH 1992 - An Agulhas ring in the South Atlantic Ocean and its interaction with the Benguela upwelling frontal system. *Deep-Sea Res.* 39(11/12): 2009-2027.

CHAPTER 6: BENGUELA SYSTEM AND AGULHAS RING INTERACTIONS

Coastal upwelling zones are well-known features of eastern boundary currents (Shannon 1985). It has recently been shown (Flament *et al.* 1985) that large volumes of cool deep water can be transported away from the coast, often in the form of narrow filaments or jets extending perpendicular to the coast. In the Benguela region, Lutjeharms *et al.* (1991) have identified several extremely long filaments extending hundreds of kilometres from the coast. Previous authors have speculated about Agulhas rings interacting with these Benguela frontal filaments and concrete evidence for such an interaction is presented here. The implication of an Agulhas ring drawing a large volume of upwelled frontal water away from the coastal region and its effect on the anchovy fishery is discussed.

6.1 RING-FILAMENT INTERACTION

Two sources of information revealed that the Vema ring entrained mature upwelled water from the Benguela Front. The first is the NOAA-11 satellite imagery for 15 June 1989, one month after the CTD transects, and the second is the appearance of low salinity (35.2 psu) water at the north-western corner of the CTD transect (Stns 8 and 9, Fig. 5.3). Referring first to the satellite imagery (Fig. 2.12), it can be seen that a cool filament of surface water with a temperature of 16.6-17°C had been entrained by the ring. This filament was also visible on other NOAA-11 images (not shown) for 24 and 30 April 1989. Using the manual feature-tracking method (Agenbag and Shannon 1988), surface velocity vectors of the order of 50 $cm.s^{-1}$ were derived (Agenbag 1992, Duncombe Rae *et al.* 1992b) in the vicinity of the cool filament and the outer edge of the ring (Fig. 5.11b). The low salinity water (35.2 psu) in Stations 8 and 9 between 50 and 150 m can be satisfactorily explained by noting that Shannon (1985) finds a salinity minimum of 35.2 psu for TS curves in the region 20° to 30°S; 7° to 18°E in the upper surface layer near the coast.

Shillington *et al.* (1990) reported that the filament they investigated (26°S; 12.5°E) had surface water with temperatures of 13° to 18°C and a salinity of 35.2 psu (between 0 and 130 m). The westward extremity

of their filament extended to 27°S; 12°E, some 340 km east of the centre of the ring being discussed here, or 160 km north of the base of the filament entrained by the ring (Fig. 5.11a). Unfortunately no simultaneous TS measurements were available from the Benguela Frontal region at the time of these cruises, but from the evidence presented above, the source region of the low salinity water is assumed to be the Benguela Frontal region.

The possible effect of such a ring on the Benguela system can be gauged by making a comparison between the volume that is normally contained in the Benguela region, and that which could be entrained by an Agulhas ring in the vicinity of the one reported here. Figure 6.1 is a schematic representation that summarizes the interaction of the ring with the Benguela Upwelling region. By taking the dimensions of the upwelling area as shown in Figure 6.1, the volume of water contained in the Benguela system can be calculated to be 1×10^{13} m^3. The volume associated with an annulus, representing a filament surrounding the ring, of width 50 km, diameter 300 km and depth 100 m, is approximately 0.5×10^{13} m^3.

Assuming that a velocity of 25 $cm.s^{-1}$ is associated with the surrounding cool filament (Fig. 5.11b shows surface velocities up to 70 $cm.s^{-1}$, but a more conservative figure is preferred in line with the geostrophic velocity calculation) and allowing the water to flow through an area 50 km wide by 100 m deep at 25 $cm.s^{-1}$, a time of 46 days is estimated to be required to entrain the volume of the annulus, 0.5×10^{13} m^3. The measured drift of the ring was 230 km over an interval of 42 days so that in a period of 1-2 months the ring will remain within an area likely to interact with the Benguela region. If the ring has a solid body rotation with a speed of 25 $cm.s^{-1}$ at its edge, and a diameter of 150 km, it will rotate once in 46 days. The water entering the filament is supplied by the coastal upwelling and the shelf edge-jet as feature tracking results have shown (Agenbag 1992). Velocities associated with the shelf-edge jet are in excess of the value used to compute the ring/filament interaction above (Nelson 1989, 1991) and it is feasible that the amount of water capable of being entrained by the ring is supplied from the jet.

6.2 EFFECT ON ANCHOVY RECRUITMENT

It is clear that Agulhas rings interacting with the Benguela Front could have significant effects on the inshore upwelling ecosystem. Acoustic estimates of the spawner biomass of the South African anchovy *Engraulis japonicus* decreased from 1.1 to 0.3 million tonnes between November 1988 and November 1990. Estimates of the abundance of 0-year-old fish at the time of their recruitment to the fishery in June were of the order of 130 000 tonnes in both 1989 and 1990, compared with a mean of about 460 000 tonnes in the period 1985-1988 (I. Hampton, Sea Fisheries Research Institute, pers. comm.). In a report prepared by the Sea Fisheries Research Institute (S.F.R.I. 1991) exact causes for the decreased abundance of anchovy could not be pinpointed. Of the factors that might have contributed to the decline in the abundance of anchovy, i.e. fishing, predation or environmental conditions, all but environmental factors were considered of minor influence during the 1988/89 season. However, at the time of the decline in anchovy, an Agulhas ring, identified on two cruises and in satellite imagery, was found to be entraining a filament from the Benguela upwelling front.

Elsewhere in the world, in the Gulf Stream and in the Kuroshio and East Australian current systems, rings and eddies shed from the currents can and do affect the continental shelf margins (Smith 1983). However, in those systems, the shelf zone and the current producing the eddies are within the same ocean basin. It is only off the south-west coast of Africa that eddies from a western boundary current, the Agulhas, can influence directly an eastern boundary current upwelling region, the Benguela.

The dynamics of rings on a rotating earth (the ß effect) are such that they tend to move westwards and equatorwards (Cushman-Roisin *et al.* 1990). In the current systems other than that off South Africa mentioned above, this motion would move the rings back towards the continental shelves they affect. Near the continental shelf, the rings are rapidly damped by being forced into contact with the continental slope (Kamenkovitch *et al.* 1986). In one such instance from the Gulf Stream, the total energy content of the ring was reduced by nearly 60% (Fornshell and Criess 1979). As a source of warm water, by generating shelf waves and by inducing mixing as they decay, the rings indirectly

affect the fishing industries of the shelf regions. In the Agulhas/ Benguela system, the rings tend to move away from the shelf forced by the β effect and the general dynamic topography. The shelf-edge topography then acts as a waveguide with minimal damping effect. If the ring has any effect on the shelf, it would act as a sink rather than as a source of water.

Eddies have been suggested as mechanisms for the loss of eggs and larvae from shelf regions elsewhere (Colton and Temple 1961, Butman *et al.* 1982). Further, Joyce *et al.* (1992) observed the transport of heat, salt and particulate matter from the continental shelf of the U.S.A. to the Gulf Stream by means of a warm-core Gulf Stream ring. Eddies as transport and retention mechanisms for plankton and phytoplankton have also been indicated in shelf, island and open-ocean environments (Boyar *et al.* 1973, Lobel and Robinson 1986, Perissinotto and Duncombe Rae 1990).

Mesoscale eddies have been known to interact with filaments from shelf-edge fronts in other parts of the world (Tintoré *et al.* 1990, Mooers and Robinson 1984) and have previously been found to be associated with the shelf-edge front of the Benguela system (Kaz'min and Sutyrin 1990, Shillington *et al.* 1990). However, those eddies interacting with the Benguela system were horizontally and vertically of too small an extent to have originated in the Agulhas Current (Duncombe Rae 1991), and they were probably generated by instabilities of the upwelling front (Strub *et al.* 1991).

In this section it is suggested that, in addition to other environmental factors outlined by the SFRI report (S.F.R.I. 1991), interaction between an Agulhas ring and the Benguela upwelling front was a contributing factor to the decline of the anchovy stock. It is hypothesized that the ring drew off pre-recruit juveniles and some late-stage larvae from the frontal jet in the vicinity of the nursery regions off the Orange River mouth, thereby removing them from the system and preventing their recruitment to the shelf fishery and the spawner stock.

6.2.1 FACTORS INFLUENCING RECRUITMENT

Anchovy spawn on the Agulhas Bank during October to January (Crawford 1981). Surface currents result in the transport of eggs and larvae from the Agulhas Bank around Cape Point and northwards. The strong shelf-edge jet carries the larvae farther north along South Africa's west coast, from the Cape Peninsula to the nursery and larval retention areas between St Helena Bay and the mouth of the Orange River (Shelton and Hutchings 1982, Boyd *et al.* 1992). The anchovy remain in those areas, recruiting to the purse-seine fishery off the west coast of South Africa. As adults, they return to the spawning grounds on the Agulhas Bank towards the end of their first year, swimming south close to the coast (Crawford 1980, Armstrong and Thomas 1989).

The SFRI report (S.F.R.I. 1991) identified fishing, predation and environmental conditions as possible causes of the poor anchovy year-classes of 1989 and 1990. Each of these is discussed very briefly as a cause below.

6.2.1.1 Fishing

Fish catches in 1987 and 1988, immediately prior to the decline in the anchovy stock, were high. However, good recruitment was also measured in those years. The biomass of the parent stock was estimated to be above average in November 1988 in spite of the high catches during 1987 and 1988. For that reason, the high catch rates were not implicated in causing the poor yearclass of 1989. Without some other factor such as adverse environmental conditions or heavy predation, recruitment should have attained at least average levels. After young anchovy were found to be scarce in June 1989 (Anon. 1989) fishing was stopped (at the end of July). Therefore, fishing alone could have had no further influence on the anchovy stock that year.

6.2.1.2 Predation

The larger predators of anchovy (cetaceans, seabirds, South African fur seals *Arctocephalus pusillus pusillus*, predatory fish such as snoek *Thyrsites atun* and squid *Loligo vulgaris reynaudii*) feed predominantly on larger sizes and tend to adjust their diet to the abundance of their prey (Nepgen 1979, Berruti 1987, Crawford 1987). As an example, this is clearly seen in the percentage of anchovy in the diet of Cape gannets *Morus capensis* (Fig. 6.2). The proportion of anchovy in the

diet of gannets closely follows the change in biomass of this prey species, as estimated by surveys. Predation by the larger predators was therefore probably not responsible for the poor anchovy year-class measured midway through 1989 (S.F.R.I. 1991). However, the proportion of anchovy in the diet of Cape gannets pin-points the timing of the most severe failure of anchovy recruitment (Fig. 6.3).

Predation of the larvae and eggs of the anchovy by planktivorous predators such as pilchard *Sardinops ocellatus* may have been higher in the 1988/89 spawning season than in previous years. However, there are no direct data to support this theory. Nevertheless, of other potential small predators, round herring and squid were abundant off western South Africa during 1989.

6.2.1.3 Environmental conditions

During the November 1988 acoustic survey of anchovy spawner biomass, it was found that, although spawner biomass was relatively high, the abundance of planktonic food for the spawning anchovy was very low on the western Agulhas Bank, a critical spawning region (Peterson *et al.* 1992). In fact, 16,9% of the fish were re-absorbing eggs, a condition usually associated with sustained poor conditions for feeding (Y.C. Melo, Sea Fisheries Research Institute, pers. comm.). During January 1989, warm water and low concentrations of chlorophyll *a* were encountered in the West Coast nursery areas, again indicating poor feeding conditions for anchovy larvae (S.F.R.I. 1991). Therefore, a series of adverse environmental conditions resulted in both poor food availability for spawning adult anchovy in the second half of the spawning season, and poor first-feeding conditions for larvae. However, no single major catastrophic event, such as the Benguela Niño of 1983/84, was identified (S.F.R.I. 1991). Anchovy in fact continued to contribute substantially to the diet of Cape gannets off western South Africa until May/June 1989 (Fig. 6.3).

6.2.2 DISCUSSION

In April 1989, an Agulhas ring was identified by means of expendable bathythermograph probes on a cruise of F.R.S. *Africana* between Cape Town and Vema Seamount (Fig. 5.1). In May 1989, a cruise of R.S. *Benguela* confirmed that the ring was of Agulhas origin. It was estimated that the ring was shed from the Agulhas retroflection south

of Cape Town during late December 1988 (Duncombe Rae *et al.* 1992b). Further, NOAA infra-red satellite imagery suggested that the ring was in the process of capturing a filament from the Benguela upwelling front (Duncombe Rae *et al.* 1989b). The first sign of this interaction with the Benguela upwelling front was seen in an image from 30 April 1989, when the base of the filament was just north of the Orange River. In images obtained in mid-June 1989, the filament is seen to extend in a loop, from between the Orange River and Lüderitz to nearly 800 km from the coast, revealing filament capture by the ring to be almost complete (Fig. 2.12). The *Benguela* survey in May 1989 confirmed the presence at the edge of the ring of frontal water from the coastal region of the Benguela system. The ring could have drawn off 5×10^{12} m^3 of upwelled surface water from the Benguela upwelling front over the period of the ring-filament interaction, representing a volume flux of 1.5×10^6 $m^3.s^{-1}$ (Lutjeharms *et al.* 1991, Duncombe Rae *et al.* 1992b).

The sharpest downward trend in acoustically determined spawner biomass of anchovy was detected between November 1988 and November 1989 (from 1 200 000 to 600 000 tonnes; Fig 6.4a), and in a similarly deduced abundance of 0-year-olds between June 1988 and June 1989 (from 500 000 to 180 000 tonnes; Fig. 6.4b). The most marked decline in the contribution of anchovy to the diet of Cape gannets feeding off western South Africa was between June and July 1989 (Fig. 6.3), coinciding with the period of the ring/filament interaction.

Juvenile anchovy have been found several times in the vicinity of the Orange River (Crawford 1981, Schülein 1986, Cruikshank *et al.* 1990). Acoustic surveys have established that the density of shoals of juvenile anchovy there can approach that of shoals on the traditional fishing grounds farther south. Indeed, shoals near the Orange River contribute a significant proportion of the recruitment to the fishery farther south (Cruikshank *et al.* 1990). Offshore transport in the upwelling zone off Lüderitz, north of the Orange River, constitutes a barrier to interchange between the Namibian and South African stocks of anchovy, which are thought to be relatively discrete (Crawford *et al.* 1988). Moreover, the coast around the mouth of the Orange River is the most northerly nursery area for the South African anchovy stock (Cruikshank *et al.* 1990). In February 1989, anchovy post-larvae and juveniles were concentrated near the mouth of the Orange River, just

south of Port Nolloth (29°15'S, 16°55'E), and in the vicinity of the Olifants River mouth (31°42'S, 18°15'E) (O'Toole and Hampton 1989).

Even if the interaction of the ring with the filament is vastly overestimated, the northernmost nursery areas for the South African anchovy stock were well within the possible range of influence of the ring. The waters off the mouth of the Orange River were adjacent to the base of the affected filament at the time the interaction began. Maximum surface current speeds within the filament, estimated from feature-tracking in the satellite imagery, were of the order of 70 $cm.s^{-1}$ (Duncombe Rae *et al.* 1992b), far greater than the swimming speed of even adult anchovy (Nelson and Hutchings 1987). Any larvae or pre-recruits still present in the frontal jet from the time of the first interaction of the ring with the front would have had great difficulty resisting entrapment by the ring. The base of the filament was 100 km wide and current speeds of up to 50 $cm.s^{-1}$ were indicated there. Although the greatest speeds of the water entering the filament are in the frontal jet, some shelf water is also involved (Agenbag 1992).

Therefore it is suggested that, with the water drawn off from the upper layers of the Benguela system, the passing ring may have extracted a significant proportion of pre-recruit anchovy, and possibly also larvae, from the coastal waters. This would have precluded their subsequent migration south to the Agulhas Bank and could have contributed to the very low abundance of 0-year-old anchovy measured acoustically in June 1989. Also, of course, it would then explain the simultaneous decline in availability of anchovy to the purse-seine fishery and Cape gannets (Fig. 6.3). The poor year-class would have drastically reduced the spawner biomass of anchovy in 1989, as indeed was subsequently measured (Fig. 6.4). This reduced spawner stock may in turn, and assuming some still-to-be-proved stock-recruit relationship, have been responsible for the poor year-class in the following year (1990).

It is estimated that nine rings are shed from the Agulhas retroflection region per year (Lutjeharms and Van Ballegooyen 1988a), of which some may enter the Antarctic Circumpolar Current and return to the Indian Ocean. Gordon and Haxby (1990) used satellite altimeter data to

estimate that five rings per year enter the South Atlantic. Of these, most move farther west than the ring detected in 1989. In addition, as the structure of Agulhas rings is dynamically coherent up to depths of 1000 m (McCartney and Woodgate-Jones 1991) and evident throughout the water column (Gordon and Haxby 1990), the proximity of the rings to the coastline is limited by the shelf topography. Rings can be expected to interact only with very long filaments from the upwelling system and such extreme filaments occur on average only 1.5 times per year (Lutjeharms *et al.* 1991). In the data from the *Discovery* ring (Mele *et al.* 1990, A.L. Gordon, Lamont-Doherty Earth Observatory, pers. comm.) anomalous salinity values in the edge of the ring suggest entrainment of a foreign water mass, possibly a Benguela upwelling filament although it is doubtful whether the ring was actively interacting with a filament at the time of its measurement. In spite of this, the likelihood of ring-filament interaction coinciding with the presence of large quantities of juvenile anchovy near the base of the filament can still be considered small.

Acknowledgment: Determining the timing of the collapse of the anchovy recruitment would not have been possible without access to the acoustic biomass data of Ian Hampton (SFRI), and the Cape gannet dietary data provided by Rob Crawford (SFRI). Rob Crawford and Alan Boyd's (SFRI) knowledge of the anchovy life-cycle were of great assistance in concluding the possible connection between the ring-filament interaction and the decline in yearclass strength.

Sources:

DUNCOMBE RAE, C.M., BOYD, A.J. and R.J.M. CRAWFORD 1992 - 'Predation' of anchovy by an Agulhas ring: a possible contributory cause of the very poor yearclass of 1989. In *Benguela Trophic Functioning.* PAYNE, A.I.L., BRINK, K.H., MANN, K.H. and R. HILBORN (Eds). *S. Afr. J. mar. Sci.* 12: 167-173.

DUNCOMBE RAE, C.M., SHILLINGTON, F.A., AGENBAG, J.J., TAUNTON-CLARK, J. and M.L. GRÜNDLINGH 1992 - An Agulhas ring in the South Atlantic Ocean and its interaction with the Benguela upwelling frontal system. *Deep-Sea Res.* 39(11/12): 2009-2027.

CHAPTER 7: AGULHAS RINGS AND INTERBASIN EXCHANGE

The formation of deep water in the Norwegian Sea (Warren 1981, Killworth 1983a) forces the circulation of North Atlantic Deep Water (NADW) through the World Ocean (Taft 1963), in what has been called the "thermohaline conveyor belt" (Broecker 1987, 1991). Shedding of rings from the Agulhas Current retroflection and intermittent direct flow have been suggested as mechanisms for the return of thermocline water to balance the outflow of NADW from the North Atlantic (Gordon 1986).

Whether the Agulhas Current is indeed a conduit for the return of mass, salt and heat is a current topic of debate. Rintoul (1991) has given arguments, based on inverse analysis of historical hydrographic sections, favouring the Drake Passage as a preferred route and opposing the Agulhas Current as a mechanism for providing the return flow. Some qualified support has been provided for this view, for example from a general circulation model modified for the South Atlantic Ocean (Matano and Philander 1993). However, other global circulation models (Semtner and Chervin 1991, 1992, FRAM Group 1991, Webb *et al.* 1991) support Gordon's (1986) hypothesis.

From work on the freshwater budget of the ocean, Wijffels *et al.* (1992) suggested that prior diagnostic inverse calculations (e.g. Fu 1981, 1986, Wunsch *et al.* 1983, Rintoul 1991) were based on incorrectly specified salt transports. Wijffels *et al.* (1992) showed that 0.7×10^6 $m^3.s^{-1}$ flows through the Bering Strait, across the Arctic Ocean and speculated that this could significantly alter the assumptions about the transport required by the thermohaline conveyor. Alternatively, Gordon *et al.* (1992) suggested a combined Drake Passage/ Agulhas Current scenario: that the NADW outflow is balanced by flow through the Drake Passage, which first circulates through the Indian Ocean before re-entering the South Atlantic via the Agulhas Current. Matano and Philander (1993) also suggest that the flux of the Antarctic Circumpolar Current (ACC) through the Drake Passage could control the thermohaline circulation of the South Atlantic Ocean (Matano 1993). They propose that when the transport of the ACC is high and the Subtropical Front is at its most northward extent, the main supplier of thermocline waters could be the flow of Intermediate water through the

Drake Passage, modified by heat exchange with the atmosphere. When the ACC transport is low, the warmer, saltier Agulhas Current transfer may become dominant.

In this Chapter, some volume, heat and salt flux results from the recently encountered Agulhas rings discussed in Chapter 5 are presented in the context of the requirements of the ocean conveyor. No attempt is made to resolve the global circulation debate from these results, which indicate that both heat and salt are transported by Agulhas rings from the Indian Ocean via the Agulhas Current system to the South Atlantic. The resolution of the problem of whether this transfer south of Africa represents a direct closing of the global ocean thermohaline conveyor, or merely a link in a coupled Indo-Atlantic super-gyre, is left to further study.

7.1 REQUIREMENTS OF THE CONVEYOR BELT

The return flow required to balance the global thermohaline circulation can be gauged from the rate of formation of NADW. Estimates of this formation rate vary from 9×10^6 $m^3.s^{-1}$ (Speer and Tziperman 1992) through 14×10^6 $m^3.s^{-1}$ (Warren 1981) to greater than 20×10^6 $m^3.s^{-1}$ (Broecker 1979).

Another indicator of the mass flux involved in the global circulation is the volume of water crossing the equator. Speer and McCartney (1991) estimated the total southward deep-water transport near 10°N close to the western boundary of the Atlantic Ocean to be about 25×10^6 $m^3.s^{-1}$. Further south they found the deep water transport close to the western boundary to be slightly less, of the order of 23×10^6 $m^3.s^{-1}$. These strong flows near the boundary are balanced in part by opposing flows in the central and eastern part of the basin since the net transports across the equator in the Atlantic are much less. In sections along the equator across the Atlantic there is general agreement among authors as to the net transports in the upper and deep layers. Net northward transport of surface, central and intermediate waters across the equator is approximately 8×10^6 $m^3.s^{-1}$ (Sverdrup *et al.* 1942; 9×10^6 $m^3.s^{-1}$ including the bottom water) to 10×10^6 $m^3.s^{-1}$ (Roemmich 1983). This surface flow was found to be balanced by a southward flow of 9×10^6 $m^3.s^{-1}$ in the deep water (Sverdrup *et al.* 1942, Wright 1970).

Within the Agulhas Current, measurements of the flow of the current when it separates from the shelf vary from 95×10^6 $m^3.s^{-1}$ (Gordon *et al.* 1987a) to 136×10^6 $m^3.s^{-1}$ (Jacobs and Georgi 1977) relative to the bottom. The retroflection is incomplete, however, and some of the current, from 3 to 14×10^6 $m^3.s^{-1}$, flows into the South Atlantic (Shannon 1966, Bang 1973, Gordon 1985, Shannon *et al.* 1990). In addition, Agulhas rings shed from the retroflection introduce a quantity of Indian Ocean water into the South Atlantic (Gordon and Haxby 1990).

7.2 FLUXES OF AGULHAS RINGS

Considering the net flux across the equator, it is reasonable to assume that the conveyor belt involves a southward flow of approximately 10×10^6 $m^3.s^{-1}$ in the deep water, carrying approximately 3.6×10^8 $kg.s^{-1}$ of salt which must be replaced in the upper layers. Whether or not this upper layer flow across the equator is supplied by the Agulhas Current in the form of rings shed from the retroflection and intermittent direct flow, the flux calculated for the transport by rings is of a similar order of magnitude. Estimates of the interbasin transfer between the Indian and the Atlantic Oceans are shown in Table 7i. Gordon and Haxby (1990) calculated a volume flux per ring of 2 to 3×10^6 $m^3.s^{-1}$ of water above the Antarctic Intermediate Water layer, while flow between the ring and the continent which was not balanced across the ring amounted to 10×10^6 $m^3.s^{-1}$.

Bennett (1988) used the 1985 data to obtain values of the heat flux westward across the retroflection region and found a heat flux of between -0.029 and -0.22 PW (westward) above 2000 m to be associated with westward transport of $12 \pm 8 \times 10^6$ $m^3.s^{-1}$ inshore of the Agulhas water-mass boundary and an eastward return transport on the south side of the Return Current. Exchange with the atmosphere could only account for 50% of the westward heat flux implying that "the steady upper-level heat flux must be balanced by more remote heat sinks" (Bennett 1988, p. 129).

Duncombe Rae *et al.* (1989b) calculated that the Vema ring contained an excess heat content relative to the South Atlantic of 7.8×10^{20} J over the upper 750 m. This was calculated from an average temperature difference between the core waters of the Vema ring and the surrounding

South Atlantic, taken along isobaths and integrated over the area and volume of the ring. It may be more informative to consider the temperature and salinity anomalies of Agulhas rings relative to representative profiles of the Agulhas Current and the South Atlantic Ocean. This is considered in the next section.

7.3 HEAT AND SALT ANOMALIES OF AGULHAS RINGS

In an attempt to define more precisely the heat and salt content of rings, and assess the ring's possible influence on the South Atlantic, sections of the temperature difference between ring cores and representative profiles in the South Atlantic and Agulhas current are presented and discussed.

Since mixing of the core waters into the surroundings can generally be considered to take place along isopycnals, the property differences are calculated at identical density levels in the ring and reference profiles. The differences are plotted at the isopycnal depth in the ring profile, giving an indication of the volume of water with the property difference, which would not be evident if the differences were plotted against density. The reference profile for the Agulhas Current water in the figures is taken from the Agulhas Bank Boundary Processes Cruise (ABBP, *Africana* V099, Stn. A12800), in January 1992, in the core of the Agulhas Current. This profile is a representative Agulhas Current core profile as shown by the comparison of this profile with another (Stn. C54: Valentine *et al.* 1988) taken in approximately the same place on the SCARC cruise, in February 1987 (Fig. 7.1). The reference profile for the South Atlantic is taken from the Benguela Sources and Transports Programme deployment cruise (BEST-1, *Africana* V105, June 1992) near the Walvis Ridge. These two profiles are also used in the comparison of the Winter ring core water with Agulhas and South Atlantic waters (Figs 5.21 and 5.22).

Sections of the temperature differential relative to the Agulhas Current along isopycnals across the Vema and Winter rings (Fig. 7.2) showed that the core of the Winter ring (Fig. 7.2b) was little changed from Agulhas Current water. Most of the water within the ring was within 1°C of the source water and a large section of the water column at the ring centre (between 300 and 750 m) was no different from

Agulhas water at the same density. The large difference in the upper 100 m indicated that the heat loss from the upper layers of the ring reduced it to the same temperature difference as the surrounding South Atlantic. The heat losses from the Vema ring referenced to the Agulhas Current (Fig. 7.2a) showed that the volume of nearly pure Agulhas water (within 1°C) had been reduced to a cone of water above 400 m depth. Mixing processes (McCartney and Woodgate-Jones 1991) contaminated the pure Agulhas water below that level.

Referenced to South Atlantic water, the entire core of the Vema ring was approximately 2°C warmer than water at the same density level in the South Atlantic (Fig. 7.3a). The conical shape indicating erosion of the lower levels was not evident. This may be due to the greater differential between ring and South Atlantic water in the deeper levels closer to the time of shedding as evidenced by the temperature difference profile for the Winter ring (Fig. 7.3b) where water at the depth of the lower stad (750 to 1000 m) was greater than 5°C warmer than the South Atlantic water of the same density. This suggests that the appearance of a lower stad (whatever its source and cause, whether produced dynamically in the formation of the ring or entrained from the surroundings: see Chapter 5) may be instrumental in maintaining the temperature difference between the invading ring and the South Atlantic gyre. However, this is inconclusive since no evidence is available for the presence of a pronounced lower stad in the early hydrographic structure of the Vema ring.

For salinity differences relative to the Agulhas Current taken in the same way as for the temperature differences, the same features are evident (Fig. 7.4). Note that the portion of the salinity differential profile indicating characteristics within the Vema ring core closest to Agulhas water lies at the same depth as the isohaline layer used to identify the Vema ring as originating from the Agulhas (Chapter 5). The Winter ring showed large salinity differences from the Agulhas at the lower stad. This reinforces the impression that the presence of a lower stad in the Winter ring is due to a dynamic process entraining a modified source of water during ring formation rather than being purely derived from the source Agulhas Current water.

Relative to South Atlantic water, the Vema ring core contained an excess of 0.4 psu between 200 and 550 m (Fig. 7.5a). The majority of the ring core contained an excess of 0.1 psu. The Winter ring showed much higher salinity differences relative to South Atlantic water, up to 0.8 psu (Fig. 7.5b).

At the translation rate of the Vema ring this represented a heat energy flux of 0.2×10^{15} W associated with a volume flux of 13×10^{6} $m^3.s^{-1}$ and a salt flux of 2×10^{13} $kg.s^{-1}$ during the passage of the ring.

From thermal satellite imagery, Lutjeharms and Van Ballegooyen (1988a) estimated nine ring shedding events per year, while Gordon and Haxby's (1990) satellite altimeter data showed five rings entering the South Atlantic per year. Feron *et al.* (1992) determined eighteen pulses, corresponding to six ring-shedding events per year, from principal component and harmonic analysis of 150 weeks of GEOSAT altimeter data.

Heat loss from the upper layers of the Vema ring between the cruises of *Africana* in April and *Benguela* in May was of the order of 1.8×10^{19} J (Duncombe Rae *et al.* 1989b). This is consistent with an estimated heat loss of 80 $W.m^{-2}$, which is considered to be the climatic mean for this region (Höflich 1984). Duncombe Rae *et al.* (1989b) also estimated that the volume flux of the ring per annum was about 1.2×10^{6} $m^3.s^{-1}$ per ring per year.

In addition to the thermal energy input, the available potential and kinetic energies associated with the Vema ring were calculated (38.8 and 2.3×10^{15} J respectively). These values are of the same order as those obtained for similar Agulhas rings by Olson and Evans (1986) and also an order of magnitude greater than similar Gulf Stream rings. The kinetic energy of the Vema ring is slightly lower, suggesting that some of this energy has already been lost by friction to the South Atlantic, due to the longer time elapsed since shedding from the Agulhas.

7.4 DISCUSSION

In this Chapter, some results of volume and heat flux transports have been presented for the Agulhas rings discussed in Chapter 5. Some

previously published results have been recalculated and the compensating fluxes of the global ocean circulation have been reviewed.

It is seen that the Agulhas rings and the associated flows between the rings and the South African shelf represent a pulsed, "instantaneous", input equivalent to the volume, heat and salt budget requirements of the thermohaline circulation. Each ring provides its input over a period of approximately one month. Intuitively then, for the flux of Agulhas rings to close the thermohaline circulation alone, Agulhas rings should move through the South Atlantic at the rate of one per month. Results from analysis of satellite observations (Lutjeharms and Van Ballegooyen 1988a, Gordon and Haxby 1990, Feron *et al.* 1992) suggest that from 50 to 80% of this requirement may be met.

The differences between the property values of Agulhas rings and their "source" and "destination" water masses were also examined. It is noted that the Agulhas rings retain their Agulhas water characteristics, and can be seen to be significantly distinct from the South Atlantic surroundings into which they move. Some of the comparisons need to be treated with caution however. It is not established that the thick isopycnal layer (lower stad) in the Winter ring is typical of newly shed Agulhas rings and since no further measurements were made on this ring, it is not known how the presence of this layer affects the later evolution of the ring. The seasonal variations which might be present due to the different times of sampling of the comparison stations is also unknown. The South Atlantic station was sampled in winter (June) and could thus reasonably be expected to correspond in season to the sampling of the Vema ring, in late autumn/early winter (May), and the Winter ring, in late winter (August). The Agulhas Current station was sampled in summer (January) and might be expected to differ seasonally from the rings. However, it is evident from Figure 7.2 that only the upper few hundred metres show any marked differences which might be due to seasonality. Parts of the rings' water column show no difference from the Agulhas profile and indeed the Winter ring shows large positive anomalies (opposite to that which would be expected if seasonality were an issue) due to the presence of the thick isopycnal layer.

Sources:

DUNCOMBE RAE, C.M., SHANNON, L.V. and F.A. SHILLINGTON 1989 - An Agulhas ring in the South Atlantic ocean. *S. Afr. J. Sci.* 85, 747-748.

DUNCOMBE RAE, C.M. and F.A. SHILLINGTON in prep. - A winter ring from the Agulhas.

DUNCOMBE RAE, C.M., SHILLINGTON, F.A., AGENBAG, J.J., TAUNTON-CLARK, J. and M.L. GRÜNDLINGH 1992 - An Agulhas ring in the South Atlantic Ocean and its interaction with the Benguela upwelling frontal system. *Deep-Sea Res.* 39(11/12): 2009-2027.

CHAPTER 8: CONCLUSION

The major accomplishments of this work are three-fold: it describes the first hydrographic detection of an Agulhas ring within the South Atlantic Ocean to which a second cruise has been able to return; it describes for the first time, the confirmed interaction of an Agulhas ring with a filament from the Benguela upwelling system; and it describes some unique features observed in an Agulhas ring shed during winter from the Agulhas retroflection. Three rings encountered hydrographically in the South Atlantic are described: the Vema, Winter, and BEST rings. It has been possible to use these and other data to characterize Agulhas rings, establish some limits to their ability to contribute to the global thermohaline circulation and to speculate on their possible influence on the Benguela upwelling ecosystem.

8.1 CHARACTERISTICS OF AGULHAS RINGS

Two Agulhas rings encountered hydrographically within the South Atlantic Ocean were examined in detail. One ring, the Vema ring, was surveyed on two cruises. Temperature sections from these two cruises were used to calculate heat fluxes to the atmosphere and the mean drift rate of the ring, first encountered during April 1989. The second, more detailed, CTD survey, in May 1989, revealed the basic physical structure of the ring in a position adjacent to the Benguela Frontal region. Water mass and nutrient characteristics in the upper 300 m at the centre of the ring, energy considerations and the general translation of the ring revealed by GEOSAT altimetry, confirmed its Agulhas origin.

The ring was elliptical, with dimensions 530 km from east to west, and 180 km from north to south. Maximum geostrophic surface speeds of 55 $cm.s^{-1}$ with respect to 1150 db were calculated at the north-western edge of the ring. Using a two-layer model (Olson and Evans 1986) the available potential energy (APE) and kinetic energy (KE) of the ring were estimated to be 38.8 and 2.3×10^{15} J respectively. A translation speed of 6.4 $cm.s^{-1}$ was determined from different observations (Duncombe Rae *et al.* 1992b).

A second ring was encountered in August 1990 and the data examined in detail. This anticyclonic ring shed from the Agulhas retroflection in late June or early July 1990 (austral mid-winter) was discovered in the South Atlantic Ocean south-west of Cape Town. The maximum diameter of the ring was 430 km E-W and 385 km N-S while the diameter of the maximum geostrophic velocity was 180 km. Isotherm depression was approximately 500 m and the temperature anomaly of the centre with respect to the edge was 4°C at 500 m. The APE and KE for the Winter ring were calculated to be 26.0×10^{15} J and 2.6×10^{15} J respectively. Maximum geostrophic velocities were 74 $cm.s^{-1}$ with respect to 1150 db. Translation speeds for the ring could not be determined.

Water masses observed at the centre of the Winter ring were compared with the water masses of the Cape Basin and Agulhas Current system and showed substantial differences from the South Atlantic water and a marked similarity to Agulhas Current water. Some modification of the Winter ring relative to Agulhas water was observed in the AAIW layer and was ascribed to stripping off of the deeper layers in its movement away from the retroflection. The surface layer of the Winter ring was seen to correspond to cooled STMW, while a deep pycnostad (between 800 and 950 m) had the characteristics of SAMW, but could not be positively identified as such since other dynamic explanations of this layer within rings exist. Three possible sources for this thick pycnostad were suggested: the Agulhas Current itself; modified Agulhas Bank bottom water; and water entrained from the Subtropical Front during ring shedding.

The Winter ring showed a deep isothermal (16.3°C) surface mixed-layer, extending from the surface to a depth of 320 m. This is the deepest mixed layer for Agulhas rings thus far reported and its formation was attributed to a combination of ocean to atmosphere heat exchange and wind mixing.

In a comparative study of Agulhas rings encountered in the South Atlantic, depression of the 10°C isotherm for most of rings was observed to be 300-400 m. Anomalously large or small isotherm depressions were identified and could have been attributable to the time of sampling of the ring relative to the time of ring shedding (large isotherm depressions were identified close to the retroflec-

tion), the surrounding water mass conditions (rings with a more westerly motion, being further south and closer to subantarctic water showed large isotherm depressions) or artifacts of the sampling strategy (some rings may not have been adequately covered in the sections across them).

The radii of Agulhas rings varied from 90 to 150 km. Marked elipticity of ring radius was observed in some of the rings encountered (Vema, Winter, and BEST rings). Whether this is typical of Agulhas rings is uncertain. However, diagrams of the Discovery ring from GEOSAT altimetry also suggest that it was elliptical during much of its passage through the Cape Basin (Gordon and Haxby 1990).

In general Agulhas rings retain their Agulhas water mass characteristics sufficiently to provide an unambiguous identification of their origin. Some rings show little evidence of intermixing with the South Atlantic thermocline at the core, in general those closer to the retroflection. Further from the retroflection modifications to the original Agulhas characteristics were evident (Vema ring; Oceanus ring: McCartney and Woodgate-Jones 1991; Discovery ring: Gordon and Haxby 1990). The longer time since shedding allows greater opportunity for mixing of the core waters. However, some rings close to the retroflection experience substantial mixing of the core water with the South Atlantic thermocline (e.g. Cape Town eddy: Olson and Evans 1986, Chapman *et al.* 1987, Fine *et al.* 1988).

The ratio of available potential (APE) to kinetic (KE) energies was seen to increase with distance from the retroflection: the Cape Town and Agulhas eddies (Olson and Evans 1986), relatively recently shed, have the lowest ratios, the Vema ring, shed six months prior to detection, the highest. The Winter ring is somewhat anomalous. In approximately the same position as the Cape Town eddy (Fig. 2.5), slightly further west, it could have been expected to have nearly the same characteristics. However, its energy ratio is a factor of two greater than that of the Cape Town eddy. The Vema ring, in spite of its greater distance from the retroflection, shows one of the highest values of APE in the Table. These observations suggest that the Vema ring was atypical. This is supported by the observations of Feron *et al.* (1992) who examined variability of the Agulhas retroflection from

GEOSAT imagery. Their data show an anomalously large peak in the time for decorrelation of the retroflection during the period when the Vema ring was shed.

Agulhas rings within the South Atlantic thus showed a range of characteristics. As a class, however, they are amongst the most energetic in the World Ocean (Olson and Evans 1986) and their influence on the Cape Basin through which they pass could be profound.

8.2 AGULHAS RINGS AND THE BENGUELA UPWELLING SYSTEM

NOAA-11 infra-red imagery and feature tracking showed that water from the Benguela upwelling frontal had been entrained into the outer perimeter of the Vema ring. Water mass characteristics of hydrographic stations occupied at the edge of the ring confirmed that the filament originated in the upwelling region. It was demonstrated that this interaction could have exerted significant influence on the functioning of the upwelling system. For this interaction to be effective, the Agulhas ring had to be in close proximity to the Benguela for a month or more. NOAA-11 images for 24 April 1989 showed that the ring had already been interacting with the Benguela, forming a long, cool filament. It was postulated that the Agulhas ring/Benguela Front interaction could have important implications for plankton and fisheries in the Benguela system and the interaction recorded during April - June 1989 was put forward as a possible contributor to the very poor yearclass of anchovy of 1989.

8.3 AGULHAS RINGS IN THE GLOBAL CIRCULATION

The heat, salt and volume fluxes associated with the rings examined in this study were compared to the volume flux associated with the thermohaline circulation of the conveyor belt. Analysis of the temperature and salinity differences between sections across rings and profiles representative of the Agulhas Current and South Atlantic Ocean suggest that Agulhas rings do transfer a significant flux of these properties from the Indian to the Atlantic Ocean. Instantaneous fluxes of the rings were approximately of the same order of magnitude as the cross-equatorial flow, but because only from 5 to 9 rings enter the South Atlantic in the course of a year the average flux contributed by

Agulhas rings may be less than the net flux required to balance the deep water outflow.

APPENDIX A: REFERENCES

AGENBAG, J.J. 1992 - *A procedure for the computation of sea-surface advection velocities from satellite thermal band imagery, with application to the south-east Atlantic Ocean.* Unpublished Ph.D. thesis, University of Cape Town: 394 pp.

AGENBAG, J.J. and L.V. SHANNON 1988 - A suggested physical explanation for the existence of a biological boundary at 24° 30'S in the Benguela system. *S. Afr. J. mar. Sci.* 6: 119-132.

ANON. 1985 - *Physical, Chemical and in-situ CTD Data from the Ajax Expedition in the South Atlantic Ocean, aboard RV Knorr. Leg I: 7 October - 6 November 1983. Leg II: 11 January - 19 February 1984.* University of California Scripps Institute of Oceanography and Texas A&M University Department of Oceanography. SIO Reference 85-24, TAMU Reference 85-4-D: 275pp.

ANON. 1989 - Anchovy recruitment poor, season closes. *S. Afr. Shipp. News Fishg. Ind. Rev.* 44(4): 22.

ARMSTRONG, M.J. and R.M. THOMAS 1989 - Clupeoids. In *Oceans of Life off Southern Africa.* PAYNE, A.I.L. and R.J.M. CRAWFORD (Eds). Cape Town; Vlaeberg: 105-121.

ARNAULT, S. 1987 - Tropical Atlantic geostrophic currents and ship drifts. *J. geophys. Res.* 92: 5076-5088.

BANG, N.D. 1970a - Major eddies and frontal structures in the Agulhas current retroflexion area in March, 1969. In *Proceedings of the Symposium on Oceanography in South Africa 1970.* Council for Scientific and Industrial Research: 16 pp.

BANG, N.D. 1970b - Dynamic interpretations of a detailed surface temperature chart of the Agulhas Current retroflexion and fragmentation area. *S. Afr. geogrl J.* 52: 67-76.

BANG, N.D. 1973 - Characteristics of an intense ocean frontal system in the upwell regime west of Cape Town. *Tellus* 25: 256-265.

BANG, N.D. and W.R.H. ANDREWS 1974 - Direct current measurements of a shelf-edge frontal jet in the Southern Benguela system. *J. mar. Res.* 32: 405-417.

BANG, N.D. and F.C. PEARSE 1970 - *Hydrological data. Agulhas Current Project, March 1969.* Data Report No 4. University of Cape Town; Institute of Oceanography: iii + 26 pp.

BENNETT, S.L. 1988 - *Where three oceans meet: the Agulhas retroflection region.* Ph.D. thesis, Woods Hole; Massachusetts Institute of Technology/Woods Hole Oceanographic Institution: xxvii + 367 pp. WHOI-88-51.

BERRUTI, A. 1987 - *The use of Cape gannets Morus capensis in management of the purse-seine fishery of the Western Cape.* Ph.D. thesis. Durban; University of Natal: 304 pp.

BOUDRA, D.B. and E.P. CHASSIGNET 1988 - Dynamics of Agulhas retroflection and ring formation in a numerical model. Part I: The vorticity balance. *J. phys. Oceanogr.* 18(2): 280-303.

BOUDRA, D.B. and W.P.M. DE RUIJTER 1986 - The wind-driven circulation in the South Atlantic-Indian Ocean - II. Experiments using a multi-layer numerical model. *Deep-Sea Res.* 33(4A): 447-482.

BOUDRA, D.B., MAILLET, K.A. and E.P. CHASSIGNET 1989 - Numerical modelling of Agulhas retroflection and ring formation with isopycnal outcropping. In *Mesoscale/Synoptic Coherent Structures in Geophysical Turbulence*. NIHOUL, J.C.J. and B.M. JAMART (Eds). Amsterdam; Elsevier: 315-335.

BOYAR, H.C., MARAK, R.R., PERKINS, F.E. and R.A. CLIFFORD 1973 - Seasonal distribution and growth of larval herring (*Clupea harengus* L.) in the Georges Bank-Gulf of Maine area from 1962 to 1970. *J. Cons. perm. int. Explor. Mer* 35(1): 36-51.

BOYD, A.J., TAUNTON-CLARK, J. and G.P.J. OBERHOLSTER 1992 - Spatial features of the near-surface and midwater circulation patterns off western and southern South Africa and their role in the life histories of various commercially fished species. In *Benguela Trophic Functioning*. PAYNE, A.I.L., BRINK, K.H., MANN, K.H. and R. HILBORN (Eds). *S. Afr. J. mar. Sci.* 12: 189-286.

BRADSHAW, A. and K.E. SCHLEICHER 1965 - The effect of pressure on electrical conductance of sea water. *Deep-Sea Res.* 12: 151-162.

BRINK, K.H. 1992 - Cold-water filaments in the California Current system. In *Benguela Trophic Functioning*. PAYNE, A.I.L., BRINK, K.H., MANN, K.H. and R. HILBORN (Eds). *S. Afr. J. mar. Sci.* 12: 53-60.

BROECKER, W.S. 1979 - A revised estimate for the radiocarbon age of North Atlantic Deep Water. *J. geophys. Res.* 84: 3218-3266.

BROECKER, W.S. 1987 - Unpleasant surprises in the greenhouse? *Nature* 328: 123-126.

BROECKER, W.S. 1991 - The great ocean conveyor. *Oceanogr.* 4(2): 79-89.

BROWN, N. and B. ALLENTOFT 1966 - Salinity, conductivity and temperature relationships of seawater over the range of 0 to 60 p.p.t. Bissett-Berman Corp., Manuscript report. (Cited in Brown and Morrison 1978)

BROWN, N.L. and G.K. MORRISON 1978 - *W.H.O.I./Brown Conductivity, Temperature and Depth Microprofiler.* Woods Hole Oceanographic Institution Technical Report WHOI-78-23, unpublished manuscript.

BRUNDRIT, G.B. and L.V. SHANNON 1989 - Cape storms and the Agulhas Current: a glimpse of the future? *S. Afr. J. Sci.* 85: 619-620.

BRYAN, K. 1962 - Measurements of meridional heat transport by ocean currents. *J. geophys. Res.* 67: 3403-3414.

BUTMAN, B., BEARDSLEY, R.C., MAGNELL, B., FRYE, D., VERMERSCH, J.A., SCHLITZ, R., LIMEBURNER, R., WRIGHT, W.R. and M.A. NOBLE 1982 - Recent observations of the mean circulation on Georges Bank. *J. phys. Oceanogr.* 12: 569-591.

BYRNE, D.A. 1993 - *Agulhas eddies: a synoptic view using Geosat ERM data.* Unpubl. M.A. thesis. New York; Columbia University: 33 pp.

CAMP, D.B., HAINES, W.E., HUBER, B.A., RENNIE, S.E. and A.L. GORDON 1986 - Agulhas Retroflection Cruise, November-December 1983. Hydrographic (CTD) data. *Tech. Rep. Lamont-Doherty geol. Observatory* LDGO-86-1: 390 pp.

CHAPMAN, P., DUNCOMBE RAE, C.M. and B.R. ALLANSON 1987 - Nutrients, chlorophyll and oxygen relationships in the surface layers at the Agulhas Retroflection. *Deep-Sea Res.* 34(8A): 1399-1416.

CHAPMAN, P. and J.L. LARGIER 1989 - On the origin of Agulhas Bank bottom water. *S. Afr. J. Sci.* 85(8): 515-519.

CHAPMAN, P., SHANNON, L.V., SMYTHE-WRIGHT, D. and C.M. DUNCOMBE RAE (in prep.) - Observations on the Subtropical Front in the Cape Basin. Manuscript in preparation.

CHASSIGNET, E.P. and D.B. BOUDRA 1988 - Dynamics of Agulhas retroflection and ring formation in a numerical model. Part II: Energetics and ring formation. *J. phys. Oceanogr.* 18(2): 304-319.

CHASSIGNET, E.P., OLSON, D.B. and D.B. BOUDRA 1990 - Motion and evolution of oceanic rings in a numerical model and in observations. *J. geophys. Res.* 95(C12): 22121-22140.

CHELTON, D.B., SCHLAX, M.G., WITTER, D.L. and J.G. RICHMAN 1990 - Geosat altimeter observations of the surface circulation of the Southern Ocean. *J. geophys. Res.* 95(C10): 17877-17903.

CHENEY, R.E., MARSH, J.G. and B.D. BECKLEY 1983 - Global mesoscale variability from collinear tracks of SEASAT altimeter data. *J. geophys. Res.* 88(C7): 4343-4354.

COCHRANE, A.J., KELLY (Jr.), F.J. and C.R. OLLING 1979 - Subthermocline countercurrents in the western equatorial Atlantic Ocean. *J. phys. Oceanogr.* 9: 724-738.

COLTON, J.B. and R.F. TEMPLE 1961 - The enigma of Georges Bank spawning. *Limnol. Oceanogr.* 6(3): 280-291.

CRAWFORD, R.J.M. 1980 - Seasonal patterns in South Africa's Western Cape purse-seine fishery. *J. Fish Biol.* 16(6): 649-664.

CRAWFORD, R.J.M. 1981 - Distribution, availability and movements of anchovy *Engraulis capensis* off South Africa, 1964-1976. *Fish. Bull. S. Afr.* 14: 51-94.

CRAWFORD, R.J.M. 1987 - Food and population variability in five regions supporting large stocks of anchovy, sardine and horse mackerel. *S. Afr. J. mar. Sci* 5: 735-757.

CRAWFORD, R.J.M., SHANNON, L.V. and P.A. SHELTON 1988 - Characteristics and management of the Benguela as a large marine ecosystem. In *Biomass Yields and Geography of Large Marine Ecosystems.* SHERMAN, K. and L.M. ALEXANDER (Eds). Washington, D.C.; American Association for the Advancement of Science: 169-219 (AAAS Selected Symposium 111).

CRESSWELL, G.R. 1982 - The coalescence of two East Australian Current warm-core eddies. *Science, N.Y.* 215(4529): 161-164.

CRUIKSHANK, R.A., HAMPTON, I. and M.J. ARMSTRONG 1990 - The origin and movements of juvenile anchovy in the Orange River region as deduced from acoustic surveys. *S. Afr. J. mar. Sci.* 9: 101-114.

CUSHMAN-ROISIN, B., CHASSIGNET, E.P. and B. TANG 1990 - Westward motion of mesoscale eddies. *J. phys. Oceanogr.* 20: 758-768.

DARBYSHIRE, J. 1972 - The effect of bottom topography on the Agulhas Current. *Pure appl. Geophys.* 101: 208-220.

DEACON, G.E.R. 1933 - A general account of the hydrology of the South Atlantic Ocean. *Discovery Reports* 7: 171-238.

DE RUIJTER, W.[P.M.] 1982 - Asymptotic analysis of the Agulhas and Brazil Current systems. *J. phys. Oceanogr.* 12: 361-373.

DE RUIJTER, W.P.M. and D.B. BOUDRA 1985 - The wind-driven circulation in the South Atlantic-Indian Ocean - I. Numerical experiments in a one-layer model. *Deep-Sea Res.* 32(5): 557-574.

DOUGLAS, B.C. and R.E. CHENEY 1990 - Geosat: beginning a new era in satellite oceanography. *J. geophys. Res.* 95(C3): 2833-2836.

DOWER, K.M. and M.I. LUCAS submitted - Photosynthesis-irradiance relationships for phytoplankton within a warm-core ring shed from the Agulhas Current Retroflection. Submitted to *Mar. Ecol. Prog. Ser.*

DUNCAN, C.P. 1968 - An eddy in the subtropical convergence southwest of South Africa. *J. geophys. Res.* 73(2): 531-534.

DUNCAN, C.P. 1970 - *The Agulhas Current.* Ph.D. Thesis, University of Hawaii: 76 pp.

DUNCOMBE RAE, C.M. 1991 - Agulhas retroflection rings in the South Atlantic Ocean: an overview. *S. Afr. J. mar. Sci.* 11: 327-344.

DUNCOMBE RAE, C.M., BOYD, A.J. and R.J.M. CRAWFORD 1992a - 'Predation' of anchovy by an Agulhas ring: a possible contributory cause of the very poor yearclass of 1989. In *Benguela Trophic Functioning.* PAYNE, A.I.L., BRINK, K.H., MANN, K.H. and R. HILBORN (Eds). *S. Afr. J. mar. Sci.* 12: 167-173.

DUNCOMBE RAE, C.M., CHAPMAN, P. and L.V. SHANNON 1989a - *Data Report of R.S. Africana Voyage 071 - South East Atlantic Ocean, April 1989 (Vema, Walvis Ridge, Tristan da Cunha, Gough).* Internal report, Sea Fisheries Research Institute, manuscript in preparation.

DUNCOMBE RAE, C.M. and M. ROBERTS in prep. - Subantarctic Mode Water in the Agulhas Current system. In preparation.

DUNCOMBE RAE, C.M., SHANNON, L.V. and F.A. SHILLINGTON 1989b - An Agulhas ring in the South Atlantic ocean. *S. Afr. J. Sci.* 85: 747-748.

DUNCOMBE RAE, C. M. and F. A. SHILLINGTON 1989 – *Data Report of R.S. Benguela Voyage 246 - South Atlantic Eddy Cruise, May 1989.* Internal report, Sea Fisheries Research Institute, manuscript in preparation.

DUNCOMBE RAE, C.M. and F.A. SHILLINGTON in prep. - A winter ring from the Agulhas. In preparation.

DUNCOMBE RAE, C.M., SHILLINGTON, F.A., AGENBAG, J.J., TAUNTON-CLARK, J. and M.L. GRÜNDLINGH 1992b - An Agulhas ring in the South Atlantic Ocean and its interaction with the Benguela Upwelling Frontal system. *Deep-Sea Res.* 39(11/12): 2009-2027.

ERIKSEN, C.C. and E.J. KATZ 1987 - Equatorial dynamics. *Rev. Geophys.* 25: 217-226.

FERON, R.C.V., DE RUIJTER, W.P.M. and D. OSKAM 1992 - Ring shedding in the Agulhas Current System. *J. geophys. Res.* 97(C6): 9467-9477.

FINE, R.A., WARNER, M.J. and R.F. WEISS 1988 - Water mass modification at the Agulhas retroflection: chlorofluoromethane studies. *Deep-Sea Res.* 35(3A): 311-332.

FLAMENT, P., ARMI, L. and L. WASHBURN 1985 - The evolving structure of an upwelling filament. *J. geophys. Res.* 90: 11765-11778.

FLIERL, G.R. 1981 - Particle motions in large-amplitude wave fields. *Geophys. astrophys. Fluid Dynam.* 18: 39-74.

FLIERL, G.R. 1984a - Model of the structure and motion of a warm-core ring. *Austr. J. mar. Freshw. Res.* 35: 9-23.

FORNSHELL, J.A. and W.A. CRIESS 1979 - Anticyclonic eddy observations in the slope water aboard CGC *Evergreen*. *J. phys. Oceanogr.* 9(5): 992-1000.

FRAM GROUP 1991 - An eddy-resolving model of the Southern Ocean. *EOS* 72(15): 169, 174-175.

FU, L.-L. 1981 - The general circulation and meridional heat transport of the subtropical South Atlantic determined by inverse methods. *J. phys. Oceanogr.* 11: 1171-1193.

FU, L.-L. 1986 - Mass, heat and freshwater fluxes in the south Indian Ocean. *J. phys. Oceanogr.* 16(10): 1683-1693.

FUGLISTER, F.C. 1960 - *Atlantic Ocean Atlas of Temperature and Salinity Profiles and Data from the International Geophysical Year of 1957-1958.* Woods Hole Oceanographic Institution, Mass. WHOI Contribution 1108. 209 pp.

FUGLISTER, F.C. 1972 - Cyclonic rings formed by the Gulf Stream 1965-66. In *Studies in Physical Oceanography* 1. GORDON, A.L. (Ed.). New York; Gordon and Breach: 137-168.

FUJIO, S., KADOWAKI, T. and N. IMASATO 1992a - World ocean circulation diagnostically derived from hydrographic and wind stress fields. 1. The velocity field. *J. geophys. Res.* 97(C7): 11163-11176.

FUJIO, S., KADOWAKI, T. and N. IMASATO 1992b - World ocean circulation diagnostically derived from hydrographic and wind stress fields. 2. The water movement. *J. geophys. Res.* 97(C9): 14439-14452.

GARZOLI, S.L. 1987 - Forced oscillations on the Equatorial Atlantic Basin during the Seasonal Response of the Equatorial Atlantic Program. *J. geophys. Res.* 92(C5): 5089-5100.

GARZOLI, S.L. and A. BIANCHI 1987 - Time-space variability of the local dynamics of the Malvinas-Brazil Confluence as revealed by inverted echo sounders. *J. geophys. Res.* 92(C2): 1914-1922.

GARZOLI, S.L. and M.E. CLEMENTS 1986 - Indirect wind observations in the southwestern Atlantic. *J. geophys. Res.* 91: 10551-10556.

GARZOLI, S.L. and Z. GARRAFFO 1989 - Transports, frontal motions and eddies at the Brazil-Malvinas Currents Confluence. *Deep-Sea Res.* 36(5): 681-703.

GARZOLI, S.[L.] and P.L. RICHARDSON 1989 - Low-frequency meandering of the Atlantic North Equatorial Countercurrent. *J. geophys. Res.* 94(C2): 2079-2090.

GEORGI, D.T. 1979 - Modal properties of Antarctic Intermediate Water in the southeast Pacific and the South Atlantic. *J. phys. Oceanogr.* 9: 456-468.

GILL, A.E. 1982 - *Atmosphere-ocean dynamics.* London; Academic Press: xv +662 pp.

GORDON, A.L. 1985 - Indian-Atlantic transfer of thermocline water at the Agulhas retroflection. *Science, N.Y.* 227(4690): 1030-1033.

GORDON, A.L. 1986 - Interocean exchange of thermocline water. *J. geophys. Res.* 91(C4): 5037-5046.

GORDON, A.L. 1989 - Brazil-Malvinas Confluence – 1984. *Deep-Sea Res.* 36(3A): 359-384.

GORDON, A.L. and K.T. BOSLEY 1991 - Cyclonic gyre in the tropical South Atlantic. *Deep-Sea Res.* 38(Suppl. 1): S323-S343.

GORDON, A.L. and C.L. GREENGROVE 1986 - Geostrophic circulation of the Brazil-Falkland confluence. *Deep-Sea Res.* 33(5A): 573-585.

GORDON, A.L. and W.F. HAXBY 1990 - Agulhas eddies invade the South Atlantic: evidence from Geosat altimeter and shipboard Conductivity-Temperature-Depth survey. *J. geophys. Res.* 95(C3): 3117-3125.

GORDON, A.L., LUTJEHARMS, J.R.E. and M.L. GRÜNDLINGH 1987a - Stratification and circulation at the Agulhas retroflection. *Deep-Sea Res.* 34(4A): 565-599.

GORDON, A.L., LUTJEHARMS, J.R.E. and M.L. GRÜNDLINGH 1987b - *Select hydrographic sections from the Agulhas research cruises of the research vessels Knorr and Meiring Naudé 1983.* Technical Report LDGO-87-1, Lamont-Doherty Geological Observatory Columbia University: 28 pp.

GORDON, A.L. and A.R. PIOLA 1983 - Atlantic Ocean upper layer salinity budget. *J. phys. Oceanogr.* 13: 1293-1300.

GORDON, A.L., WEISS, R.F., SMETHIE, W.M. and M.J. WARNER 1992 - Thermocline and Intermediate Water communication between the South Atlantic and Indian Oceans. *J. geophys. Res.* 97(C5): 7223-7240.

GOSCHEN, W.S. and E.H. SCHUMANN 1990 - Agulhas Current variability and inshore structures off the Cape Province, South Africa. *J. geophys. Res.* 95(C1): 667-678.

GRÜNDLINGH, M.L. 1978 - Drift of a satellite-tracked buoy in the southern Agulhas Current and Agulhas Return Current. *Deep-Sea Res.* 25: 1209-1224.

GRÜNDLINGH, M.L. 1979 - Observation of a large meander in the Agulhas Current. *J. geophys. Res.* 84(C7): 3776-3778.

GRÜNDLINGH, M.L. 1983 - Eddies in the southern Indian Ocean and Agulhas Current. In *Eddies in Marine Science.* ROBINSON, A.R. (Ed.). Berlin; Springer: 245-264.

GRÜNDLINGH, M.L. 1985 - Occurrence of Red Sea Water in the southwestern Indian Ocean, 1981. *J. phys. Oceanogr.* 15(2): 207-212.

GRÜNDLINGH, M.L. 1988 - Review of cyclonic eddies of the Moçambique Ridge Current. *S. Afr. J. mar. Sci.* 6: 193-206.

GRÜNDLINGH, M.L., CARTER, R.A. and R.C. STANTON 1991 - Circulation and water properties of the southwest Indian Ocean, spring 1987. *Prog. Oceanogr.* 28(4): 305-342.

GRÜNDLINGH, M.L. and A.F. PEARCE 1984 - Large vortices in the northern Agulhas Current. *Deep-Sea Res.* 31(9): 1149-1156.

HARRIS, T.F.W. 1972 - Sources of the Agulhas Current in the spring of 1964. *Deep-Sea Res.* 19(9): 633-650.

HARRIS, T.F.W. and N.D. BANG 1974 - Topographic Rossby waves in the Agulhas Current. *S. Afr. J. Sci.* 70(7): 212-214.

HARRIS, T.F.W. and D. VAN FOREEST 1978 - The Agulhas Current in March 1969. *Deep-Sea Res.* 25: 549-561.

HÖFLICH, O. 1984 - Climate of the South Atlantic Ocean. In *Climates of the Oceans. World Survey of Climatology* 15. VAN LOON, H. (Ed.). Amsterdam; Elsevier: 1-191.

JACOBS, S.S. and D.T. GEORGI 1977 - Observations on the Southwest Indian/Antarctic Ocean. In *A Voyage of Discovery, George Deacon 70th anniversary volume*. ANGEL, M.[V.] (Ed.) Oxford; Pergamon: pp. 43-84 (*Deep-Sea Res.* **24** Suppl.).

JONES, P.G.W. 1971 - The southern Benguela Current region in February, 1966: Part I, Chemical observations with particular reference to upwelling. *Deep-Sea Res.* **18**: 193-208.

JOYCE, T.M. 1985 - Gulf Stream warm-core ring collection: an introduction. *J. geophys. Res.* **90**(C5): 8801-8802.

JOYCE, T.M., BISHOP, J.K.B. and O.B. BROWN 1992 - Observations of offshore shelf-water transport induced by a warm-core ring. *Deep-Sea Res.* **39**(Suppl. 1): S97-S113.

KAMENKOVITCH, V.M., KOSHLYAKOV, M.N. and A.S. MONIN 1986 - *Synoptic Eddies in the Ocean*. Dordrecht; D. Reidel: ix + 433 pp.

KAWASE, M. 1987 - Establishment of deep ocean circulation driven by deep-water production. *J. phys. Oceanogr.* **17**: 2294-2317.

KAZ'MIN, A.S., LEGECKIS, R. and K.N. FEDEROV 1990 - Evolution of the temperature field in the Benguela upwelling using ship and satellite measurements. *Sov. J. Remote Sensing* **7**(3): 427-444.

KAZ'MIN, A.S. and G.G. SUTYRIN 1990 - Anticyclone blocking of the Benguela Current: satellite and shipborne data analysis. *Sov. J. Remote Sensing* **7**(6): 986-995.

KILLWORTH, P.D. 1983a - Deep convection in the world ocean. *Rev. Geophys. Space Physics* **21**(1): 1-26.

KITANO, K. 1975 - Some properties of the warm eddies generated in the confluence zone of the Kuroshio and Oyshio currents. *J. phys. Oceanogr.* **5**: 245-252.

LAI, D.Y. and P.L. RICHARDSON 1977 - Distribution and movement of Gulf Stream rings. *J. phys. Oceanogr.* **7**: 670-683.

LEGECKIS, R. and A.L. GORDON 1982 - Satellite observations of the Brazil and Falkland Currents — 1975 to 1976 and 1978. *Deep-Sea Res.* **29**(3A): 375-401.

LEVITUS, S. 1982 - *Climatological Atlas of the World Ocean*. NOAA Professional Paper 13. Washington, D.C.; U.S. Department of Commerce: 173 pp.

LEWIS, E.L. and R.G. PERKIN 1981 - The Practical Salinity Scale 1978: conversion of existing data. *Deep-Sea Res.* **28A**(4): 307-328.

LEWIS, L. 1990a - *Satellite Altimetry Data System report: The NOAA GEOSAT Programs*. Council for Scientific and Industrial Research, South Africa, Report EMA-I 8934, 32pp.

LEWIS, L. 1990b - *Satellite Altimetry Data System (SADS). Part 1: The design of SADS*. Council for Scientific and Industrial Research, South Africa, Report EMA-T 8905/01, 15pp.

LEWIS, L. 1990c - *Satellite Altimetry Data System (SADS). Part 2: Programmers reference manual.* Council for Scientific and Industrial Research, South Africa, Report EMA-T 8905/02, 40pp. plus source code listing.

LEWIS, L. and U.V. St. ANGE 1990 - *Satellite Altimetry Data System (SADS). Part 3: User's manual.* Council for Scientific and Industrial Research, South Africa, Report EMA-T 8905/03, 20pp.

LOBEL, P.S. and A.R. ROBINSON 1986 - Transport and entrapment of fish larvae by ocean mesoscale eddies and currents in Hawaiian waters. *Deep-Sea Res.* 33(4A): 483-500.

LUCAS, M.I., ATTWOOD, C., DOWER, K.M. and G. RIGG in prep. a - Chlorophyll and primary production associated with a warm core ring shed from the Agulhas Current retroflection south of Africa: potential implications for carbon flux.

LUCAS, M.I., SEARSON, S. and T.A. PROBYN in prep. b - Size-fractionated nitrogen uptake and regeneration within a warm-core ring shed from the Agulhas Current retroflection.

LUTJEHARMS, J.R.E. 1976 - The Agulhas Current system during the North-east Monsoon season. *J. phys. Oceanogr.* 6: 665-670.

LUTJEHARMS, J.R.E. 1981a - Features of the southern Agulhas Current circulation from satellite remote sensing. *S. Afr. J. Sci.* 77(5): 231-236.

LUTJEHARMS, J.R.E. 1981b - Spatial scales and intensities of circulation in the ocean areas adjacent to South Africa. *Deep-Sea Res.* 28(11A): 1289-1302.

LUTJEHARMS, J.R.E. 1987 - Die subtropiese konvergensie en Agulhasretrofleksievaart (SCARC). *S. Afr. J. Sci.* 83(8): 454-456.

LUTJEHARMS, J.R.E. 1988a - On the role of the East Madagascar Current as a source of the Agulhas Current. *S. Afr. J. Sci.* 84(4): 236-238.

LUTJEHARMS, J.R.E. 1988b - Examples of extreme circulation events at the Agulhas retroflection. *S. Afr. J. Sci.* 84: 584-586.

LUTJEHARMS, J.R.E. 1989 - The role of mesoscale turbulence in the Agulhas Current system. In *Mesoscale/Synoptic Coherent Structures in Geophysical Turbulence*. NIHOUL, J.C.J. and B.M. JAMART (Eds). Amsterdam; Elsevier: 357-372.

LUTJEHARMS, J.R.E., BANG, N.D. and C.P. DUNCAN 1981 - Characteristics of the currents east and south of Madagascar. *Deep-Sea Res.* 28(9A): 879-899.

LUTJEHARMS, J.R.E., CATZEL, R. and H.R. VALENTINE 1989 - Eddies and other boundary phenomena of the Agulhas Current. *Continent. Shelf Res.* 9(7): 597-616.

LUTJEHARMS, J.R.E. and A.L. GORDON 1987 - Shedding of an Agulhas Ring observed at sea. *Nature, Lond.* 325(7000): 138-140.

LUTJEHARMS, J.R.E. and H.R. ROBERTS 1988 - The Natal pulse: an extreme transient on the Agulhas Current. *J. geophys. Res.* 93(C1): 631-645.

LUTJEHARMS, J.R.E., SHILLINGTON, F.A. and C.M. DUNCOMBE RAE 1991 - Observations of extreme upwelling filaments in the Southeast Atlantic Ocean. *Science, N.Y.* 253(5021): 774-776.

LUTJEHARMS, J.R.E. and H.R. VALENTINE 1988b - Evidence for persistent Agulhas rings south-west of Cape Town. *S. Afr. J. Sci.* 84(9): 781-783.

LUTJEHARMS, J.R.E. and R.C. VAN BALLEGOOYEN 1984 - Topographic control in the Agulhas Current system. *Deep-Sea Res.* 31(11): 1321-1337.

LUTJEHARMS, J.R.E. and R.C. VAN BALLEGOOYEN 1988a - The retroflection of the Agulhas Current. *J. phys. Oceanogr.* 18(11): 1570-1583.

LUTJEHARMS, J.R.E. and R.C. VAN BALLEGOOYEN 1988b - Anomalous upstream retroflection in the Agulhas Current. *Science, N.Y.* 240: 1770-1772.

MATANO, R.P. 1993 - On the separation of the Brazil Current from the coast. *J. phys. Oceanogr.* 23(1): 79-90.

MATANO, R.P. and S.G.H. PHILANDER 1993 - Heat and mass balances of the South Atlantic Ocean calculated from a numerical model. *J. geophys. Res.* 98(C1): 977-984.

MAZEIKA, P.A. 1967 - Thermal domes in the eastern tropical Atlantic Ocean. *Limnol. Oceanogr.* 12: 537-539.

McCARTNEY, M.S. 1977 - Subantarctic Mode Water. In *A Voyage of Discovery*. ANGEL, M.V. (Ed.). New York; Pergamon: 103-119 (Supplement to *Deep-Sea Res.* 24).

McCARTNEY, M.S. 1982 - The subtropical recirculation of Mode Waters. *J. mar. Res.* 40(Suppl.): 427-464.

McCARTNEY, M.S. and M.E. WOODGATE-JONES 1991 - A deep-reaching anticyclonic eddy in the subtropical gyre of the eastern South Atlantic. *Deep-Sea Res.* 38(Suppl. 1): S411-S443.

McDOUGALL, T.J. 1987 - Neutral surfaces. *J. phys. Oceanogr.* 17: 1950-1964.

McDOUGALL, T.J. 1989 - Dianeutral advection. *'Aha Huliko'a. Parameterisation of small scale processes.* MÜLLER, P. and D. HENDERSON (Eds.). Proceedings of Hawaiian Winter Workshop, University of Hawaii at Manoa, January 17-20 1989: pp. 289-315.

MELE, P.A., HAINES, W.E., HUBER, B.A. and A.L GORDON 1990 - *CTD and Hydrographic Data from Cruise 165B of RRS Discovery - Benguela.* LDGO-90-2 Palisades; Lamont-Doherty Geological Observatory: 273 pp.

MEY, R.D., WALKER, N.D. and M.R. JURY 1990 - Surface heat fluxes and marine boundary layer modification in the Agulhas retroflection region. *J. geophys. Res.* 95(C9): 15997-16015.

MILLERO, F.J., CHEN, C.-T., BRADSHAW, A. and K. SCHLEICHER 1980 - A new high pressure equation of state for seawater. *Deep-Sea Res.* 27A: 255-264.

MILLERO, F.J. and A. POISSON 1981 - International one-atmosphere equation of state for seawater. *Deep-Sea Res.* **28A**: 625-629.

MOLINARI, R.L., VOITURIEZ, B. and P. DUNCAN 1981 - Observations in the subthermocline undercurrent of the equatorial South Atlantic Ocean: 1978-1980. *Oceanologica Acta* **4**: 451-456.

MOOERS, C.N.K. and A.R. ROBINSON 1984 - Turbulent jets and eddies in the California Current and inferred cross-shore transports. *Science, N.Y.* **223**(4631): 51-53.

MOROSHKIN, K.V., BUBNOV, V.A. and R.P. BULATOV 1970 - Water circulation in the eastern South Atlantic Ocean. *Oceanology* **10**(1): 27-34.

MOSTERT, S.A. 1983 - Procedures used in South Africa for the automatic photometric determination of micro nutrients in sea-water. *S. Afr. J. mar. Sci.* **1**: 189-198.

MOSTERT, S.A. 1988 - Notes on improvements and modifications to the automatic methods for determining dissolved micronutrients in seawater. *S. Afr. J. mar. Sci.* **7**: 295-298.

NELSON, G. 1989 - Poleward motion in the Benguela area. In *Poleward Flows Along Eastern Ocean Boundaries*. NESHYBA, S.J., MOOERS, C.N.K., SMITH, R.L. and R.T. BARBER (Eds). New York; Springer: 110-130 (*Coastal and Estuarine Studies* **34**).

NELSON, G. 1991 - An equatorward shelf-edge jet west of Cape Town. Poster at IUGG XX General Assembly, Vienna, 11-24 August 1991.

NELSON, G. and L. HUTCHINGS 1983 - The Benguela upwelling area. *Prog. Oceanogr.* **12**(3): 333-356.

NELSON, G. and L. HUTCHINGS 1987 - Passive transportation of pelagic system components in the southern Benguela area. In *The Benguela and Comparable Ecosystems*. PAYNE, A.I.L., GULLAND, J.A. and K.H. BRINK (Eds). *S. Afr. J. mar. Sci.* **5**: 223-234.

NEPGEN, C.S.De V. 1979 - The food of the snoek *Thyrsites atun*. *Fish. Bull. S. Afr.* **11**: 39-42.

NILSSON, C.S. and G.R. CRESSWELL 1981 - The formation and evolution of East Australian Current warm-core eddies. *Prog. Oceanogr.* **9**: 133-183.

NOF, D. 1981 - On the beta-induced movements of isolated baroclinic eddies. *J. phys. Oceanogr.* **11**: 1662-1672.

OLSON, D.B. 1980 - The physical oceanography of two rings observed by the Cyclonic Ring Experiment. Part II: Dynamics. *J. phys. Oceanogr.* **10**(4): 514-528.

OLSON, D.B. 1991 - Rings in the ocean. *A. Rev. Earth planet. Sci.* **19**: 283-311.

OLSON, D.B. and R.H. EVANS 1986 - Rings of the Agulhas Current. *Deep-Sea Res.* 33(1A): 27-42.

OLSON, D.B., FINE, R.A. and A.L. GORDON 1992 - Convective modifications of water masses in the Agulhas. *Deep-Sea Res.* **39**(Suppl. 1): S163-S181.

OLSON, D.B., SCHMITT, R.W., KENNELLY, M. and T.M. JOYCE 1985 - A two-layer diagnostic model of the long-term physical evolution of Warm-Core Ring 82B. *J. geophys. Res.* **90**(C5): 8813-8822.

ONKEN, R. 1990 - The creation of reversed baroclinicity and subsurface jets in oceanic eddies. *J. phys. Oceanogr.* **20**: 786-791.

O'TOOLE, M. and I. HAMPTON 1989 - New prospects for surveying and sampling anchovy pre-recruits. *S. Afr. Shipp. News Fishg. Ind. Rev.* **44**(5): 32-33.

OU, H.W. and W. DE RUIJTER 1986 - Separation of an inertial boundary current from a curved coastline. *J. phys. Oceanogr.* **16**: 280-289.

PEDLOSKY, J. 1979 - *Geophysical Fluid Dynamics*. New York; Springer: 624 pp.

PERISSINOTTO, R. and C.M. DUNCOMBE RAE 1990 - Occurrence of anti-cyclonic eddies on the Prince Edward Plateau (South West Indian Ocean): Effects on phytoplankton biomass and production. *Deep-Sea Res.* 37(5): 777-793.

PETERSON, R.G. and L. STRAMMA 1991 - Upper-level circulation in the South Atlantic Ocean. *Prog. Oceanogr.* **26**: 1-73.

PETERSON, W.T., HUTCHINGS, L., HUGGETT, J.A. and J.L. LARGIER 1992 - Anchovy spawning in relation to the biomass and the replenishment rate of their copepod prey on the western Agulhas Bank. In *Benguela Trophic Functioning*. PAYNE, A.I.L., BRINK, K.H., MANN, K.H. and R. HILBORN (Eds). *S. Afr. J. mar. Sci.* **12**: 487-500.

PIOLA, A.R. and D.T. GEORGI 1982 - Circumpolar properties of Antarctic Intermediate Water and Subantarctic Mode Water. *Deep-Sea Res.* **29**(6A): 687-711.

PIOLA, A.R. and A.L. GORDON 1986 - On oceanic heat and freshwater fluxes at 30°S. *J. phys. Oceanogr.* **16**(12): 2184-2190.

PIOLA, A.R. and A.L. GORDON 1989 - Intermediate waters in the southwest South Atlantic. *Deep-Sea Res.* **36**(1A): 1-16.

POLLARD, R.T., RHINES, P.B. and R.O.R.Y. THOMPSON 1973 - The deepening of the wind-mixed layer. *Geophys. Fluid Dyn.* **3**: 381-401.

REID, J.L. 1989 - On the total geostrophic circulation of the South Atlantic Ocean: Flow patterns, tracers and transports. *Prog. Oceanogr.* **23**: 149-244.

REID, R.O., ELLIOTT, B.A. and D.B. OLSON 1981 - Available potential energy: a clarification. *J. phys. Oceanogr.* **11**(1): 15-29.

RICHARDSON, P.L. 1983 - Gulf Stream Rings. In: *Eddies in Marine Science*. ROBINSON, A.R. (Ed.). Berlin; Springer: pp 19-45.

RINTOUL, S.R. 1991 - South Atlantic interbasin exchange. *J. geophys. Res.* 96(C2): 2675-2692.

ROBINSON, A.R. (Editor) 1983 - *Eddies in Marine Science*. Berlin; Springer: 609 pp.

RODEN, G.I. 1986 - Thermohaline fronts and baroclinic flow in the Argentine Basin during the austral spring of 1984. *J. geophys. Res.* 91(4): 5075-5093.

ROEMMICH, D. 1983 - The balance of geostrophic and Ekman transports in the tropical Atlantic Ocean. *J. phys. Oceanogr.* 13: 1534-1539.

S.A. WEATHER BUREAU 1990 - *Daily Weather Bulletin*. Dept. Environment Affairs, Pretoria.

SAETRE, R. and A. JORGE DA SILVA 1984 - The circulation of the Mozambique Channel. *Deep-Sea Res.* 31(5): 485-508.

SANDWELL, D.T. and B. ZHANG 1989 - Global mesoscale variability from the Geosat Exact Repeat mission: correlation with ocean depth. *J. geophys. Res.* 94(C12): 17971-17984.

SCHELL, I.I. 1968 - On the relation between the winds off South West Africa and the Benguela Current and Agulhas Current penetration in the South Atlantic. *Deuts. Hydrogr. Zeits.* 21: 109-117.

SCHMITT, R.W. 1981 - Form of the temperature-salinity relationship in the Central Water: evidence for double-diffusive mixing. *J. phys. Oceanogr.* 11: 1015-1026.

SCHÜLEIN, F.H. 1986 - Availability patterns and length distributions of anchovy in ICSEAF Divisions 1.3, 1.4, and 1.5 between 1971 and 1985. *Colln scient. Pap. int. Commn SE. Atl. Fish.* 13(2): 205-224.

SCHUMANN, E.H. and I.L. VAN HEERDEN 1988 - Observations of Agulhas Current frontal features south of Africa, October 1983. *Deep-Sea Res.* 35(8A): 1355-1362.

SEMTNER, A.[J.] and R.[M.] CHERVIN 1988 - A simulation of the global ocean circulation with resolved eddies. *J. geophys. Res.* 93(C12): 15502-15522.

SEMTNER, A.J. and R.M. CHERVIN 1991 - A thermohaline conveyor belt in the World Ocean. *WOCE Notes* 3(2): 12-15.

SEMTNER, A.J. and R.M. CHERVIN 1992 - Ocean general circulation from a global eddy-resolving model. *J. geophys. Res.* 97(C4): 5493-5550.

S.F.R.I. 1991 - An investigation into the causes of the recent fluctuations in pelagic fish stocks off South Africa. Internal Report, Sea Fisheries Research Institute, Cape Town: 3pp.

SHANNON, L.V. 1966 - Hydrology of the south and west coasts of South Africa. *Investl Rep. Div. Sea Fish. S. Afr.* 58: 22 pp.+30 pp. of Figures.

SHANNON, L.V. 1985 - The Benguela ecosystem. 1. Evolution of the Benguela, physical features and processes. In *Oceanography and Marine Biology. An Annual Review* 23. BARNES, M. (Ed.). Aberdeen; University Press: 105-182.

SHANNON, L.V., AGENBAG, J.J. and M.E.L. BUYS 1987 - Large- and meso-scale features of the Angola-Benguela Front. *S. Afr. J. mar. Sci.* 5: 11-34.

SHANNON, L.V., AGENBAG, J.J., WALKER, N.D. and J.R.E. LUTJEHARMS 1990 - A major perturbation in the Agulhas retroflection area in 1986. *Deep-Sea Res.* 37(3A): 493-512.

SHANNON, L.V., BOYD, A.J., BRUNDRIT, G.B. and J. TAUNTON-CLARK 1986 - On the existence of an El Niño-type phenomenon in the Benguela system. *J. mar. Res.* 44: 495-520.

SHANNON, L.V. and D. HUNTER 1988 - Notes on Antarctic Intermediate Water around South Africa. *S. Afr. J. mar. Sci.* 6: 107-117.

SHANNON, L.V., LUTJEHARMS, J.R.E. and J.J. AGENBAG 1989a - Episodic input of subantarctic water into the Benguela region. *S. Afr. J. Sci.* 85(5): 317-322.

SHANNON, L.V., POLLOCK, D.E., CHAPMAN, P. and A.A. ROBERTSON 1989b - South-east Atlantic expedition of R.S. Africana, April 1989: Some preliminary results. *S. Afr. J. Sci.* 85: 665-669.

SHELTON, P.A. and L. HUTCHINGS 1982 - Transport of anchovy, *Engraulis capensis* Gilchrist, eggs and early larvae by a frontal jet current. *J. Cons. perm. int. Explor. Mer* 40(2): 185-198.

SHILLINGTON, F.A., HUTCHINGS, L., PROBYN, T.A., WALDRON, H.N. and W.T. PETERSON 1992 - Filaments and the Benguela frontal zone: offshore advection or recirculating loops? In *Benguela Trophic Functioning*. PAYNE, A.I.L., BRINK, K.H., MANN, K.H. and R. HILBORN (Eds). *S. Afr. J. mar. Sci.* 12: 207-218.

SHILLINGTON, F.A., PETERSON, W.T., HUTCHINGS, L., PROBYN, T.A., WALDRON, H.N. and J.J. AGENBAG 1990 - A cool upwelling filament off Namibia, south-west Africa: preliminary measurements of physical and biological properties. *Deep-Sea Res.* 37(11A): 1753-1772.

SHUM, C.K., WERNER, R.A., SANDWELL, D.T., ZHANG, B.H., NEREM, R.S. and B.D. TAPLEY 1990 - Variations of global mesoscale eddy energy observed from Geosat. *J. geophys. Res.* 95(C10): 17865-17876.

SIEDLER, G. 1983 - Tropical and equatorial regions. In *Eddies in Marine Science*. ROBINSON, A.R. (Ed.). Berlin; Springer: 181-199.

SMITH, P.C. 1983 - Eddies and coastal interactions. In *Eddies in Marine Science*. ROBINSON, A.R. (Ed.). Berlin; Springer: 446-480.

SOLOMON, H. 1978 - Detachment and recombination of a current ring with the Kuroshio. *Nature, Lond.* 274(5671): 580-581.

SPEER, K.G. and M.S. McCARTNEY 1991 - Tracing lower North Atlantic Deep Water across the equator. *J. geophys. Res.* 96(C11): 20443-20448.

SPEER, K. and E. TZIPERMAN 1992 - Rates of water mass formation in the North Atlantic Ocean. *J. phys. Oceanogr.* 22: 93-104.

STOMMEL, H. and A.B. ARONS 1960 - On the abyssal circulation of the world ocean — II. An idealized model of the circulation pattern and amplitude in oceanic basins. *Deep-Sea Res.* 6: 217-233.

STRAMMA, L. 1989 - The Brazil Current transport south of 23°S. *Deep-Sea Res.* 36(4A): 639-646.

STRAMMA, L. 1991 - Geostrophic transport of the South Equatorial Current in the Atlantic. *J. mar. Res.* 49(2): 281-294.

STRAMMA, L., IKEDA, Y. and R.G. PETERSON 1990 - Geostrophic transport in the Brazil Current region north of 20°S. *Deep-Sea Res.* 37(12A): 1875-1886.

STRAMMA, L. and R.G. PETERSON 1989 - Geostrophic transport in the Benguela Current region. *J. phys. Oceanogr.* 19: 1440-1448.

STRUB, P.T., KOSRO, P.M. and A. HUYER 1991 - The nature of the cold filaments in the California Current system. *J. geophys. Res.* 96(C8): 14743-14768.

STRAMMA, L. and R.G. PETERSON 1990 - The South Atlantic Current. *J. phys. Oceanogr.* 20(6): 846-859.

SVERDRUP, H.U., JOHNSON, M.W. and R.H. FLEMING 1942 - *The Oceans: their Physics, Chemistry, and General Biology.* Englewood Cliffs, New Jersey; Prentice-Hall: x + 1087 pp.

SWART, V.P. and J.L. LARGIER 1987 - Thermal structure of Agulhas Bank water. In *The Benguela and Comparable Ecosystems.* PAYNE, A.I.L., GULLAND, J.A. and K.H. BRINK (Eds). *S. Afr. J. mar. Sci.* 5: 243-253.

TAFT, B.A. 1963 - Distribution of salinity and dissolved oxygen on surfaces of uniform potential specific volume in the South Atlantic, South Pacific and South Indian Oceans. *J. mar. Res.* 21: 129-146.

TAUNTON-CLARK, J. 1993 - *The identification and tracking of Agulhas rings using the techniques of satellite altimetry.* Unpublished M.Sc. thesis, University of Cape Town: 132 pp.

THE RING GROUP 1981 - Gulf Stream cold-core rings: their physics, chemistry and biology. *Science, N.Y.* 212(4499): 1091-1100.

THOMPSON, R.O.R.Y. 1973 - Stratified Ekman boundary layer models. *Geophys. Fluid Dyn.* 5: 201-210.

TINTORÉ, J., WANG, D.-P. and P.E. LA VIOLETTE 1990 - Eddies and thermohaline intrusions of the shelf/slope front off the northeast Spanish Coast. *J. geophys. Res.* 95(C2): 1627-1633.

UNESCO 1983 - Algorithms for computation of fundamental properties of seawater. *Unesco Technical Papers in Marine Science* (44): 53 pp.

UNESCO 1988 - The acquisition, calibration, and analysis of CTD data. *Unesco Technical Papers in Marine Science* (54): 94 pp.

VALENTINE, H.R. 1990 - A fine-scale volumetric census of the water masses of the Agulhas Retroflection area. *Rep. S. Afr. Coun. scient. ind. Res.* EMA-R 691: 105 pp.

VALENTINE, H.R., DUNCOMBE RAE, C.M., VAN BALLEGOOYEN, R.C. and J.R.E. LUTJEHARMS 1988 - The Subtropical Convergence and Agulhas Retroflection Cruise (SCARC) Data Report. *Rep. S. Afr. Coun. scient. ind. Res.* T/SEA 8804: 10 pp + tables + figures.

VALENTINE, H.R., LUTJEHARMS, J.R.E. and G.B. BRUNDRIT 1993 - The water masses and volumetry of the southern Agulhas Current region. *Deep-Sea Res. I* 40(6): 1285-1305.

VOITURIEZ, B. 1981 - Les sous-courants équatoriaux nord et sud et la formation des dômes thermiques tropicaux. *Oceanologica Acta* 4: 497-506.

VOITURIEZ, B. and A. HERBLAND 1982 - Comparison des systèmes productifs de l'Atlantique Tropical Est: dômes thermiques, upwellings côtiers et upwelling équatorial. *Rapports et Procès-Verbaux des Réunions Conseil International pour l'Exploration de la Mer* 180: 114-130.

WACONGNE, S. 1989 - Dynamical regimes of a fully nonlinear stratified model of the Atlantic Equatorial Undercurrent. *J. geophys. Res.* 94: 4801-4815.

WACONGNE, S. and B. PITON submitted - Current measurements along the coasts of Gabon and Congo and relevance to the larger scale circulation. Submitted to *Deep-Sea Res.* (Cited in Peterson and Stramma 1991.)

WAKKER, K.F., NAEIJE, M.C., SCHARROO, R. and B.A.C. AMBROSIUS 1990a - Extraction of mesoscale ocean current information from GEOSAT altimeter data. *Proceedings of the Space and Sea Colloquium, Paris, 24-26 September 1990*, ESA SP-312: 221-226.

WAKKER, K.F., ZANDBERGEN, R.C.A., NAEIJE, M.C. and B.A.C. AMBROSIUS 1990b - Geosat altimeter data analysis for the oceans around South Africa. *J. geophys. Res.* 95(C3): 2991-3006.

WALKER, N.D. 1990 - Links between South African summer rainfall and temperature variability of the Agulhas and Benguela Current systems. *J. geophys. Res.* 95(C3): 3297-3319.

WALKER, N.D. and R.D. MEY 1988 - Ocean/atmosphere heat fluxes within the Agulhas Retroflection region. *J. geophys. Res.* 93(C12): 15473-15483.

WARREN, B.A. 1981 - Deep circulation of the world ocean. In *Evolution of Physical Oceanography, Scientific Surveys in Honour of Henry Stommel.* WARREN, B.A. and C. WUNSCH (Eds). Cambridge, Mass.; Massachusetts Institute of Technology Press: 6-41 + Reference List.

WARREN, B.A. 1983 - Why is no deep water formed in the North Pacific? *J. mar. Res.* 41: 327-347.

WEBB, D.J., KILLWORTH, P.D., COWARD, A.C. and S.R. THOMPSON 1991 - *The FRAM Atlas of the Southern Ocean.* Swindon; Natural Environment Research Council: 67 pp.

WHITWORTH, T. and W.D. NOWLIN 1987 - Water masses and currents of the Southern Ocean at the Greenwich Meridian. *J. geophys. Res.* 92(C6): 6462-6476.

WIJFFELS, S.E., SCHMITT, R.W., BRYDEN, H.L. and A. STIGEBRANDT 1992 - Transport of freshwater by the oceans. *J. phys. Oceanogr.* 22: 155-162.

WILLIAMS, R.G. 1988 - Modification of ocean eddies by air-sea interaction. *J. geophys. Res.* 93(C12): 15523-15533.

WRIGHT, W.R. 1970 - Northward transport of Antarctic Bottom Water in the western Atlantic Ocean. *Deep-Sea Res.* 17: 367-371.

WUNSCH, C., HU, D. and B. GRANT 1983 - Mass, heat, salt and nutrient fluxes in the South Pacific Ocean.*J. phys. Oceanogr.* 13: 725-753.

WÜST, G. 1957 - Stromgeschwindigkeiten und Strommengen in den Tiefen des Atlantischen Ozeans. *Wissenschaftliche Ergebnisse der Deutschen Atlantischen Expedition Forschungs- und Vermessungsschiff Meteor 1925-1927* 6(2): 261-420. (Cited in Peterson and Stramma 1991.)

WYRTKI, K. 1971 - *Oceanographic Atlas of the International Indian Ocean Expedition.* Washington, D.C.; National Science Foundation: 531 pp.

APPENDIX B: FIGURES AND TABLES

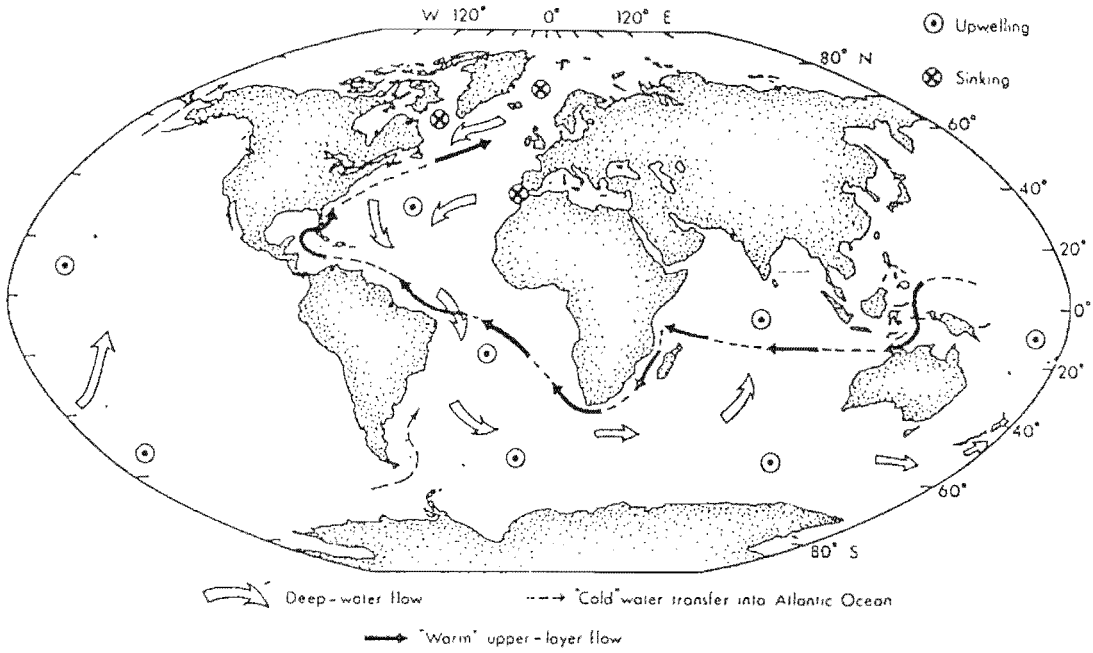

Figure 2.1: The thermohaline circulation of deep water through the World Ocean, the "conveyor belt". North Atlantic Deep Water is renewed in the Norwegian and Labrador Seas and spreads through the ocean, upwelling into the Intermediate Water. The outflow is compensated by the flow of Central Water into the South Atlantic from the Indonesian Seas via the Agulhas Current (the "warm-water path") and by Antarctic Intermediate Water through the Drake Passage (the "cool freshwater path"). (From Gordon 1986)

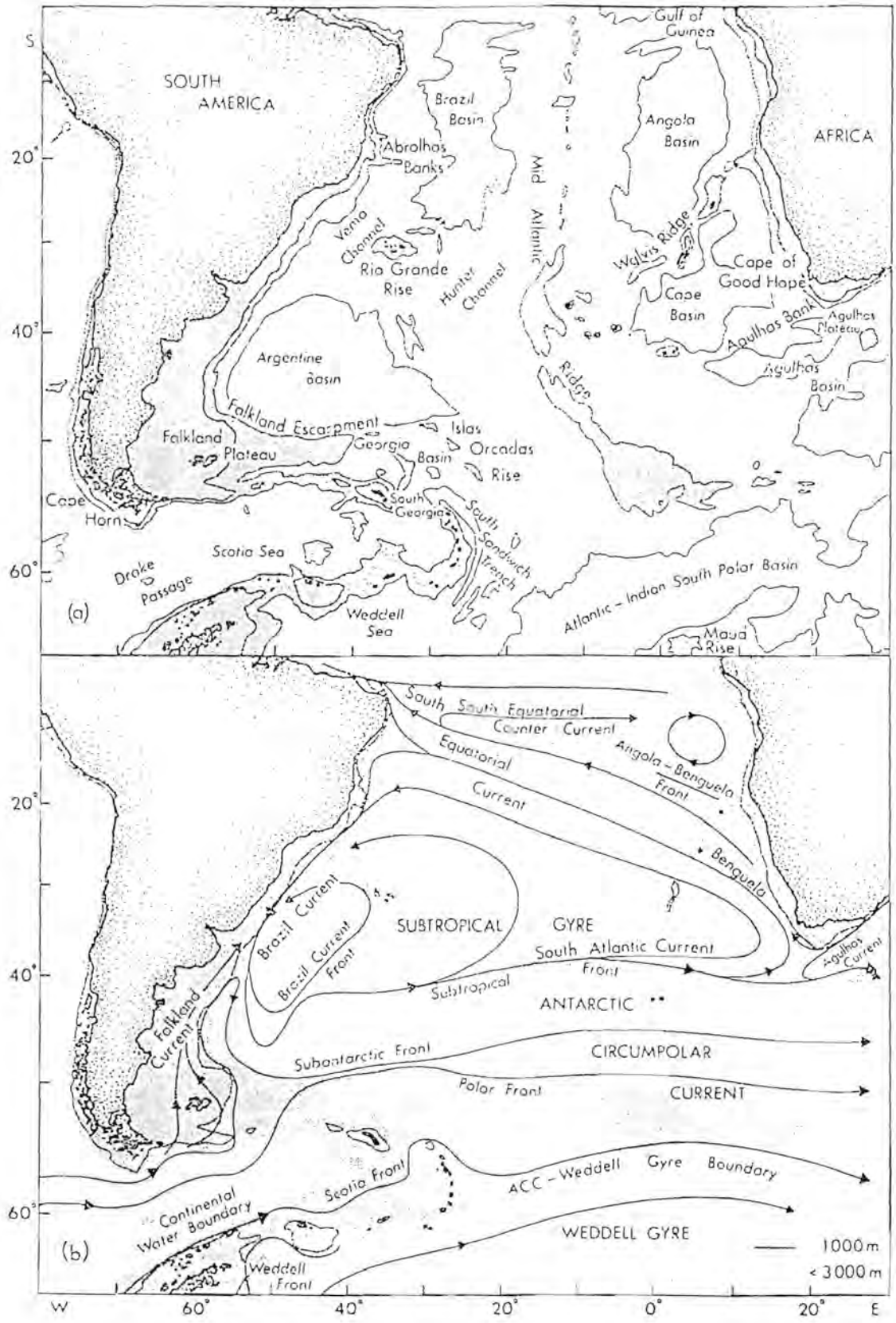

Figure 2.2: (a) The bathymetry of the South Atlantic Ocean. The contours for 1000, 3000 and 5000 m are shown, regions shallower than 3000 m deep being shaded. (b) Schematic representation of the large-scale upper-level geostrophic currents and fronts in the South Atlantic Ocean (From Peterson and Stramma 1991).

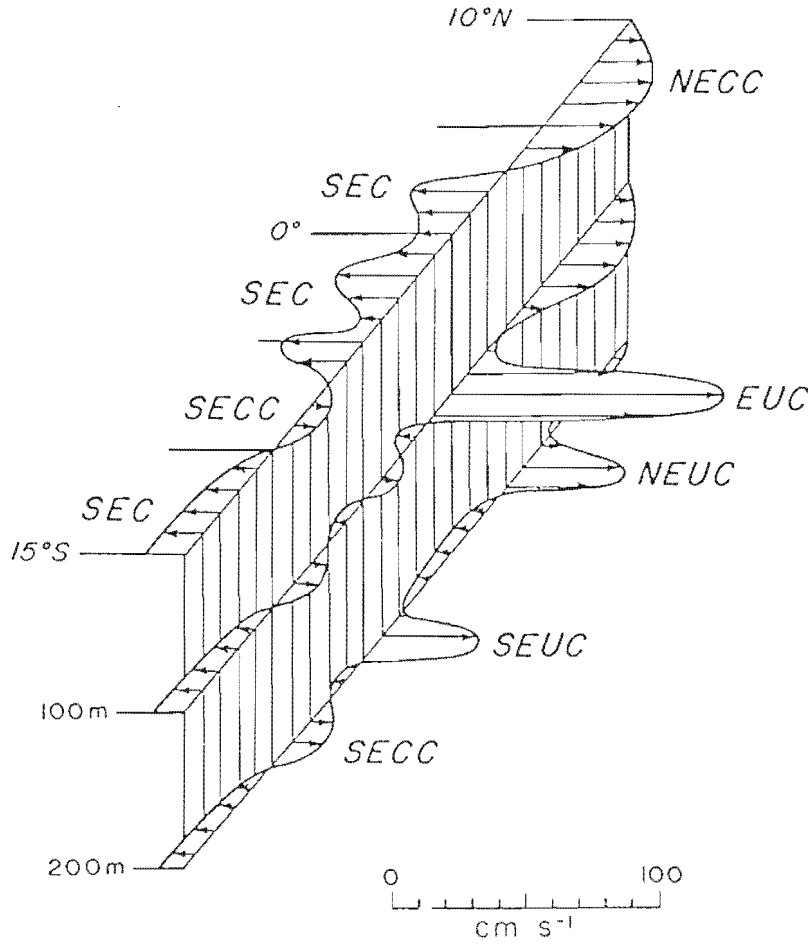

Figure 2.3: Equatorial current system of the Atlantic Ocean. (From Peterson and Stramma 1991.)

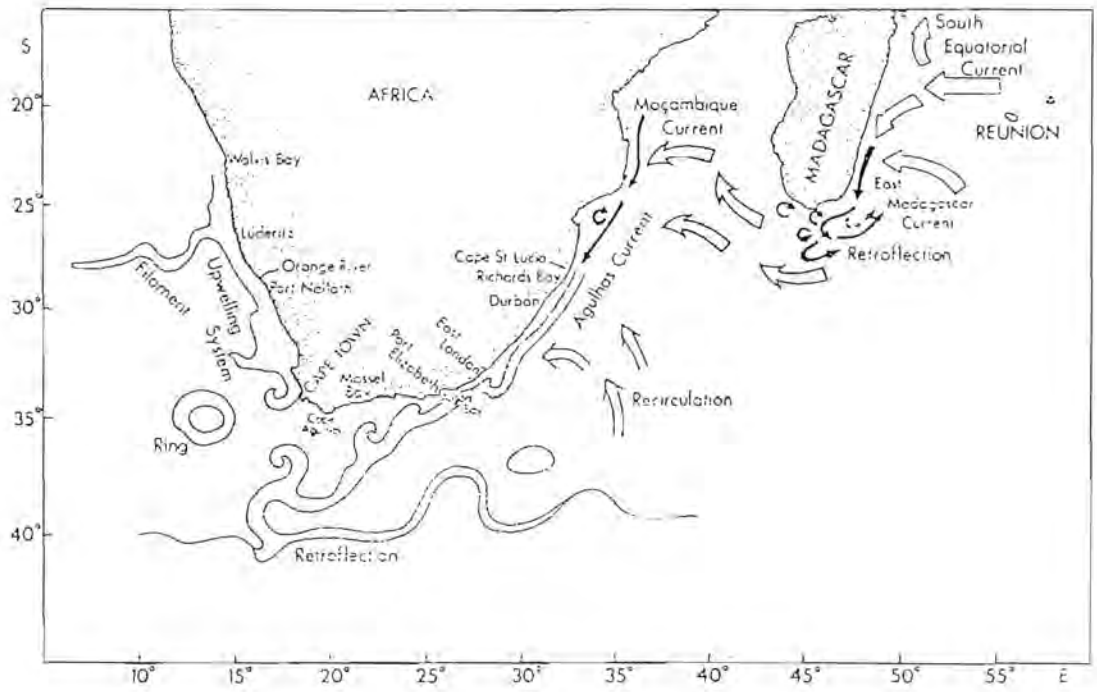

Figure 2.4: The circulation of the Agulhas Current showing its features: rings shed from the retroflection in the South Atlantic Ocean, inshore eddies and filaments on the landward side of the current over the Agulhas Bank, a Natal pulse (near East London), meanders in the current over the Agulhas Plateau and cold core rings in the Indian Ocean. (Adapted from Lutjeharms *et al.* 1981, and Lutjeharms 1981b.)

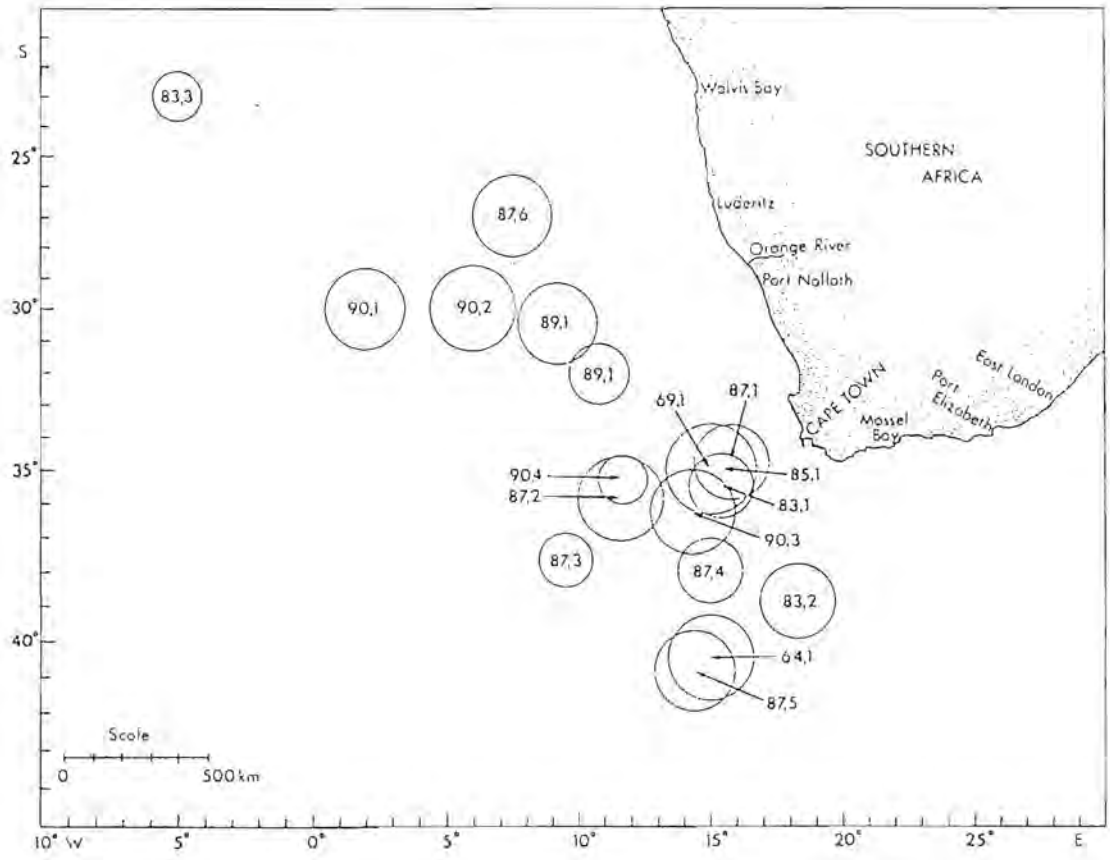

Figure 2.5: The positions of Agulhas rings detected hydrographically in the South Atlantic Ocean. Rings are numbered according to Table 2i. The circle indicates the diameter of maximum azimuthal velocity for each ring in Table 2ii. The rings for which data are not given in the Table have estimated diameters indicated. Data sources for the rings are indicated in Table 2i.

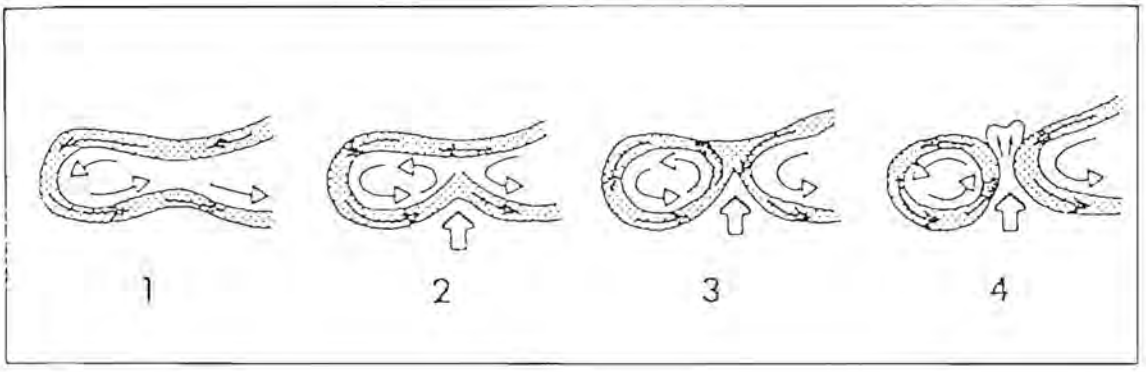

Figure 2.6: Conceptual representation of the initiation (2), development (3) and separation (4) of an Agulhas ring from the Agulhas retroflection (1) with the accompanying inflow of subantarctic water. (From Lutjeharms and Van Ballegooyen 1988a.)

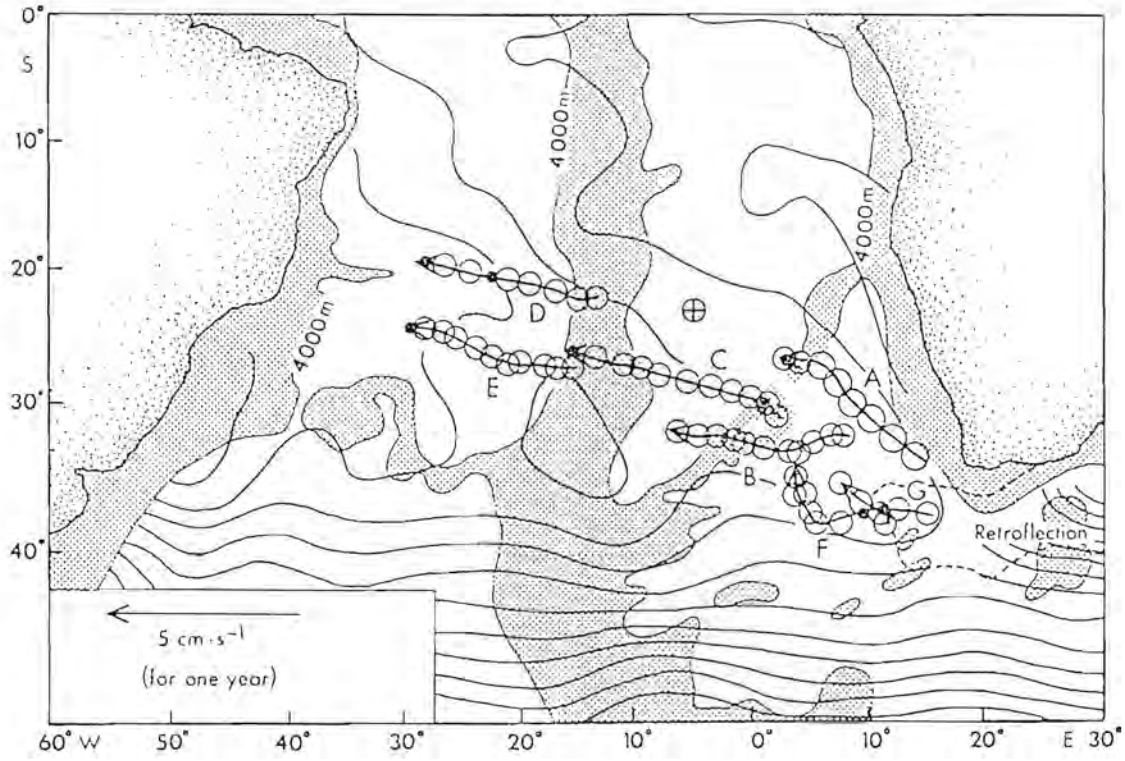

Figure 2.7: The tracks of eddies in the South Atlantic Ocean detected by means of GEOSAT altimetry, superimposed on the 0/1000 ob dynamic topography map based on Levitus (1982). The eddy position and approximate size are shown as circles at roughly one-month intervals. A dot is placed at the expected position when the eddy feature is not clearly revealed by the GEOSAT map. The *Oceanus* eddy (McCartney and Woodgate-Jones 1991) is shown by the crossed circle. Eddy A was sampled by Gordon and Haxby (1990) after whom the Figure is taken.

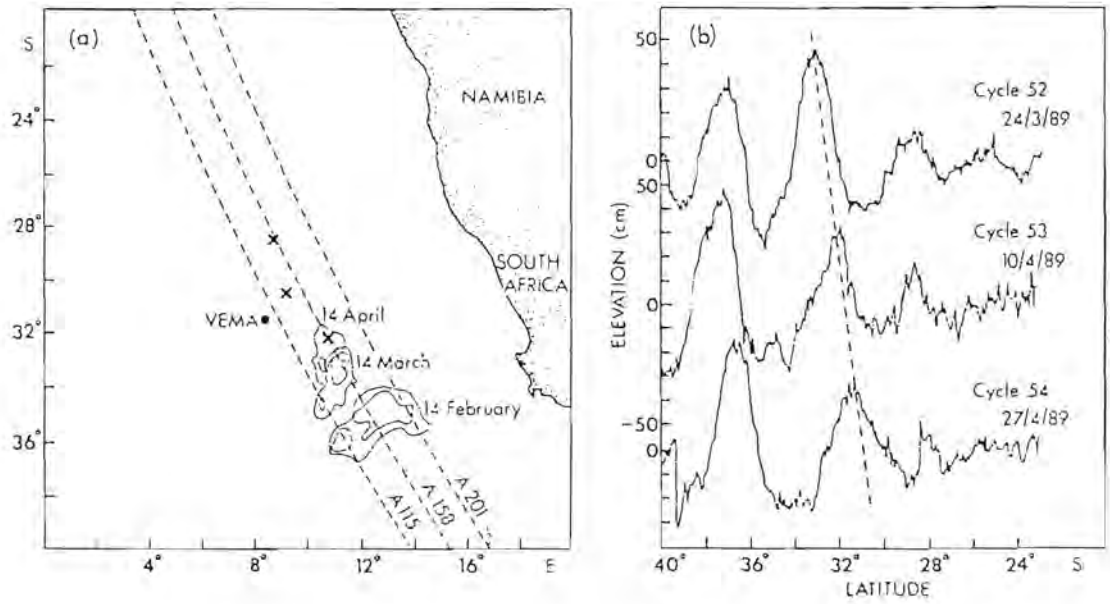

Figure 2.8: a. Positions of the Vema ring from sea-surface elevations from mid-February to mid-April, derived from GEOSAT altimetry. The ascending satellite ground tracks over the area (A115, A158, A201) are marked. The positions of the ring centre on 6 April, 20 May (determined by hydrography) and 15 June (by NOAA imagery) are indicated by crosses. b. Along-track elevations from three successive cycles (52, 53, 54) along pass A158 in March and April 1989. The progress of the elevation corresponding to the ring is indicated by the dashed line. (Figures from Duncombe Rae *et al.* 1992b.)

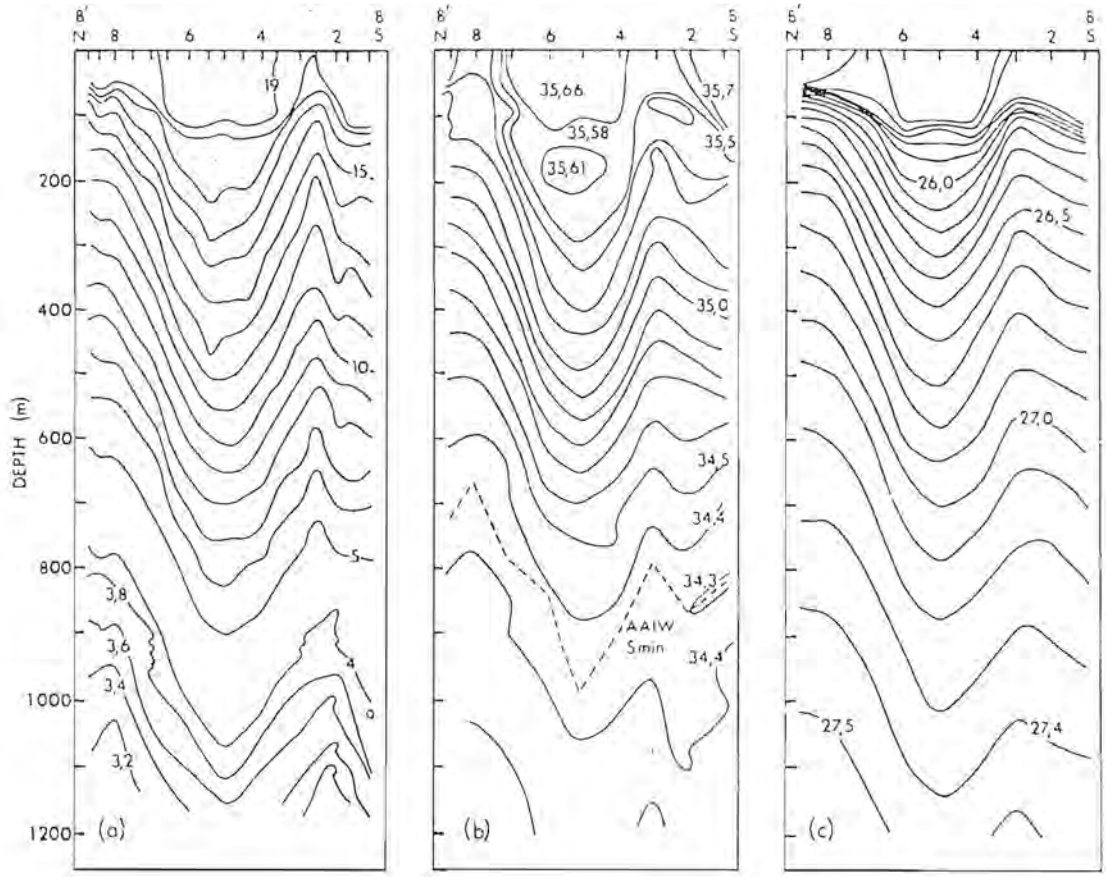

Figure 2.9: South/north section across the Vema ring (May 1989). a. Temperature (°C). b. Salinity (psu). c. Density ($kg.m^{-3}$). (From Duncombe Rae *et al.* 1992b.)

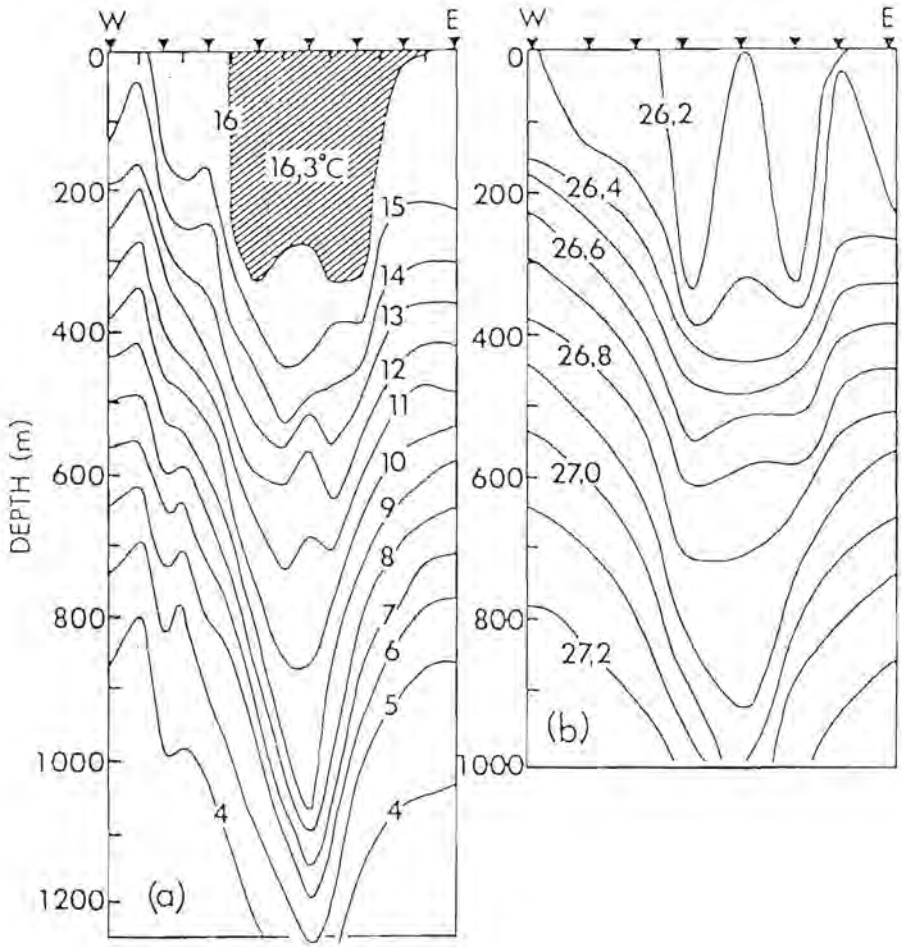

Figure 2.10: West/east section across the Winter ring (August 1990) indicating the deep isothermal mixed layer. a. Temperature (°C). b. Density ($kg.m^{-3}$). (From Duncombe Rae and Shillington in prep.)

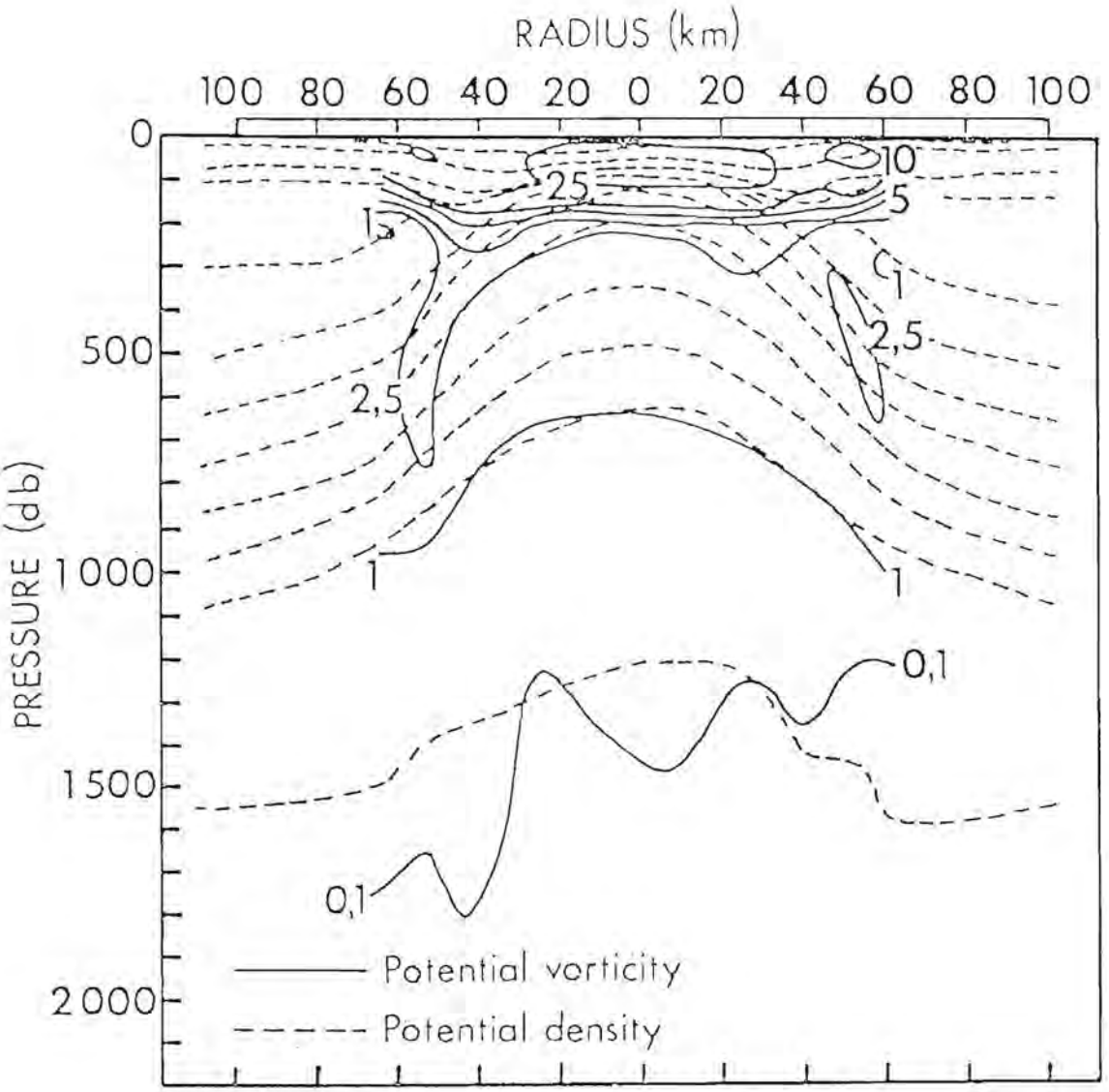

Figure 2.11: The potential vorticity superimposed on the potential density for a cyclonic ring. Preferred mixing paths along isopycnals are blocked by bands of high potential vorticity, confining the water to the ring centre. (From Olson 1980.)

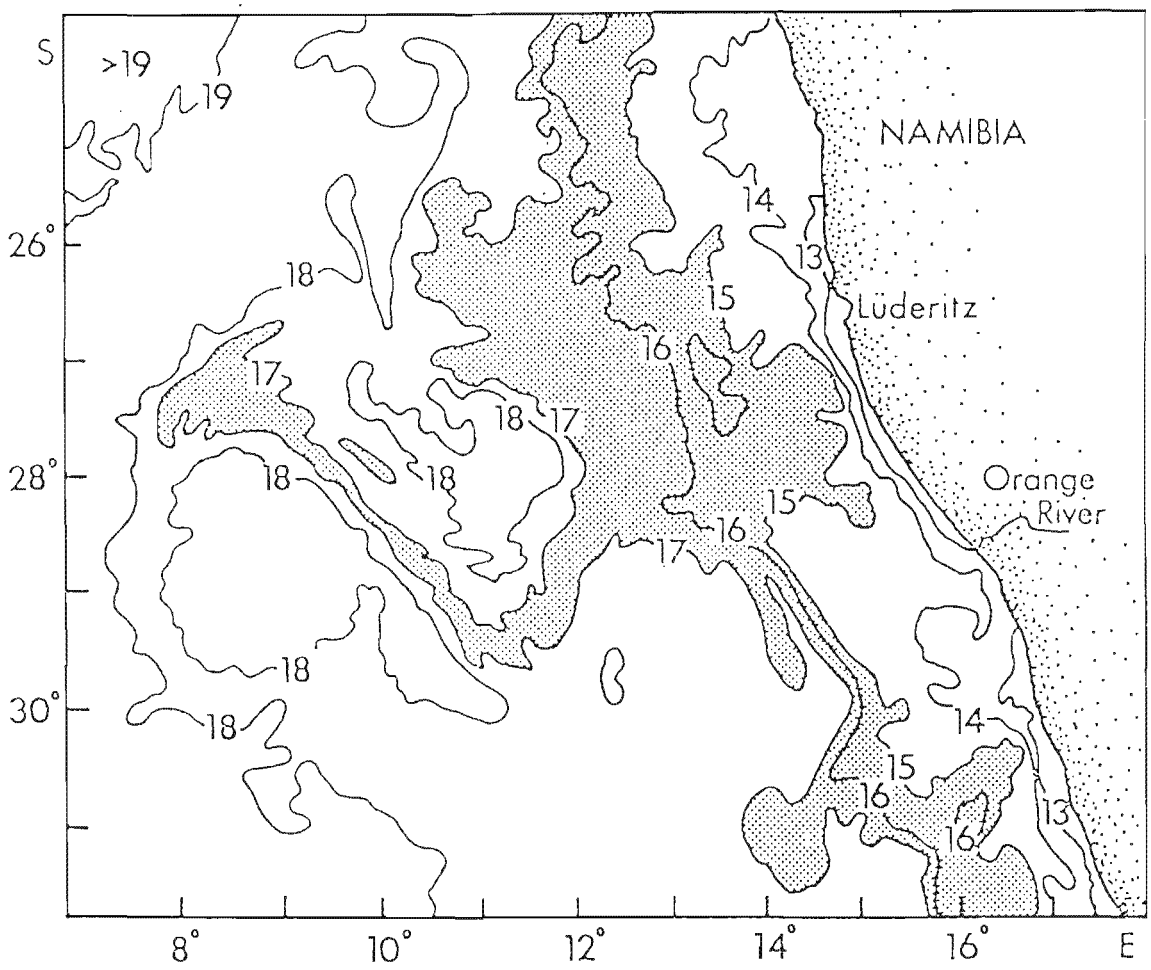

Figure 2.12: A line drawing interpretation of the surface isotherms from NOAA satellite imagery for 15 June 1989. The isotherms indicate a cold filament from the Benguela system being entrained by the ring. The cool frontal water is shown shaded. The flow of water within the front is south to north throughout. (From Lutjeharms *et al.* 1991.)

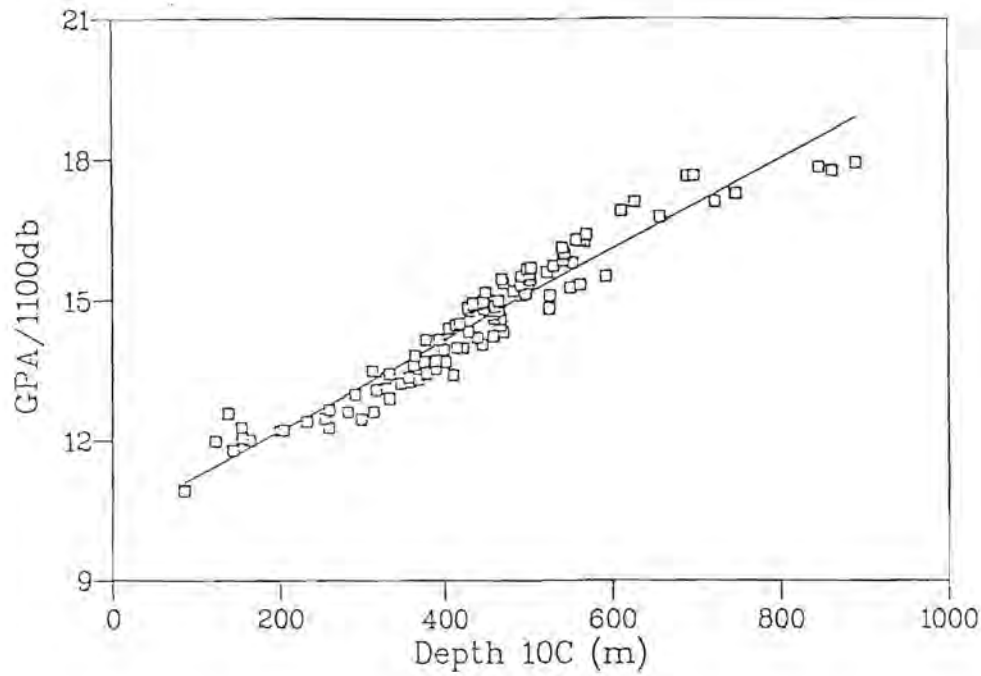

Figure 3.1: The relationship between the geopotential anomaly relative to 1100 db and the depth of the 10°C isotherm in the Cape Basin for all CTD stations occupied on the various cruises indicated in the text.

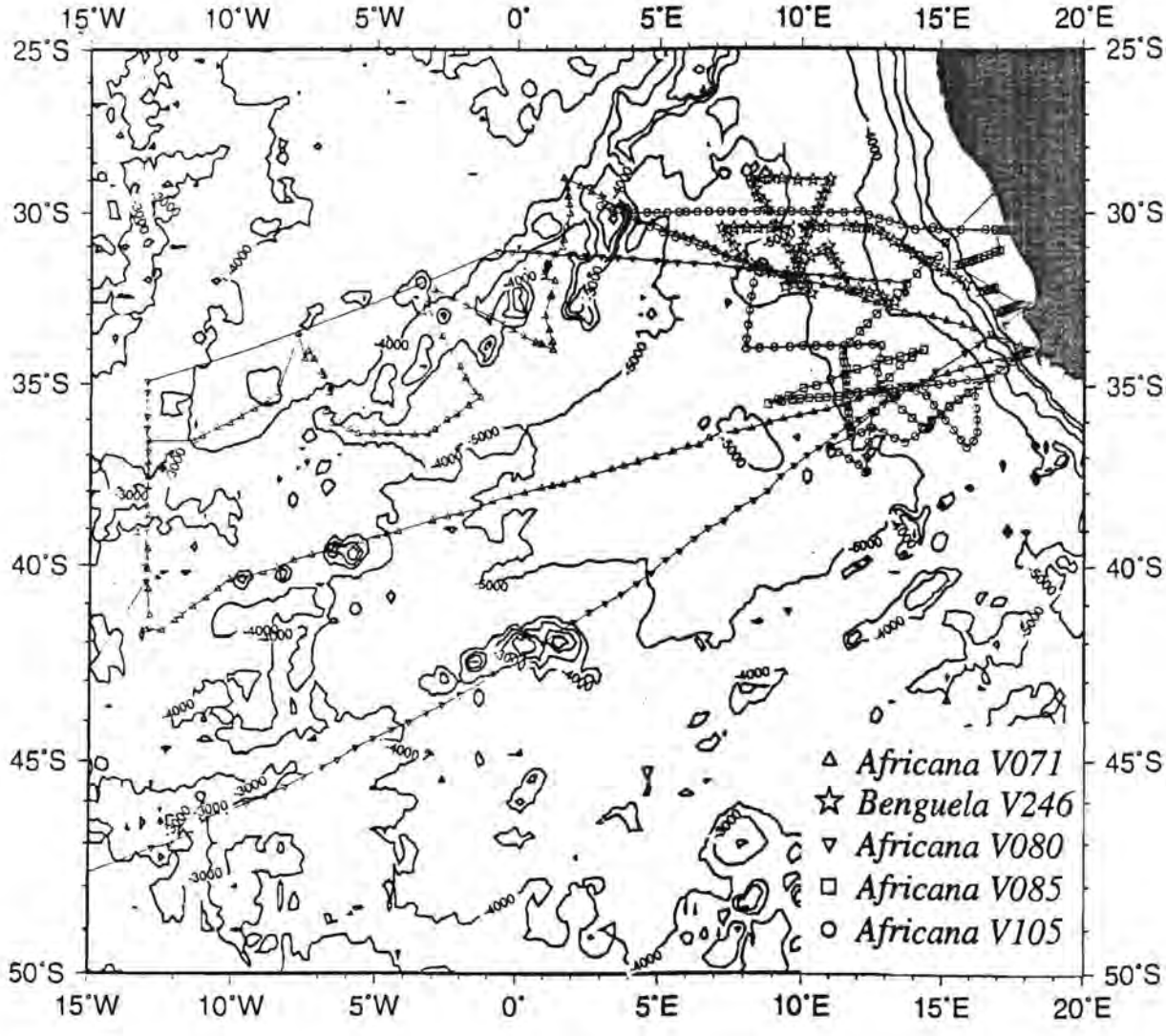

Figure 4.1: Positions of CTD and XBT stations occupied in the Cape Basin from April 1989 to June 1992 from the cruises: *Africana* V071, April to May 1989; *Benguela* V246, May 1989; *Africana* V080, northern line in February and southern line in April 1990; *Africana* V085, August 1990; *Africana* V105, June 1992.

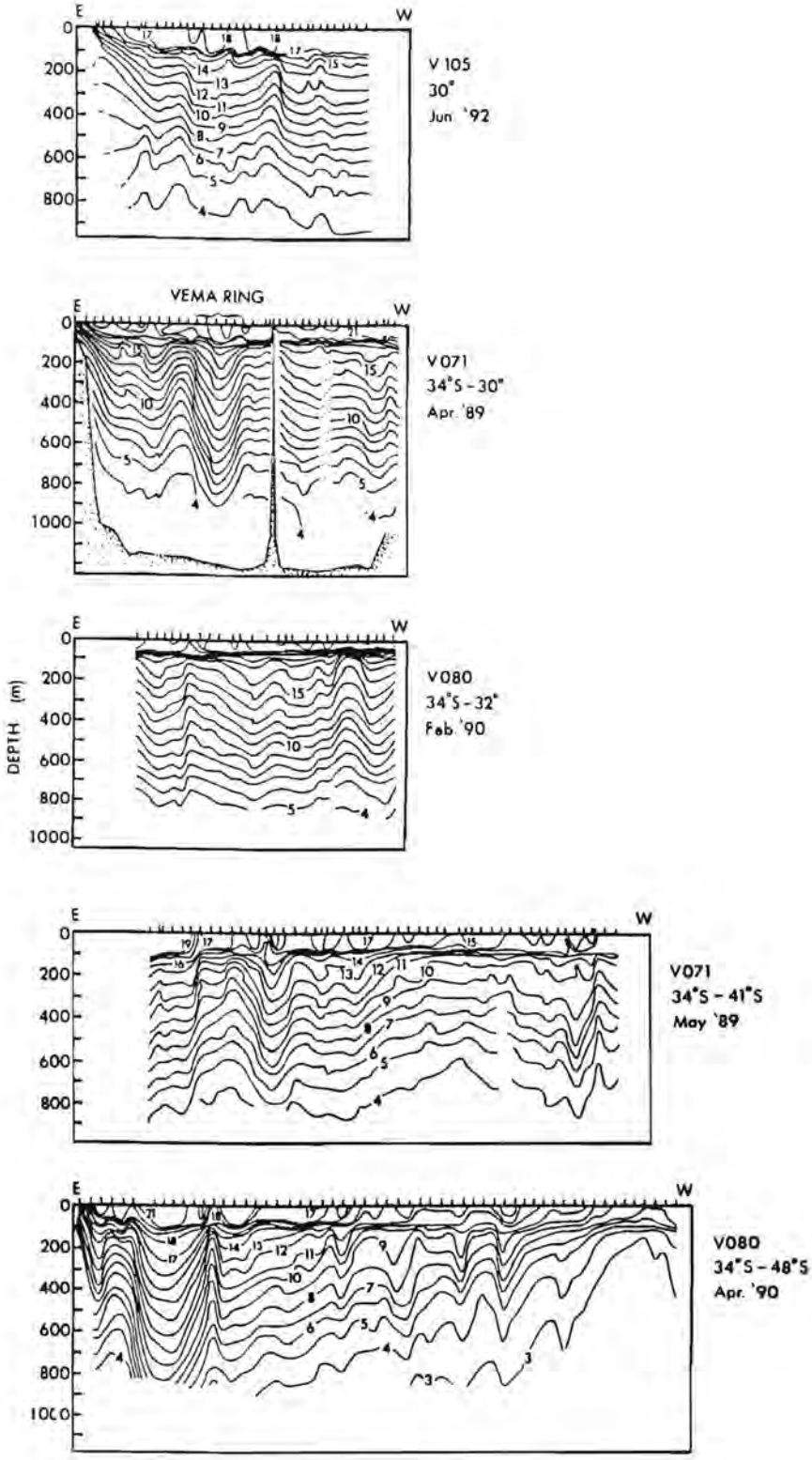

Figure 4.2: Vertical temperature sections across the Cape Basin obtained on cruises which crossed the basin to the Walvis Ridge: *Africana* V071, *Africana* V080 and *Africana* V105. The sections are arranged from (top) north to (bottom) south. a. *Africana* V105, June 1992. Hondeklip Bay to Walvis Ridge, 30°S. b. *Africana* V071, April 1989. Cape Town to Walvis Ridge. The Vema ring is indicated. c. *Africana* V080, February 1990. Cape Town to Walvis Ridge. d. *Africana* V071, May 1989. Gough Island to Cape Town. e. *Africana* V080, April 1990. Punta Arenas to Cape Town.

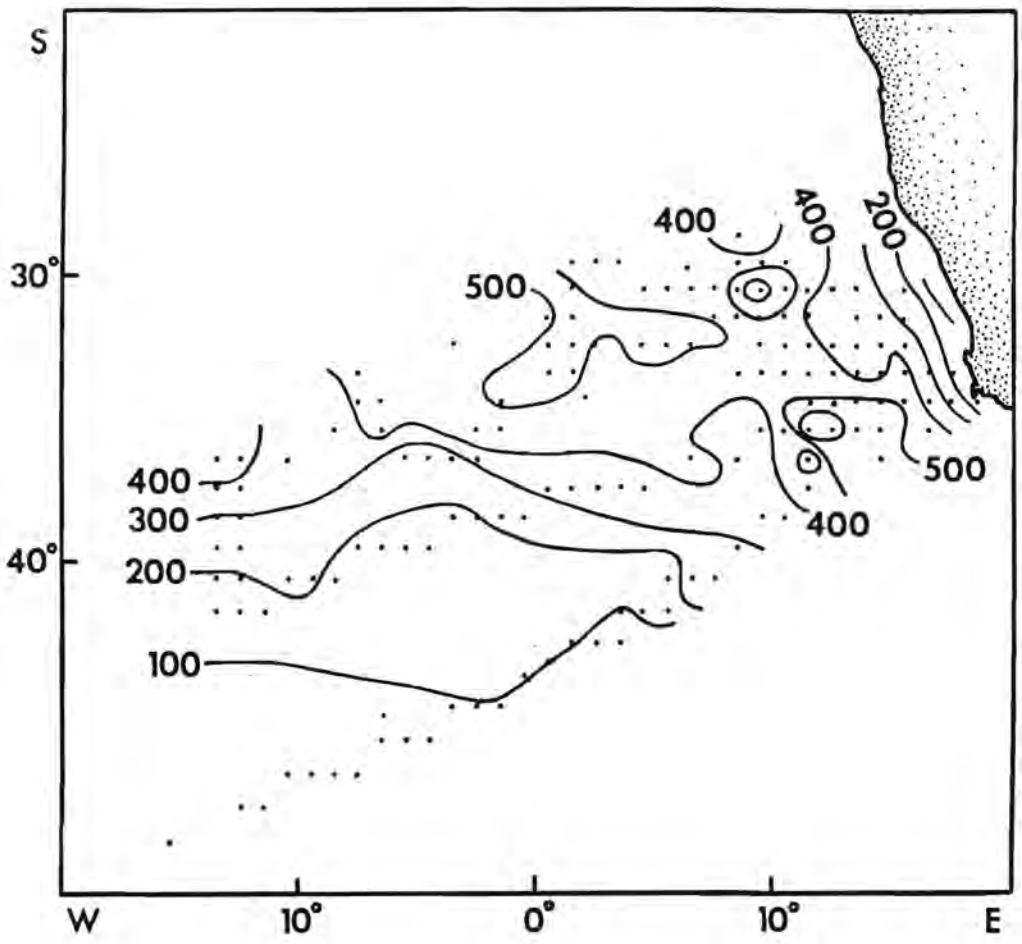

Figure 4.3: Depth of the 10° isotherm contoured from XBT and CTD data from the five cruises. The data are weighted means of the data in 1° squares. All data are included.

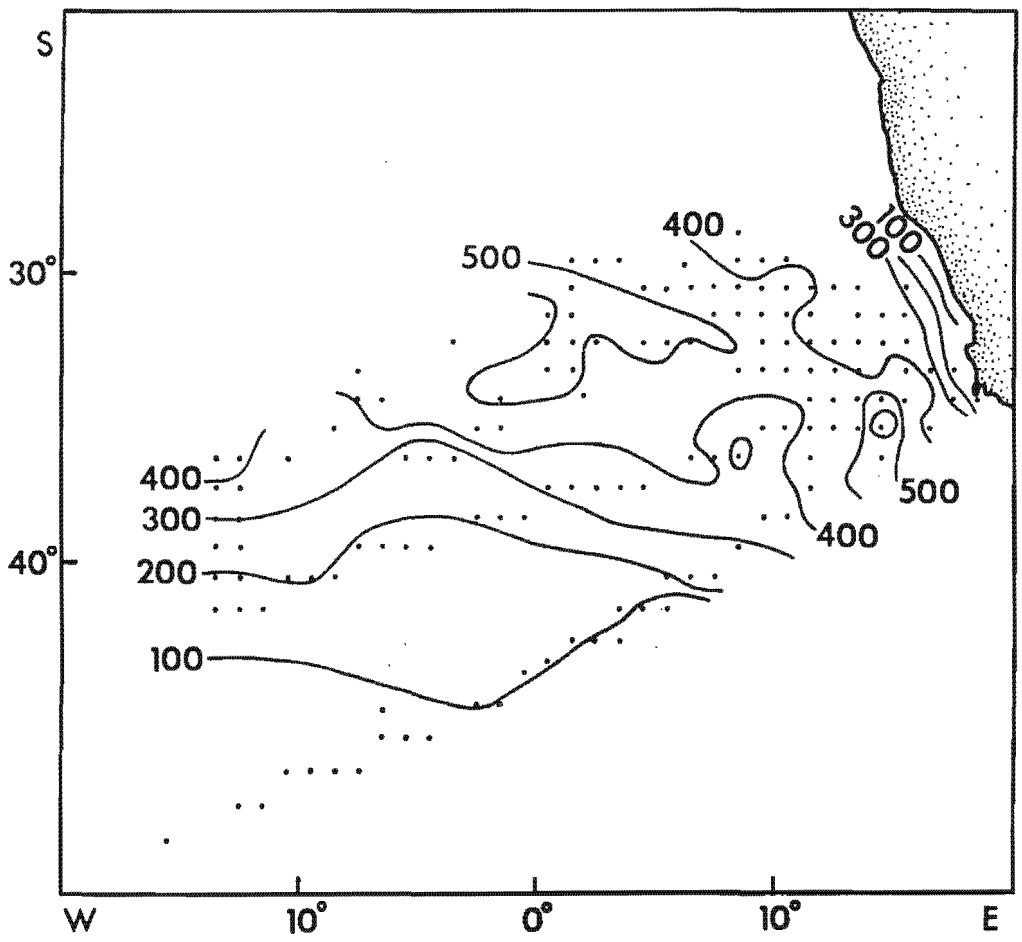

Figure 4.4: Depth of the 10° isotherm contoured from XBT and CTD data from the five cruises. The data are weighted means of the data in 1° squares. Data within known Agulhas rings were omitted from the averages.

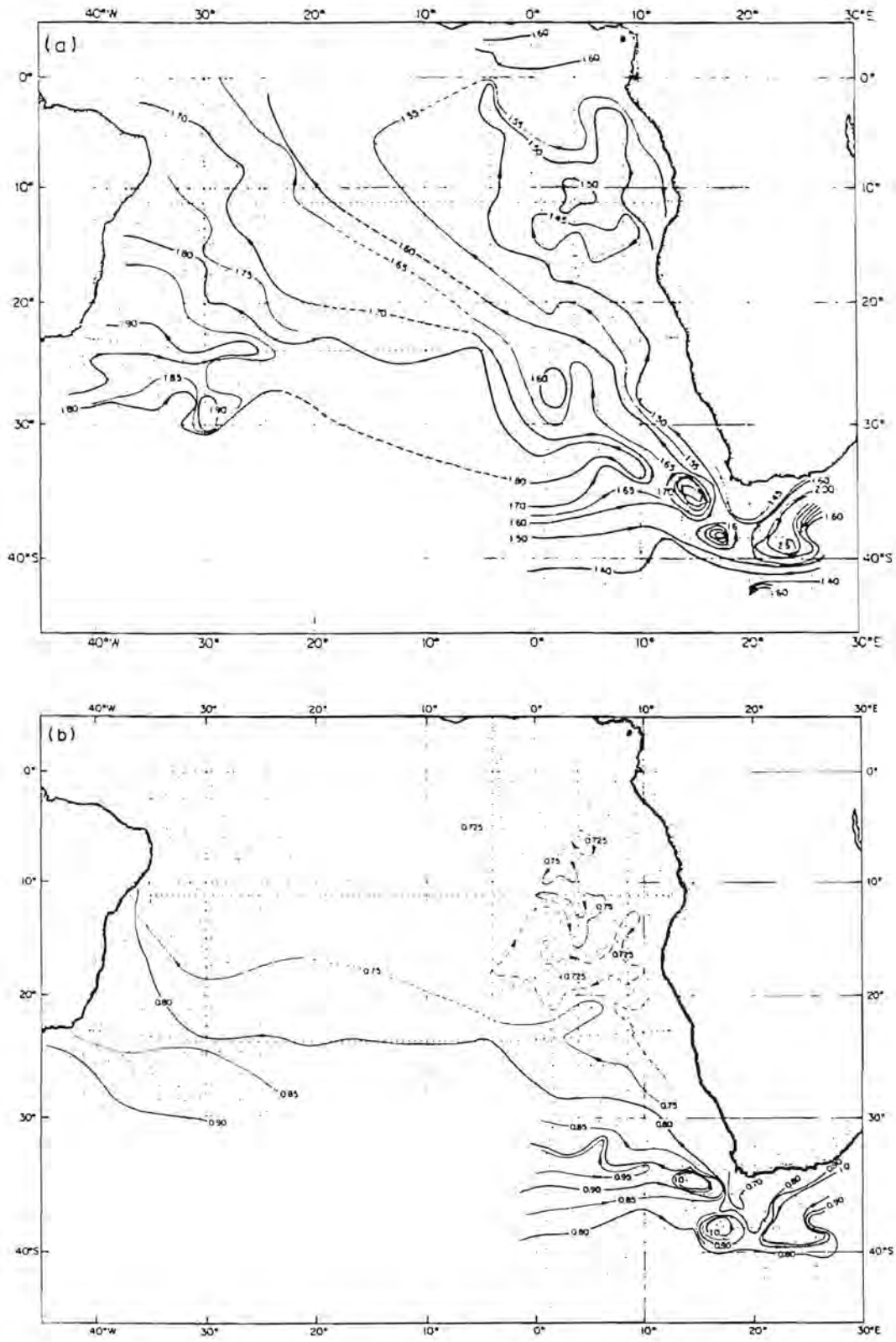

Figure 4.5: South Atlantic Ocean dynamic topographies from data collected during 1983-1984. (a) Dynamic topography of the sea surface relative to the 1500 db surface. (b) Dynamic topography of the 500 db surface relative to the 1500 db surface. (From Gordon and Bosley 1991.)

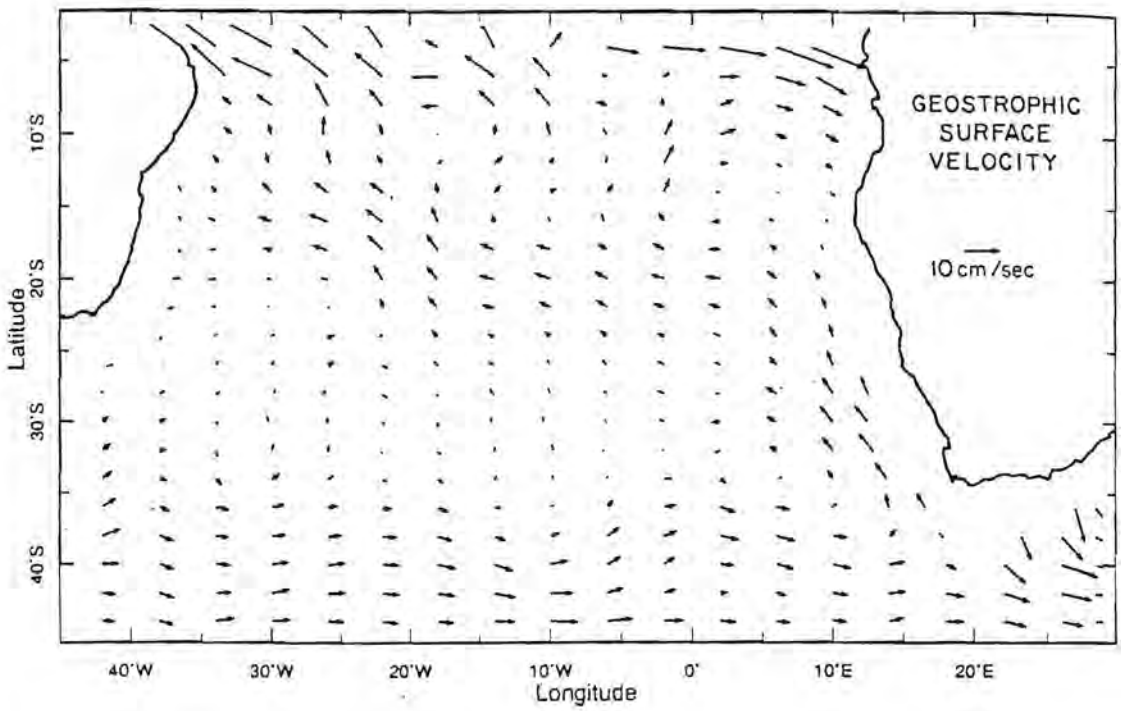

Figure 4.6: Mean annual geostrophic surface velocity (referenced to 1500 db) using Levitus (1982) historical data. (From Gordon and Bosley 1991.)

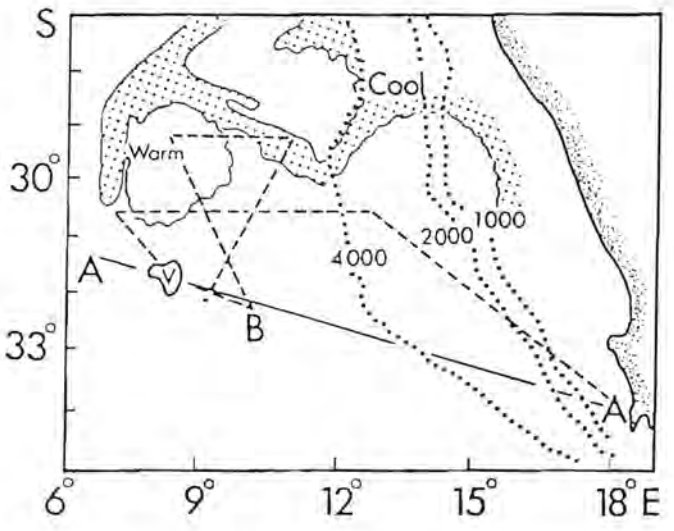

Figure 5.1: Cruise tracks for F.R.S. *Africana* (solid line A-A), April 1989, and R.S. *Benguela* (dashed line), May 1989. Isobath depths in km. Vema Seamount is marked V. The approximate position and shape of the ring as seen in NOAA infrared imagery in June 1989 is shown. (From Duncombe Rae *et al.* 1989b).

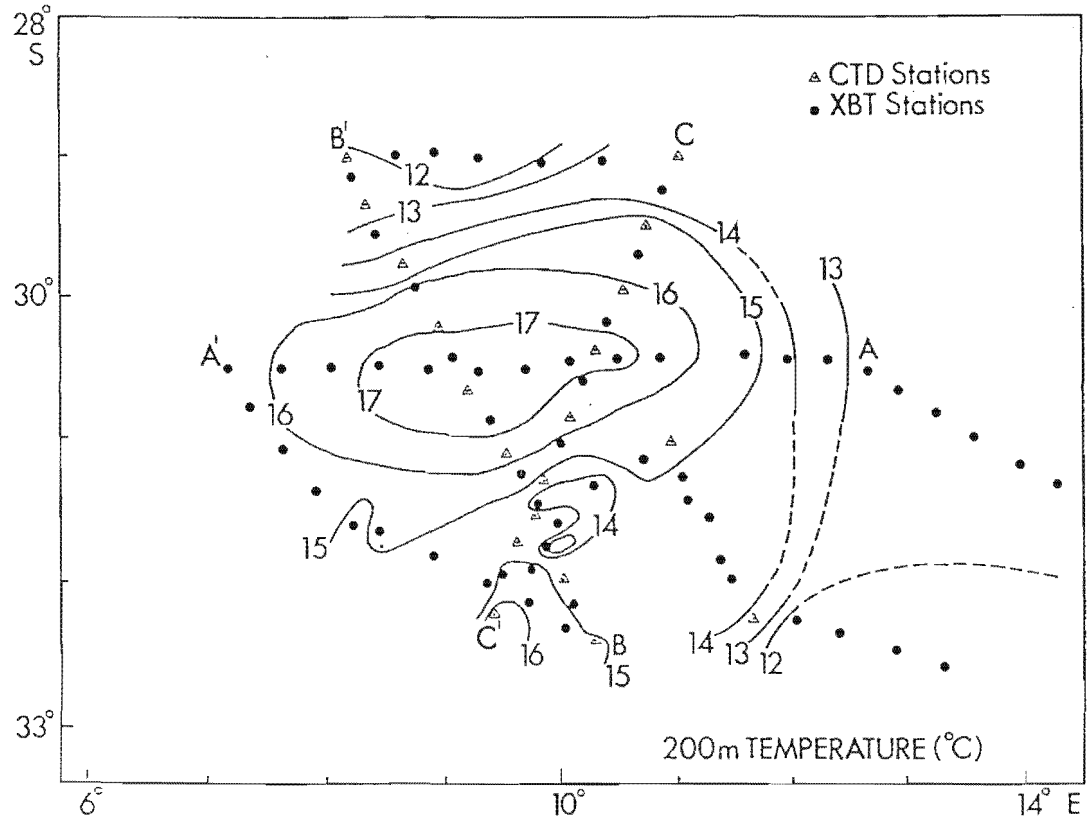

Figure 5.2: Temperatures at 200 m depth contoured from XBT and CTD data for the May 1989 *Benguela* cruise. Solid circles are XBT drops and triangles indicate CTD casts. The east - west XBT line is from A to A', the south - north CTD and XBT line is from B to B', and the north - south CTD and XBT line is from C to C'.

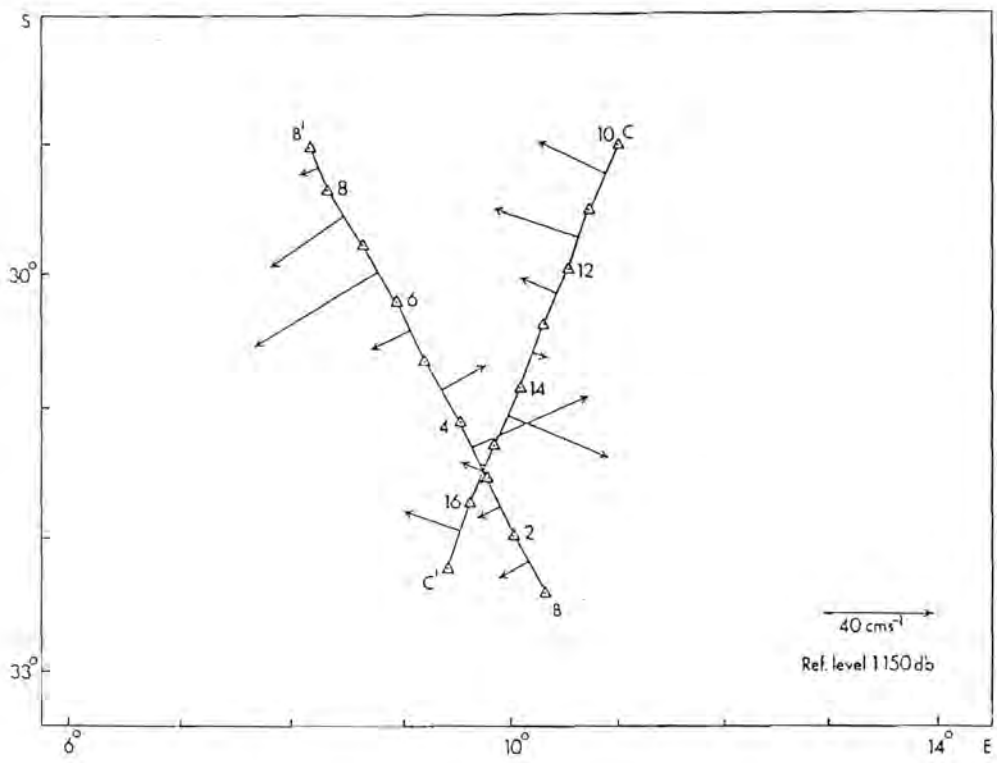

Figure 5.3: Surface geostrophic current speeds ($cm.s^{-1}$) referenced to 1150 db from the *Benguela* cruise. The lengths of the vectors are proportional to the current speed. Even-numbered CTD stations are indicated.

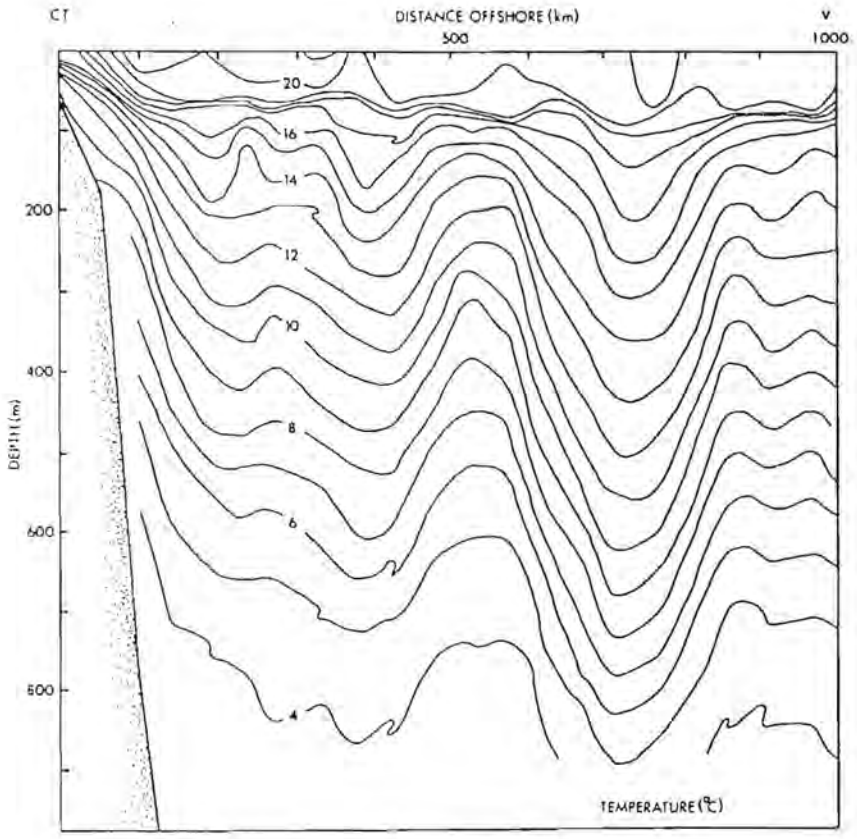

Figure 5.4: Vertical temperature section derived from XBT measurements taken from F.R.S. *Africana* in April 1989. The line of stations extends from Cape Town to Vema Seamount.

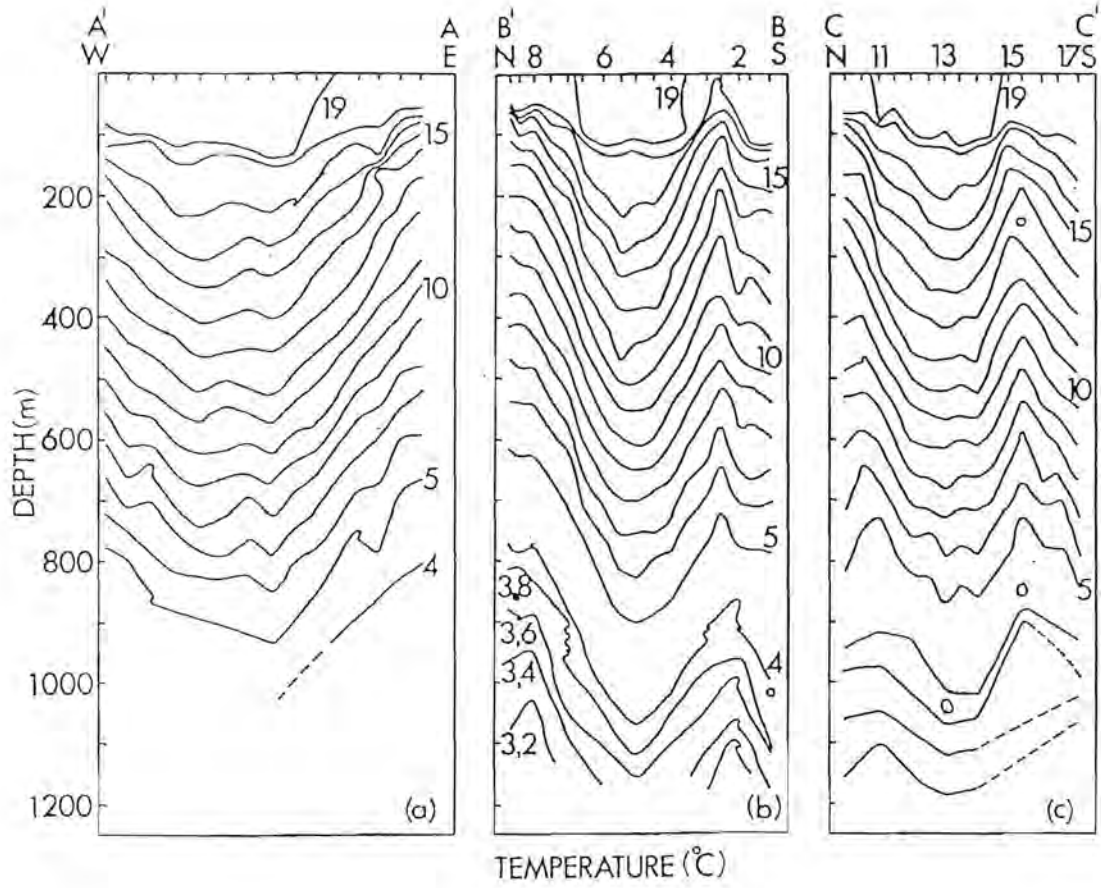

Figure 5.5: Temperature sections from XBT and CTD measurements from R.S. *Benguela* in May 1989. (a) east - west XBT section A..A', (b) south - north XBT and CTD section B..B', (c) north - south XBT and CTD section C..C' (see Figures 5.1 and 5.2 for cruise track details).

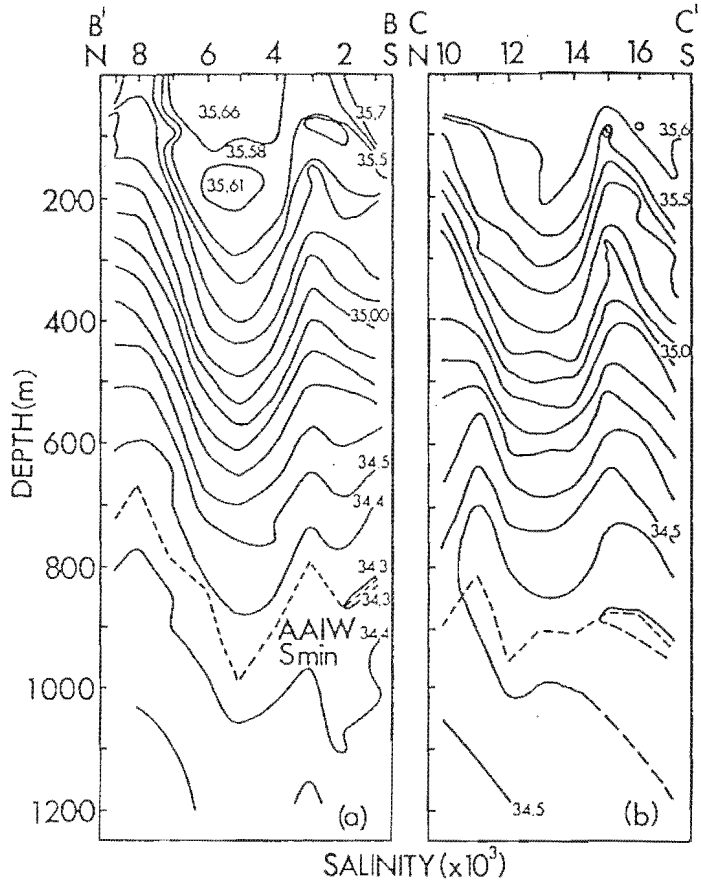

Figure 5.6: Salinity sections for the two CTD transects across the ring: (a) south - north leg B'..B (stations 1 to 9), (b) north - south leg C..C' (stations 10 to 17). The mid-water salinity minimum (S_{min}) indicating Antarctic Intermediate Water (AAIW) is shown by the dotted line.

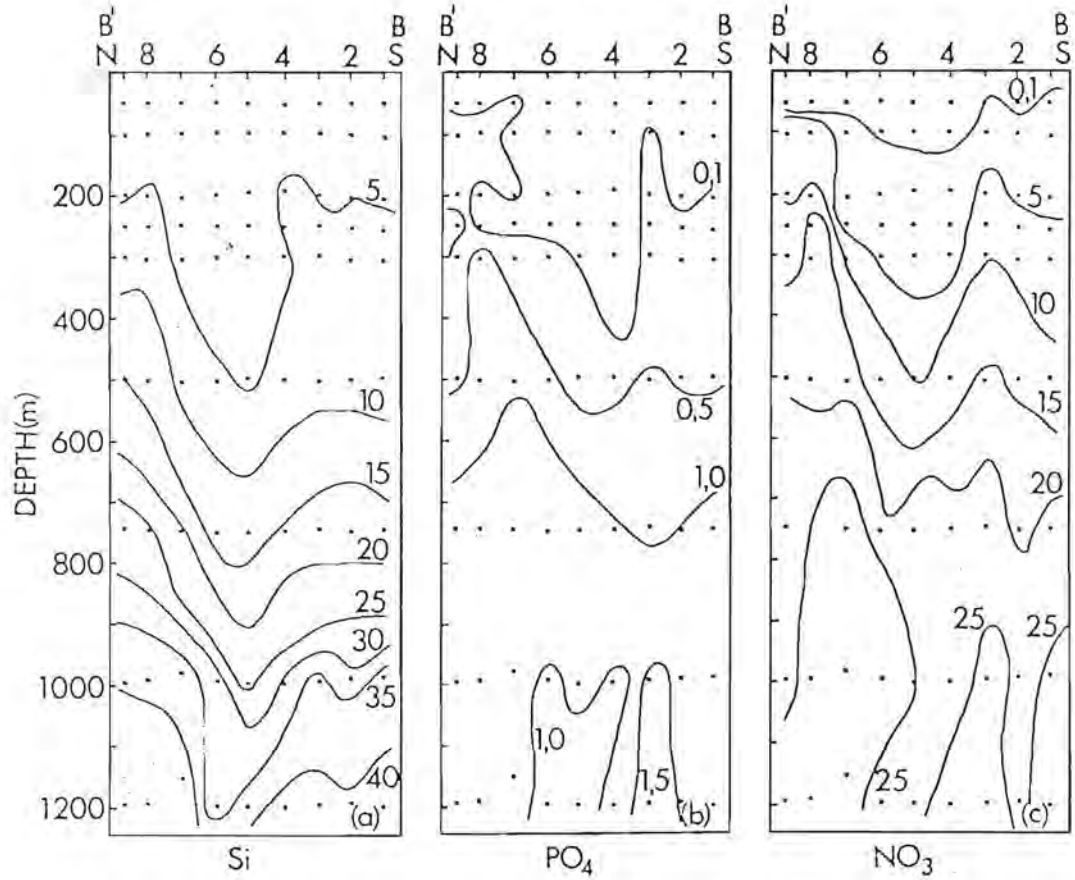

Figure 5.7: Vertical nutrient sections for south - north leg B..B' (stations 1 to 9). (a) silicate, (b) phosphate, (c) nitrate. Concentrations are in mmol.l^{-1}.

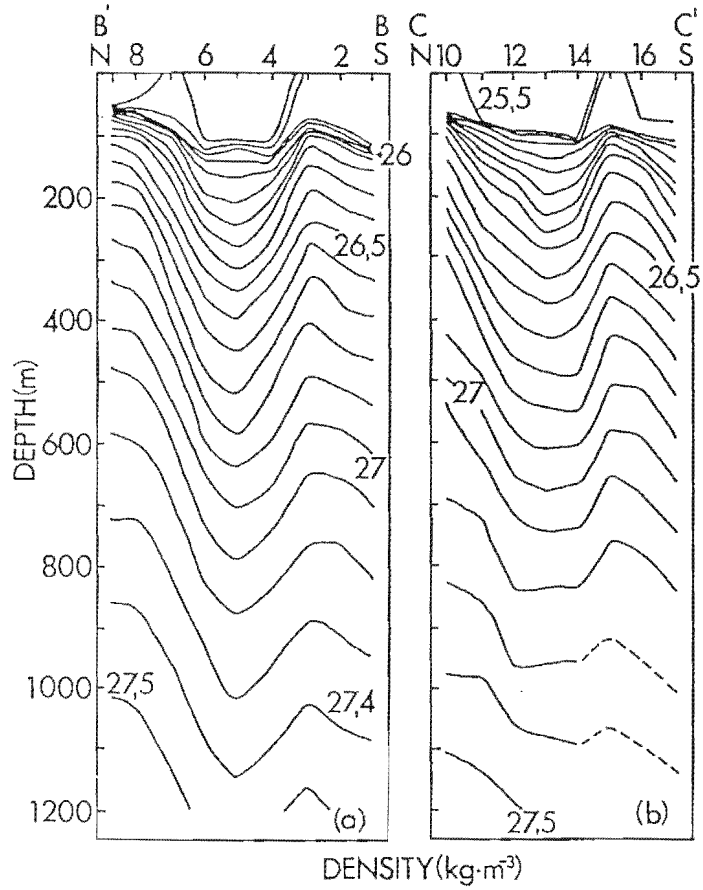

Figure 5.8: Vertical potential density (σ_t) structure for the two CTD lines on the R.S. *Benguela* cruise: (a) Leg B..B' (stations 1 to 9). (b) Leg C..C' (stations 10 to 17). Units are $kg.m^{-3}$.

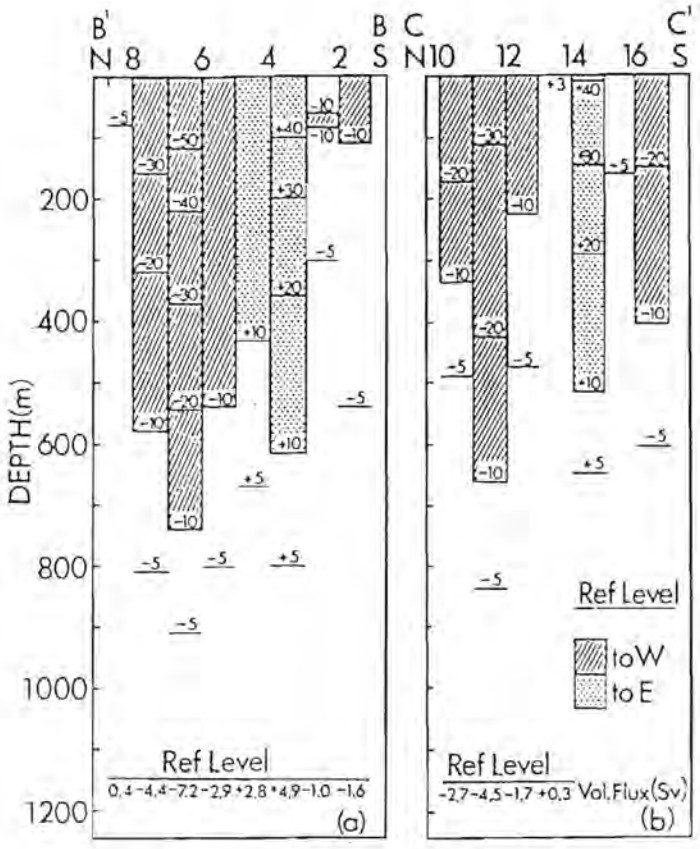

Figure 5.9: Vertical geostrophic velocity structure for the two CTD lines on the R.S. *Benguela* cruise: (a) Leg B..B' (stations 1 to 9). (b) Leg C..C' (stations 10 to 17). The reference depth level for each station pair is indicated. Below the reference level the volume flux in Sverdrup (Sv = 10^6 $m^3.s^{-1}$) is indicated.

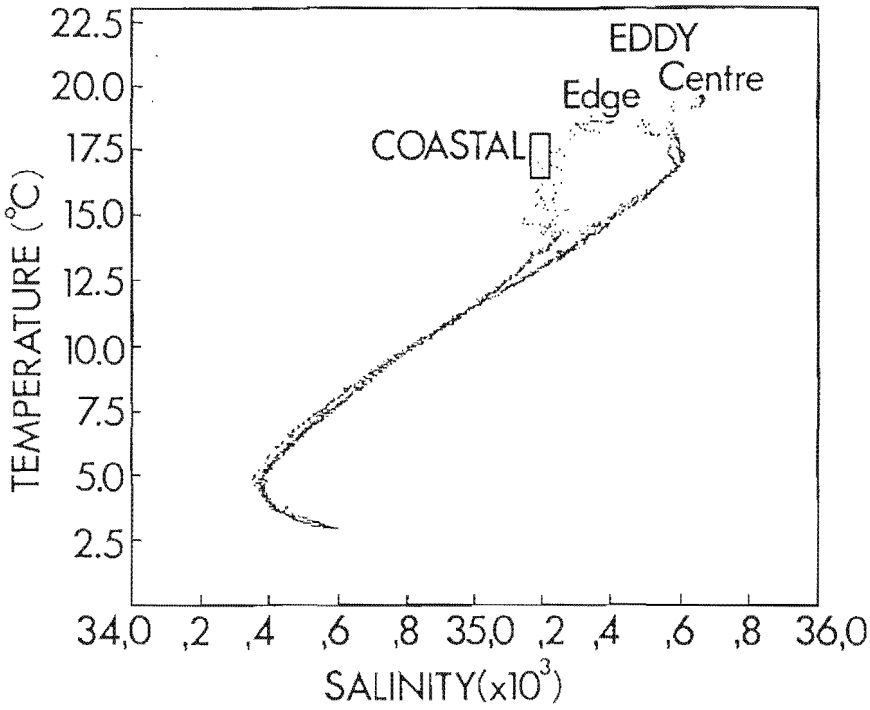

Figure 5.10: Temperature-salinity (TS) diagram for stations representative of the centre of the ring (5 and 6 on leg B..B') and of the north-western edge of the ring (stations 8 and 9 on leg B..B'). Typical surface Benguela Frontal water (Shillington *et al.* 1990) is boxed and indicated as "Coastal". The apparent splitting of the thermocline water between 5° and 10°C is not related to the salinity differences near the surface.

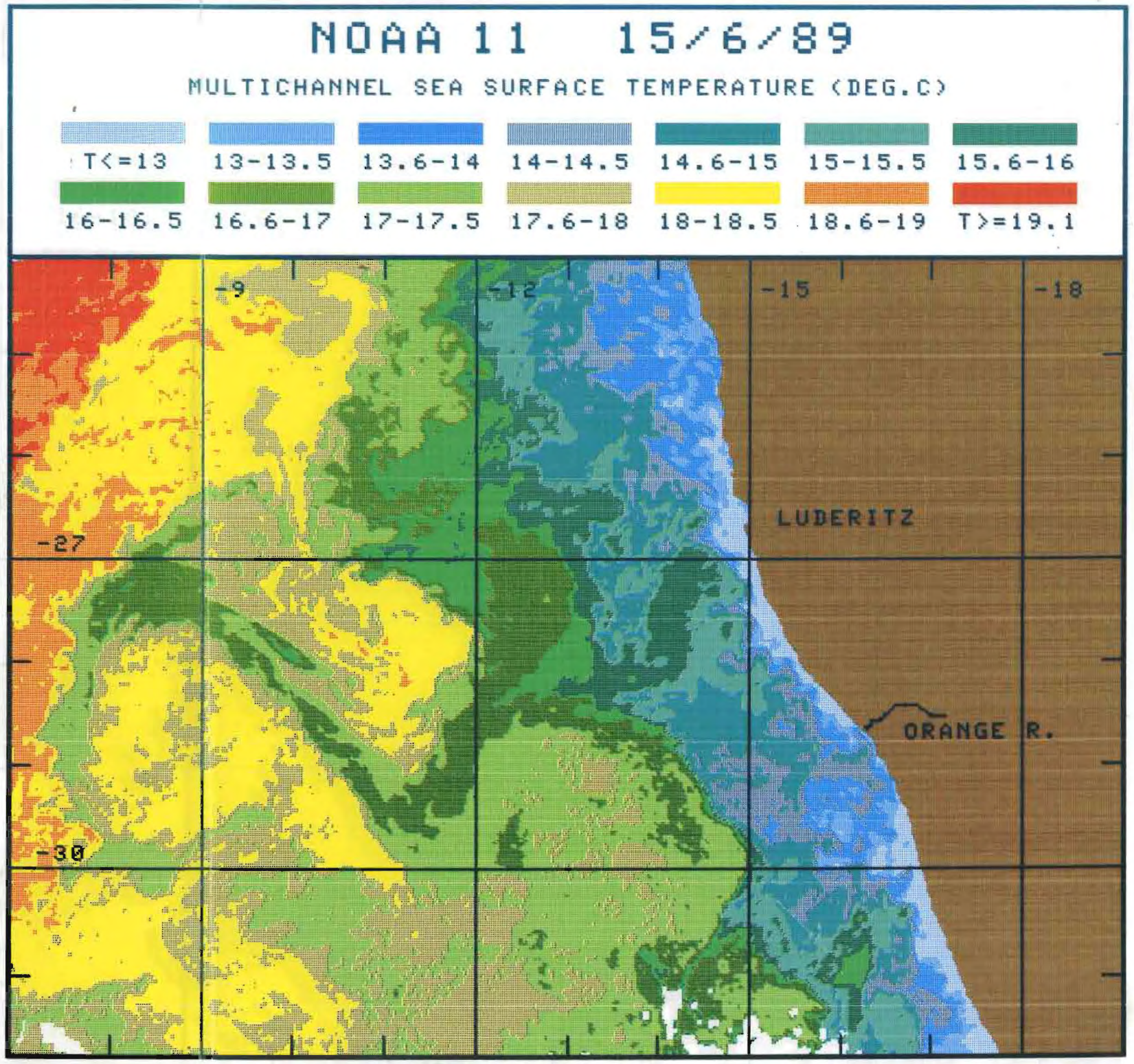

Figure 5.11a: NOAA-11 multi-channel sea surface temperatures for 15 June 1989 showing the extent of the filament drawn in from the Benguela system and the relationship of the ring with the coast.

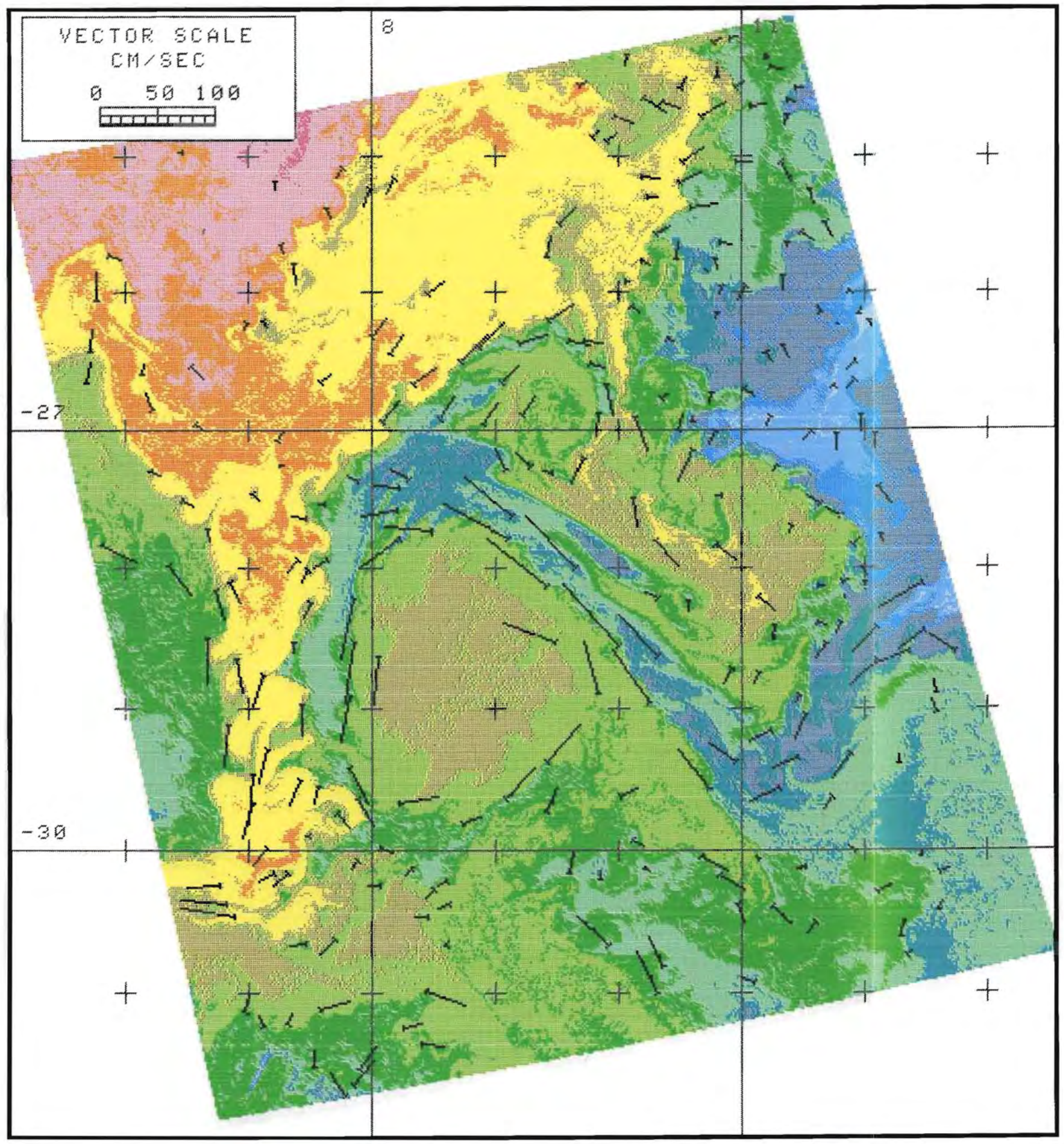

Figure 5.11b: NOAA-11 single channel infra-red image for 15 June 1989 with surface current vectors from feature tracking with two images approximately 24 hours apart.

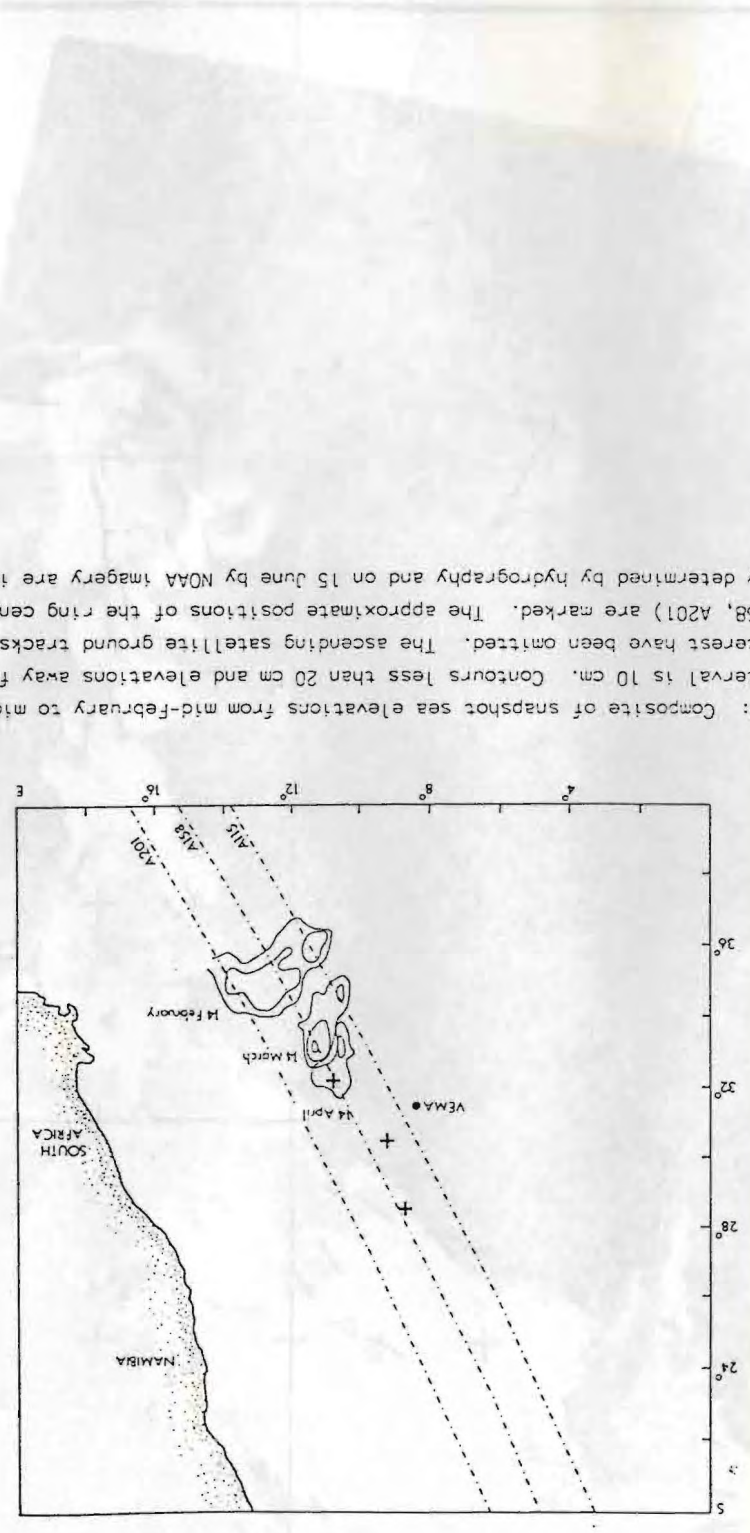

Figure 5.12: Composite of snapshot sea elevations from mid-February to mid-April. The contour interval is 10 cm. Contours less than 20 cm and elevations away from the features of interest have been omitted. The ascending satellite ground tracks over the area (A115, A158, A201) are marked. The approximate positions of the ring centre on 6 April and 20 May determined by hydrography and on 15 June by NOAA imagery are indicated by crosses.

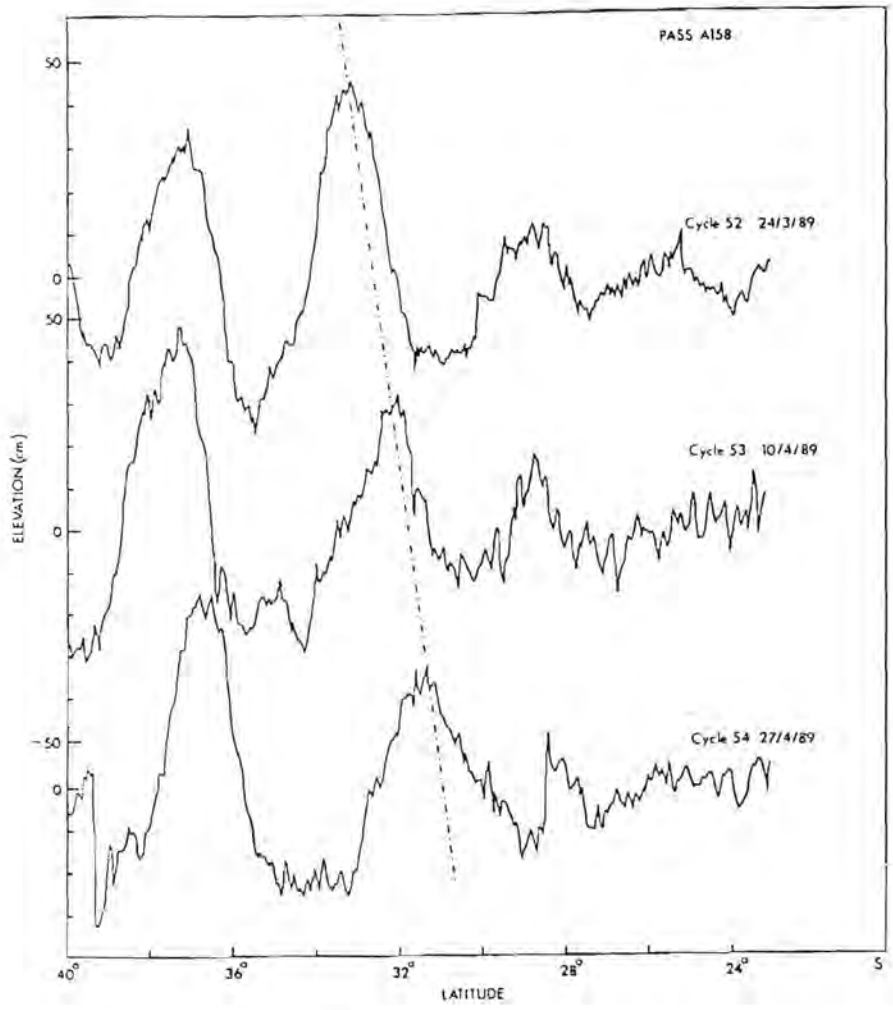

Figure 5.13: Along-track elevations from three successive cycles (52, 53, 54) along pass A158 in March and April 1989. The progress of the elevation corresponding to the ring is indicated by the dashed line.

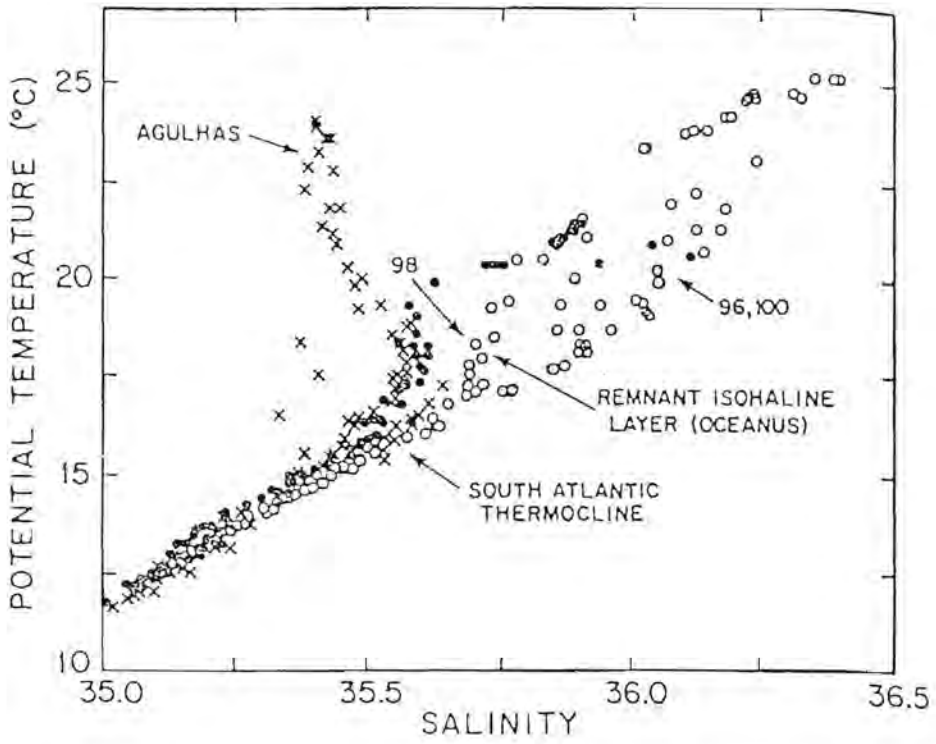

Figure 5.14: Potential temperature and salinity relation for *Discovery* stations within the ring discussed by Gordon and Haxby (1990 from whom the figure is taken) contrasted with data from the Agulhas retroflection (ARC: Camp *et al.* 1986) and the South Atlantic Ocean (AJAX Expedition: Anon. 1985).

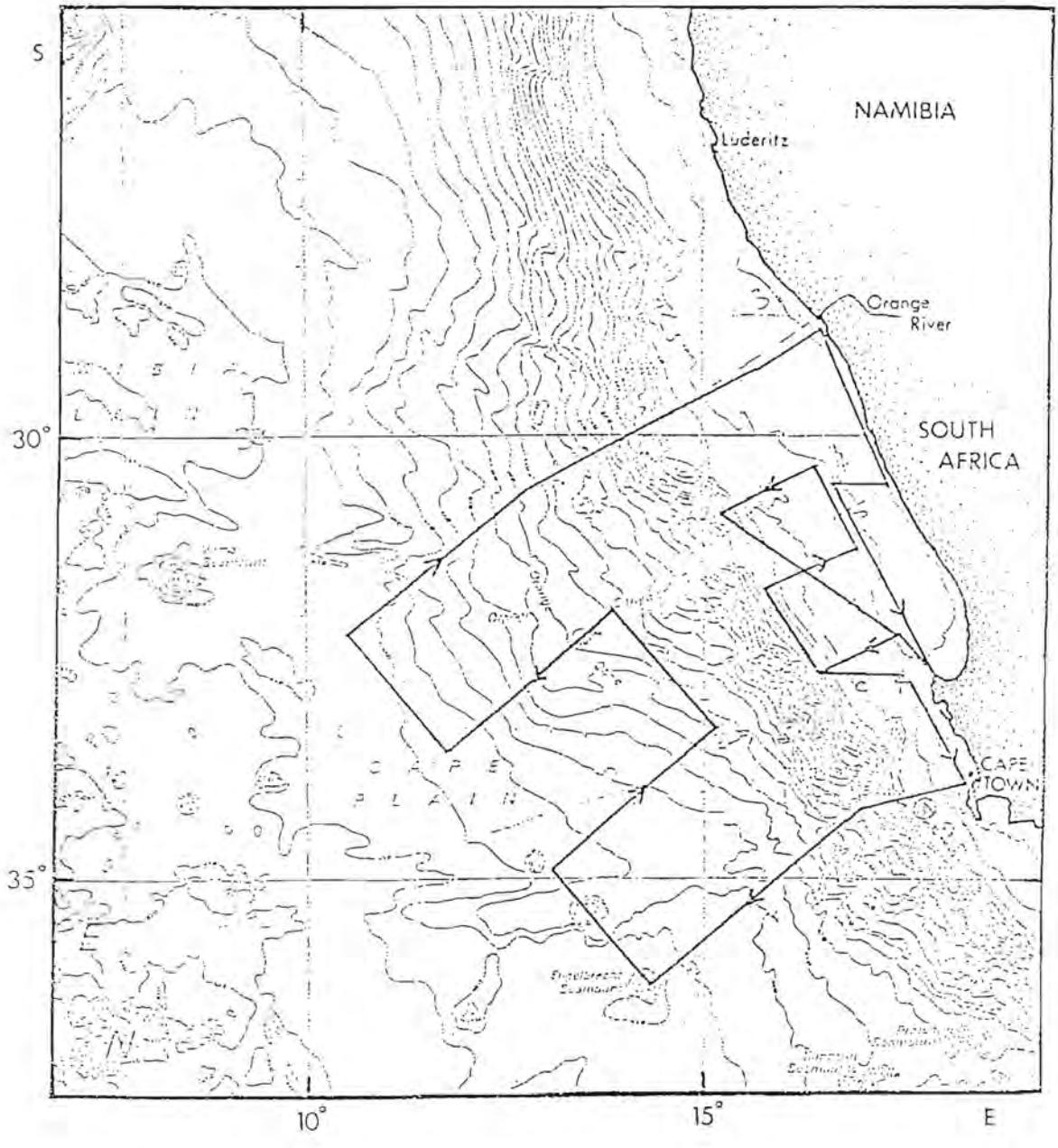

Figure 5.15: The proposed cruise track for the August 1990 cruise of F.R.S. *Africana* (V085) on which the Winter ring was encountered.

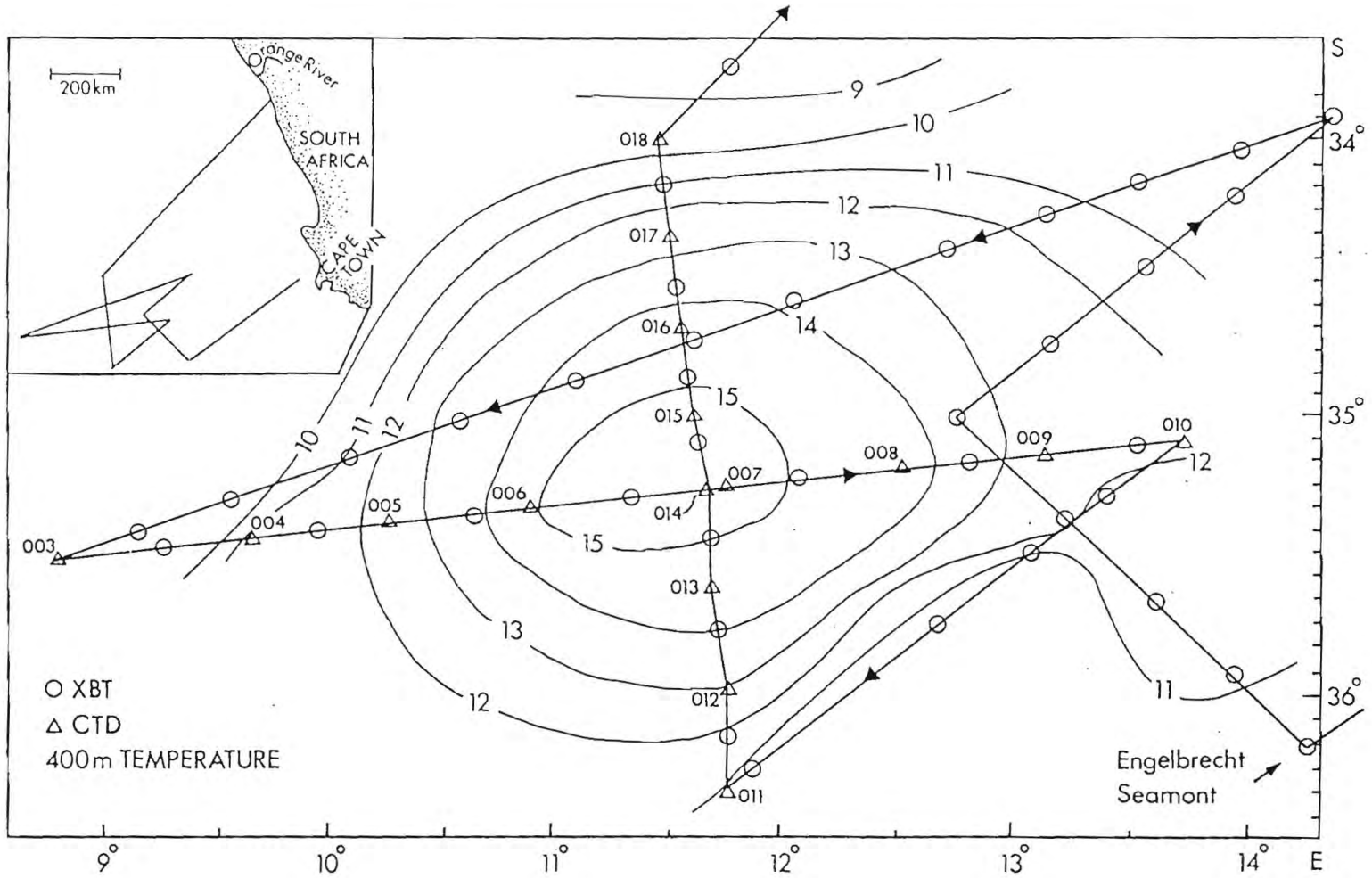

Figure 5.16: Isotherms in °C at 400 m depth for the Winter ring. The actual cruise track followed and the positions of expendable bathythermograph (circles) and conductivity-temperature-depth (triangles) stations are shown. CTD station numbers are indicated.

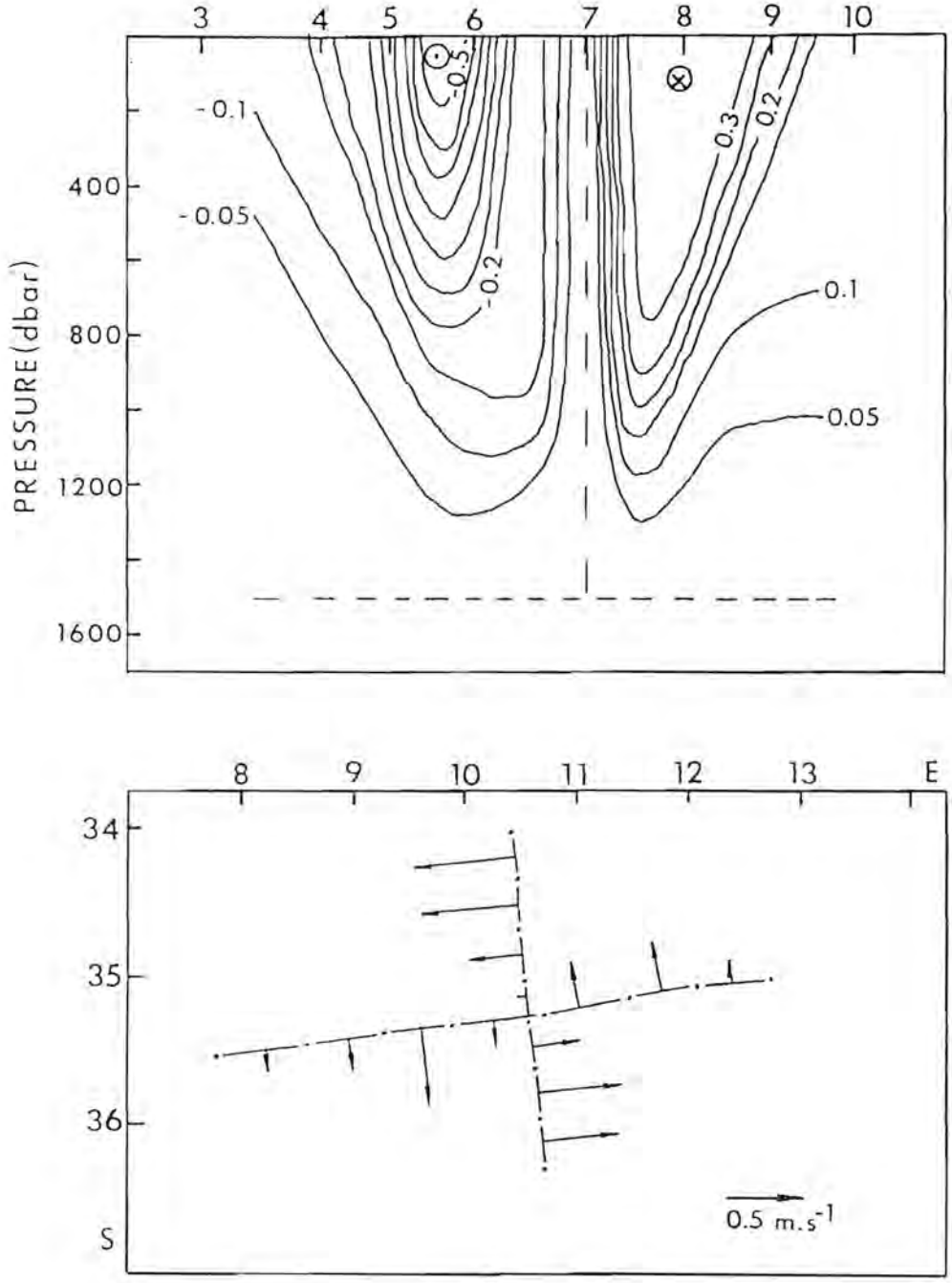

Figure 5.17: Geostrophic velocity structure for the Winter ring. (a) Vertical east-west section. Contour interval is 0.05 $m.s^{-1}$ (b) Surface vectors. The length of the arrows is proportional to the current speed.

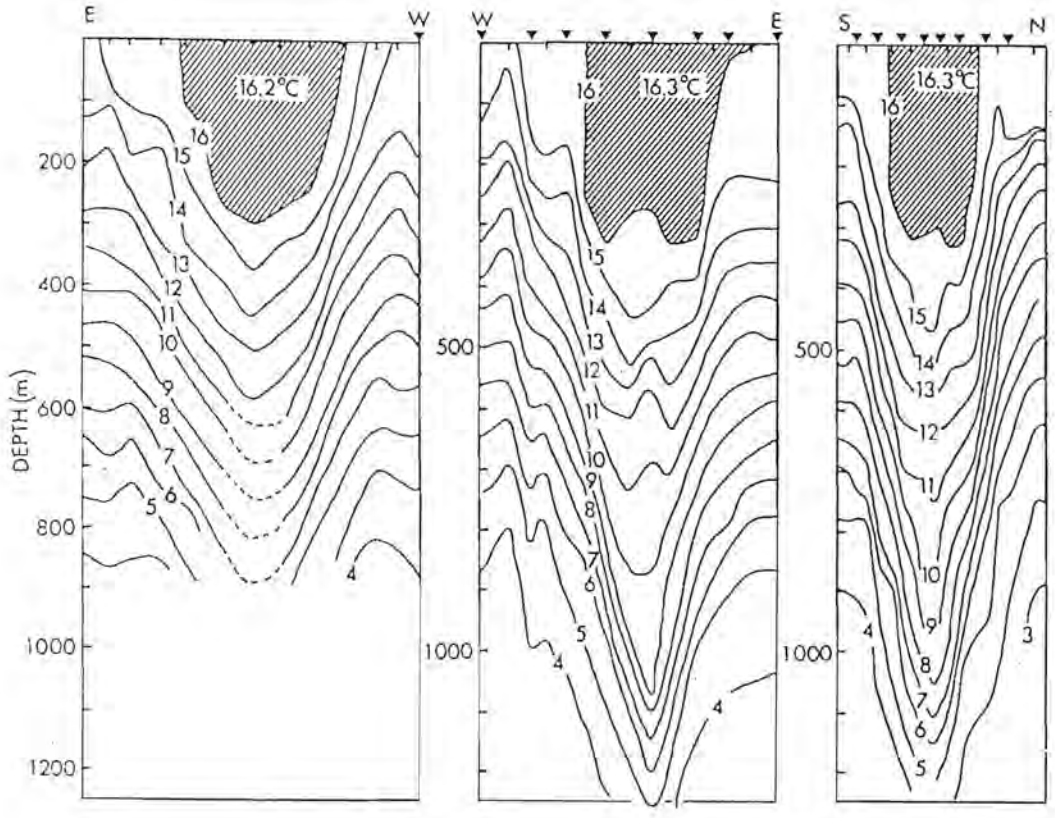

Figure 5.18: Vertical temperature sections through the Winter ring showing the deep surface mixed layer. (a) The east - west XBT section across the northern edge of the ring. (b) The west - east XBT and CTD section across the ring centre. (c) The south - north XBT and CTD section.

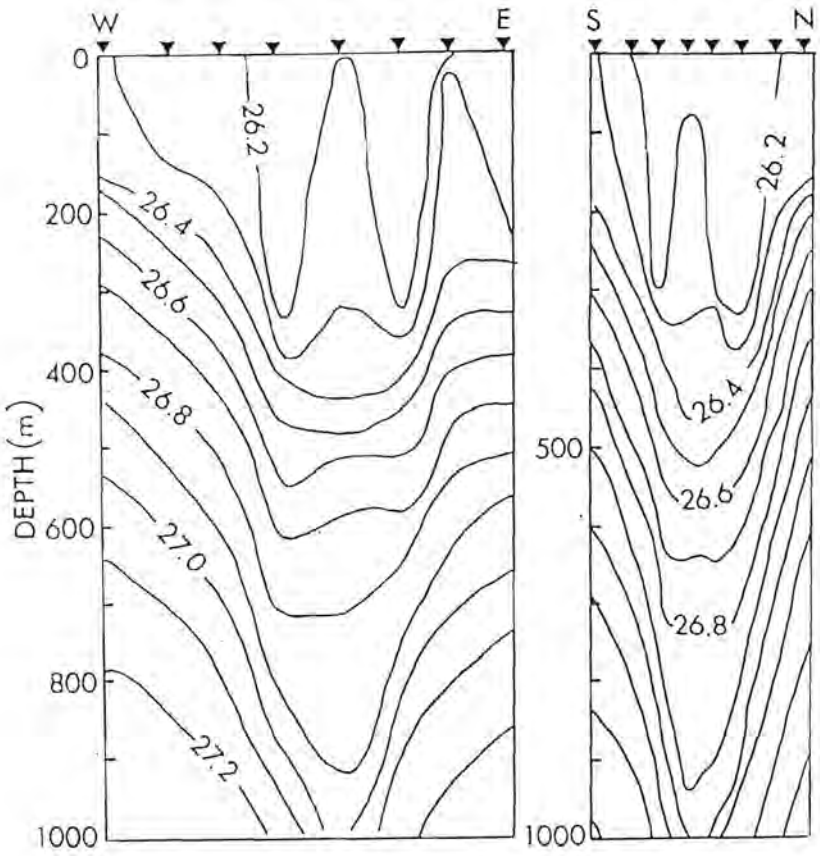

Figure 5.19: Vertical density section across the Winter ring, showing the reversal of baroclinicity at the ring centre above 400 m.

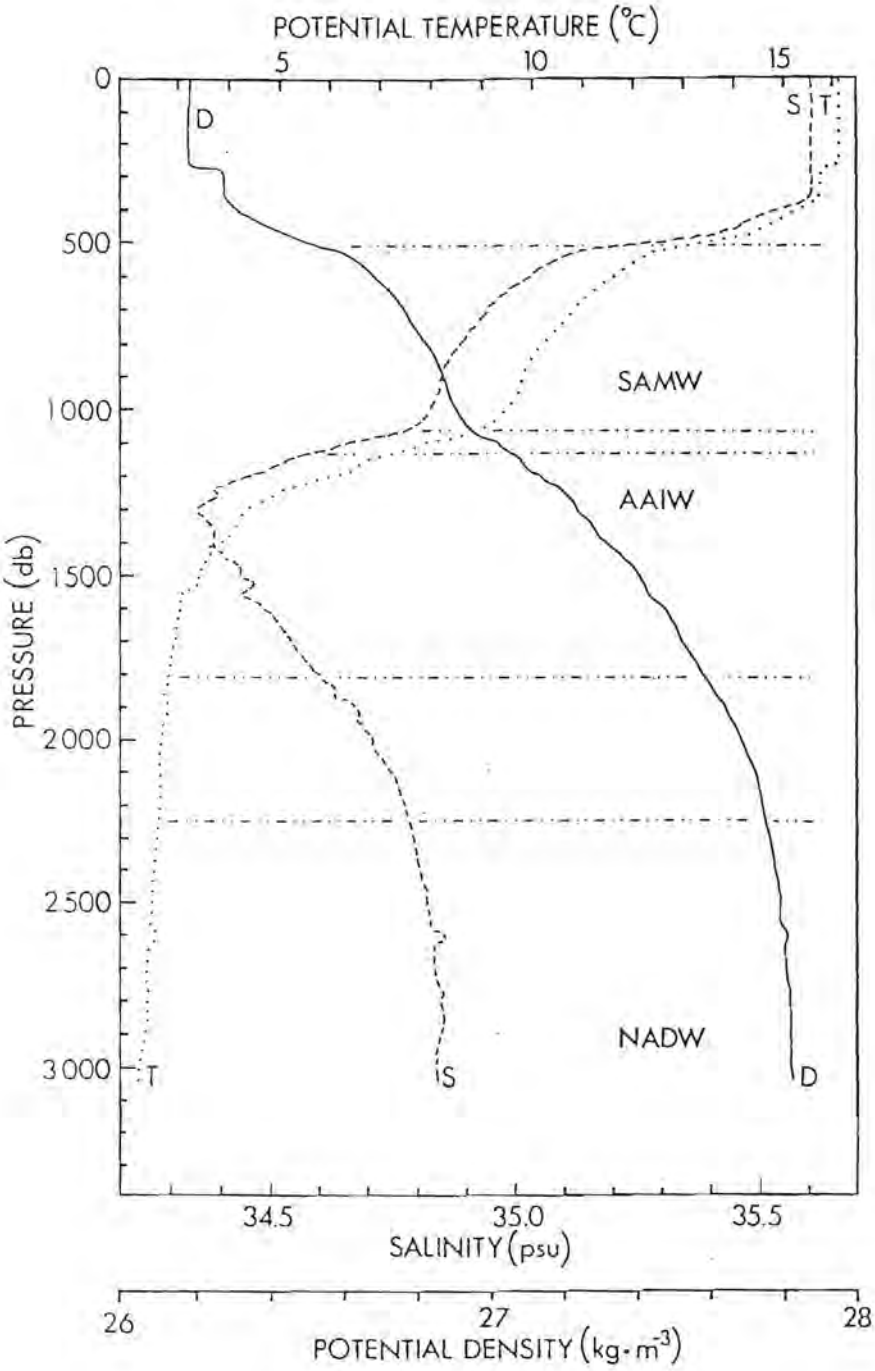

Figure 5.20: Vertical temperature, salinity and density structure at a station (Stn. 7 on Fig. 5.16) in the centre of the ring showing the deep surface mixed layer and the Agulhas ring Lower Stad Water at 900 m. The applicable water types according to Bennett's definitions (Bennett 1988) are indicated: SAMW – Subantarctic Mode Water (Bennett's salinity criterion is used here); AAIW – Antarctic Intermediate Water; NADW – North Atlantic Deep Water.

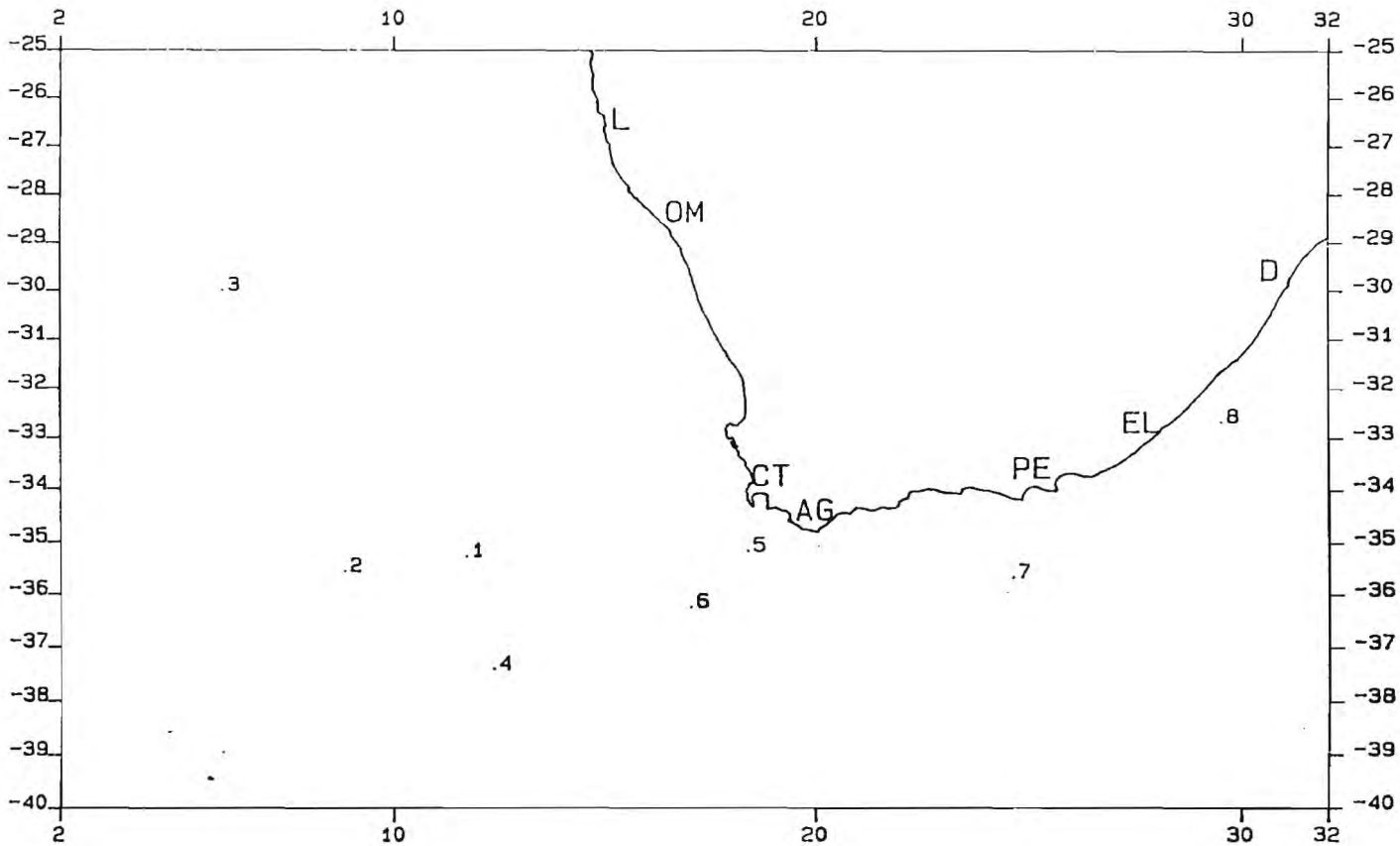

Figure 5.21: Station positions of hydrographic stations referred to in Fig. 5.22 and the text. Pos. 1: Stn 7 (Fig. 5.16) at the centre of the Winter ring. Pos. 2: Stn 3 (Fig. 5.16) at the western edge of the Winter ring. Pos. 3: Station near the Walvis Ridge from the BEST-1 cruise, *Africana* V105. Pos. 4: Station at the westernmost end of the SW line of the BEST-1 cruise. Pos. 5: Station on the western Agulhas Bank shelf-edge from the Agulhas Bank Boundary Processes (ABBP) Cruise, *Africana* V099. Pos. 6: Station in an eddy off the western Agulhas Bank from the ABBP Cruise. Pos. 7: Station in the Agulhas Current core off the eastern Agulhas Bank from the ABBP Cruise. Pos. 8: Station in the Agulhas Current core off the Transkei coast from the ABBP Cruise.

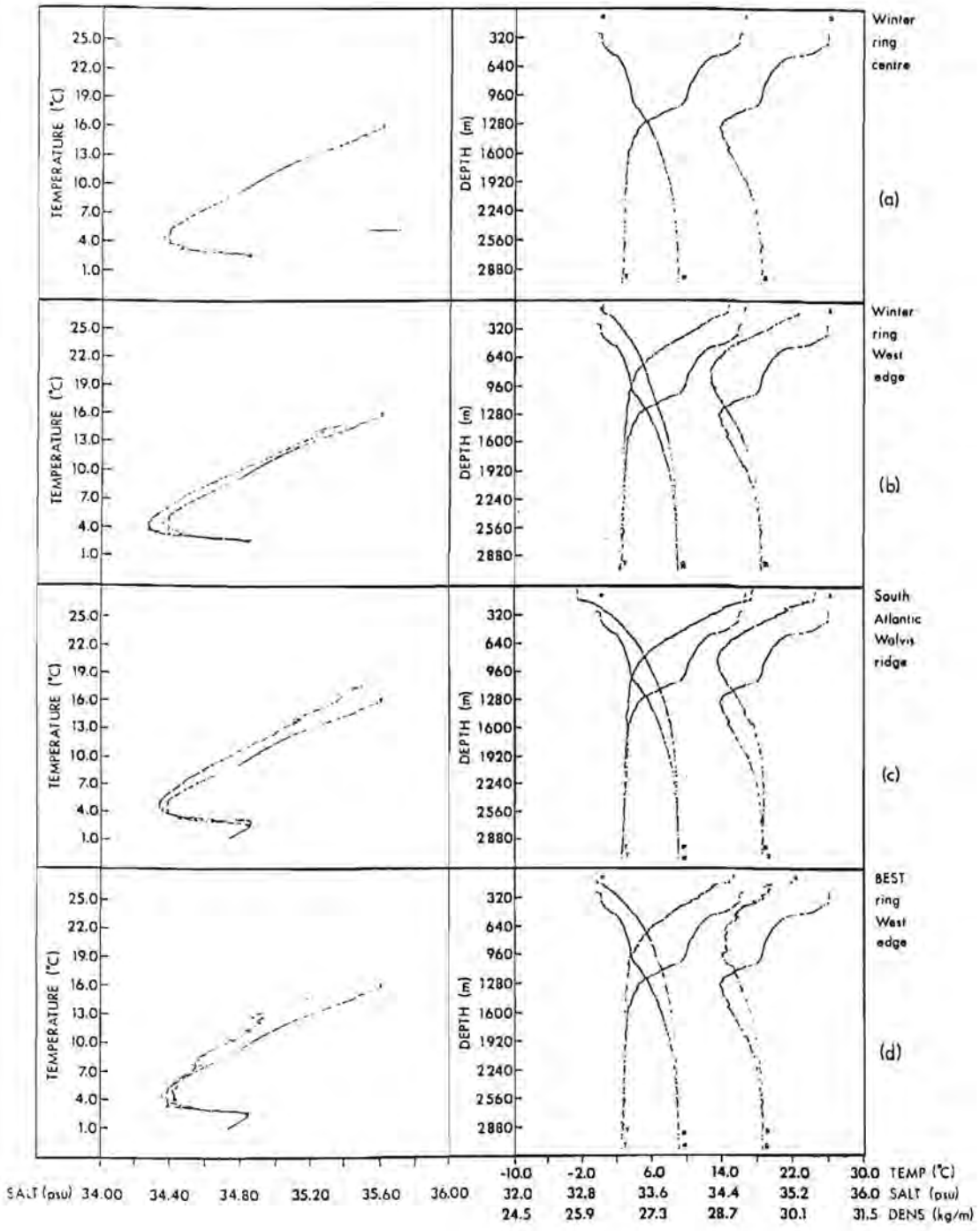

Figure 5.22: Temperature-salinity diagrams for the station positions indicated on Fig. 5.21. (a) TS diagram and water column profile for Stn 7 (Pos. 1) at the centre of the Winter ring. This TS diagram is shown with other TS diagrams for comparison with: (b) the western edge of the Winter ring (Pos. 2); (c) South Atlantic water from a station (Pos. 3) near the Walvis ridge on the BEST-1 30°S line; (d) the western edge of the BEST ring (Pos. 4)

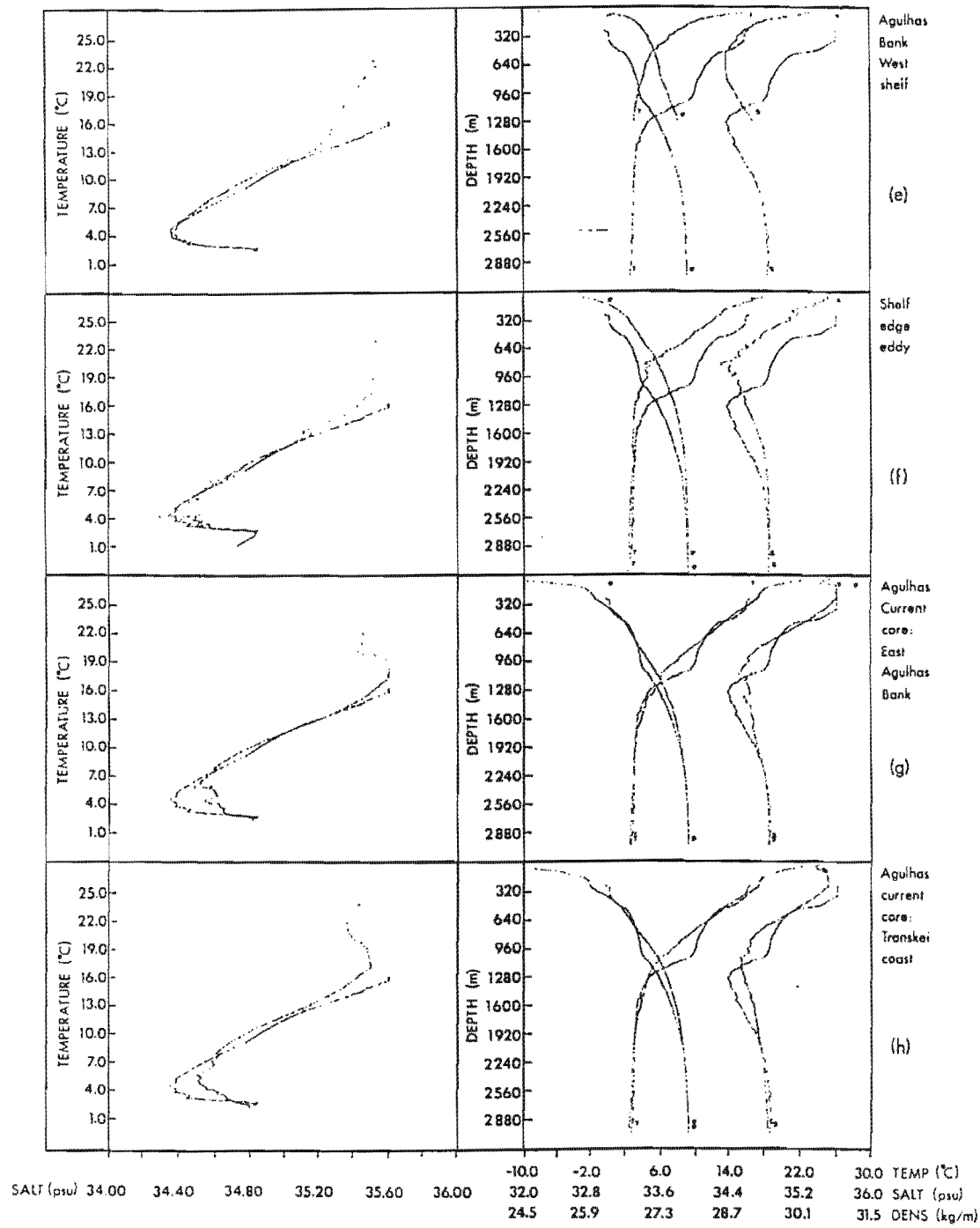

Figure 5.22: Temperature-salinity diagrams for the station positions indicated on Fig. 5.21. (e) a station (Pos. 5) on the western Agulhas Bank shelf edge from the Agulhas Bank Boundary Processes Cruise (*Africana* V099); (f) a station (Pos. 6) within an eddy encountered on V099; (g) off the eastern Agulhas Bank shelf-edge, within the Agulhas Current core, (Pos. 7) from V099; (h) the Agulhas current core off the Transkei coast (Pos. 8).

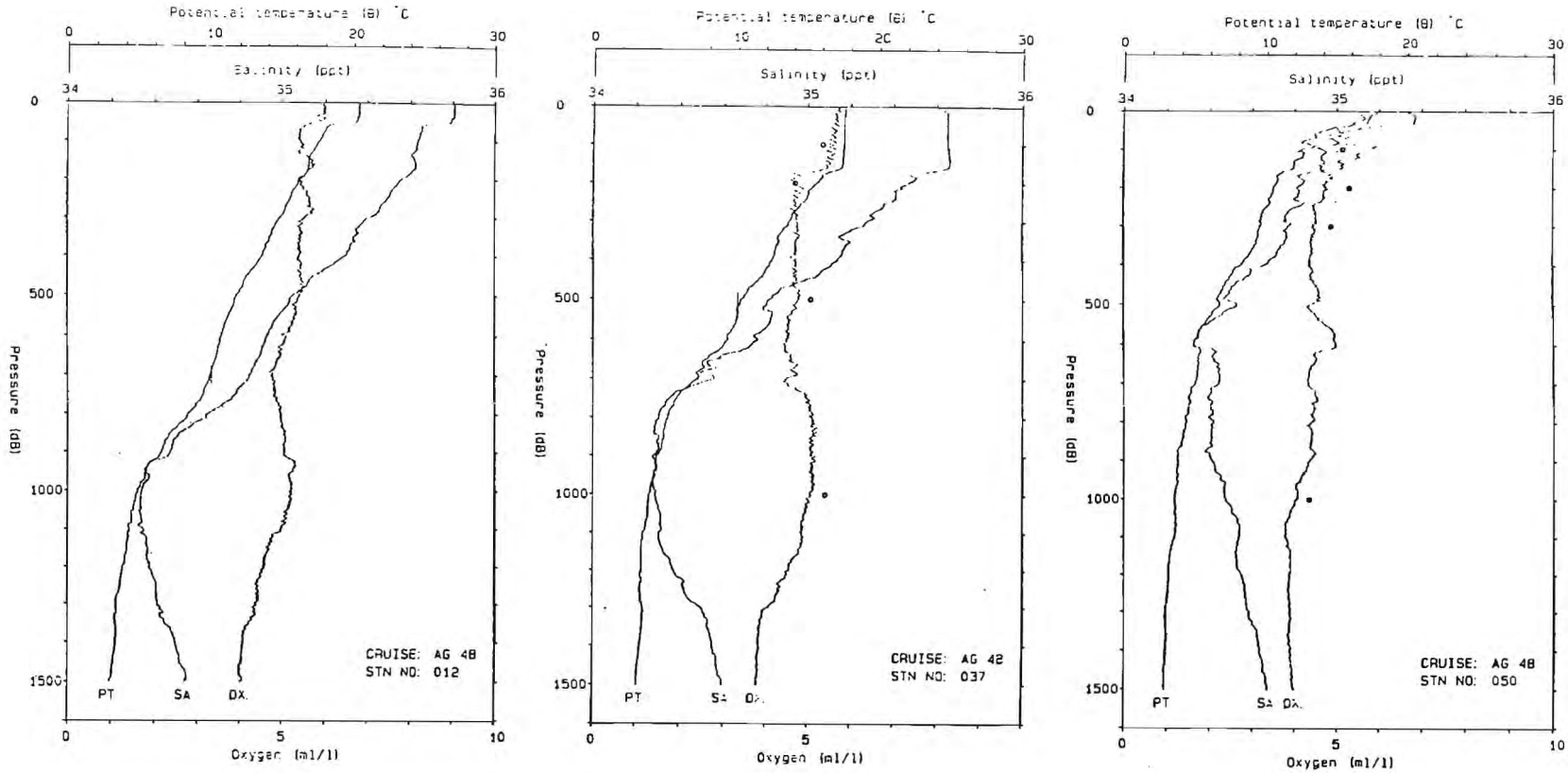

Figure 5.23: Temperature and salinity profiles at three stations from the SCARC cruise of February 1987 which showed evidence of a thick near-isopycnal layer with TS characteristics close to T=10°C and S=34.7 psu. (a) Stn. 12 at the centre of ring Rosemary (Table 2i). (b) Stn. 37 at the centre of ring Helen (Table 2i). (c) Stn 50 on the edge of a cold-core feature within the Agulhas Return Current. (Data from Valentine *et al.* 1988.)

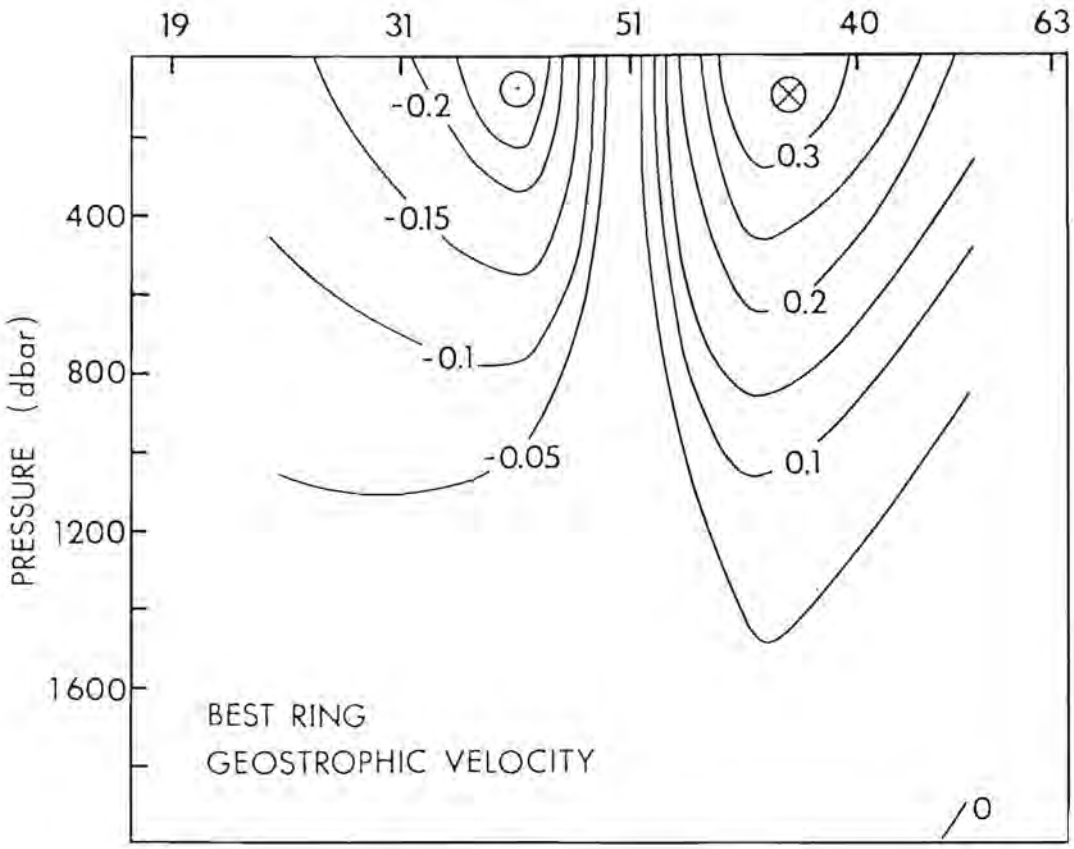

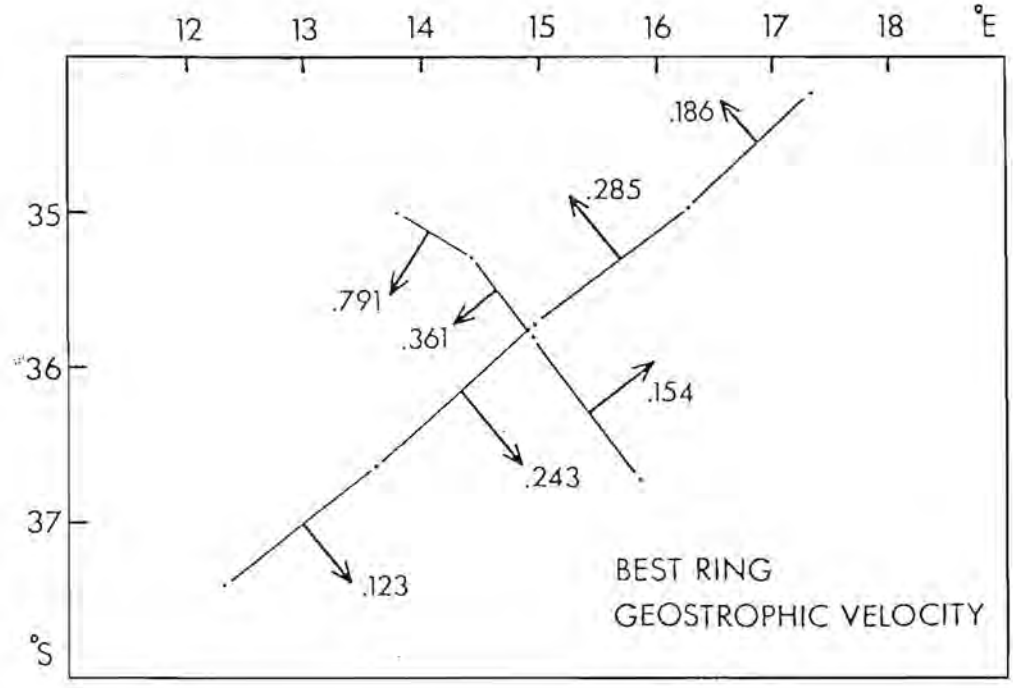

Figure 5.25: Geostrophic velocity structure of the BEST-1 ring. (a) Velocities across the vertical west to east section referrenced to the bottom (b) Surface geostrophic velocities referenced to the bottom. Velocities are in $m.s^{-1}$

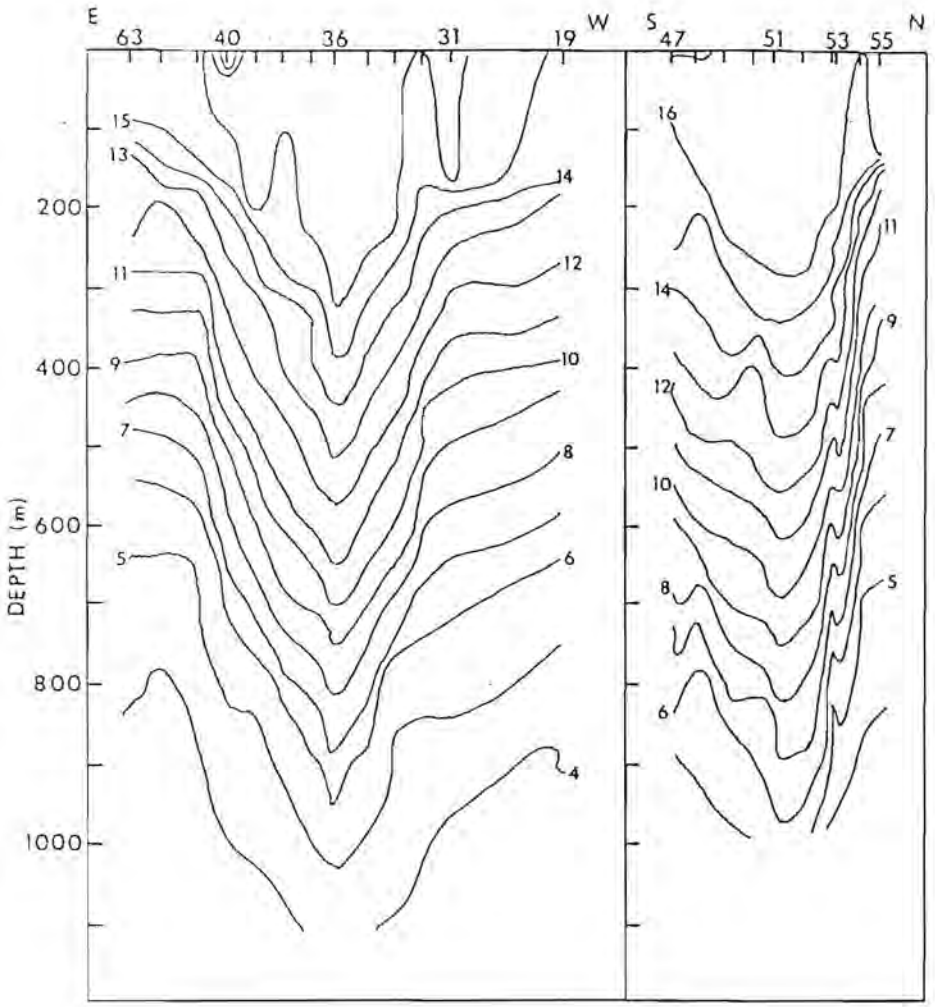

Figure 5.24: Vertical temperature sections along the two CTD station lines across the BEST ring.

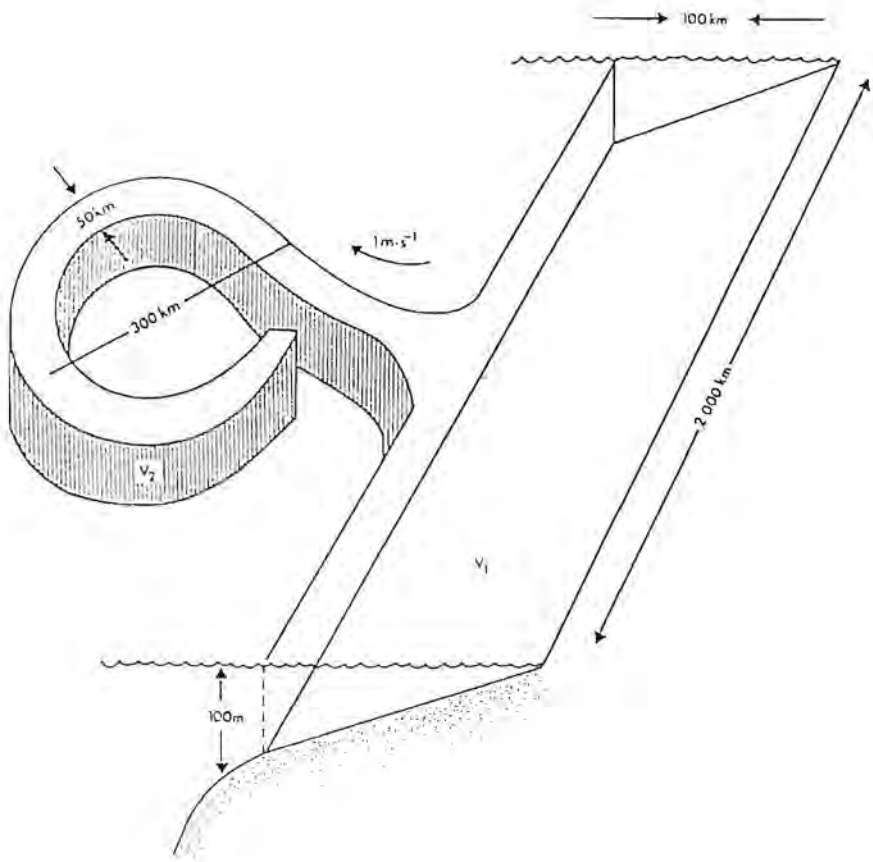

Figure 5.1: Schematic representation of the interaction between the Vema ring and a filament from the Benguela upwelling system, showing the volumes of water which the ring may extract from the system.

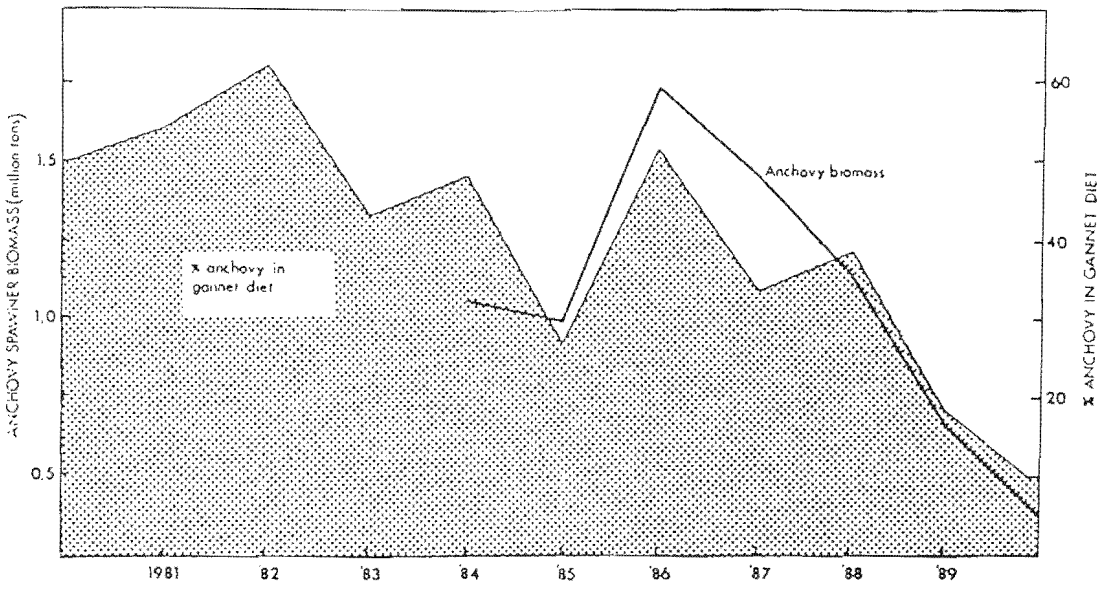

Figure 6.2: The proportion by weight of anchovy in the diet of Cape gannets off western South Africa contrasted with acoustic estimates of anchovy spawner biomass, 1980-1990.

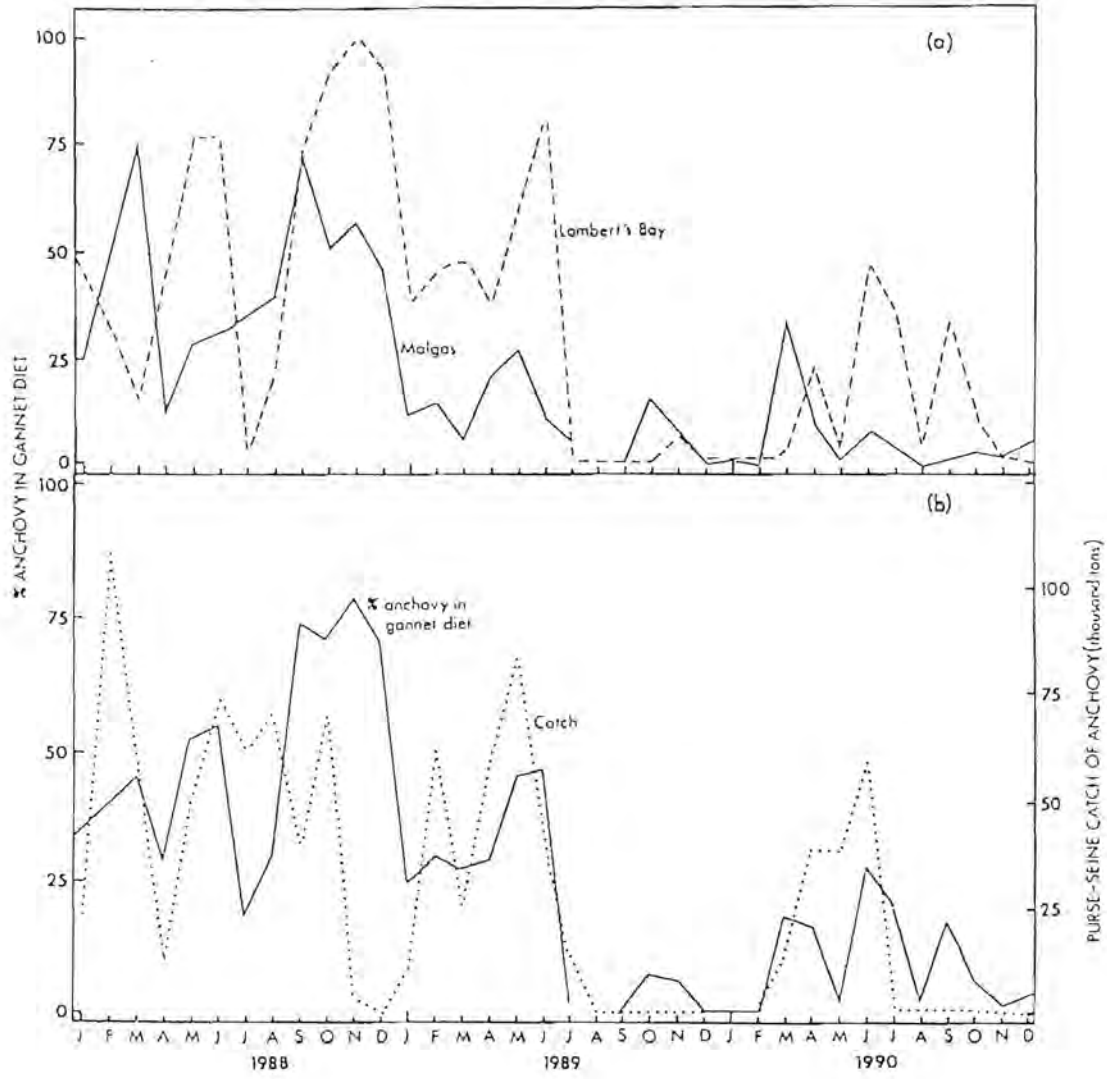

Figure 6.3: (a) The percentage by weight of anchovy in the diet of Cape gannets at two sites off western South Africa, Lambert's Bay (32°05'S; 18°18'E) and Malgas Island (33°03'S; 17°55'E). (b) Combined gannet diet data for the two sites contrasted with the purse-seine catch of anchovy, January 1988 - December 1990, showing the collapse of anchovy in mid-1989. At the end of July 1989 the fishery was closed.

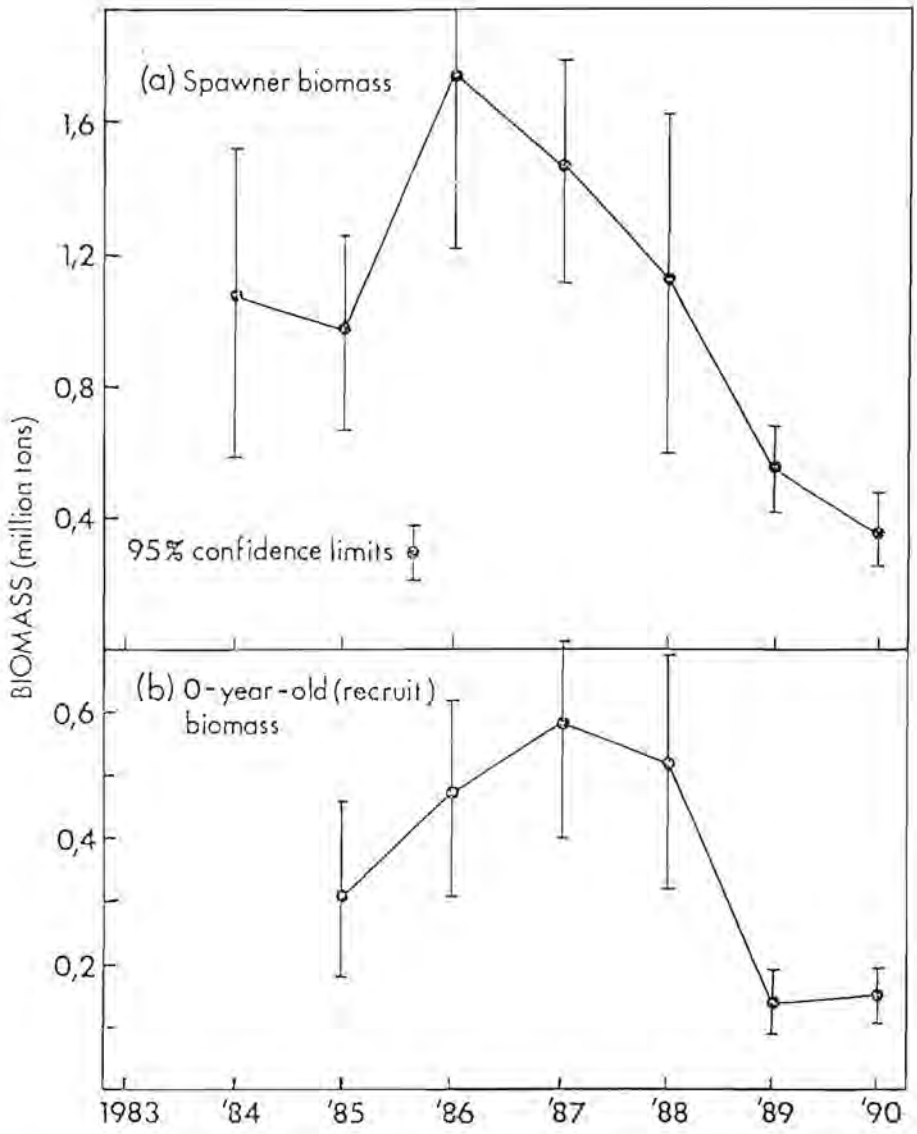

Figure 6.4: Acoustic estimates of (a) spawner biomass of anchovy in November and (b) abundance of 0-year-old anchovy in June, 1984-1990. (From S.F.R.I. 1991).

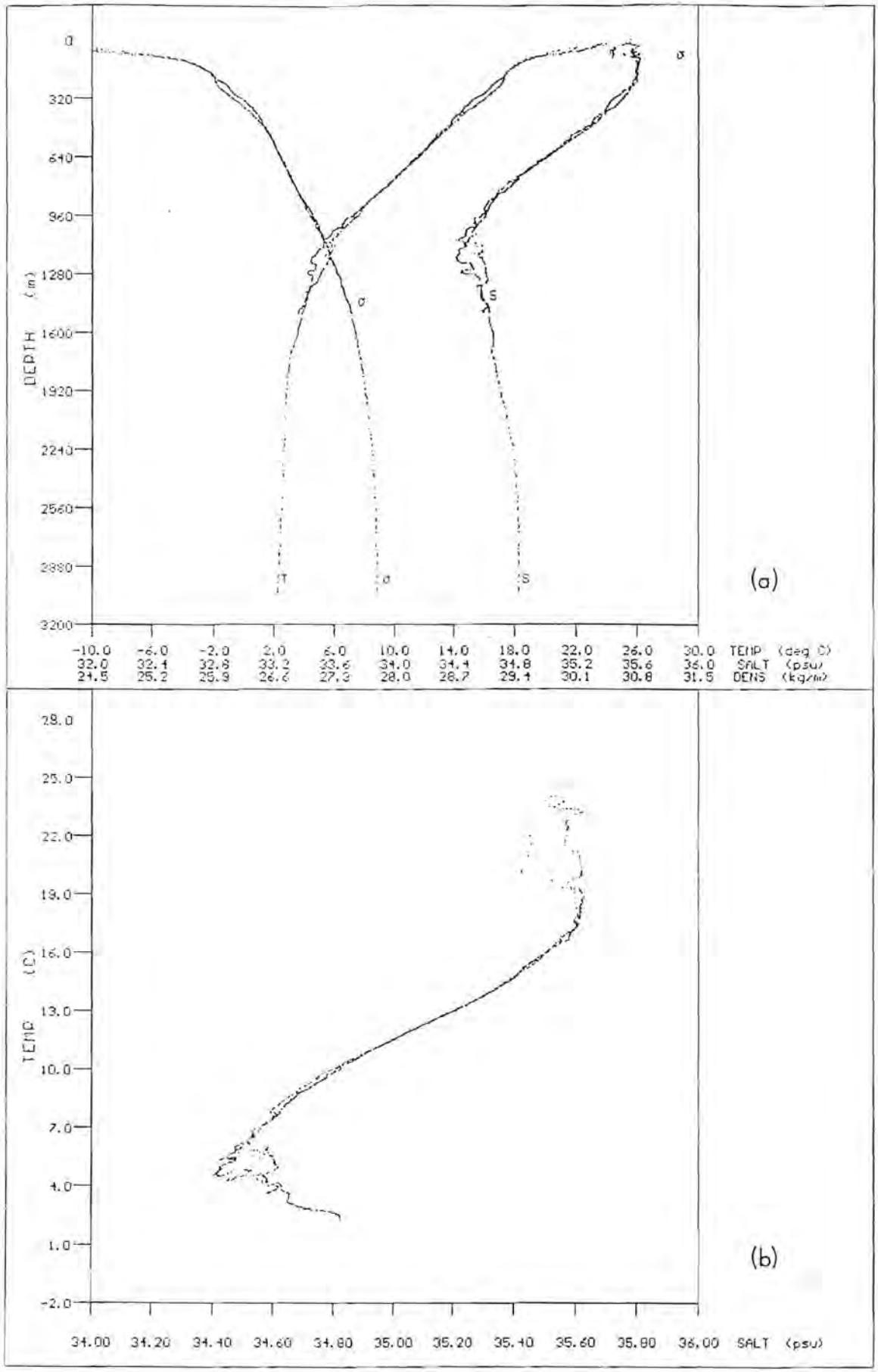

Figure 7.1: Comparison between temperature and salinity profiles taken within the Agulhas Current core, showing that the current property distributions are consistent from year to year. Profiles were obtained on the SCARC (February 1987) and ABBP (January 1992) cruises. a. Property/depth. b. Temperature-salinity.

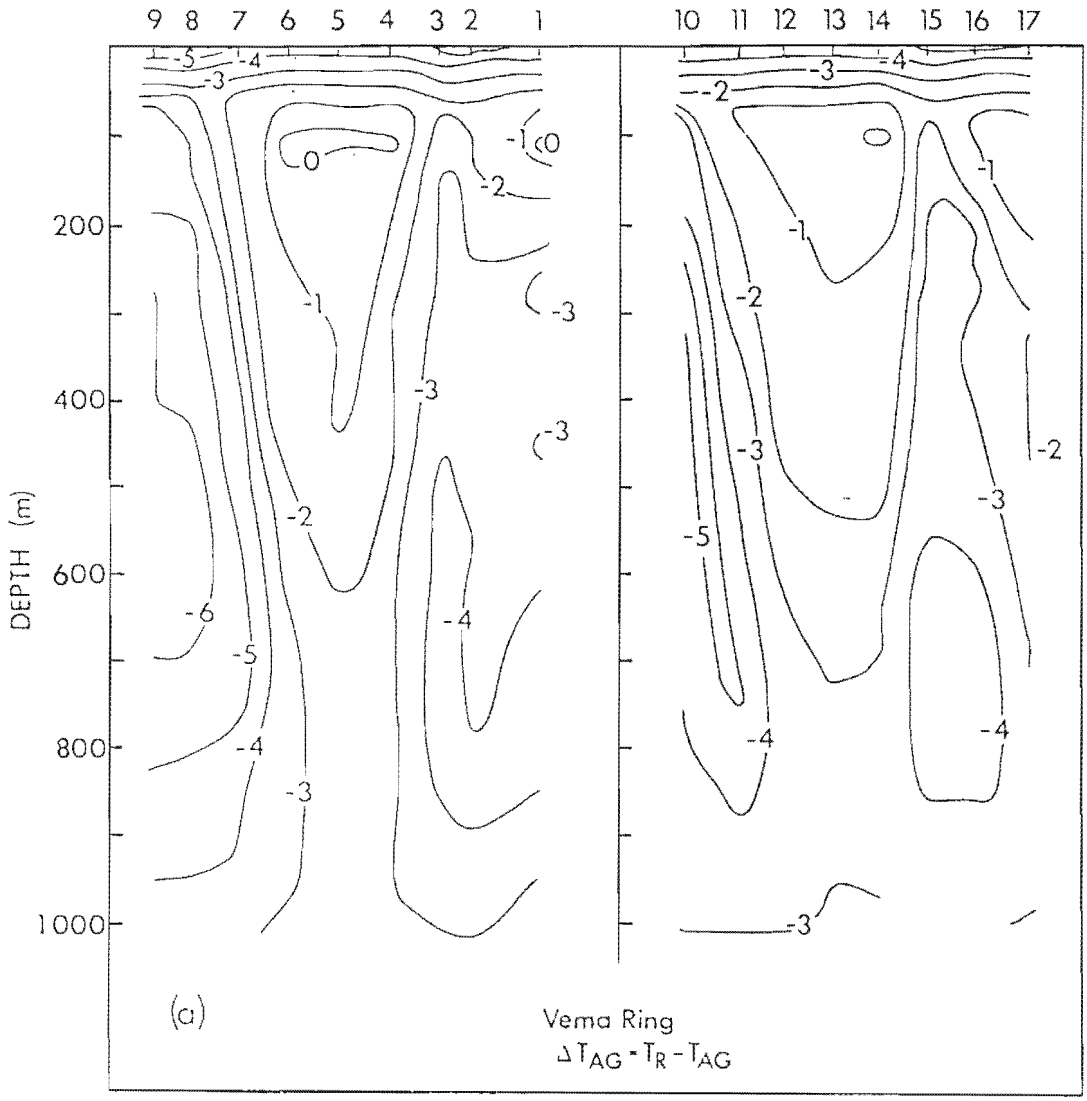

Figure 7.2a: Section of the temperature difference between ring water and a station in the Agulhas Current core taken along isopycnals and plotted against depth of isopycnal within the ring. a. the Vema ring.

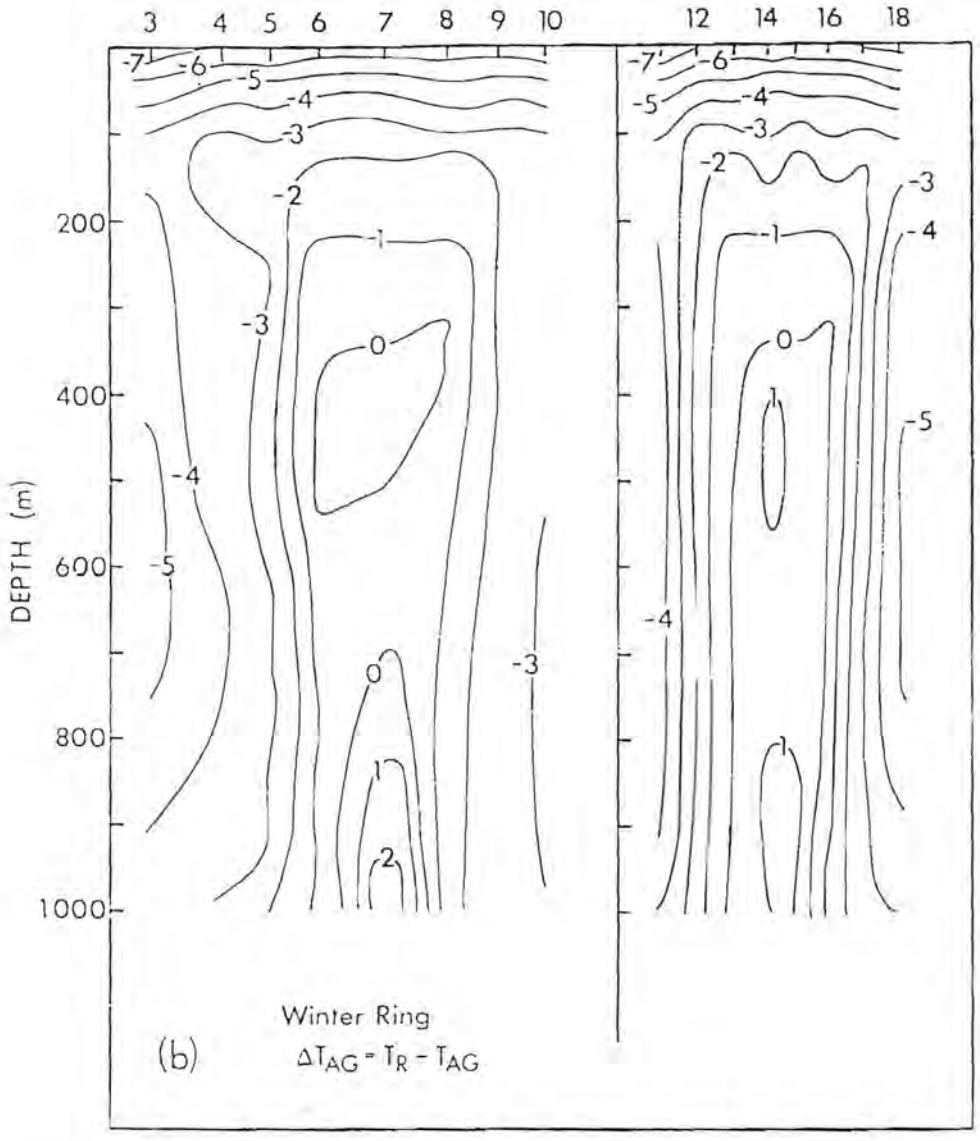

Figure 7.2b: Section of the temperature difference between ring water and a station in the Agulhas Current core taken along isopycnals and plotted against depth of isopycnal within the ring. b. the Winter ring

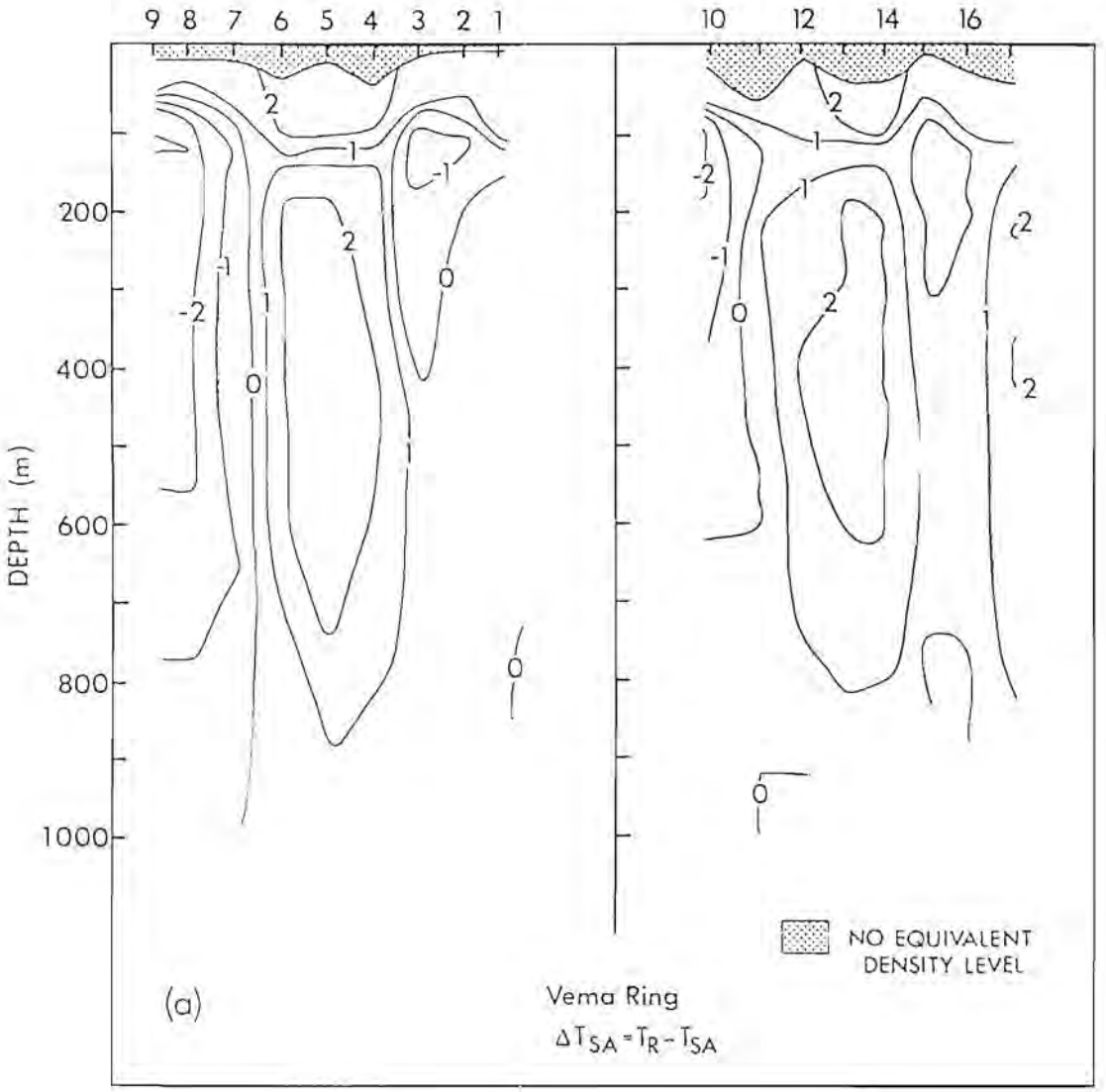

Figure 7.3a: Section of the temperature differences along isopycnals, between ring water and a station in the South Atlantic Ocean near the Walvis Ridge and plotted against depth of isopycnal within the ring. a. the Vema ring.

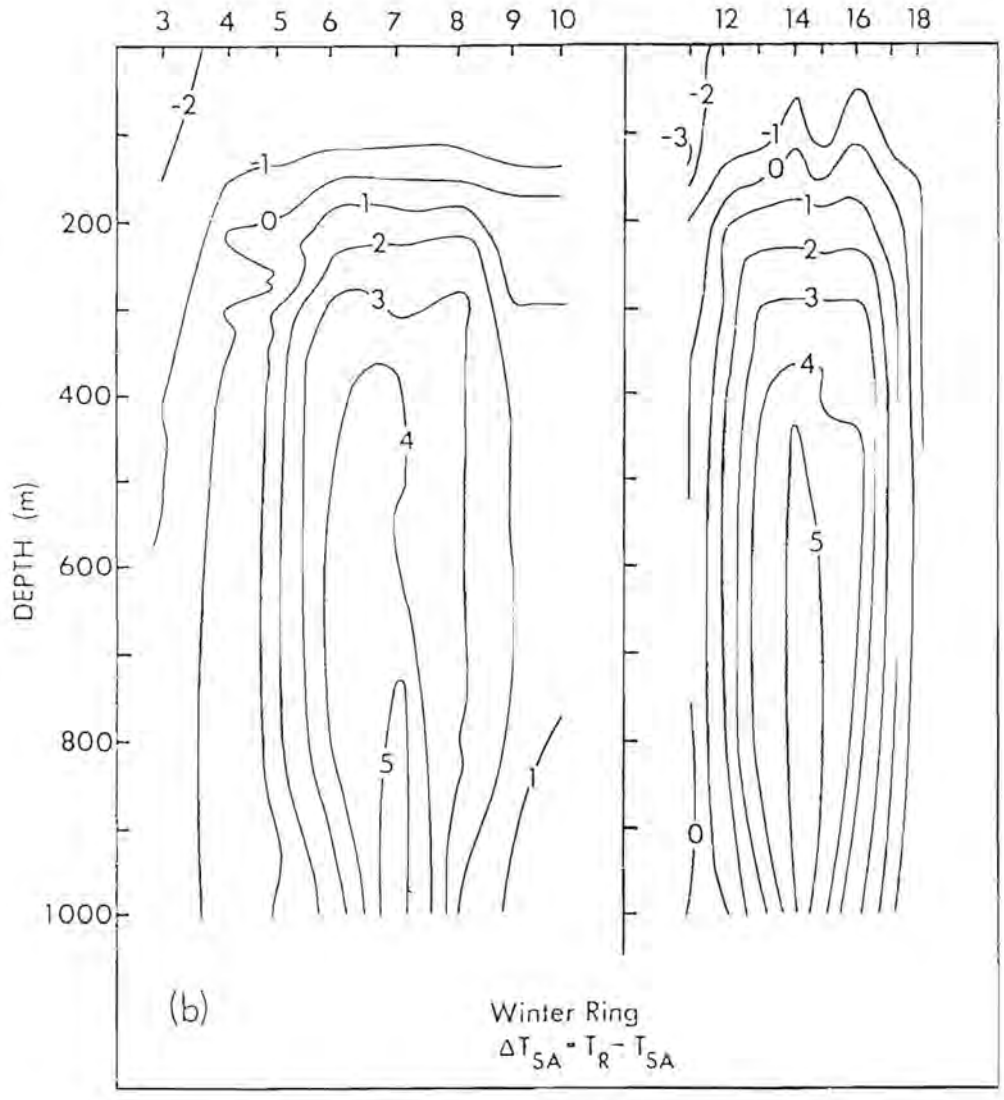

Figure 7.3b: Section of the temperature differences along isopycnals, between ring water and a station in the South Atlantic Ocean near the Walvis Ridge and plotted against depth of isopycnal within the ring. b. the Winter ring

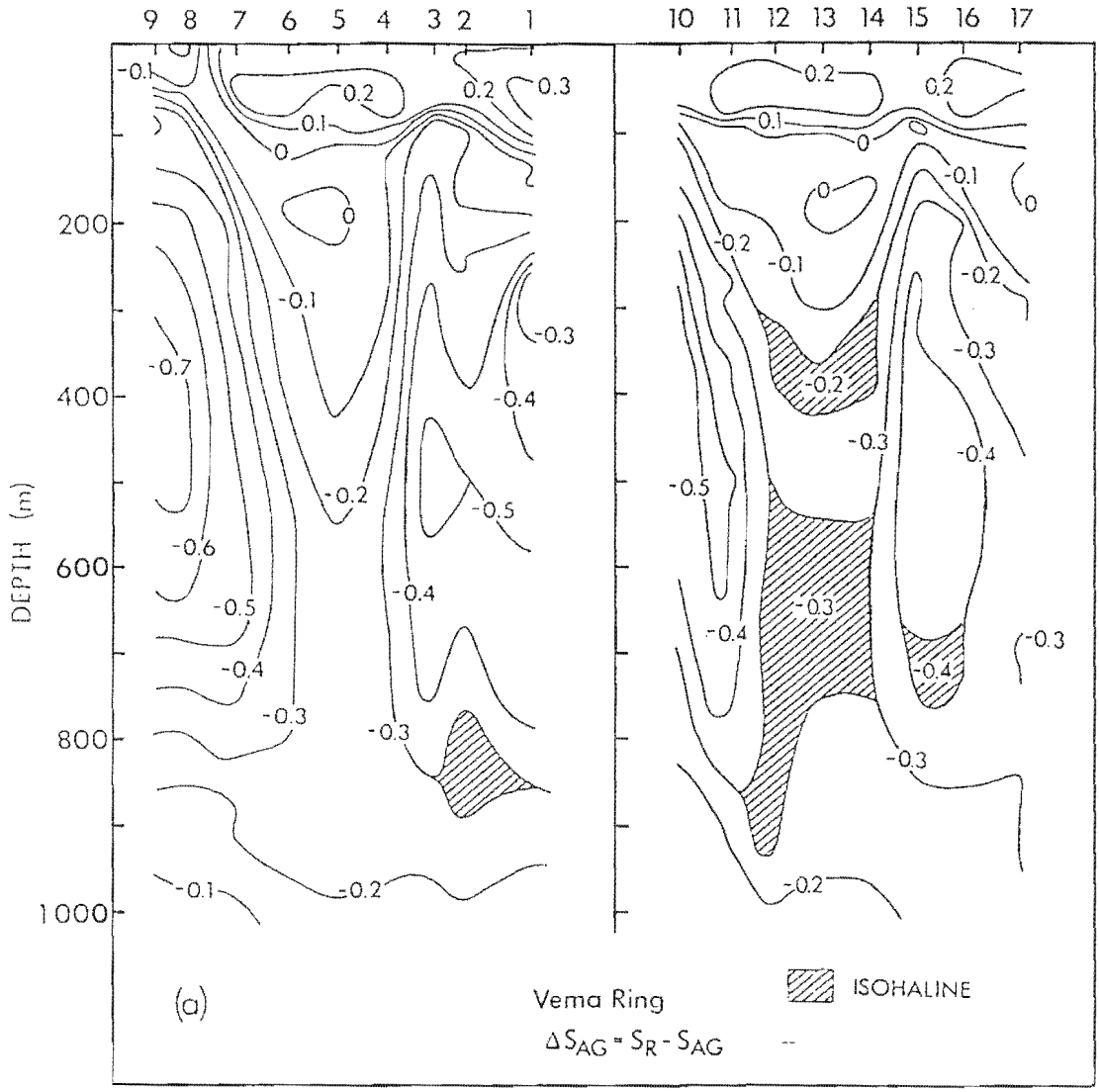

Figure 7.4a: Section of the salinity differences between ring water and a station in the Agulhas Current core taken along isopycnals and plotted against depth of isopycnal within the ring. a. the Vema ring.

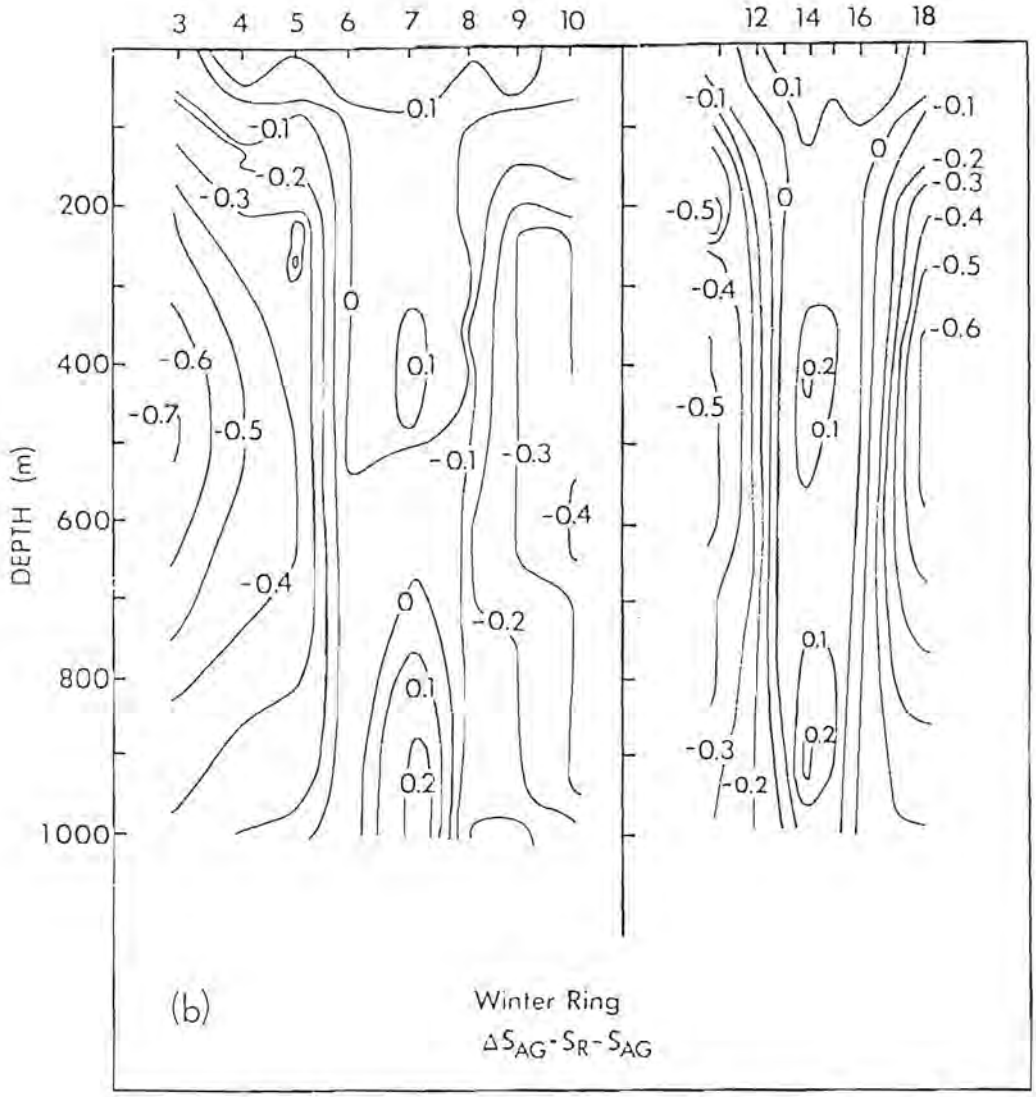

Figure 7.4b: Section of the salinity differences between ring water and a station in the Ag..lhas Current core taken along isopycnals and plotted against depth of isopycnal within the ring. b. the Winter ring

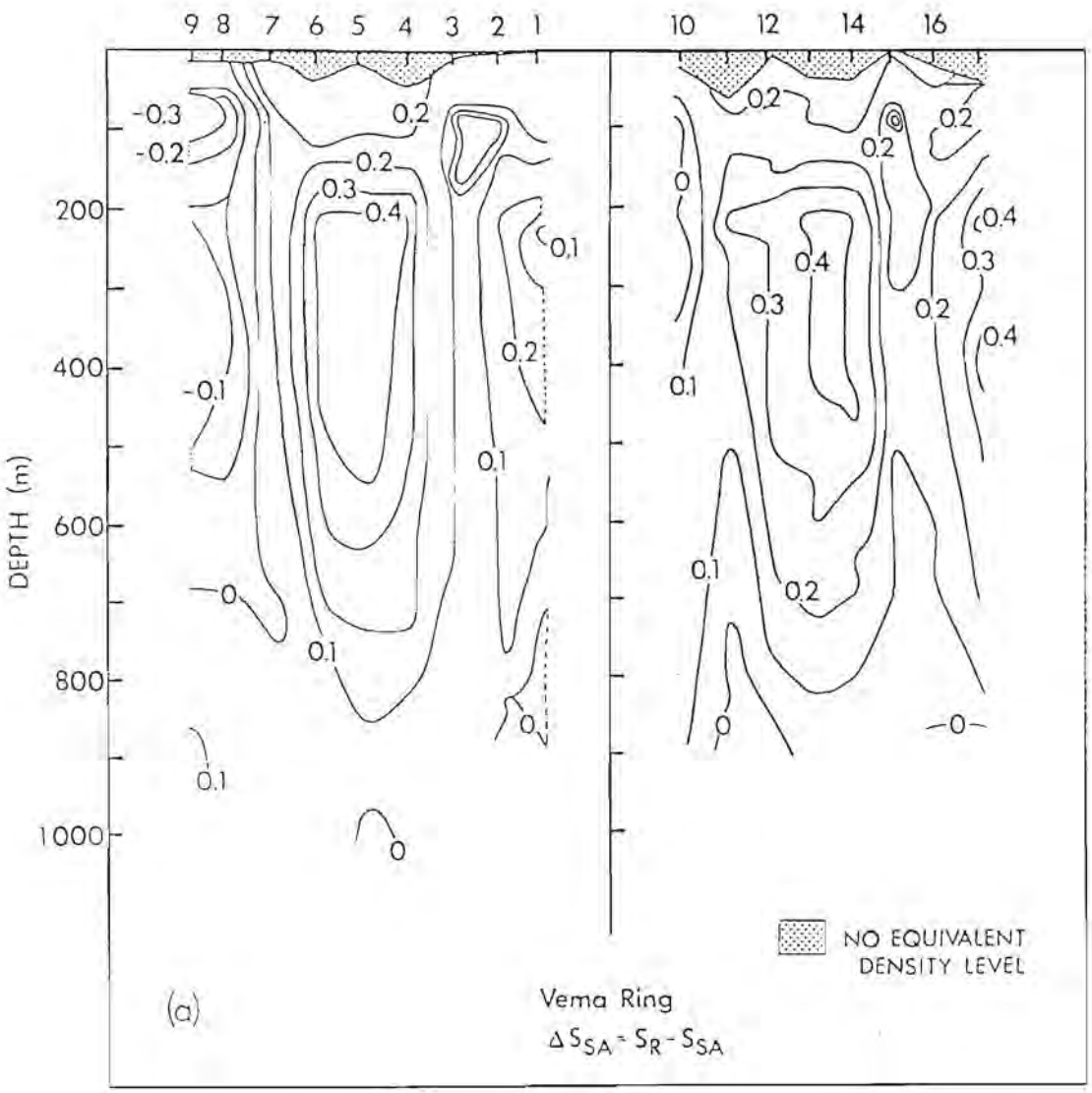

Figure 7.5a: Section of the salinity differences along isopycnals, between ring water and a station in the South Atlantic Ocean near the Walvis Ridge and plotted against depth of isopycnal within the ring. a. the Vema ring.

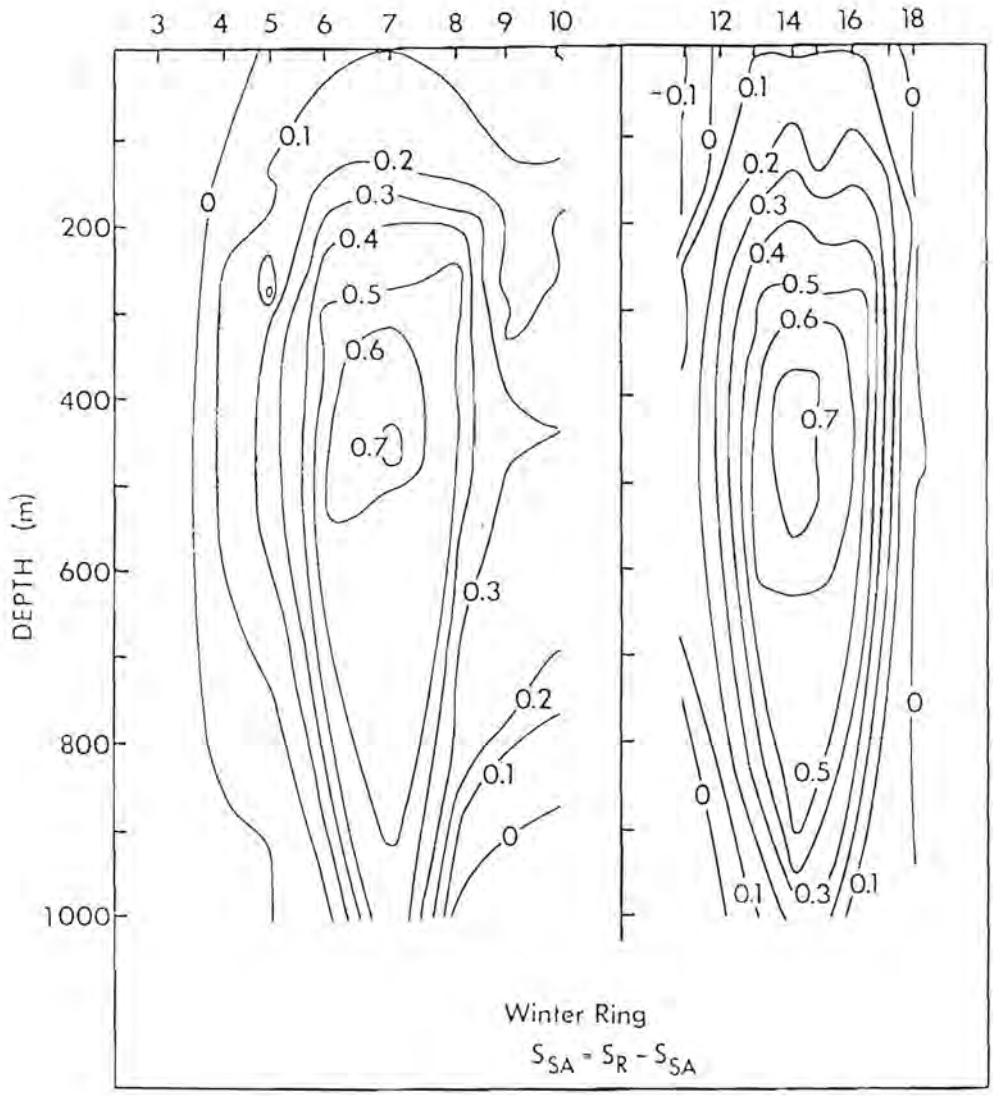

Figure 7.5b: Section of the salinity differences along isopycnals, between ring water and a station in the South Atlantic Ocean near the Walvis Ridge and plotted against depth of isopycnal within the ring. b. the Winter ring

Table 2i. A list of rings encountered hydrographically in the South Atlantic Ocean. The rings are named chronologically according to the year encountered. The position refers to the time at which hydrographic measurements were made. The sources are: Duncan (1968); H&VF - Harris and Van Foreest (1978); O&E - Olson and Evans (1986); M&WJ - McCartney and Woodgate-Jones (1991); B - Bennett (1988); L,V+ - Lutjeharms (1987), Valentine *et al.* (1988); G&H - Gordon and Haxby (1990); DR+ - Duncombe Rae *et al.* (1992b); DR&S - Duncombe Rae and Shillington (in prep.); G+ - Gordon *et al.* (1992); Po - Personal observation.

Ring	Vessel	Voyage	Date	Lati °S	Long °E	Source	Comment
R64.1	Afr. II*	?	64-3	40.5	15	Duncan	Wide station spacing. Reversing bottles.
R69.1	Afr. II*	?	69-3	35	15	H&VF	Wide station spacing. Reversing bottles.
R83.1	Knorr	104-5	83-11	35.5	15.4	O&E	ARC (Cape Town eddy)
R83.2				38.9	18.3		ARC (Retroflection eddy)
R83.3	Oceanus	133	83-2	23.0	-5.0	M&WJ	Detected on CTD line along 23°S
R85.1	R/V TW#	?	85-3	35	15.5	B	CTD line (Cape Town eddy 85)
R87.1	Agulhas	48	87-2	34.8	15.8	L,V+	2 lines SCARC (ring Susan)
R87.2				35.9	11.6		1 line SCARC (ring Rosemary)
R87.3				37.7	9.5		2 lines SCARC (ring Mariaan)
R87.4				38.0	15.0		2 lines SCARC (ring Erina)
R87.5				40.9	14.4		1 line SCARC (ring Helen)
R87.6	Discovery	165B	87-4	27.0	7.5	G&H	1 CTD line, GEOSAT
R89.1a	Africana	71	89-4	32.1	10.8	DR+	1 XBT line (Vema ring), GEOSAT
R89.1b	Benguela	246	89-5	30.5	9.2	DR+	R89.1a revisited, 3 lines (Vema ring)
R90.1	Melville	?	90-1	30	2	G+	CTD line SAVE-4
R90.2				30	6		
R90.3	Africana	81	90-5	36.3	14.3	Po	Feature on return from S.Am. Ring?
R90.4	Africana	85	90-7	35.3	11.7	DR&S	Search for ring. (Winter ring)
R92.1	Africana	105	92-6	35.8	14.9	Po	CTD, XBT 2 lines, IES line BEST-1
R93.1	Meteor	22/5	93-1	30.0	-3.0	Po	WOCE Line A10

* Afr. II - Africana II; # R/V TW - R/V Thomas Washington

Table 2ii. Parameters measured for some of the rings listed in Table 2i. Radius is the radius of the maximum radial velocity, with values in parentheses indicating estimates; h_{10} is the depth of the 10° isotherm at the ring centre; δh_{10} is the difference between the depth of the 10°C isotherm at the centre and at the edge of the ring; v_t and v_r refer to the translation and maximum radial speeds respectively (negative speeds indicate anticyclonic flow); APE is the available potential energy; and KE is the kinetic energy.

Ring	Radius km	h_{10} m	δh_{10} m	v_t $cm.s^{-1}$	v_r $cm.s^{-1}$	APE $10^{15}J$	KE $10^{15}J$
R83.1	115	750	370	4.8	-60	30.5	6.2
R83.2	130	740	420	8.5	-90	51.4	8.7
R83.3	90	560	140	?	-29	?	?
R87.1	(130)	425	145	?	?	?	?
R87.2	(150)	700	350	?	?	?	?
R87.3	(100)	650	300	?	?	?	?
R87.4	(115)	770	455	?	?	?	?
R87.5	(140)	520	370	?	?	?	?
R87.6	145	520	300	8.3	-43	?	?
R89.1b	145	600	300	6.4	-55	38.8	2.3
R90.4	90	870	510	?	-60	26.2	2.6
R92.1	140	750	350	?	-80	?	?

Table 2iii. Water masses of the Agulhas Retroflection region and the property extremes associated with them. Compiled from Bennett (1988).

Depth Range	Water Mass	Extreme	Density ($kg.m^{-3}$)	Temp (°C)	Salt (psu)	Water Type	Abbr
Shallow - 50 to 300m	Surface	S max	σ_0=25.8	17.7	35.60	South Indian Subtropical Surface Water	SSW
		PV max		17.4±0.7	35.58±0.04	Local Subtropical Mode Water	STMW
		O_2 max					
		O_2 min				South Indian Tropical Thermocline Water	TTW
		O_2 min				Benguela Shelf Bottom Water	BBW
Thermocline 200 to 800m	Central	PV min	$26.6 \leq \sigma_0 \leq 26.8$	10-12	34.8-35.2	South Indian Subantarctic Mode Water	SAMW
		O_2 max					
600 to 1800m	Intermediate	S min	σ_1=31.8	4.6	34.3-34.6	Antarctic Intermediate Water	AAIW
		O_2 min	$32.1 \leq \sigma_1 \leq 32.2$			Deep North Indian Water (Red Sea Water)	RSW
2000 to bottom	Deep	O_2 min				Upper Circumpolar Deep Water	UCDW
		S max				North Atlantic Deep Water	NADW
		O_2 max					
		O_2 min				Lower Circumpolar Deep Water	LCDW

Table 2iv. Characteristic ranges of temperature and salinity for the water masses of the Agulhas Retroflection. NADW - North Atlantic Deep Water; CDW - Circumpolar Deep Water; AABW - Antarctic Bottom Water (From Valentine 1990.)

Water Mass	Temperature (°C)	Salinity (psu)
Surface Water	~16 - 26	>35.5
Central Water		
Southeast Atlantic Ocean	6.0 - 16.0	34.5 - 35.5
Southwest Indian Ocean	8.0 - 15.0	34.6 - 35.5
Antarctic Intermediate Water		
Characteristic	~2.2	~33.87
1) SE Atlantic	2.0 - 6.0	33.8 - 34.8
2) SW Indian	2.0 - 10.0	33.8 - 34.8
Deep Water		
NADW (SE Atlantic)	1.5 - 4.0	34.8 - 35.00
CDW (SW Indian)	0.1 - 2.0	34.63 - 34.73
AABW	-0.9 - 1.7	34.64 - 34.72

Table 5i: Scales and dimensionless numbers for Agulhas rings. Ring numbers refer to those in Tables 2i and 2ii: R83.1 and R83.2 are the Cape Town and Agulhas eddies, respectively, referred to by Olson and Evans (1986); R89.1b is the Vema ring; R90.4 is the Winter ring; WCR.82B refers to Gulf Stream Warm Core Ring 82B. L is the length scale at the radius of maximum velocity; V is the maximum velocity; h is the depth of 10°C isotherm; δh is the displacement of the 10°C isotherm; g' is the reduced gravity for the two-layer model; f is the Coriolis parameter; $R_o = (-1 \pm (1 + 4B')^{\frac{1}{2}})/2$ is the Rossby number; $R_d = (g'h)^{\frac{1}{2}}/f$ is the Rossby radius; $B' = g'\delta h/f^2L^2$ is a Burger number for the displacement of the isotherms; $B = g'h/f^2L^2$ is the conventional Burger number; $R_i = g'h/V^2$ is the Richardson number; E_R = APE/KE is the ratio of available potential to kinetic energies. Data are obtained from: * Olson and Evans (1986); $ Olson *et al.* (1985 in Olson 1991).

Ring	L 10^3 m	V m.s^{-1}	h m	δh m	g' m.s^{-2}	f 10^{-5} s^{-1}	R_o	R_d 10^3 m	B'	B	R_i	E_R
R83.1	115*	-0.60*	750*	-370*	0.018*	-8.4	-0.04*	43.5	-0.071	0.143	37.5	4.9
R83.2	130*	-0.90*	740*	-420*	0.018*	-9.1	-0.07*	40.0	-0.054	0.094	16.4	5.9
R89.1b	145	-0.55	600	-300	0.01513	-7.4	-0.041	40.8	-0.040	0.079	30.0	16.9
R90.4	90	-0.60	870	-510	0.00933	-8.4	-0.091	33.9	-0.083	0.142	22.5	10.1
WCR.82B	55$	-0.55$					-0.11$	26$		0.16$		

Table 7i: Volume transport estimates of the inter-basin transfer between the Indian and Atlantic Oceans

Source	Volume Flux Estimate $\times 10^6$ $m^3.s^{-1}$	Date	Type of measurement	Suggested mechanism for transfer
FRAM Group 1991	10	N/A	Circulation model	In eddies
Harris & Van Foreest 1978	5	1969	Geostrophic calculation from bottle data	Not discussed, leakage implied
Gordon *et al.* 1987a	10	Late 1983	Geostrophic calculation from CTD data	Within IOCW+AAIW
Whitworth & Nowlin 1987	19	Early 1984	Geostrophic calculation from CTD data	Leakage. Figure represents net flux
Bennett 1988	6.3	1983	Geostrophic calculation	Water > 8°C
	9.6	1984		
	2.8	1985		
Stramma & Peterson 1990	8	1983	Recalculated from RV *Knorr* sections	Leakage between eddy and coast
Gordon and Haxby 1990	10 to 15	1987	GEOSAT and geostrophic calculations	Eddy field
McCartney & Woodgate-Jones 1991	2 to 5.5	early 1983	Inferred from hydrographic measurements	Eddy field

APPENDIX C: CURRICULUM VITAE

C.1 BIOGRAPHY

I was born in Port Elizabeth, South Africa, where I received my primary and secondary education. A first attempt at tertiary education was interrupted by my conscription into the SADF to undergo National Service.

My path into research in oceanography started after finally completing a Bachelor of Science degree with Physics and Chemistry majors at Rhodes University in Grahamstown in 1982. I began working for Prof. Brian Allanson as his research assistant with the Institute for Fresh Water Studies in January 1983. My first insight into what oceanographers do was provided by the Fifth National Oceanographic Symposium, held in Grahamstown during that month. Work for Prof. Allanson included application of a one-dimensional model of the thermal structure of P.K. Le Roux Dam, and research cruises to the Prince Edward Islands and Prydz Bay, Antarctica, all of which fuelled an interest in the physical structure and dynamics of water, particularly ocean water. My first experience with Agulhas rings came in November 1983, when I participated in Prof. Arnold Gordon's Agulhas Retroflection Cruise to measure chlorophyll concentrations for Prof. Allanson.

In 1985 I attended the University of Cape Town to take a B.Sc. Honours degree in Physical Oceanography. Between 1986 and 1988 I held a position as research officer in the Southern Oceans Group at Rhodes University under the Foundation for Research Development Antarctic Programme. During this time I renewed my acquaintance with Agulhas rings in February 1987 on the SCARC cruise organised by Prof. Johann Lutjeharms. At the beginning of 1989, I moved to Cape Town to a post in the Sea Fisheries Research Institute.

Collecting XBT data from deep-sea cruises in the South Atlantic suggested the topic of an M.Sc. thesis on upper layer temperatures of the South Atlantic (some remnants of this work are retained as Chapter 4 of this thesis). My interest in Agulhas rings was re-kindled by the cruises to the Vema ring (*Africana* V071 and *Benguela* V246) and the Winter ring. By the end of 1990 I knew more about Agulhas rings than I did about "the upper layer thermal structure of the Cape Basin" and in early 1992 I formally changed topic and upgraded my thesis proposal to a Ph.D.

My current and future research interests lie closer inshore, associated with the Agulhas Bank shelf-edge: the influence of the Agulhas Current on the Agulhas Bank and the demersal and pelagic fisheries in the region; the possible influence of the Agulhas Bank on the Agulhas Current; and the coupling between the western Agulhas Bank and the Benguela ecosystem.

C.2 LIST OF PUBLICATIONS

Papers contributing to the body of the thesis are indicated *.

C.2.1 PUBLICATIONS RELEVANT TO THE THESIS (Excluding unpublished data reports and unpublished conference presentations.)

CHAPMAN, P., DUNCOMBE RAE, C.M. and B.R. ALLANSON 1987 - Nutrients, chlorophyll and oxygen relationships in the surface layers at the Agulhas Retroflection. *Deep-Sea Res.* **34**(8A): 1399-1416.

*DUNCOMBE RAE, C.M. 1991 - Agulhas retroflection rings in the South Atlantic Ocean: an overview. *S. Afr. J. mar. Sci.* 11: 327-344.

*DUNCOMBE RAE, C.M., BOYD, A.J. and R.J.M. CRAWFORD 1992 - 'Predation' of anchovy by an Agulhas ring: a possible contributory cause of the very poor yearclass of 1989. In *Benguela Trophic Functioning.* PAYNE, A.I.L., BRINK, K.H., MANN, K.H. and R. HILBORN (Eds). *S. Afr. J. mar. Sci.* 12: 167-173.

DUNCOMBE RAE, C.M., SHANNON, L.V. and F.A. SHILLINGTON 1989 - An Agulhas ring in the South Atlantic ocean. *S. Afr. J. Sci.* 85: 747-748.

*DUNCOMBE RAE, C.M. and F.A. SHILLINGTON in prep. - A winter ring from the Agulhas. In preparation.

*DUNCOMBE RAE, C.M., SHILLINGTON, F.A., AGENBAG, J.J., TAUNTON-CLARK, J. and M.L. GRÜNDLINGH 1992 - An Agulhas ring in the South Atlantic Ocean and its interaction with the Benguela Upwelling Frontal system. *Deep-Sea Res.* **39**(11/12): 2009-2027.

LUTJEHARMS, J.R.E., SHILLINGTON, F.A. and C.M. DUNCOMBE RAE 1991 - Observations of extreme upwelling filaments in the Southeast Atlantic Ocean. *Science, N.Y.* 253(5021): 774-776.

VALENTINE, H.R., DUNCOMBE RAE, C.M., VAN BALLEGOOYEN, R.C. and J.R.E. LUTJEHARMS 1988 - The Subtropical Convergence and Agulhas Retroflection Cruise (SCARC) Data Report. *Rep. S. Afr. Coun. scient. ind. Res.* **T/SEA 8804**: 10 pp + tables + figures.

C.2.2 OTHER REFEREED PUBLICATIONS

ALLANSON, B.R., BODEN, B.P., PARKER, L.D. and C.M. DUNCOMBE RAE 1985 - A contribution to the oceanology of the Prince Edward Islands. In *Antarctic Nutrient Cycles and Food Webs.* SIEGFRIED, W.R., CONDY, P.R. and R.M. LAWS (Eds). Heidelberg; Springer: pp. 38-45.

ALLANSON, B.R. and C.M. DUNCOMBE RAE 1984 - Values for the first and second apparent dissociation constants, K_1' and K_2', of carbonic acid for estuarine and brackish waters as a function of temperature and chlorinity. *J. limnol. Soc. s. Afr.* 10(2): 74-75.

BODEN, B.P., DUNCOMBE RAE, C.M. and J.R.E. LUTJEHARMS 1988 - The distribution of the diatoms of the surface waters of the South West Indian Ocean between Cape Town and the Prince Edward Islands archipelago. *S. Afr. J. Sci.* **84**: 811-818.

DUNCOMBE RAE, C.M. 1984 - Preliminary results of the South African SIBEX I Cruise to the Prydz Bay region, Antarctica, 15 March - 3 May 1984: V. Nutrient analysis. *S. Afr. J. Antarct. Res.* 15: 20-22.

DUNCOMBE RAE, C.M. 1989 - Frontal systems encountered between southern Africa and the Prince Edward Islands during April/May 1987. *S. Afr. J. Antarct. Res.* 19(1): 21-25.

DUNCOMBE RAE, C.M. 1989 - Physical and chemical marine environment of the Prince Edward Islands (Southern Ocean) during April/May 1987. *S. Afr. J. mar. Sci.* 8: 301-311.

PERISSINOTTO, R. and C.M. DUNCOMBE RAE 1990 - Occurrence of anti-cyclonic eddies on the Prince Edward Plateau (South West Indian Ocean): effects on phytoplankton biomass and production. *Deep-Sea Res.* 37(5): 777-793.

PERISSINOTTO, R., DUNCOMBE RAE, C.M., BODEN, B.P. and B.R. ALLANSON 1990 - Vertical stability as a controlling factor of the marine phytoplankton production at the Prince Edward Archipelago (Southern Oceans). *Mar. Ecol. Progr. Ser.* 60: 205-209.

C.2.3 NON-REFEREED PUBLICATIONS

BODEN, B.P., PARKER, L.D. and C.M. DUNCOMBE RAE 1987 - *An investigation of the distribution and production of plankton in the seas around the Prince Edward Islands: final project report to SASCAR.* SANARP Final Project Reports. Pretoria; Foundation for Research Development, CSIR: 28pp.

DUNCOMBE RAE, C.M. 1987 - Summary of the April/May 1987 cruise for the Marion Offshore Ecological Study (MOES) component of the SASCAR Southern Ocean Programme. *SASCAR Newsl.* (27): 2-4.

DUNCOMBE RAE, C.M. 1989 - *Data Report of the First Cruise of the Marion Off-shore Ecological Study (MOES-1).* South African National Scientific Programmes Reports No. 159. Pretoria; C.S.I.R.: 384pp.

DUNCOMBE RAE, C.M., BODEN, B.P. and D. GIANAKOURAS 1987 - *Marion Offshore Ecosystems Study (first cruise - biological component): Report on ship-based scientific work conducted aboard S.A. Agulhas during Voyage 49 (Marion Island Base relief).* S.A. Agulhas Chief Scientists' Reports. Pretoria; C.S.I.R.: 10pp.

C.2.4 UNPUBLISHED REPORTS (Including unpublished data reports relevant to the thesis.)

ALLANSON, B.R. and C.M. DUNCOMBE RAE 1984 - Chlorophyll-a distribution during ARC (a) The RV *Knorr* cruise. In: *South African Participation in Agulhas Retroflection Cruise Programme.* LUTJEHARMS, J.R.E. (Ed.). NRIO Data Report D8406. Stellenbosch; N.R.I.O. (Preliminary report not for publication).

DUNCOMBE RAE, C.M. 1987 - *Oceanographic programs, subroutines and functions.* Internal Report, Southern Oceans Group, Zoology Department, Rhodes University, Grahamstown.

DUNCOMBE RAE, C.M. and H.M. BARBER 1987 - *Methods of nutrient analysis using the Technicon Autoanalyzer II system: a handbook for using the AAII system at Rhodes University.* Internal Report, Southern Oceans Group, Zoology Department, Rhodes University, Grahamstown.

*DUNCOMBE RAE, C.M., CHAPMAN, P. and L.V. SHANNON 1989 - *Data Report of R.S. Africana Voyage 071 - South East Atlantic Ocean, April 1989 (Vema, Walvis Ridge, Tristan da Cunha, Gough).* Internal report, Sea Fisheries Research Institute, manuscript in preparation.

*DUNCOMBE RAE, C. M. and F. A. SHILLINGTON 1989 - *Data Report of R.S. Benguela Voyage 246 - South Atlantic Eddy Cruise, May 1989.* Internal report, Sea Fisheries Research Institute, manuscript in preparation.

C.2.5 UNPUBLISHED CONFERENCE PRESENTATIONS

BODEN, B.P., DUNCOMBE RAE, C.M. and D. LAPOTA 1987 - Bioluminescence as an adjunct indicator of activity at ocean frontal regions. Oral presentation at 6 National Oceanographic Symposium, Stellenbosch.

DUNCOMBE RAE, C.M. and F.A. SHILLINGTON 1990 - An Agulhas eddy in the South Atlantic Ocean and interactions with the Benguela System. Oceans '90, 7th National Oceanographic Symposium, San Lameer, South Africa, 25-29 June 1990. Abstract. Oral presentation.

PERISSINOTTO, R., DUNCOMBE RAE, C.M. and B.R. ALLANSON 1990 - Physical, chemical and biological control of marine phytoplankton production and biomass at the Prince Edward Islands (1982-1989). Oceans '90, 7th National Oceanographic Symposium, San Lameer, South Africa, 25-29 June 1990. Abstract. Poster presentation.

VAN BALLEGOOYEN, R.C. and C.M. DUNCOMBE RAE 1989 - Features of the mesoscale ocean circulation in the vicinity of the Prince Edward Island group. Oral presentation at South African Society for Atmospheric Sciences, 6th Annual Conference, November 1989.

VAN BALLEGOOYEN, R.C., DUNCOMBE RAE, C.M., PERISSINOTTO, R., LUTJEHARMS, J.R.E. and B.R. ALLANSON 1990 - The oceanic environment surrounding the Prince Edward Island Group. Oceans '90, 7th National Oceanographic Symposium, San Lameer, South Africa, 25-29 June 1990. Abstract. Oral presentation.